**Title**
Stromal Modulation of Radiation Carcinogenesis in Breast Cancer



**Author**
Nguyen, David Hiendat Hua

**Publication Date**
2011

Peer reviewed|Thesis/dissertation

# Stromal Modulation of Radiation Carcinogenesis in Breast Cancer

By

David Hiendat Hua Nguyen

A dissertation submitted in partial satisfaction of the
requirements for the degree of
Doctor of Philosophy
in
Endocrinology
in the
Graduate Division
of the
University of California, Berkeley

Committee in charge:
Professor Mary Helen Barcellos-Hoff, Co-Chair
Professor Gertrude Buehring, Co-Chair
Professor Gary L. Firestone
Professor Qing Zhong

Spring 2011

To my parents and family.

Love, care, sacrifice, you gave to me;

braving oceans of oppression, sweatshop labor, and poverty.

To my teachers and mentors.

Reason, imitate;

Wisdom, emulate;

Wonder, perpetuate.

And to the roots of America's ideals.

Liberty, reciprocate.

**Table of Contents**

**Abstract**

**Stromal Modulation of Radiation Carcinogenesis in Breast Cancer**

by

David Hiendat Hua Nguyen

Doctor of Philosophy in Endocrinology

University of California, Berkeley

Professor Mary Helen Barcellos-Hoff, Co-Chair

Professor Gertrude Buehring, Co-Chair

Our experimental data and that of others suggest that the carcinogenic action of ionizing radiation (IR) is a two-compartment problem: IR can alter genomic sequence as a result of DNA damage and radiation-induced signal transduction can alter phenotype and multicellular interactions. Rather than being accessory or secondary to genetic damage, we propose that such non-targeted radiation effects create the critical context that promotes cancer development. This review focuses on experimental studies that clearly define molecular mechanisms by which cell interactions contribute to cancer in different organs, and addresses how non-targeted radiation effects may similarly act though the microenvironment. The definition of non-targeted radiation effects and their dose dependence could modify the current paradigms for radiation risk assessment. Since radiation non-targeted effects, unlike DNA damage, are amenable to intervention, we discuss the implication that long term cancer risk could be limited after exposure.

## Chapter 1

## Introduction

A fundamental challenge in radiation research related to human health is to predict the biological impact of exposure to low dose (<0.1 Gy) ionizing radiation (IR). Excess cancers have been observed in the Japanese atomic-bomb survivors at doses of 0.1 to 4 Gy, which are 40 to 1600 times the average yearly background levels in the USA. The excess risks vary significantly with gender, attained age, and age at exposure for all solid cancers as a group and many individual sites as a consequence of the atomic bomb (Preston et al., 2007). It has been estimated that if radiation exposure occurs at age 30, the solid cancer rates at age 70 is increased by about 35% per Gy (90% CI 28%; 43%) for men and 58% per Gy (90% CI 43%; 69%) for women (Preston et al., 2007). Predicting cancer risk in populations exposed to doses lower than ~0.1 Gy is limited by statistical considerations. Therefore, radiation risk models extrapolate in the region below which epidemiological data are robust using an assumption of linearity. This linear-no-threshold (LNT) regulatory paradigm is based in large part on observations that cancer incidence increases with increasing dose above 0.1 Gy, as well as pragmatic, regulatory and societal considerations to protect the population.

A recent review study of the National Academy of Sciences (BEIR VII) concluded that human health risks continue in a linear fashion at low doses without a threshold such that that the smallest dose has the potential to increase risk in humans. The scientific rationale for linearly extrapolating radiation health effects is underpinned by biophysical theory of how energy interacts with DNA, which is thought to be the major biological target. This area of radiation biology has made significant progress in identifying the critical mechanisms, processes and pathways by which DNA is damaged, repaired or misrepaired. The efficiency and frequency by which IR induces mutations and chromosomal aberrations is thought by most to be the best surrogate of its carcinogenic potential, in part because there is a clear mechanistic understanding of their induction from energy deposition, and in part because these events are strongly associated with cancer. A fundamental principle of target theory is that the effect (e.g. DNA damage, cell kill, mutation) is linear or linear/linear-quadratic as a function of dose due to biophysical considerations that energy deposition (i.e. dose) is proportional to damage. In terms of immediate damage, so-called targeted radiation effects, this conclusion is very well supported for DNA damage that can be measured directly or indirectly over several logs of radiation exposure (1-100 Gy).

However biological responses to radiation damage quickly evolve and amplify in a non-linear manner, particularly at low doses, which has been broadly documented both in cell culture and in vivo (reviewed in (Brooks, 2005; Wright and Coates, 2006). There are now myriad experimental reports that low doses radiation alters the response to subsequent challenge doses (i.e. adaptive responses, AR), affects daughter cell fates such as differentiation and senescence, induces long-range signals that affect non-irradiated cells, and generates a state of chronic genomic instability (GIN). Although there are several definitions of non-targeted effects, we define non-targeted effects as those that are inconsistent with either direct energy deposition, such as bystander phenomenon (Barcellos-Hoff and Ravani, 2000; Hei et al., 1997;

Kaplan et al., 1956b; Mothersill et al., 2001), or those that are exhibited in the daughters of irradiated cells, but not mediated by a mutational mechanism, such as radiation-induced genomic instability (Clutton et al., 1996; Kadhim et al., 1994; Kadhim et al., 1995; Kadhim et al., 1992; Limoli et al., 1997) and persistent phenotypic changes (Herskind and Rodemann, 2000; Park et al., 2003; Rave-Frank et al., 2001; Tsai et al., 2005). Although the extent to which these phenomena reflect different molecular mechanisms is not clear, experimental results to date suggest that significant deviation from linearity at low doses may impact the ability to predict cancer risk in humans (Barcellos-Hoff and Brooks, 2001; Baverstock, 2000; Huang et al., 2003; Little, 2003; Wright, 2000).

These non-linear radiation responses could have significant implications for the LNT regulatory assumption. Indeed the French Academy of Medicine concluded that there is compelling evidence that the mechanisms of response to low dose/dose rate are sufficiently different from those operating at high doses and that the current policy may lead to an overestimation of risks (2005). Nonetheless, there is considerable debate regarding the relevance of non-targeted effects in radiation protection paradigms. Do non-targeted radiation effects alter the predicted dose dependence of radiation carcinogenesis at low doses? Although we believe that different modes of radiation action contribute to health effects, it is unlikely that that they will be incorporated into the regulatory perspective unless a more comprehensive biological paradigm of radiation carcinogenesis is generally accepted.

Our overarching hypothesis is that cancer *emerges* as a result of a complex, but ultimately predictable, interplay between targeted and non-targeted effects in the context of host genetics and physiology (Barcellos-Hoff, 2007). Just as DNA damage elicits a dramatic transition in signaling within a cell, each irradiated tissue has its own set of signals and cell types, distinct from those of un-irradiated tissue and different from other irradiated tissues. The sum of these events, occurring in different organs and highly modulated by genotype, predicates the consequence to the organism. We propose that radiation exposure culminates in cancer as a result of oncogenic mutations from targeted DNA damage that occur in the context of the biology of irradiated tissues driven in large part by non-targeted radiation effects (Barcellos-Hoff, 2005; Barcellos-Hoff, 2007). The dose dependence of the former is well-established; the dose dependence of the latter is crucial to understanding risk.

**Carcinogenesis in Context**

Many models of cancer risk and mitigation are focused on 'targets', i.e. the cell that will undergo neoplastic transformation or the genetic alterations that initiate and promote this event. There is growing recognition that as a disease, cancer results from a systemic failure in which many cells other than those with oncogenic genomes determine the frequency of clinical cancer. Even though the prevalence of cancer in humans (1 of 3 Americans will be diagnosed during their lives), cancer is much more frequent at the tissue level according to autopsy studies. At age 50, 1 of 4000 people will be diagnosed with thyroid cancer although 99% of autopsy specimens contain frank malignancies (Tulinius, 1991). Similarly, many more Western men compared to Japanese men develop clinical prostate cancer by age 60, even though carcinomas are equally prevalent in autopsy specimens (Stemmermann et al., 1992). Autopsy data also show that breast cancer is much more prevalent at the tissue level than is clinically

evident (Nielsen, 1989; Nielsen et al., 1984) Thus, random genetic changes occur sufficiently frequently to produce malignant cells in large part as a result of normal living but do not progress at the tissue level. It is thought that these cancers fail to execute the angiogenic switch, or that proliferation is balanced by apoptotic programs, or that dormancy is enforced by organismal biology like immune response (reviewed by (Folkman et al., 2000)). Together, these processes point to system integration that resists change to maintain integrity.

Pioneering studies by Mintz and Pierce during the '70s showed that malignancy could be suppressed by normal tissues (Mintz and Illmensee, 1975; Pierce et al., 1978). Dvorak proposed that cancer is analogous to a wound that never heals (Dvorak, 1986), an idea that implicates the importance of tissue remodeling and inflammation, both of which involve the functions of tissues. It has become increasingly evident that tissue structure, function and dysfunction are highly intertwined with the microenvironment during the development of cancer (Barcellos-Hoff and Medina, 2005; Bissell et al., 2002a) and that tissue biology and host physiology are subverted to drive malignant progression (Coussens and Werb, 2001). Recent studies, examples of which are discussed in this section, have identified specific signals and cells that contribute to carcinogenesis. These experimental models provide strong mechanistic support for dominant control by the microenvironment even in highly efficient carcinogenesis driven by strong oncogenic programs.

Coussens and colleagues employed a transgenic mouse model that expressed the human papillomavirus type 16 (HPV16) early region genes under the control of the keratin 14 promoter in order to examine the link between chronic inflammation and skin cancer (de Visser et al., 2006). They hypothesized that interactions between adaptive immune cells and initiated, "at risk," cells were determinants of skin cancer progression which was tested by crossing the transgenic model with a RAG-1-/- mouse that lacks mature B and T lymphocytes. Unlike the K14-HPV16 mice that exhibit leukocyte recruitment and chronic inflammation in premalignant skin, HPV16/RAG-1-/- mice did not possess these features or the subsequent parameters necessary for full malignant progression (i.e. release of proangiogenic factors, activated vasculature, and hyperproliferation of oncogene-positive keratinocytes). Transfer of either B lymphocytes or serum from K14-HPV16 mice effectively restored the chronic inflammation and malignant progression in HPV16/RAG-1-/- mice. Interestingly, B lymphocytes did not infiltrate the skin tumors in this study, but were found to exert their effects by depositing immunoglobulins in a paracrine fashion.

A study by Pollard and colleagues used a mammary restricted polyoma middle T oncoprotein, of which tumors undergo pre-malignant stages prior to advanced carcinomas (Lin et al., 2001). The investigators examined the kinetics and contribution of tumor associated macrophages in the development of the vasculature that is essential for progression, otherwise known as the "angiogenic switch." Enhanced macrophage infiltration was found to always precede the increase in vessel density that characterized the transition between pre-malignant and early carcinoma stages. Genetic depletion of macrophages by homozygous deletion of the macrophage growth factor, CSF-1, resulted in a delay in both angiogenic switch and malignant progression, suggesting that macrophages regulated angiogenesis. In addition, transgenic over expression of CSF-1 under the mammary specific mouse mammary tumor virus promoter in this model resulted in very early recruitment of macrophages and the development of a late-stage

vessel density during the early pre-malignant stage of hyperplasia. Thus, premature macrophage recruitment was sufficient to stimulate a degree of angiogenesis that could support a late-stage carcinoma, indicating that angiogenic activity is not simply in response to enhanced tumor size (and hypoxia) but was controlled by the host, independent of tumor stage.

Evan and colleagues engineered a OH-Tamoxifen-inducible form of the transcription factor c-Myc, restricted to islets of the mouse pancreas by the proximal insulin promoter, as a model to study the in vivo mechanisms of its oncogenic potential (Shchors et al., 2006). They found that sustained c-Myc activation drives proliferation of β-cells of the islets and also indirectly increases proliferation of endothelial cells. The cytokine IL-1β, which was transcriptionally induced after activation of c-Myc, was determined to be necessary and sufficient for the angiogenic effects of c-Myc activation. Systemic administration of neutralizing antibodies against IL-1β had no effect on Myc-induced β-cell proliferation, but severely impaired the activation and redistribution of the angiogenic factor VEGF-A, which remains dormant in the islet extracellular matrix until activated. Thus, though c-Myc exerts a potent proliferative push in β islet cells, an important aspect of its action in tumor promotion is the production of IL-1β, which serves as a paracrine trigger to modify the microenvironment around the islet.

Human epithelial cells are also subject to the influence of the microenvironment. A human mammary model developed by Weinberg underscores both the requirement for the appropriate microenvironment in the ability of epithelial cells to perform in a tissue-appropriate manner and a critical role of abnormal stroma in cancer promotion (Kuperwasser et al., 2004). The model employs the mouse mammary gland as the host for human fibroblasts, which, when irradiated in vitro, take up permanent residence in the cleared fat pad. This humanized stroma supports the growth and morphogenesis of subsequently transplanted human mammary epithelial organoids. Proper ductal morphogenesis depends on the admixture of primary normal breast fibroblasts to these organoids prior to engraftment into humanized fat pads. Although specimens from most individuals gave rise to apparently normal ductal outgrowths, one specimen gave rise to hyperplastic growth, suggesting the presence of neoplastically initiated, but dormant, cells. When that preparation was transplanted in a murine stroma humanized with stromal cells engineered to over express either HGF or TGFß1, the organoids developed into growths that closely resembled human comedo-type and basal-type invasive carcinomas, respectively. The authors conclude that these observations indicate that an altered stromal environment can promote human breast cancer formation by abnormal epithelial cells present, but dormant, in the normal human breast.

These examples provide specific mechanisms at play in carcinogenesis driven by experimentally induced oncogenes. Radiation carcinogenesis is much more challenging to similarly dissect given the random nature of initiation, the genetic variation between individuals, and the susceptibility of a particular tissue. We propose that cancer initiation (defined as mutations resulting from misrepaired DNA damage caused by IR) is only half the story, and that radiation-induced host biology is a critical action of radiation as a carcinogen and in the development of clinical cancer. Unlike the random interaction of energy with DNA, resulting in damage and mutation, tissue response to radiation is orchestrated, predictable and may ultimately be amenable to intervention.

**Radiation Carcinogenesis**

Although the prevailing risk paradigm focuses on radiation-induced DNA damage leading to mutations in susceptible cells, numerous studies over the last 50 years have provided evidence that radiation carcinogenesis is more complex. Terzaghi-Howe demonstrated that the expression of dysplasia *in vivo* and neoplastic transformation in culture of irradiated tracheal epithelial cells is inversely correlated with the number of cells seeded (Terzaghi-Howe, 1986; Terzaghi-Howe, 1989; Terzaghi and Little, 1976; Terzaghi and Nettesheim, 1979) and identified TGF as a key mediator (Terzaghi-Howe, 1990). Greenberger proposed in 1996 that irradiated stromal cells function as biologic tumor promoters in leukemia through their release of reactive oxygen species, and production of altered adhesion molecules or growth factors that block apoptosis and induce DNA strand breaks in closely associated self-renewing stem cells (Greenberger et al., 1996b). Long term bone marrow cultures were used in which irradiated bone marrow stroma actively contributes to leukemogenesis via growth factors, reactive oxygen and altered adhesion molecules that regulate the expansion of hematopoietic stem cells. The bone marrow stromal cell alterations of CBA/B mice irradiated with 200 cGy persisted 6 months after explant of the cells to culture (Greenberger et al., 1996a). Irradiated bone marrow stromal cell line D2XRII express persistently altered fibronectin splicing, increased expression of several transcriptional splice variants of macrophage-colony-stimulating factor, and increased TGFβ (Greenberger et al., 1996c).

Extensive studies were published by Kaplan and colleagues in a series of four papers in the '50s. C57BL mice are very susceptible to thymic lymphomas after radiation exposure. Young mice underwent thymectomy, and 2-7 days later received the first of four consecutive doses of 168 cGy, spaced apart by 8-day intervals. Several hours after the last irradiation, a single thymus from a non-irradiated mouse was transplanted subcutaneously under the right chest or upper abdomen of each of the previously thymectomized, irradiated hosts. Tumors were then tracked by palpation for 15 months thereafter. Amazingly, the incidence and latency of the thymic lymphomas arising from the grafts matched that observed in irradiated, intact mice (39% and 214 days, respectively). Furthermore, the tumors were histologically identical to those found in the intact mice, and exhibited a similar pattern of metastasis (Kaplan et al., 1956b). This study showed that radiation induced thymic lymphomas can occur even when the grafted thymus was never exposed to radiation, suggesting a systemic effect of tumor induction inherent to the host.

This systemic mechanism of tumor induction was elucidated in their second study, which showed that shielding a thigh of the host during irradiation or promptly injecting fresh bone marrow into the host shortly after the last irradiation could neutralize the tumor inducing effect of IR. Using the same experimental approach as in the first study, but varying the time of implantation after the last irradiation, the authors showed that the tumor promoting effect of IR through the host persisted for up to 8 days, yielding tumor incidences that were not significantly different from implantations performed 1-3 hrs post-irradiation (Kaplan et al., 1956a).

In the third study, Kaplan and colleagues examined the physiological status of the un-irradiated thymic graft after it was transplanted into a previously thymectomized and irradiated

host. Massive necrosis was observed at 24 hrs after implantation, with only a few surviving cells under the capsular membrane. These regions of survival, however, would eventually be repopulated within the course of the next 14 days into a graft with a regenerated cortex. At this time point grafts increased in total size and even reformed lobes, though not always two nor complete lobes. Comparing graft regeneration in thymectomized, irradiated or un-irradiated hosts revealed that prior radiation exposure impaired regeneration. Consistent with the finding that bone marrow injection neutralized tumor induction through the irradiated host, thigh-shielded mice exhibited an identical degree of graft regeneration as observed in un-irradiated mice, while unshielded mice had significantly impaired regeneration (Carnes et al., 1956). The authors thus concluded that a systemic bone marrow factor in the host was necessary for proper regeneration of un-irradiated thymic grafts, and that radiation compromised this factor in the host as a mechanism of tumor induction.

In a fourth study, Kaplan and colleagues provided conclusive evidence that the tumors that arose in the un-irradiated thymic grafts were indeed composed of donor cells and not invading host cells that had received radiation. The susceptible C57BL strain of mice was crossed with the C3H strain, which is resistant to radiation-induced lymphomas, to generate an F1 hybrid. Using the same experimental approach of transplantation into previously irradiated hosts, the authors revealed that though host irradiation could induce lymphomas, the genetic background of the graft donor heavily determined tumor incidence. Hosts bearing grafts from the susceptible C57BL or F1 hybrid strains had more tumors than those bearing grafts from C3H donors, thus indicating that susceptibility to radiation induced lymphomas was a property that was inherent to the thymus, even though the mechanism of induction can occur through the host. Lastly, to prove that tumors induced through host exposure, but arising in the graft were truly cells from the un-irradiated implant, tumor fragments were excised from grafts that were either C57BL or F1 hybrid, and then implanted, subcutaneously or intraperitoneally, back into hosts from each of the three genetic backgrounds. The tumor fragments from C57BL grafts only grew in the C57BL and F1 host, not in the C3H host; and that fragments from hybrid grafts grew only in hybrid hosts. Thus, the fact that there was rejection of tumor fragments when they were placed into hosts of a different background shows that the tumor cells were derived from the graft and not the host (Kaplan et al., 1956c). This series of papers highlight the host as an effective target of radiation in the induction of thymic lymphomas in grafts that were never irradiated. Similarly, a study of skin carcinogenesis done by Billingham and colleagues used the carcinogen methylcholanthrene to determine which compartment was the sight of carcinogenic action in mouse skin. Skin grafts of various thicknesses (including or excluding hair follicles) from carcinogen treated sites were transplanted to untreated sites in the same animal. Such an approach revealed that the underlying dermis layer conferred equivalent tumorigenic potential, even if the overlying epidermis was untreated. Tumors occurred when untreated grafts were transplanted into treated dermis, but not when treated grafts were placed into untreated dermis (Billingham et al., 1951).

Ethier and Ullrich showed that dissociated cells from mouse mammary gland irradiated with 1 Gy, 24 hr after exposure transplanted to unirradiated mice increased the frequency and persistence of dysplasia over that of intact tissues (Ethier and Cundiff, 1987; Ethier et al., 1987). Clifton and colleagues showed that dissociated cells from irradiated rat mammary gland

exhibited a very high frequency of initiation (i.e. 1/100) when transplanted into unirradiated tissue. We had shown that IR induces rapid remodeling of the mammary microenvironment (Barcellos-Hoff, 1993; Barcellos-Hoff, 1998a; Barcellos-Hoff, 1998b), which led us to hypothesize that the irradiated stroma modified tumorigenic potential. To test this hypothesis, we created a radiation chimera by transplanting unirradiated, preneoplastic mammary cells to the mammary glands of irradiated hosts (Barcellos-Hoff and Ravani, 2000). The undeveloped mammary epithelium is surgically removed at puberty, the animal irradiated, and some time later non-irradiated mammary epithelial cells are transplanted into the irradiated host. These studies used COMMA-1D mammary epithelial cells, which are non-tumorigenic if injected into the cleared fat pads of 3-week old mice, or subcutaneously in immature, adult mice or into nude mice, undergo mammary morphogenesis when transplanted into 3 week old mammary gland. Although clonal in origin, COMMA-1D cells harbor two mutant Trp53 alleles that may confer neoplastic potential (Jerry et al., 1994). When transplanted into mice irradiated 1-14 days earlier with 4 Gy, outgrowths rapidly developed tumors, ranging from a peak of 100% at day 3 and twice that of sham-irradiated mice at 14 days post-irradiation. Furthermore, tumors from irradiated animals were nearly 5 times larger than the few tumors that arose in sham-irradiated hosts, indicating that tumor biology, as well as frequency, was affected. These data support the idea that high dose radiation promotes carcinogenesis by inducing a hospitable tissue environment.

If host microenvironment created by radiation can promote neoplastic progression in un-irradiated epithelial cells, then events "outside of the box" do significantly increase cancer risk. We believe that this adverse "bystander effect" of irradiated cells on un-irradiated cells is due to extracellular signaling from the microenvironment that supports progression. The effect of the irradiated microenvironment on neoplastic progression persisted for several weeks and appears to be independent of systemic radiation effects (as tested by hemi-body irradiation), which support the hypothesis that non-mutagenic effects of radiation can contribute significantly to radiation carcinogenesis in vivo. If key signals that promote carcinogenesis in irradiated tissues are identified, then irradiated microenvironment can be a therapeutic target to mitigate the long term consequences of inadvertent radiation exposures.

**Contribution of TGFβ to carcinogenesis**

Radiation-induced DNA damage elicits checkpoints for genome integrity that coordinate with the cell cycle machinery to ensure accurate transmission of genetic information and are complemented by preemptive apoptotic triggers that eliminate damaged cells that could compromise tissue integrity. Such cellular responses to damage must be integrated within the context of multicellular tissues to maintain homeostasis. Radiation also rapidly induces extracellular signaling via growth factors and cytokines that regulate stromal remodeling, vascular integrity and inflammatory responses (reviewed in (Barcellos-Hoff, 1998a; Dent et al., 2003; Hallahan et al., 1993; McBride, 1995)). In particular, IR induces the activation of TGFβ a growth factor that is produced and widely distributed extracellularly as a latent complex (Barcellos-Hoff et al., 1994; Ehrhart et al., 1997). TGFβ mediates epithelial fate decisions by regulating proliferation and apoptosis (reviewed in (Derynck et al., 2001)).

TGFβ has been widely implicated in radiation responses. Terzaghi-Howe showed that TGFβ produced by the differentiated normal epithelial cells inhibited the growth and phenotype of radiation transformed cells (Terzaghi-Howe, 1986). Bauer described three distinct, but competing, roles for TGFβ (reviewed in (Häufel et al., 1999)) during transformation: TGFβ actually helps maintain the transformed state of mesenchymal cells, but it also enables non-transformed neighbors to recognize transformed cells and trigger an apoptosis-inducing signal. Bauer and collegues recently showed that the latter two processes are enhanced following very low radiation doses (Portess et al., 2007).

Similarly, we postulated a positive role of the extracellular signaling from TGFβ, whose activity is induced by radiation *in vivo* and *in vitro* (Barcellos-Hoff and Brooks, 2001). We demonstrated that radiation-induced apoptosis is significantly decreased in *Tgfb1* heterozygote embryonic liver and skin and adult mammary gland while *Tgfb1* null embryos fail to undergo either apoptosis or inhibition of cell cycle in response to IR (Ewan et al., 2002). Either chronic TGFβ depletion by gene knockout and transient depletion by TGFβ neutralizing antibody reduced phosphorylation of p53 serine 18 in irradiated mammary gland (Ewan et al., 2002). Together, these data implicate TGFβ in the genotoxic stress program of epithelial tissues.

This led us to the surprising demonstration that TGFβ plays an essential role in the intrinsic cellular response to DNA damage mediated by ataxia telangiectasia mutated (ATM) checkpoint kinase (Abraham, 2003; Bakkenist and Kastan, 2003). We found that these the intracellular and extracellular damage response programs are functionally linked in epithelial cells. TGFβ has a direct regulatory function in the ATM damage response since irradiated primary epithelial cultures from *Tgfb1* null murine epithelial cells or human mammary epithelial cells in which TGFβ signaling was blocked exhibited hypophosphorylation of ATM and reduced kinase activation (Kirshner et al., 2006). TGFβ treatment prior to radiation restored damage-responses, supporting a specific requirement for TGFβ signaling in the genotoxic stress programs via modulation of ATM kinase activation.

If TGFβ has a fundamental role in regulating the response to DNA damage activity, and is commonly lost during neoplastic progression, then what are the commonalities among its tumor suppressor functions? Inability of the cell to properly repair DNA damage caused by radiation or other DNA damaging agents can lead to genomic instability (reviwed in (Kastan and Bartek, 2004; Khanna and Jackson, 2001). Epithelial cells deficient for TGFβ show genetic instability (Glick et al., 1996), increased tumor progression (Glick et al., 1993) and haploid insufficiency for carcinogenesis (Tang et al., 1998). Thus we tested whether TGFβ was involved in radiation-induced genomic instability that occurs in clonally expanded, finite life span, normal human mammary epithelial cells (HMEC) as measured by aberrant karyotypes and supernumerary centrosomes (Sudo et al., 2008). TGFβ addition reduced while inhibition increased genomic instability in irradiated and control HMEC. Rather than preventing genomic instability, TGFβ selectively deleted genomically unstable cells via apoptosis, resulting in an overall increase in population stability. Thus, endogenous TGFβ suppresses radiation-induced and spontaneous genomic instability, while attenuation of TGFβ signaling permits survival of genomically unstable cells. This interaction between intrinsic radiation effects and the

microenvironment determine the prevalence of unstable human cells (Maxwell et al. unpublished) and transformed rodent cells (Portess et al., 2007; Terzaghi-Howe, 1989).

However, if treated chronically with TGFβ, there is more to the story. We found that the progeny of irradiated HMEC undergo disrupted alveolar morphogenesis when embedded in reconstituted basement membrane (Park et al., 2003). Single irradiated HMEC gave rise to colonies exhibiting decreased localization of E-cadherin, β-catenin, and connexin-43, which are proteins necessary for the establishment of cell polarity and communication. Severely compromised acinar organization was manifested by most irradiated HMEC progeny, arguing against a mutational mechanism. We compared the effect of IR on ability of MCF-10A and HMT3522 S1, which are cell lines, to that of 184 extended life span HMEC, which are completely stable by both karyotype and comparative genomic hybridization. Surprisingly, all three non-tumorigenic HMEC are susceptible and undergo disrupted acinar morphogenesis and loss of E-cadherin. These data point to a heritable, non-mutational mechanism whereby IR compromises cell polarity and multicellular organization. Notably, we found a dose response similar to that observed in non-targeted phenomena, i.e. a steep response at low dose (<10 cGy) followed by a plateau. Is this a novel radiation response exhibited only in culture? Interestingly, urinary bladder carcinogenesis in humans exposed to long-term low-dose radiation exhibit significant increases of TGFβ1 and altered localization of E-cadherin/β-catenin complexes (Romanenko et al., 2006). Also, a recent study by Arteaga and colleagues showed that IR induced TGFβ promotes metastatic breast cancer (Biswas et al., 2007).

Indeed, TGFβ promotion of carcinogenesis is often ascribed to its ability to drive phenotypic switching (Han et al., 2005; Zavadil and Bottinger, 2005). Further studies show that the underlying mechanism of disrupted morphogenesis by irradiated cells is that radiation disposes HMEC to undergo TGFβ mediated epithelial to mesenchymal transition (EMT; (Andarawewa et al., 2007a). As found with morphogenesis, and consistent with a non-targeted effect, irradiation with either 2 or 200 cGy appear to be equally effective in priming HMEC to undergo TGFβ mediated EMT (Andarawewa et al. in preparation). Although radiation-induced TGFβ was demonstrable by media transfer, endogenous radiation-induced TGFβ was insufficient to drive EMT. Rather, EMT was the product of the intersection of the intrinsic response to IR, in this case activation of the MAP-K pathway, and chronic TGFβ signaling from the microenvironment. Thus, while endogenous TGF primarily eliminates genomically unstable cells via apoptosis, exogenous chronic exposure promotes phenotypic instability.

Overexpression of constitutively active TGFβ can induce EMT during tumor progression *in vivo* (Portella et al., 1998) and the overexpression of TGFβ has been associated with poor prognosis of many human cancers (Bierie and Moses, 2006). In support of a dominant pro-carcinogenic action, polymorphisms, 509T and 869T, that increase TGFβ production are associated between risk of advanced cancer. Compared with other genotypes, high *TGFβ1* producer genotypes were associated with an increased risk of colorectal adenoma (Berndt et al., 2007), nasopharyngeal cancer (Wei et al., 2007), malignant melanoma (Nikolova et al., 2007) and lung cancer (Kang et al., 2006). While the role of *TGFβ1* polymorphisms in breast cancer is complex (Cox et al., 2007b), a recent large consortium confirmed a 869T dose dependent increase in breast cancer risk (Cox et al., 2007a). Contrary to its characterization as a tumor suppresser,

*TGFβ1* polymorphisms associated with high levels/activity of TGFβ seem to be associated with increased solid cancer risk.

TGFβ is classically described as a tumor suppressor since it is a profound inhibitor of epithelial cell proliferation. Consistent with this, *Tgfb1* heterozygote mice, which express only 10-30% of wild type protein levels, in combination with oncogene expression or chemical carcinogen exposure, exhibit increased tumor incidence and size (Tang et al., 1998) as well as decreased tumor latency (Forrester et al., 2005; Glick et al., 1994). TGFβ is implicated in tumor processes that affect angiogenesis (Ueki et al., 1992), reactive stroma (Iozzo and Cohen, 1994; Mahara et al., 1994), and immunosuppression (Hojo et al., 1999; Li et al., 1993). Based on the paradigm in which TGFβ acts as a tumor suppressor, one would expect TGFβ compromised mice, like those in which the TGFβ receptor was floxed (Bhowmick et al., 2004), to be extremely cancer prone. However many labs including ours have observed that spontaneous cancer is not increased in *Tgfb1* heterozygote mice, even when aged for 2 years (unpublished data). *Tgfb1* null mice crossed onto a immune deficient background (which prevents neonatal death from gross inflammatory disease shortly after birth (Shull et al., 1992)), but have little evidence of spontaneous cancer when housed under germ-free conditions. These mice do develop gastrointestinal cancer under standard mouse husbandry (Engle et al., 2002), indicating that TGFβ mediates the interactions between inflammation and epithelial cancer. The lack of spontaneous cancer in mice that have reduced TGFβ appears to contradict the thesis that TGFβ acts primarily as a tumor suppressor in the intact organism. Our unpublished data (Nguyen and Barcellos-Hoff) using the radiation chimera model of *Tgfb1* heterozygote BALB/c mice transplanted with p53 null mammary epithelium suggests that host TGFβ promotes mammary cancer and is a major mediator of radiogenic cancer. Given *TGFβ1* polymorphisms in humans, and the complex roles TGFβ plays in tissues, it is difficult to predict whether TGFβ inhibition, but it is clearly a hub that warrants significant investigation.

**Systems Radiation Biology**

Many have argued, even at the height of focus on identifying critical mutations, that disruption of the cell interactions and tissue architecture are primary drivers of carcinogenesis (Barcellos-Hoff, 1998b; Bissell and Radisky, 2001; Rubin, 1985; Sonnenschein and Soto, 2000; Wiseman and Werb, 2002). Recent experiments demonstrating the key role of normal cells in cancer (Bhowmick et al., 2001; de Visser et al., 2006; Kuperwasser et al., 2004; Maffini et al., 2004) offer provocative evidence that microenvironment composition determines whether cancer ensues following mutational activation of oncogenes or loss of tumor suppressors. Since an oncogenic genome can be effectively suppressed by normal tissues, and radiation-induced microenvironments promote oncogenesis, then understanding non-targeted mechanisms can readily lead to testable hypotheses, and possible interventions, for health risks in future populations. Strategies that block the effects of IR mediated by the microenvironment are likely to significantly reduce long term cancer risk.

Non-targeted radiation phenomena are also an impetus to reevaluate whether extrapolation of risk from high to low doses, or from acute to chronic exposures, is reasonable. Our experimental data and that of others suggest that the action of radiation as a carcinogen is a two-compartment problem: IR alters the genome of the target, e.g. epithelium, in the context

of radiation-induced phenotypes of other cells of the tissue. Therefore cancer following radiation is the end result of both mutations and altered signaling via the microenvironment. At least three aspects of cancer are underappreciated when DNA damage and mutation is used as the scientific rationale for linear-no-threshold extrapolation of radiation risks from high to low doses. First, recognition that IR alters cell phenotype as well as genotype (reviewed in (Barcellos-Hoff et al., 2005). Second, that initiated cells progress in the context of accessory/host cells that ultimately determine whether cancer progresses (Coussens and Werb, 2002). Third, that specific signals, like TGFβ, play a global role in orchestrating tissue functions (Akhurst, 2002). Even if the nature and dose dependence of these processes are not as yet completely understood, there is more than sufficient evidence that they, in conjunction with DNA damage, determine the cancer risk at high doses.

Multicellular responses and extracellular signaling following radiation exposure are integral, rather than secondary in evaluating radiation risks. Some dose responses show increased response with increased dose (e.g. TGFβ activation *in situ* (Ehrhart et al., 1997)) while others like phenotypic responses appear to act like switches at low dose (<10 cGy) (e.g. EMT (Park et al., 2003) and unpublished data). If cancer is a function of both genomic alterations and microenvironment disruption, then it is critical to ascertain whether microenvironment changes are linearly related to direct energy deposition.

Clearly defining the complex processes that lead to cancer is important in order to accurately predict radiation health effects. Although a biological model in which radiation risk is the sum of dynamic and interacting processes may not readily replace a pragmatic risk model, it could provide the impetus to reassess our assumptions about radiation health effects in populations, and possibly spur new approaches to intervention or countermeasures. Systems radiation biology is an approach to integrate information across time and scale that are determined by experimentation. A key property of a system is that some phenomena emerge as a property of the system rather than the parts. Systems biology attempts to quantitatively evaluate interactions and relationships to predict complex events. A model that analyzes the irradiated tissue/organ/organism as a system rather than a collection of non-interacting or minimally interacting cells, leads to the idea of cancer as an emergent phenomenon of a perturbed system (Barcellos-Hoff, 2007). Given the current research goal to determine the consequences of high versus low radiation exposures, then broadening the scope of radiation studies to include systems biology concepts should benefit risk modeling of radiation carcinogenesis.

**References**


Abraham RT. Checkpoint signaling: epigenetic events sound the DNA strand-breaks alarm to the ATM protein kinase. Bioessays 25: 627-30; 2003.

Akhurst RJ. TGF-{beta} antagonists: Why suppress a tumor suppressor? J. Clin. Invest. 109: 1533-1536; 2002.

Andarawewa KL, Erickson AC, Chou WS, Costes SV, Gascard P, Mott JD, Bissell MJ, Barcellos-Hoff MH. Ionizing Radiation Predisposes Nonmalignant Human Mammary Epithelial Cells to Undergo Transforming Growth Factor {beta} Induced Epithelial to Mesenchymal Transition. Cancer Res 67: 8662-8670; 2007.

Bakkenist CJ, Kastan MB. DNA damage activates ATM through intermolecular autophosphorylation and dimer dissociation. Nature 421; 2003.

Barcellos-Hoff MH. Radiation-induced transforming growth factor b and subsequent extracellular matrix reorganization in murine mammary gland. Cancer Res 53: 3880-3886; 1993.

Barcellos-Hoff MH. How do tissues respond to damage at the cellular level? The role of cytokines in irradiated tissues. Radiat Res 150: S109-S120; 1998.

Barcellos-Hoff MH. The potential influence of radiation-induced microenvironments in neoplastic progression. J Mammary Gland Biol Neoplasia 3: 165-175; 1998.

Barcellos-Hoff MH. Integrative radiation carcinogenesis: interactions between cell and tissue responses to DNA damage. Semin Cancer Biol 15: 138-48; 2005.

Barcellos-Hoff MH. Cancer as an Emergent Phenomenon in Systems Radiation Biology. Radiat Env Biophys 47: 33-8; 2007.

Barcellos-Hoff MH, Brooks AL. Extracellular signaling via the microenvironment: A hypothesis relating carcinogenesis, bystander effects and genomic instability. Radiat Res 156: 618-627; 2001.

Barcellos-Hoff MH, Derynck R, Tsang ML-S, Weatherbee JA. Transforming growth factor-b activation in irradiated murine mammary gland. J Clin Invest 93: 892-899; 1994.

Barcellos-Hoff MH, Medina D. New highlights on stroma-epithelial interactions in breast cancer. Breast Cancer Res 7: 33-36; 2005.

Barcellos-Hoff MH, Park C, Wright EG. Radiation and the microenvironment - tumorigenesis and therapy. Nat Rev Cancer 5: 867-75; 2005.

Barcellos-Hoff MH, Ravani SA. Irradiated mammary gland stroma promotes the expression of tumorigenic potential by unirradiated epithelial cells. Cancer Res 60: 1254-1260; 2000.

Baverstock K. Radiation-induced genomic instability: a paradigm-breaking phenomenon and its relevance to environmentally induced cancer. Mutat Res 454: 89-109; 2000.

Berndt SI, Huang W-Y, Chatterjee N, Yeager M, Welch R, Chanock SJ, Weissfeld JL, Schoen RE, Hayes RB. Transforming growth factor beta 1 (TGFB1) gene polymorphisms and risk of advanced colorectal adenoma
10.1093/carcin/bgm155. Carcinogenesis 28: 1965-1970; 2007.

Bhowmick NA, Chytil A, Plieth D, Gorska AE, Dumont N, Shappell S, Washington MK, Neilson EG, Moses HL. TGF-{beta} Signaling in Fibroblasts Modulates the Oncogenic Potential of Adjacent Epithelia. Science 303: 848-851; 2004.

Bhowmick NA, Ghiassi M, Bakin A, Aakre M, Lundquist CA, Engel ME, Arteaga CL, Moses HL. Transforming growth factor-b1 mediates epithelial to mesenchymal transdifferentiation through a Rho-A-dependent mechanism. Mol Biol Cell 12: 27-36; 2001.
Bierie B, Moses HL. Tumour microenvironment: TGFbeta: the molecular Jekyll and Hyde of cancer. Nat Rev Cancer 6: 506-20; 2006.
Billingham RE, Orr JW, Woodhouse DL. Transplantation of skin components during chemical carcinogenesis with 20-methylcholanthrene. Br J Cancer 5: 417-32; 1951.
Bissell MJ, Radisky D. Putting tumours in context. Nat Review: Cancer 1: 1-11; 2001.
Bissell MJ, Radisky D, Rizki A, Weaver VM, Petersen OW. The organizing principle: microenvironmental influences in the normal and malignant bresat. Differentiation 70: 537-546; 2002.
Biswas S, Guix M, Rinehart C, Dugger TC, Chytil A, Moses HL, Freeman ML, Arteaga CL. Inhibition of TGF-{beta} with neutralizing antibodies prevents radiation-induced acceleration of metastatic cancer progression
10.1172/JCI30740. J. Clin. Invest. 117: 1305-1313; 2007.
Brooks AL. Paradigm Shifts in Radiation Biology: Their Impact on Intervention for Radiation-Induced Disease. Radiation Research: 454-461; 2005.
Carnes WH, Kaplan HS, Brown MB, Hirsch BB. Indirect Induction of Lymphomas in Irradiated Mice: III. Role of the Thymic Graft. Cancer Res 16: 429-433; 1956.
Clutton SM, Townsend KM, D.T. G, J.D A, Wright EG. Differentiation and delayed cell death in embryonal stem cells exposed to low doses of ionising radiation. Cell Death Differ 3: 141-8; 1996.
Coussens LM, Werb Z. Inflammatory cells and cancer: Think different! J Exp Med 193: 23F-26; 2001.
Coussens LM, Werb Z. Inflammation and cancer. Nature 420: 860-7; 2002.
Cox A, Dunning AM, Garcia-Closas M, Balasubramanian S, Reed MWR, Pooley KA, Scollen S, Baynes C, Ponder BAJ, Chanock S, Lissowska J, Brinton L, Peplonska B, Southey MC, Hopper JL, McCredie MRE, Giles GG, Fletcher O, Johnson N, dos Santos Silva I, Gibson L, Bojesen SE, Nordestgaard BG, Axelsson CK, Torres D, Hamann U, Justenhoven C, Brauch H, Chang-Claude J, Kropp S, Risch A, Wang-Gohrke S, Schurmann P, Bogdanova N, Dork T, Fagerholm R, Aaltonen K, Blomqvist C, Nevanlinna H, Seal S, Renwick A, Stratton MR, Rahman N, Sangrajrang S, Hughes D, Odefrey F, Brennan P, Spurdle AB, Chenevix-Trench G, Beesley J, Mannermaa A, Hartikainen J, Kataja V, Kosma V-M, Couch FJ, Olson JE, Goode EL, Broeks A, Schmidt MK, Hogervorst FBL, Veer LJVt, Kang D, Yoo K-Y, Noh D-Y, Ahn S-H, Wedren S, Hall P, Low Y-L, Liu J, Milne RL, Ribas G, Gonzalez-Neira A, Benitez J, Sigurdson AJ, Stredrick DL, Alexander BH, Struewing JP, Pharoah PDP, Easton DF. A common coding variant in CASP8 is associated with breast cancer risk. 39: 352-358; 2007.
Cox DG, Penney K, Guo Q, Hankinson SE, Hunter DJ. TGFB1 and TGFBR1 polymorphisms and breast cancer risk in the Nurses' Health Study. BMC Cancer 7: 175; 2007.
de Visser KE, Eichten A, Coussens LM. Paradoxical roles of the immune system during cancer development. 6: 24-37; 2006.

Dent P, Yacoub A, Contessa J, Caron R, Amorino G, Valerie K, Hagan MP, Grant S, Schmidt-Ullrich R. Stress and radiation-induced activation of multiple intracellular signaling pathways. Radiat Res. 159: 283-300; 2003.

Derynck R, Akhurst RJ, Balmain A. TGF-b signaling in tumor suppression and cancer progression. Nature Genet 29: 117-129; 2001.

Dvorak HF. Tumors: wounds that do not heal. Similarities between tumor stroma generation and wound healing. N Engl J Med 315: 1650-9; 1986.

Ehrhart EJ, Carroll A, Segarini P, Tsang ML-S, Barcellos-Hoff MH. Latent transforming growth factor-b activation in situ: Quantitative and functional evidence following low dose irradiation. FASEB J 11: 991-1002; 1997.

Engle SJ, Ormsby I, Pawlowski S, Boivin GP, Croft J, Balish E, Doetschman T. Elimination of Colon Cancer in Germ-free Transforming Growth Factor Beta 1-deficient Mice. Cancer Res 62: 6362-6366; 2002.

Ethier SP, Cundiff KC. Importance of extended growth potential and growth factor independence on in vivo neoplastic potential of primary rat mammary carcinoma cells. Cancer Res. 47: 5316-5322; 1987.

Ethier SP, Kudla A, Cundiff KC. Influence of hormone and growth factor interactions on the proliferative potential of normal rat mammary epithelial cells öin vitroò. J. Cell. Physiol. 132: 161-167; 1987.

Ewan KB, Henshall-Powell RL, Ravani SA, Pajares MJ, Arteaga CL, Warters RL, Akhurst RJ, Barcellos-Hoff MH. Transforming Growth Factor-b1 Mediates Cellular Response to DNA Damage in Situ. Cancer Res 62: 5627-5631; 2002.

Folkman J, Hahnfeldt P, Hlatky L. Cancer: looking outside the genome. Nat Rev Mol Cell Biol 1: 76-9; 2000.

Forrester E, Chytil A, Bierie B, Aakre M, Gorska AE, Sharif-Afshar AR, Muller WJ, Moses HL. Effect of conditional knockout of the type II TGF-beta receptor gene in mammary epithelia on mammary gland development and polyomavirus middle T antigen induced tumor formation and metastasis. Cancer Res 65: 2296-302; 2005.

Glick AB, Kulkarni AB, Tennenbaum T, Hennings H, Flanders KC, O'Reilly M, Sporn MB, Karlsson S, Yuspa SH. Loss of expression of transforming growth factor b in skin and skin tumors is associated with hyperproliferation and a high risk for malignant conversion. Proc Natl Acad Sci USA 90: 6076-6080; 1993.

Glick AB, Lee MM, Darwiche N, Kulkarni AB, Karlsson S, Yuspa SH. Targeted deletion of the TGF-b1 gene causes rapid progression to squamous cell carcinoma. Genes Dev 8: 2429-2440; 1994.

Glick AB, Weinberg WC, Wu IH, Quan W, Yuspa SH. Transforming growth factor beta 1 suppresses genomic instability independent of a G1 arrest, p53, and Rb. Cancer Res 56: 3645-50; 1996.

Greenberger JS, Anderson J, Berry LA, Epperly M, Cronkite EP, Boggs SS. Effects of irradiation of CBA/CA mice on hematopoietic stem cells and stromal cells in long-term bone marrow cultures. Leukemia 10: 514-27.; 1996.

Greenberger JS, Epperly MW, Jahroudi N, Pogue-Geile KL, Berry L, Bray J, Goltry KL. Role of bone marrow stromal cells in irradiation leukemogenesis. Acta Haematologica 96: 1-15; 1996.

Greenberger JS, Epperly MW, Zeevi A, Brunson KW, Goltry KL, Pogue-Geile KL, Bray J, Berry L. Stromal cell involvement in leukemogenesis and carcinogenesis. In Vivo 10: 1-17.; 1996.
Hallahan DE, Haimovitz-Friedman A, Kufe DW, Fuks Z, Wichselbaum RR. The role of cytokines in radiation oncology. Important Advances in Oncology 1993: 71-90; 1993.
Han G, Lu S-L, Li AG, He W, Corless CL, Kulesz-Martin M, Wang X-J. Distinct mechanisms of TGF-{beta}1-mediated epithelial-to-mesenchymal transition and metastasis during skin carcinogenesis
10.1172/JCI24399. J. Clin. Invest. 115: 1714-1723; 2005.
Häufel T, Dormann S, Hanusch J, Schwieger A, Bauer G. Three distinct roles for TGF-beta during intercellular induction of apoptosis: a review. Anticancer Research 19: 105-11; 1999.
Hei TK, Wu LJ, Liu SX, Vannais D, Waldren CA, Randers-Pehrson G. Mutagenic effects of a single and an exact number of alpha particles in mammalian cells. Proc Natl Acad Sci U S A 94: 3765-70.; 1997.
Herskind C, Rodemann HP. Spontaneous and radiation-induced differentiationof fibroblasts. Experimental Gerontology 35: 747-755; 2000.
Hojo M, Morimoto T, Maluccio M, Asano T, Morimoto K, Lagman M, Shimbo T, Suthanthiran M. Cyclosporine induces cancer progression by a cell-autonomous mechanism. Nature 397: 530-534; 1999.
Huang L, Snyder AR, Morgan WF. Radiation-induced genomic instability and its implications for radiation carcinogenesis. Oncogene 22: 5848-54; 2003.
Iozzo RV, Cohen I. Altered proteoglycan gene expression and the tumor stroma. Exs 70: 199-214; 1994.
Jerry DJ, Medina D, Butel JS. p53 mutations in COMMA-D cells. In Vitro Cell. Dev. Biol. 30A: 87-89; 1994.
Kadhim MA, Lorimore SA, Hepburn MD, Goodhead DT, Buckle VJ, Wright EG. Alpha-particle-induced chromosomal instability in human bone marrow cells. Lancet 344: 987-8; 1994.
Kadhim MA, Lorimore SA, Townsend KM, Goodhead DT, Buckle VJ, Wright EG. Radiation-induced genomic instability: delayed cytogenetic aberrations and apoptosis in primary human bone marrow cells. Int J Radiat Biol 67: 287-93; 1995.
Kadhim MA, Macdonald DA, Goodhead DT, Lorimore SA, Marsden SJ, Wright EG. Transmission of chromosomal instability after plutonium alpha-particle irradiation [see comments]. Nature 355: 738-40; 1992.
Kang H-G, Chae MH, Park JM, Kim EJ, Park JH, Kam S, Cha SI, Kim CH, Park R-W, Park SH, Kim YL, Kim I-S, Jung TH, Park JY. Polymorphisms in TGF-[beta]1 gene and the risk of lung cancer. Lung Cancer 52: 1-7; 2006.
Kaplan HS, Brown MB, Hirsch BB, Carnes WH. Indirect Induction of Lymphomas in Irradiated Mice: II. Factor of Irradiation of the Host. Cancer Res 16: 426-428; 1956.
Kaplan HS, Carnes WH, Brown MB, Hirsch BB. Indirect Induction of Lymphomas in Irradiated Mice: I. Tumor Incidence and Morphology in Mice Bearing Nonirradiated Thymic Grafts Cancer Res 16: 422-425; 1956.
Kaplan HS, Hirsch BB, Brown MB. Indirect Induction of Lymphomas in Irradiated Mice: IV. Genetic Evidence of the Origin of the Tumor Cells from the Thymic Grafts. Cancer Res 16: 434-436; 1956.

Kastan MB, Bartek J. Cell-cycle checkpoints and cancer. Nature 432: 316-323; 2004.
Khanna KK, Jackson SP. DNA double-strand breaks: signaling, repair and the cancer connection. Nat Genet 27: 247-54; 2001.
Kirshner J, Jobling MF, Pajares MJ, Ravani SA, Glick A, Lavin M, Koslov S, Shiloh Y, Barcellos-Hoff MH. Inhibition of TGFb1 Signaling Attenuates ATM Activity in Response to Genotoxic Stress. Cancer Res 66: 10861-68; 2006.
Kuperwasser C, Chavarria T, Wu M, Magrane G, Gray JW, Carey L, Richardson A, Weinberg RA. From The Cover: Reconstruction of functionally normal and malignant human breast tissues in mice. PNAS 101: 4966-4971; 2004.
Li XF, Takiuchi H, Zou JP, Katagiri T, Yamamoto N, Nagata T, Ono S, Fujiwara H, Hamaoka T. Transforming growth factor-b (TGF-b)-mediated immunosuppression in the tumor-bearing state: enhanced production of TGF-b and a progressive increase in TGF-b susceptibility of anti-tumor $CD4^{+}$T Cell Function. Japanese Journal of Cancer Research 84: 315-325; 1993.
Limoli CL, Kaplan MI, Corcoran J, Meyers M, Boothman DA, Morgan WF. Chromosomal instability and its relationship to other end points of genomic instability. Cancer Res 57: 5557-63; 1997.
Lin EY, Nguyen AV, Russell RG, Pollard JW. Colony-stimulating factor 1 promotes progression of mammary tumors to malignancy. J Exp Med 193: 727-40.; 2001.
Little JB. Genomic instability and bystander effects: a historical perspective. Oncogene 22: 6978-87; 2003.
Maffini MV, Soto AM, Calabro JM, Ucci AA, Sonnenschein C. The stroma as a crucial target in rat mammary gland carcinogenesis. J Cell Sci 117: 1495-1502; 2004.
Mahara K, Kato J, Terui T, Takimoto R, Horimoto M, Murakami T, Mogi Y, Watanabe N, Kohgo Y, Niitsu Y. Transforming growth factor beta 1 secreted from scirrhous gastric cancer cells is associated with excesss collagen deposition in the tissue. Br. J. Cancer 69: 777-783; 1994.
McBride WH. Cytokine cascades in late normal tissue radiation responses. Int J Radiat Oncol Biol Phys 33: 233-4; 1995.
Mintz B, Illmensee K. Normal genetically mosaic mice produced from malignant teratocarcinoma cells. Proc Natl Acad Sci U S A 72: 3585-9; 1975.
Morgan JE, Gross JG, Pagel CN, Beauchamp JR, Fassati A, Thrasher AJ, Di Santo JP, Fisher IB, Shiwen X, Abraham DJ, Partridge TA. Myogenic cell proliferation and generation of a reversible tumorigenic phenotype are triggered by preirradiation of the recipient site. J. Cell Biol. 157: 693-702; 2002.
Mothersill C, Rea D, Wright EG, Lorimore SA, Murphy D, Seymour CB, O'Malley K. Individual variation in the production of a 'bystander signal' following irradiation of primary cultures of normal human urothelium. Carcinogenesis 22: 1465-1471; 2001.
Nielsen M. Autopsy studies of the occurrence of cancerous, atypical and benign epithelial lesions in the female breast. APMIS Suppl. 10: 1-56; 1989.
Nielsen M, Jensen J, Anderson J. Precancerous and cancerous breast lesions during lifetime and at autopsy: a study of 83 women. Cancer 54: 612-5; 1984.
Nikolova P, N., Pawelec GP, Mihailova SM, Ivanova MI, Myhailova AP, Baltadjieva DN, Marinova DI, Ivanova SS, Naumova EJ. Association of cytokine gene polymorphisms with malignant melanoma in Caucasian population. Cancer Immunol Immunother 56: 371-9; 2007.

Park CC, Henshall-Powell R, Erickson AC, Talhouk R, Parvin B, Bissell MJ, Barcellos-Hoff MH. Ionizing Radiation Induces Heritable Disruption of Epithelial Cell-Microenvironment Interactions. Proc Natl Acad Sci 100: 10728-10733; 2003.

Pierce GB, Shikes R, Fink LM. Cancer: A Problem of Developmental Biology. Englewood Cliffs: Prentice-Hall, Inc.; 1978.

Portella G, Cumming SA, Liddell J, Cui W, Ireland H, Akhurst RJ, Balmain A. Transforming growth factor beta is essential for spindle cell conversion of mouse skin carcinoma in vivo: implications for tumor invasion. Cell Growth Differ 9: 393-404; 1998.

Portess DI, Bauer G, Hill MA, O'Neill P. Low dose irradiation of non-transformed cells stimulates the selective removal of pre-cancerous cells via intercellular induction of apoptosis. Cancer Res. 67: 1246-53; 2007.

Preston DL, Ron E, Tokuoka S, Funamoto S, Nishi N, Soda M, Mabuchi K, Kodama K. Solid cancer incidence in atomic bomb survivors: 1958-1998. Radiat Res 168: 1-64; 2007.

Rave-Frank M, Virsik-Kopp P, Pradier O, Nitsche M, Grunefeld S, H. S. In vitro response of human dermal fibroblasts to X-irradiation: relationship between radiation-induced clonogenic cell death, chromosome aberrations and markers of proliferative senescence or differentiation. Int J Radiat Biol 77: 1163-74; 2001.

Romanenko A, Morell-Quadreny L, Ramos D, Nepomnyaschiy V, Vozianov A, Llombart-Bosch A. Extracellular matrix alterations in conventional renal cell carcinomas by tissue microarray profiling influenced by the persistent, long-term, low-dose ionizing radiation exposure in humans. Virchows Archiv: 1-7; 2006.

Rubin H. Cancer as a dynamic developmental disorder. Cancer Res. 45: 2935-2942; 1985.

Shchors K, Shchors E, Rostker F, Lawlor ER, Brown-Swigart L, Evan GI. The Myc-dependent angiogenic switch in tumors is mediated by interleukin 1beta 10.1101/gad.1455706. Genes Dev 20: 2527-2538; 2006.

Shull MM, Ormsby I, Kier AB, Pawlowski S, Diebold RJ, Yin M, Allen R, Sidman C, Proetzel G, Calvin D, Annnunziata N, Doetschman T. Targeted disruption of the mouse transforming growth factor-b1 gene results in multifocal inflammatory disease. Nature 359: 693-699; 1992.

Sonnenschein C, Soto AM. Somatic mutation theory of carcinogenesis: why it should be dropped and replaced. Molecular Carcinogenesis 29: 205-11; 2000.

Stemmermann G, Nomura A, Chyou P, Yatani R. A prospective comparison of prostate cancer at autopsy and as a clinical event: the Hawaii Japanese experience. Cancer Epidemiol Biomarkers Prev 1: 189-193; 1992.

Sudo H, Garbe J, Stampfer M, Barcellos-Hoff MH, Kronenberg A. Karyotypic instability and centrosome aberrations in the progeny of finite life-span human mammary epithelial cells exposed to sparsely or densely ionizing radiation. Radiat Res 170: 23-32; 2008.

Tang B, Bottinger EP, Jakowlew SB, Bangall KM, Mariano J, Anver MR, Letterio JJ, Wakefield LM. Transforming growth factor-beta1 is a new form of tumor supressor with true haploid insufficiency. Nature Med 4: 802-807; 1998.

Terzaghi M, Little JB. X-radiation-induced transformation in C3H mouse embryo-derived cell line. Cancer Res. 36: 1367-1374; 1976.

Terzaghi M, Nettesheim P. Dynamics of neoplastic development in carcinogen-exposed tracheal mucosa. Cancer Res. 39: 3004-3010; 1979.

Terzaghi-Howe M. Inhibition of carcinogen-altered rat tracheal epithelial cell proliferation by normal epithelial cells in vivo. Carcinogenesis 8: 145-150; 1986.
Terzaghi-Howe M. Changes in response to, and production of, transforming growth factor type b during neoplastic progression in cultured rat tracheal epithelial cells. Carcinogenesis 10: 973-980; 1989.
Terzaghi-Howe M. Interactions between cell populations influence expression of the transformed phenotype in irradiated rat tracheal epithelial cells. Radiat. Res. 121: 242-247; 1990.
Tsai KKC, Chuang EY-Y, Little JB, Yuan Z-M. Cellular Mechanisms for Low-Dose Ionizing Radiation-Induced Perturbation of the Breast Tissue Microenvironment. Cancer Res 65: 6734-6744; 2005.
Tulinius H. Latent malignancies at autopsy: a little used source of information on cancer biology. IARC Sci Publ. 112: 253-61; 1991.
Ueki N, Nakazato M, Ohkawa T, Ikeda T, Amuro Y, Hada T, Higasino K. Excessive production of transforming growth-factor b 1 can play an important role in the development of tumorigenesis by its action for angiogenesis: validity of neutralizing antibodies to block tumor growth. Biochimica et Biophysica Acta 1137: 186-196; 1992.
Wei Y-S, Zhu Y-H, Du B, Yang Z-H, Liang W-B, Lv M-L, Kuang X-H, Tai S-H, Zhao Y, Zhang L. Association of transforming growth factor-[beta]1 gene polymorphisms with genetic susceptibility to nasopharyngeal carcinoma. Clinica Chimica Acta 380: 165-169; 2007.
Wiseman BS, Werb Z. Stromal effects on mammary gland development and breast cancer. Science 296: 1046-9.; 2002.
Wright EG. Inducible genomic instability: new insights into the biological effects of ionizing radiation. Med Confl Surviv 16: 117-30; 2000.
Wright EG, Coates PJ. Untargeted effects of ionizing radiation: Implications for radiation pathology. Mutation Res 597: 119-132; 2006.
Zavadil J, Bottinger EP. TGF-beta and epithelial-to-mesenchymal transitions. Oncogene 24: 5764-74; 2005.

## Chapter 2

## Abstract

### Radiation Acts on the Microenvironment to Affect Breast Carcinogenesis by Distinct Mechanisms that Decrease Breast Cancer Latency and Affect Tumor Type

Tissue microenvironment is an important determinant of carcinogenesis. We demonstrate that ionizing radiation, a known carcinogen, affects cancer frequency and characteristics by acting on the microenvironment. Using a mammary chimera model in which an irradiated host is transplanted with oncogenic *Trp53* null epithelium, we show accelerated development of aggressive tumors whose molecular signatures were distinct from non-irradiated hosts. Molecular and genetic approaches show that TGFβ mediated tumor acceleration; molecular signatures implicated TGFβ and genetically reducing TGFβ abrogated the effect on latency. Surprisingly, tumors from irradiated hosts were predominantly estrogen receptor negative. This effect was TGFβ independent and linked to mammary stem cell activity. Thus the irradiated microenvironment affects latency and clinically relevant features of cancer through distinct and unexpected mechanisms. Compared to sporadic breast cancer, women treated with radiation for childhood cancers are diagnosed with early onset breast cancer that is more likely to be estrogen receptor negative and have a worse prognosis. Our mammary chimera model shows that host irradiation alone can reduce latency, increase aggressive tumor growth and promote estrogen receptor-negative cancers. Thus changes to the stromal microenvironment rather than DNA damage accounts for many of the features that are observed in radiation-preceded breast cancer. We combined molecular and genetic approaches to identify distinct mechanisms via TGFβ activity and stem cell deregulation. Our study further shows that host biology significantly alters cancer molecular signatures and such microenvironmental changes are an important biological conduit for cancer risk in humans.

**Chapter 2 in context**

The introduction discussed the effects of ionizing radiation as a carcinogen and the importance of understanding its actions through the tumor microenvironment. Tumors arise via complex interactions between the initiated cells and the stromal compartments that can either suppress or aid the carcinogenic process. Radiation effects both stromal and epithelial compartments in breast cancer, and in this chapter we use the radiation chimera model to study the effects of host-irradiation on un-irradiated *Trp53* null mammary transplants. We show that host-irradiation is sufficient to promote *Trp53* null breast cancer and has persistent effects that can be detected long after exposure.

## Chapter 2

### Introduction

Currently, very little is known about how early changes in the microenvironment contribute to breast cancer. Ionizing radiation is one of a few demonstrable human breast carcinogens (Land et al., 1980). The prevailing view is that radiation induces cancer through DNA damage (NAS/NRC, 2006). However, this viewpoint is an oversimplification that is inconsistent with many experimental studies showing that ionizing radiation evokes acute and persistent, short and long range, effects (Amundson et al., 1999a; Ehrhart et al., 1997; Kaplan et al., 1956b; Mancuso et al., 2008). We and others have postulated that radiation's carcinogenic potential is perpetuated via so-called non-targeted radiation effects like altered signaling and microenvironment changes (Barcellos-Hoff et al., 2005; Durante and Cucinotta, 2008; Little et al., 2005). We established a radiation chimera model in which the mammary gland is cleared of endogenous epithelium before the mouse is irradiated and subsequently transplanted with unirradiated, non-malignant epithelial cells (Barcellos-Hoff and Ravani, 2000). Mice irradiated with a high dose (400 cGy) that were transplanted up to two weeks later with unirradiated, immortalized mammary epithelial cells develop large, aggressive tumors even though normal outgrowths form in non-irradiated hosts.

The challenge remains to demonstrate that non-targeted radiation effects contribute to carcinogenesis following doses relevant to human populations. In the present studies, we use the radiation chimera to assess the frequency, rate and/or characteristics of carcinogenesis of a donor epithelium primed to undergo neoplastic transformation by genetic loss of p53. Carcinogenesis in *Tp53* null tissue is similar to human breast cancer in that tumors exhibit genomic instability, differential expression of estrogen receptor $\alpha$ (ER) and heterogeneous histology (Jerry et al., 2000; Medina et al., 2002). Over the course of a more than a year, most (~70%) *Trp53* null mammary epithelial transplants in wildtype mouse mammary stroma progress *in situ* from ductal outgrowths to ductal carcinoma *in situ* to invasive breast carcinomas (Medina et al., 2002). To test whether specific signals induced by radiation in the microenvironment contribute to its carcinogenic action, we used the *Trp53* null mammary chimera in which only the host was exposed to low radiation doses (10-100 cGy) to determine the effect on the latency and type of cancer.

### Results

#### Host irradiation affects development of spontaneous Trp53 null breast cancer

The radiation chimera model consists of surgically clearing the mammary epithelium from the inguinal glands of 3-week old BALB/c mice, irradiating with 400 cGy or sham irradiating these mice at 10-12 weeks of age, and transplanting 3 days later with syngeneic mammary fragments (Figure 1A). Based on our prior study using 400 cGy, we first asked whether host irradiation was sufficient to promote cancer of orthotopically transplanted wild type mammary epithelium. Mice were monitored by palpation for 60 weeks yet no palpable tumors arose from wild type epithelium in either sham or irradiated hosts. These data indicated that neither transplantation

itself (Figure 1B) nor host irradiation alone is sufficient to induce neoplastic transformation in wild type epithelium.

In contrast to wild type epithelium, most *Trp53* null transplants developed palpable tumors. The percentage of successful transplants into cleared fat pads was 81±2% S.D. in control hosts (n=55) and 77±10% in irradiated hosts (n=54) in 4 consecutive experiments. Syngeneic *Trp53* null mammary outgrowths in wild type hosts are morphologically normal at weeks 6 and 10 post transplantation (Figure 1C,D). Tumors developed with a similar mean latency in sham (61 weeks ±7.4 S.D.) and irradiated (63±5.5 S.D.) hosts (Figure 1E), which were confirmed to contain the p53 null allele (Figure 1F). The growth rate of tumors that arose in hosts irradiated with 400 cGy was increased in comparison to sham-irradiated hosts (Figure 1F). As described previously, *Trp53* null mammary tumors were diverse in terms of histology, proliferation, lineage markers and ER (Figure 1H). Tumor histological types included poorly differentiated, solid adenocarcinomas with little stroma, spindle-cell morphology, and squamous cell carcinomas.

Unexpectedly, the frequency of *Trp53* null tumors in irradiated hosts was reduced by 21% ($p<0.01$) compared to sham-irradiated hosts. Since women who receive an ovarian dose of >500 cGy have a greatly reduced risk of breast cancer (Inskip et al., 2009) and ovariectomy decreases cancer development by *Trp53* null mammary transplants (Medina et al., 2003), we considered the possibility that radiation exposure compromised ovarian function. To test this idea, *Trp53* 8 week ductal outgrowth were examined. Outgrowths from 400 cGy irradiated mice were noted to have thinner mammary gland ducts and significantly ($p<0.001$) fewer branches (0.31±0.1/unit length) compared to controls (0.56±0.1). This defect in branching morphogenesis persisted one year after transplantation into hosts irradiated with 200 cGy or more but *Trp53 null* mammary outgrowths in hosts irradiated with 100 cGy or less were histologically indistinguishable from those of sham-irradiated mice (Figure 1H-K).

To avoid confounding by ovarian effects, and to better represent relevant human exposures, we focused subsequent radiation-chimera experiments on doses of 10-100 cGy (Figure 2). The rate at which tumors developed in transplants increased in irradiated hosts compared to sham-irradiated hosts (Figure 2A). When all radiation dose groups were pooled and compared to the sham-irradiated control group, host irradiation unequivocally accelerated tumorigenesis (Figure 2B). The first tumors were detected at about 170 days post transplantation in both irradiated and non-irradiated hosts but by 300 days, 100% of transplants in hosts irradiated with either 10 or 100 cGy had developed tumors compared to 54% of transplants in un-irradiated hosts. Median tumor latency was significantly reduced by 72 day for 10 cGy, 82 days for 100 cGy, and 63 days for all doses pooled compared to sham irradiated mice. At 365 days after transplantation, all outgrowths in irradiated hosts (n=45) had developed tumors compared to 69% (n= 20/29) in sham-irradiated mice (Figure 2C, $p<0.05$, Chi-square test). Furthermore, as was observed in hosts irradiated with 400 cGy, tumor growth rate increased with increasing host radiation exposure (Figure 2D). Thus, low doses of ionizing radiation altered the course of carcinogenesis, even when radiation was administered in the absence of the epithelium and exposure preceded detectable cancer by many months.

**Molecular features of breast cancer are altered by host irradiation**

Breast cancer in women is a heterogeneous disease in terms of histology, marker expression and prognosis (Parise et al., 2009), as are breast tumors that develop in *Trp53* knockout mice (Jerry et al., 2000). We next considered the possibility that acceleration in irradiated hosts was because the specific tumor type was affected. We classified *Trp53* null tumors arising in un-irradiated hosts and low dose irradiated hosts by histological type (n=81). Most tumors from un-irradiated mice were adenocarcinomas (43%) or spindle cell carcinomas (33%), the remaining tumors were myoepitheliomas or squamous carcinoma (Table S1). Tumor type was not significantly associated with host irradiation status or latency *per se*.

To further explore how tumors arising in irradiated hosts are distinct from those that occur in non-irradiated hosts, we used Affymetrix gene chips to profile total RNA from individual adenocarcinoma or spindle cell tumors that arose in non-irradiated mice (n=9) and irradiated mice (n=23). Raw data was background normalized and unsupervised hierarchical clustering (UHC) was performed using a 1 S.D. filter cut-off of gene expression change of at least 2-fold that yielded 2,547 probes. UHC did not readily separate tumors on the basis of host irradiation status (Figure 3A). To explicitly compare tumors from irradiated hosts and non-irradiated hosts (reference group), we performed a supervised analysis of genes with a p-value of 0.05 and a minimum 2-fold change, using significance of analysis of microarray (SAM) methodology and permutation analysis under a leave-one-out bootstrap scheme (Tusher et al., 2001). This strategy resulted in 24 genes, which we referred to as the irradiated host core signature (24-IHC), enriched in tumors that developed in irradiated hosts. Using the 24-IHC gene expression list, UHC segregated tumors of non-irradiated hosts from those of irradiated hosts (Figure 3B). Ingenuity pathway analysis (IPA) resulted in two major networks (Figure S1A,B). The first containing 12/21 identified genes described a network characterizing cell morphology and amino acid metabolism; the second containing 10/21 identified genes, associated with cellular movement, cellular growth and proliferation, and cancer. Quantigene validation of expression differences confirmed 22 genes of the 24-IHC; this subset still segregated tumors from irradiated or non-irradiated hosts.

To define the global biology of tumors arising in irradiated hosts, a gene list was generated using a 1.5 fold-change threshold (Table S2), which also segregated tumors from irradiated or non-irradiated hosts (Figure S1C). IPA using these 156 genes invoked cell-cell interaction, cancer, hematological system development, and DNA replication, recombination, and repair (Figure 3C and D). IPA analysis of the 156-IHC also revealed enrichment for genes involved leukocyte chemo-attraction and binding (Figure 3E, p=0.007), monocyte maturation (Figure 3F, p=0.006), and proliferation of tumor cell lines (Figure 3G p=0.0007).

The top-ranked networks contained a node occupied by the cytokine TGFβ1, which although not transcriptionally regulated, is known to play a central role in the response of tissues to radiation. Consistent with this, we found that the 156 gene list significantly overlapped (p=<0.01) gene lists describing mouse mammary tumors driven by cooperation between Wnt and TGFβ (Labbe et al., 2007). Previous work from our group has shown that TGFβ is persistently activated in the irradiated mouse mammary gland (Barcellos-Hoff et al., 1994; Ehrhart et al., 1997). Thus we hypothesized the TGFβ mediates tumor promotion of *Trp53* null transplants in irradiated wild type mice.

**TGFβ mediates persistent tissue radiation responses**

To determine the extent to which radiation changes in gene expression can be attributed to TGFβ, we next conducted comprehensive analysis of the contribution of TGFβ signaling in irradiated mammary gland by expression profiling *Tgfb1* heterozygote and wild type mammary glands at 1 and 4 weeks after whole body exposure to 10 cGy, the lowest dose used in the tumor experiment. Microarray analysis showed that radiation regulated 178 identified genes (p=0.05 and 1.25-fold differences) similarly in *Tgfb1* wild type and heterozygote mammary gland (Figure 4A; Table S3), which constitutes those genes that are independent of TGFβ dose. The top down-regulated genes in both irradiated genotypes suggested that epithelial cell differentiation was affected. Down regulation of amphiregulin (*Areg*), inhibin beta b (*Inhibb*), *Wnt5a* and suppressor of cytokine signaling 3 (*Socs3*) also suggest decreased differentiation. Up-regulated genes included *Adamts18*, which is a disintegrin-like and metallopeptidase with thrombospondin type 1 motif indicative of extracellular matrix remodeling, heat shock protein 8 (*Hspa8*) reflecting persistent stress, and chemokine (C-X-C motif) receptor 4 (*Cxcr4*) associated with expanding vascular networks. Consistent with these, IPA networks invoked antigen presentation, cell-to-cell signaling and interaction, hematological system development and function.

In contrast, more than twice as many genes (n=488) were regulated by radiation in a TGFβ-dose dependent manner (Figure 4B). TGFβ transcriptional targets, including *Tgfbi*, *Col1a1*, and *Gadd45b* were increased in the wild type but not *Tgfb1* heterozygote gland, consistent with prior studies showing that radiation induces TGFβ activation (Barcellos-Hoff, 1993). IPA of genes regulated only in wild type mice (Table S4) and TGFβ-dependent, radiation regulated genes (Table S5) identified cell-to-cell signaling, cell signaling and development, and cancer as the top wild type networks. These analyses support the premise that a low radiation dose elicits persistent changes in gene expression (Amundson et al., 1999b), one third of which are independent and two thirds of which are dependent upon TGFβ dose. In contrast, antigen presentation, cellular assembly and organization, and cell cycle were identified in the expression profiles of irradiated *Tgfb1* +/- mammary glands compared to un-irradiated tissue, which implicates TGFβ signaling as a critical determinant of the pattern of radiation response. We noted that 29 genes regulated by radiation in mammary gland overlapped the IHC-156 list from tumors arising in irradiated hosts.

**TGFβ mediates tumor latency in irradiated hosts**

Although the specific epithelial actions of TGFβ suggest that it functions as a tumor suppressor early in cancer (Cui et al.), its roles on development of epithelial cancers in the context of irradiated tissue are unknown. To investigate whether host TGFβ contributes to the radiation effect on *Trp53* null carcinogenesis, the radiation-chimera experiment was repeated using syngeneic *Tgfb1* +/- hosts. Strikingly, *Tgfb1* +/- host irradiation did not affect the frequency, latency, or growth rate of *Trp53* null carcinomas (Figure 5A-D), nor molecular characteristics (Table S6), providing strong genetic proof that a critical threshold of TGFβ is an essential facet of radiation induced tumorigenesis and acceleration.

Given that genetically reducing host TGFβ rescued tumor promotion caused by host irradiation, we asked whether the 24-IHC derived from tumors of irradiated wild type hosts could segregate tumors that arose in non-irradiated *Tgfb1* +/- mice (n=6) from those that arose in irradiated hosts (n=10). Neither the 24-IHC nor a similar SAM bootstrap analysis could segregate tumors from non-irradiated versus irradiated *Tgfb1* +/- hosts (Figure 3H). As radiation did not accelerate carcinogenesis in the *Tgfb1* +/- hosts, these tumors can be considered a validation set of the distinct biology of the microenvironment that accelerates carcinogenesis.

Given that reducing the host TGFβ abolished the radiation effect on tumor latency, we next sought to test whether chronic TGFβ could alter malignant progression. To do so we used a derivative of COMMA-1D cells, CDβGeo, which produce ductal and alveolar structures when transplanted in cleared fat pads (Deugnier et al., 2006) and exposed them to 14 days of continuous TGFβ treatment (5ng/ml) in vitro. These and the parental cells were then injected (500,000 cells/gland) into contralateral inguinal cleared mammary fat pads of WT BALB/c host mice (n=15). As shown previously (Barcellos-Hoff and Ravani, 2000), un-treated parental cells injected into cleared mammary glands mostly gave rise to ductal outgrowths (Figure 5E) and a few nodular tumors (2/15; Figure 5F). In contrast, TGFβ treated CDβGeo cells rapidly formed solid tumors (Figure 5G) with a mean latency of 44 days, such that by 9 weeks all fat pads had tumors compared to 13% of those injected with parental cells (Figure 5H). Together these data support chronic TGFβ activity as the mechanism by which host irradiation accelerates *Trp53* null mammary carcinogenesis.

**Host Irradiation Mediates Tumor ER Status Independently of TGFβ dosage**

The presence of estrogen receptor is perhaps the most important clinical marker in breast cancer and is associated with distinct risk factors, pathological features, and clinical behavior (Jensen and Jordan, 2003). We determined the ER status of *Trp53* null tumors using the Allred scoring system (Harvey et al., 1999). Host irradiation significantly increased development of ER-negative tumors ($p=0.002$, Fisher's exact test). Sixty-five percent of tumors that arose in sham-irradiated hosts were ER-positive (28/45, both genotypes) compared to only 35% of tumors (33/93, pooled radiation doses, both genotypes) in irradiated hosts (Figure 6A). This effect of host irradiation to increase ER-negative tumors was observed in both genotypes irradiated with 10 cGy ($p<0.05$; 5B) and therefore was not associated with the effect of radiation on latency *per se*.

To confirm the distinct biology associated with ER status, we localized progesterone receptor (PR) in a subset of 20 tumors. Most (8/10) ER-positive tumors were PR-positive, while few (4/10) ER-negative tumors were PR-positive. We considered the possibility that the frequency of ER-positive cells *Trp53* null outgrowths was affected by host irradiation but the frequency of ER positive cells was unaffected in irradiated compared to control hosts (Figure 6 C,D).

What determines the prevalence of ER negative cancer is not well-understood (Allred et al., 2008). ER negative breast cancer is most frequent in young women and certain racial groups, particularly African-American women (Parise et al., 2009). The observation that irradiated hosts were significantly more likely to give rise to ER-negative and PR-negative tumors implicates radiation-induced heterotypic signaling in determining critical clinical features of breast cancer. We then asked how different the expression profiles of ER-negative tumors were in sham and

irradiated hosts as a means to infer whether they develop via similar paths. SAM-tandem-bootstrap identified 115 genes (Table S7) that cluster ER-negative tumors from irradiated versus sham-irradiated hosts (Figure 6E), but not ER-positive tumors (Figure 6F).

It is has been proposed that breast cancer heterogeneity is determined in part by the cell of origin and its position within the epithelial lineage hierarchy of normal organs (Sell and Pierce, 1994). A corollary is that the tumors retain fundamental programming that remains evident in the biology, behavior, and signature of the cancer subtype. Indeed the expression profiles of isolated mammary stem cells (MaSC), thought to give rise to luminal progenitor (LP) cells that in turn generate mature luminal (ML) cells segregate breast cancers with specific markers and prognosis (Lim et al., 2010a). Mouse *Trp53* null tumors are similar to claudin-low breast cancer (Prat et al., 2010b) and both are enriched in the MaSC signature (Lim et al., 2010a). Moreover, neoplastic transformation in this model is thought to be enhanced by increased stem cell self-renewal (Cicalese et al., 2009b), which is mediated by Notch signaling (Tao et al., 2010b). Notch is preferentially activated in the normal ductal luminal epithelium and promotes commitment of MaSC *in vivo* (Bouras et al., 2008a). We noted significant core enrichment for the Notch pathway in irradiated tissues of both genotypes at 4 weeks when compared to corresponding sham controls. Activation of this pathway was confirmed in an independent experiment using qRT-PCR of Jag1 and Rbpj, which are a key effector and transducer of Notch signaling respectively. Both genes are significantly induced in *Tgfb1* wild type and heterozygote tissues following irradiation with 10 cGy. We then used high content image analysis to localize epithelial Notch based on β-catenin immunoreactivity (Figure 7C, D). We found that nuclear co-localization of both proteins was significantly increased by radiation (Figure E,F). These data suggested that radiation could affect stem cell activity by inducing key regulators of mammary self-renewal and lineage commitment.

Since the mammary stem cell is ER-negative, as are tumors that are enriched in the MaSC signature, we asked whether the MaSC profile relates to IHC-156 and ER-115 profiles (Figure 8A). Genes up-regulated in the IHC-156 showed a highly significant (p=5.4 E-05) enrichment using ConceptGen for genes up regulated in the MaSC profile, as was the ER-115 signature (p=0.01). These data suggest that tumors arising in the irradiated host have a strong MaSC profile. Similarly, MaSC genes were significantly enriched after irradiation in mammary gland (Figure 8B). Together these data suggested the hypothesis that low dose host irradiation might affect the mammary lineage hierarchy by altering self-renewal in mammary stem cells.

To test this idea, mice were irradiated with graded low doses at 3 weeks of age and cells isolated from fully mature glands were analyzed by FACs using $Cd24^{med}/Cd49^{hi}$ mammary repopulation markers (Shackleton et al., 2006). Similar cell numbers were recovered from irradiated mouse mammary gland, which is expected for these very low doses and the extended recovery period. The proportion of lin-/ $Cd24^{med}/Cd49^{hi}$ cells in irradiated mice was significantly increased ($p<0.05$) compared to sham-irradiated mice (Figure 8C). Note the absence of dose dependence, indicating that this effect is not mediated by cell kill *per se*. Functional analysis of repopulating potential is the gold standard to assess mammary stem cells (Purton and Scadden, 2007). Thus we isolated mammary cells from 8 week old mice that were sham-irradiated or irradiated with 10 cGy at 3 weeks. Mammary repopulating activity increased

~1.7 fold ($p<0.05$) in irradiated mice compared to sham-irradiated mice, again without evidence of dose dependence (Figure 8D).

Thus, low doses of ionizing radiation induce a tumor promoting microenvironment by two distinct mechanisms (Figure 8E). One mechanism is the induction of TGFβ activity that acts to accelerate tumorigenesis. The other mechanism, which is not affected by host *Tgfb1* haploinsufficiency and hence appears to be unaffected by TGFβ dosage, radiation induction of Notch pathway and mammary stem cell activity, correlates with the increased frequency of ER-negative tumors.

**Discussion**

Even though engineered mouse models have shown that microenvironment is critical in determining whether cancer ensues from a specific oncogenic event (Bhowmick et al., 2004; de Visser et al., 2006; Kuperwasser et al., 2004), few studies have examined whether carcinogens modify stroma to actively participate in multistep carcinogenesis. Here, we employ the radiation chimera model to provide compelling evidence that a known human carcinogen, ionizing radiation, promote breast cancer through effects on the microenvironment. Several features of carcinogenesis in irradiated hosts parallel those documented in irradiated women: early onset, a more aggressive phenotype and worse prognosis defined by markers. We identified TGFβ in gene expression profiles of irradiated tissue and tumors arising in irradiated hosts, and used a genetic knockdown model to confirm that radiation-induced host TGFβ accelerated carcinogenesis. We also used this combined molecular and genetic approach to show that the effect of radiation on tumor ER status was independent of TGFβ host status and genetically separable from the effect on latency. Rather, radiation induced Notch pathway activation and deregulation of mammary stem cell activity was correlated with ER status of tumors, a mechanism in which radiation alters tissue composition, thus affecting development of specific breast cancer types.

Although it is common in risk modeling to extrapolate from high to low radiation doses, our data demonstrate that radiation effects on cell interactions and host physiology is different at high versus low doses. High dose (4Gy) host irradiation inhibited *Trp3* null tumor development, even though mammary ductal outgrowth occurred efficiently. We observed that branching morphogenesis was reduced in mice irradiated with high doses, consistent with ovarian hormone deficiency. Similarly, young women whose cancer treatment induces premature ovarian failure (Inskip et al., 2009) and older women who undergo radiotherapy have reduced risk of breast cancer because ovarian hormones regulate mammary proliferation (Morin Doody et al., 2000).

In contrast, even though many months elapsed between host irradiation and tumor appearance, low radiation doses accelerated cancer and increased tumor growth rate, suggesting a paradigm in which radiation promotes carcinogenesis by altered heterotypic cell interactions. Distinct from rapid molecular responses to DNA damage, signals from irradiated cells can induce a range of events both in distant un-irradiated cells and in the progeny of irradiated cells. These phenomena are encompassed under a class of actions now called non-targeted effects postulated to impact radiation carcinogenesis (Barcellos-Hoff et al., 2005). The

few studies to explicitly test this hypothesis have used high doses that may alter host physiology (Barcellos-Hoff and Ravani, 2000; Kaplan et al., 1956b). The lowest dose reported herein is near that at which humans show increased cancer risk.

Prior studies using expression profiles have argued that the biology following low dose radiation differs from that following high doses, but it has proven difficult to use these differences to identify key drivers of processes that affect cancer risk. We identified a gene signature that clustered tumors arising in irradiated hosts from those that arose in naïve hosts. Network analysis of the IHC-156 revealed TGFβ hubs and enrichment of TGFβ mediated genes. Our earlier functional studies showed that radiation-induced TGFβ activation *in vivo* mediates extracellular matrix remodeling, cell fate decisions, ATM kinase control of the DNA damage response, and EMT (reviewed in (Andarawewa et al., 2007b)). Expression analysis of irradiated *Tgfb1* heterozygote and wild type mammary gland further underscored the considerable influence of TGFβ in the tissue response to radiation and motivated the radiation chimera experiment using *Tgfb1* heterozygote hosts. The radiation chimera model unequivocally demonstrates that radiation-induced host TGFβ mediates promotion in this model, even though the transplanted epithelium is competent to both produce and respond to TGFβ. Consistent with this, we found that mammary epithelial cells chronically exposed to TGFβ *in vitro* readily progress to tumors in vivo.

The radiation chimera not only showed accelerated carcinogenesis, but altered the expression profiles of tumors that arose from un-irradiated epithelium many months after host exposure. Broeks and colleagues reported that gene expression profiles of breast cancers in women treated with radiation for Hodgkin's lymphoma cluster separately from tumors from un-irradiated women diagnosed at the same age and were consistent with a more aggressive tumor type (Broeks et al., 2010). More to the point, young women treated with radiation for childhood cancer not only have a significantly increased risk of breast cancer at an early age, but a much greater likelihood to have ER-negative cancer compared to age matched controls (Castiglioni et al., 2007). Importantly, even though the epithelium is not irradiated in the radiation chimera model, unlike the breasts of women exposed to radiation by diverse medical sources, it recapitulates all of the clinically relevant features of radiation-preceded breast cancer. Thus it not only provides a relevant model of radiation carcinogenesis but also unequivocally shows that the stroma is a pathologically relevant target of radiation.

We found that the frequency of ER-negative mammary tumors increased in irradiated hosts, which was independent of host *Tgfb1* haploinsufficiency, was associated with radiation-induced Notch pathway activation and stem cell activity. ER-negative cancers are thought to arise from the early, undifferentiated cells of the mammary gland, either mammary stem cells or luminal progenitor cells (Lim et al., 2010a). We hypothesize that radiation exerts significant effects on mammary epithelial hierarchy because the expression profiles of tumors arising in irradiated hosts as well as the irradiated mammary gland significantly overlapped the MaSC profile, recently described by Visvader and colleagues (Lim et al., 2010a). Lifetime breast cancer risk is correlated with factors that drive stem cell proliferation (Savarese et al., 2007). We explicitly tested this idea using cell surface markers and functional repopulating capacity in cells isolated from irradiated mice, which showed that radiation significantly increased the mammary repopulating activity, and could thereby increase the number of target cells that could initiate

cancer. Taken together these data lead to the hypothesis that aberrant heterotypic interactions induced by radiation early in life may set the stage for stem cell expansion and increase the risk of developing ER-negative breast cancer, as observed in the radiation-chimera and in women treated with radiation for childhood cancers (Castiglioni et al., 2007).

It has become increasingly evident that cell function and dysfunction during cancer development are highly intertwined with the microenvironment (Barcellos-Hoff and Medina, 2005; Bissell et al., 2002b; Gonda et al., 2009). Our studies suggest that radiation has very early and persistent effects on the tissue microenvironment that are critical to its carcinogenic potential. Although radiation therapy for cancer is effective, it comes at the price of increased cancer risk that is a life-long burden for cancer patients, particularly those diagnosed during childhood. Radiotherapy for childhood cancers in which breasts are exposed, dramatically increases risk of breast cancer at an early age (Castiglioni et al., 2007). Our study raises the possibility that cancer risk could be decreased by targeting host biology mediated by TGFβ after radiation exposure.

**Experimental Procedures**

Mice. All animal experiments were performed at Lawrence Berkeley National Laboratory with institutional review and approval. BALB/c mice were purchased from Simonsen Laboratories (Gilroy, CA) and housed four per cage, fed with Lab Diet 5008 chow and water *ad libidum*. *Trp53* null and *Tgfb1* heterozygote BALB/c mice were bred in-house under similar conditions. For transplantation experiments, the epithelial rudiments in inguinal glands of 3-week-old mice were surgically removed. These host mice were irradiated whole body at 10-12 weeks of age to the indicated dose at a rate of 23 cGy/min using $^{60}$Co $\gamma$ -radiation. Three days after irradiation, the cleared mammary glands of host mice were transplanted with a 1 mm$^3$ fragment of non-irradiated *Trp53* null BALB/c mammary gland harvested and pooled from 3 or more inguinal glands of 8-10 week old donor mice. Mice were monitored for 365 days.

An informative transplant was defined as that which had an epithelial outgrowth evident by tumor development or confirmation at sacrifice at 12 months. Time to tumor occurrence was plotted using Kaplan-Meier with significance determined by the log-rank test (Graphpad Prizm). Tumor growth curves in a treatment group were fitted to an exponential curve and averaged. Tumors were divided and frozen in liquid nitrogen, embedded in OCT and formalin fixed followed by paraffin embedding.

For tissue analysis, 10 week old *Tgfb1* heterozygote and wild type mice were injected with estrogen (1 μg) and progesterone (1 mg) dissolved in sesame oil 2 days before irradiation with 10 cGy. The lymph node was removed from inguinal mammary glands used to isolate RNA. For mammary stem cell activity, cells were isolated from 5-8 mice sham or irradiated 6 weeks before and processed for lin-/ Cd24$^{med}$/Cd49$^{hi}$ FACS analysis as described (Shelton et al., 2010) in three experiments with technical triplicates. Mammary repopulation frequency was measured by limiting dilution as described (Illa-Bochaca et al., 2010) using 5 cell doses and 58 mice as recipients per treatment. The repopulating capacity in sham and irradiated mice was compared using L-Calc V1.1.1 (StemCell Technologies).

Immunohistochemistry. Sections were deparaffinized and rehydrated prior to antigen unmasking according to manufacturer's instructions (Vector Labs, #H-3300), washed once with phosphate buffer saline and blocked with 0.5% casein and 0.1% Tween 20/PBS for 1 hr at room temperature. Primary antibody for ER C1355 (Millipore/Upstate, #06-935), PR (Neomarkers), αSMA (Sigma, # A2547), K6 (Covance, #PRB-169P), and K14 (Covance, #PRB-155P) were diluted in Superblock Blocking Buffer (Pierce, #37515) and refrigerated overnight. The slides were washed, followed by incubation with fluorochrome-conjugated secondary antibody, washed and counterstained with DAPI (2 μg/ml; Molecular Probes). Histopathological characteristics of the tumors were reviewed by two observers blinded to the experimental details of the mouse models. Tumors were classified and staining was analyzed by two pathologists (JSR-F & FCG) as previously described (McCarthy et al., 2007). ER scoring using the Allred scoring system (Harvey et al., 1999). Notch and β–catenin dual localization was assessed using multiscale *in situ* sorting (Fernandez-Gonzalez et al., 2009).

Expression Profiling. Total RNA quality and quantity was determined using Agilent 2100 Bioanalyzer and Nanodrop ND-1000. Affymetrix mouse Genechip MG-430 2.0 arrays were used according to manufacturer's protocol. Background normalization was done using R software v2.10.1 with widgets specific to the Affymetrix platform. UHC was done using Gene Cluster v3.0 software and heatmaps were visualized using Java TreeView v1.1.4r3 software. No filter was used unless specified as a SD of 1.0 relative to the expression values of that gene across all samples. Adjusted data means of gene expression values was centered by medians. Gene clustering was done by an uncentered-correlation and array clustering was done by Spearman Rank correlation.

Affymetrix CEL files were normalized using Robust Multichip Average algorithm (Bolstad et al., 2003) in GeneSpring GX software (Agilent Technologies) and each probe was normalized to the median value of the un-irradiated specimens for each genotype. Genes differentially regulated in mammary gland tissues were identified by feature selection algorithm Pavlidis template matching (Pavlidis and Noble, 2001) using a p-value <0.05 for pathway analysis. Heatmaps were incorporated in the multi-experiment viewer of the TIGR TM4 Analysis package (Saeed et al., 2003). Pathways were identified with Ingenuity Pathway Analysis, ConceptGen (http://conceptgen.ncibi.org/core/conceptGen/index.jsp), L2L (Newman and Weiner, 2005), or Gene Set Enrichment Analysis using MolDig v3 database. QuantiTect primers for murine Gapdh, Notch1, Jag1, Jag2, and Rbpj (Qiagen) were used with Qiagen's QuantiTect SYBR Green PCR Kit on a BioRad CFX96 Thermal Cycler according to manufacturer's protocols.

Accession Number. NCBI Gene Expression Omnibus database accession number for irradiated mammary glands and tumors is GSE18216.

Statistical Analysis. Statistical analysis was performed using Prism (GraphPad). Differences between treatment groups was determined using the Chi-square test or two tailed Student's t-test for differences, which were considered statistically significant at $P<0.05$.

**Figure Legends**

**Figure 1. Host irradiation affects tumor features.** (A) Schematic of the experimental protocol. Wholemounts of (B) cleared mammary gland; (C) 6 week *Trp53* null outgrowth; (D) 10 week *Trp53* null outgrowth; (E) tumor bearing *Trp53* null outgrowth. (F) Examples of tumor genotype defined by PCR of wild type and null allele. (G) Tumor growth rate as a function of host irradiation. Tumors that arose in irradiated hosts grew significantly faster compared to those in the sham group (top panel). Tumor doubling time was approximately 2 days in the irradiated host group compared to 8 days in the sham group (bottom panel). (H) Histopathology of *Trp53* mouse mammary tumors: left, adenocarcinoma, middle, squamous cell carcinoma, and right, spindle cell carcinoma; scale bar=100 μm. Wholemounts from Trp53 null epithelium transplanted to mice that were sham-irradiated (I) or irradiated with (J) 100 cGy, (K) 200 cGy, or (L) 400 cGy before transplantation. Doses of 200 cGy and above exhibit reduced branching, thinner ducts (arrows), and lack of alveolar buds (arrow heads), indicative of ovarian insufficiency. Scale bar=1 mm.

**Figure 2. Low dose irradiation promotes tumor development.** (A) Analyses of the time-to-tumor occurrence of tumors in sham (black) and hosts irradiated with 10 (blue), 50 (grey), or 100 (red) cGy. Significance was calculated by the log-rank test. (B) Tumor occurrence in transplants pooled from all radiation doses groups (purple, n=45) compared to sham irradiated controls (black, n=29) was accelerated ($p<0.0005$, log-rank test). (C) Tumor frequency at experiment termination in each dose group (sham, 20/29; 10, 14/14; 50, 17/17 ; 100 cGy, 14/14; $p<0.05$, Chi-square test). (D) *Trp53 null* tumor growth rate was increased in hosts previously irradiated with 100 cGy (open symbols) compared to sham (closed symbols) hosts (bars, SEM). Host irradiation at lower doses showed a similar trend but with wider variance. See also Table S1.

**Figure 3. Tumors from irradiated hosts exhibit distinct gene expression.** (A) UHC of *Trp53* null mouse tumors based on SD of 1.0 from sham (red) or irradiated (purple) hosts that were either spindle cell carcinoma (gold) or adenocarcinoma (turquoise). Latency for each tumor is listed below the column. (B) Supervised hierarchical clustering of permutation analysis using SAM with a threshold of 2-fold change identified 24 genes that classified tumors that arose in irradiated (purple) hosts versus sham-irradiated (red). The genes of the irradiated host core (24-IHC) are listed at the right. IPA networks of gene interactions among the 24-IHC include cell-to-cell signaling and interaction, cellular development, hematopoiesis, and cellular assembly and organization. (C,D) IPA network of the top two gene networks generated from the 156-IHC. Note that TGFβ is a central node in both networks (yellow circle). IPA of 156-IHC also revealed enrichment for genes involved (E) leukocyte chemo-attraction and binding ($p=0.007$), (F) monocyte maturation ($p=0.006$), and (G) proliferation of tumor cell lines ($p=0.0007$). Red ovals, induced; green ovals, suppressed. (H) Dendrogram of tumor expression profiles based on the 24–IHC genes indicates that unsupervised hierarchical clustering did not segregate tumors from sham-irradiated (red) versus irradiated (purple) *Tgfb1 +/-* mice. See also Figure S1 and Table S2.

**Figure 4. A single low radiation dose elicits persistent changes in gene expression that are highly modulated by TGFβ.** (A) Heat map based on PTM ($p<0.05$ and threshold of 1.25-fold) for radiation-induced genes common to mammary gland from *Tgfb1* wildtype (black) and heterozygote (grey) littermates at 1 (orange) and/or 4 (blue) weeks after sham irradiation (yellow) or 10 cGy (green) exposure. (B) Heat map based on PTM ($p<0.05$) and threshold of 1.25-fold change for genes that are down regulated (blue) or up regulated (red) in mammary gland from irradiated wild type (black) but not *Tgfb1* heterozygote (grey) littermates at 1 (orange) or 4 (blue) weeks after sham (yellow) or 10 cGy (green) radiation exposure. (C) IPA networks of the genes up-regulated by radiation in both genotypes invoked cellular growth and proliferation, reproductive system development and function, and organismal development. Note TGFβ is a node (yellow circle). (D) IPA network of the genes induced by radiation only in wildtype hosts included functions involved in hematological disease, metabolic disease, and connective tissue development and function. See also Tables S3, S4, and S5.

**Figure 5. TGFβ promotes carcinogenesis in irradiated hosts.** (A) Kaplan-Meier analyses of the time-to-tumor occurrence in *Tgfb1* heterozygote hosts irradiated with sham (black), 10 (blue), 50 (grey), and 100 (red) cGy. Host irradiation did not decrease tumor latency. Significance was calculated by the log-rank test. (B) Tumor occurrence in transplants into *Tgfb1* heterozygote hosts pooled from all radiation doses groups (purple, n=86) compared to sham irradiated controls (black, n=26). (C) Tumor incidence of *Trp53 null* outgrowths does not significantly increase in irradiated *Tgfb1* heterozygote hosts compared to sham hosts at 365 days post transplantation. Sham, n=15/26; 10 cGy, n=21/31; 50 cGy, n=16/22; and 100 cGy, n=20/33 (ns, not significant). (D) Tumor growth rate was not affected by host irradiation (bars, SEM). (E) TGFβ treatment significantly ($p<0.0001$) increased mammary tumor incidence (black) compared to control parental CDβGeo cells (grey) transplanted to cleared mammary glands. (F) Most CDβGeo cells give rise to ductal outgrowths, as shown in a representative tissue section (H&E, bar=50 μm). (G) A few CDβGeo injections give rise to nodular tumors (H&E, bar=50 μm). (H) CDβGeo cells exposed to prolonged TGFβ in vitro rapidly generate solid tumors (H&E, bar=50 μm). See also Table S6.

**Figure 6. The frequency of ER negative *Trp53* null tumors is increased by host irradiation.** (A) The frequency ER-negative tumors was significantly greater ($p<0.002$) in irradiated hosts compared to sham hosts. (B) The frequency of ER-negative *Trp53 null* tumors arising of hosts irradiated with 10 cGy was significantly increased in either host genotype (black, $p<0.05$; grey, *Tgfb1* +/-, $p<0.05$). (C) ER immunohistochemistry in 5 week old outgrowths *of Trp53* null mammary outgrowths; scale bar=100 μm. (D) The frequency ER-positive cells in outgrowths was not affected by host irradiation (sham hosts, 34±6% SEM, n=3 vs irradiated hosts, 31±2% SEM, n=9). (E) The ER-115 profile clusters ER-negative tumors that arose in irradiated (purple) from sham-irradiated (red) hosts. (F) Dendrogram showing the ER-115 does not cluster ER-positive tumors. See also Table S7.

**Figure 7. Radiation induces Notch and β-catenin activity.** (A) Notch ligand, Jag1, is increased at 1 wk and a transducer of Notch signaling, Rpbj, is increased at 4 wk after irradiation as measured by qRT-PCR (bars, SEM). (B) Notch ligand, Jag1, and a transducer of Notch signaling, Rpbj, are increased at 4 wk in irradiated *Tgfb1* heterozygote mammary tissue as measured by qRT-PCR (bars, SEM). (C, D) Dual immunostaining of Notch (green) and β-catenin (red) in mammary epithelium in which nuclei are stained with DAPI (blue; Bar=25 μm). Arrowheads indicate cells that have high nuclear Notch immunoreactivity and β-catenin that are increased in irradiated tissues (D) compared to sham-irradiated tissue (C). (E,F) Multiscale *in situ* sorting of nuclear Notch and β-catenin immunoreactivity shows that radiation (F; n=486 cells) significantly increased the frequency of Notch positive cells ($p<0.05$, Fisher's exact test) and dual stained cells ($p<0.001$, Fisher's exact test) compared to sham-irradiated tissues (E; n=424 cells).

**Figure 8. Radiation affects the mammary stem cell pool.** (A) The overlap between the MaSC signature (Lim et al., 2010a), IHC-156 and ER-115 is indicated within the Venn diagram and the p-value for enrichment determined with ConceptGen is shown outside the regions of interest. (B) Venn diagram showing the overlap between the MaSC signature and the genes regulated by radiation in the *Tgfb1* wild type (WT) and heterozygote (HT) mammary gland as described for A. (C) Radiation significantly ($p<0.01$) increased the proportion of lin-/Cd24$^{med}$/Cd49$^{hi}$ cells determined by FACS analysis of mammary epithelial cells isolated from tissue of mice irradiated 6 weeks before compared to sham-irradiated mice (bars, SEM). Dose was not associated with the degree of response. (D) The mammary repopulating capacity of cells from mice irradiated as in C is significantly increased ($p<0.05$) as determined by limiting dilution estimation ($\pm$95% C.I.). (E) Schematic of distinct mechanisms by which host irradiation affects tumor latency and type.

**Figure 1**

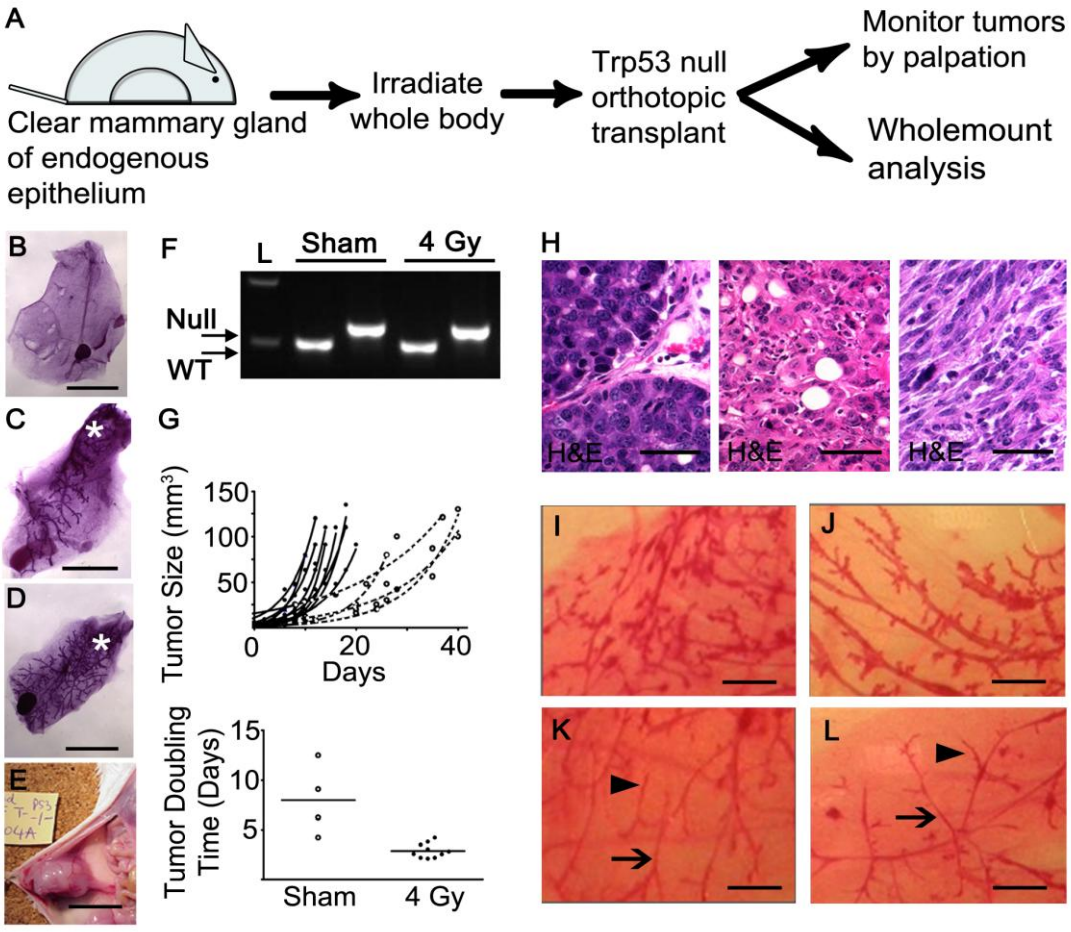
A
Clear mammary gland of endogenous epithelium
Irradiate whole body
Trp53 null orthotopic transplant
Monitor tumors by palpation
Wholemount analysis
B
C
D
E
F
L
Sham
4 Gy
Null
WT
G
Tumor Size (mm³)
150
100
50
0
20
40
Days
Tumor Doubling Time (Days)
15
10
5
Sham
4 Gy
H
H&E
H&E
H&E
I
J
K
L

**Figure 2**

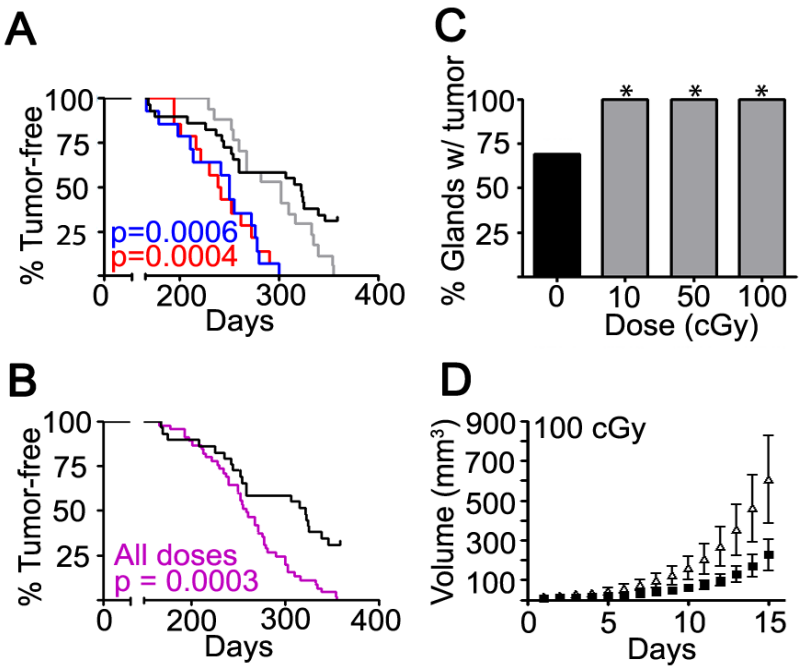
A
% Tumor-free
100
75
50
25
0
200
300
400
Days
p=0.0006
p=0.0004
C
% Glands w/ tumor
100
75
50
25
0
10
50
100
Dose (cGy)
*
*
*
B
% Tumor-free
100
75
50
25
0
200
300
400
Days
All doses
p = 0.0003
D
Volume (mm³)
900
700
500
300
100
0
5
10
15
Days
100 cGy

**Figure 3**

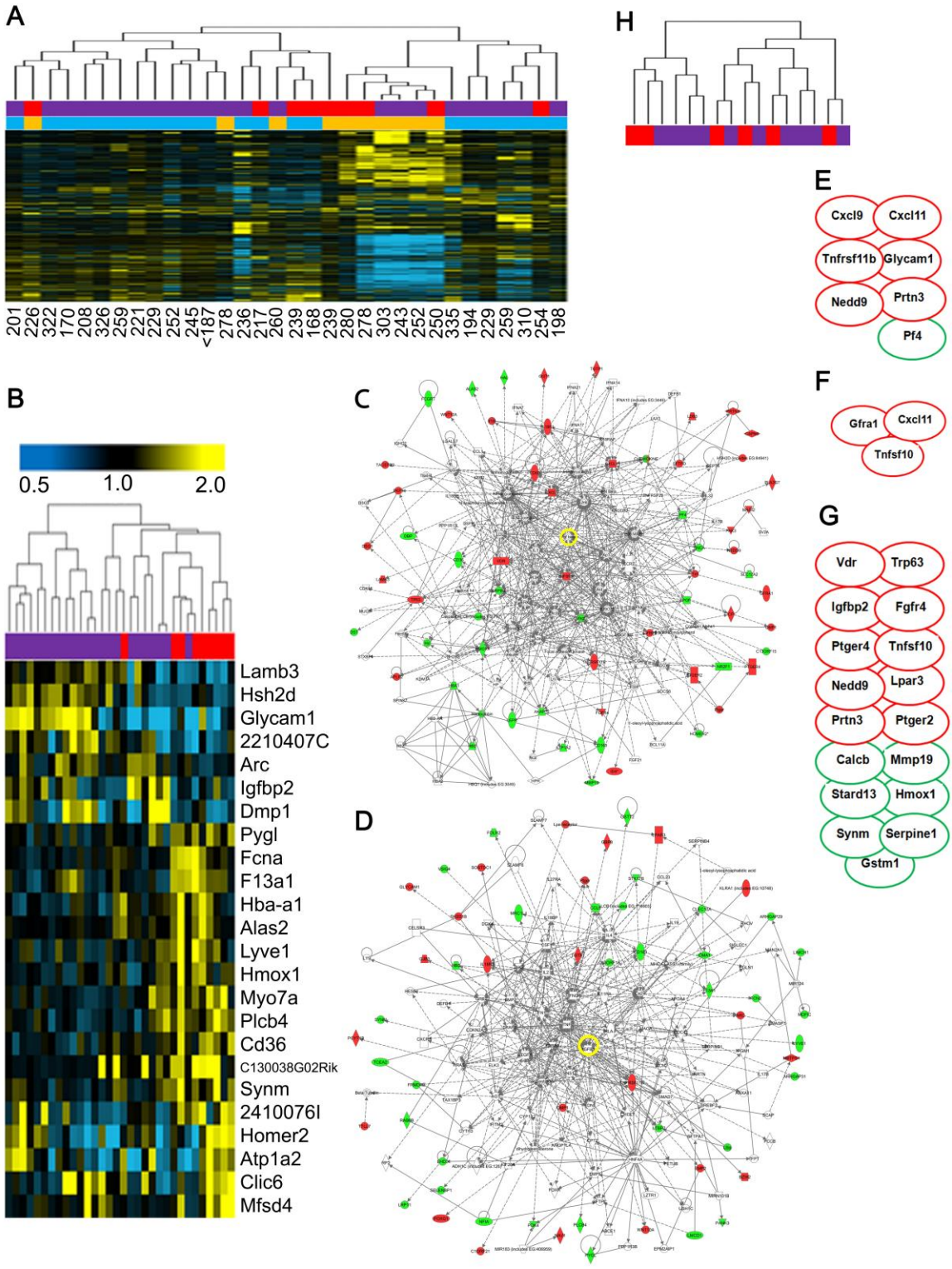
A
201 226 322 170 208 326 259 221 229 252 245 <187 278 236 217 260 239 168 239 280 278 303 243 252 250 335 194 229 259 310 254 198
H
E
Cxcl9
Cxcl11
Tnfrsf11b
Glycam1
Nedd9
Prtn3
Pf4
F
Gfra1
Cxcl11
Tnfsf10
B
0.5
1.0
2.0
Lamb3
Hsh2d
Glycam1
2210407C
Arc
Igfbp2
Dmp1
Pygl
Fcna
F13a1
Hba-a1
Alas2
Lyve1
Hmox1
Myo7a
Plcb4
Cd36
C130038G02Rik
Synm
2410076I
Homer2
Atp1a2
Clic6
Mfsd4
C
D
G
Vdr
Trp63
Igfbp2
Fgfr4
Ptger4
Tnfsf10
Nedd9
Lpar3
Prtn3
Ptger2
Calcb
Mmp19
Stard13
Hmox1
Synm
Serpine1
Gstm1

**Figure 4**

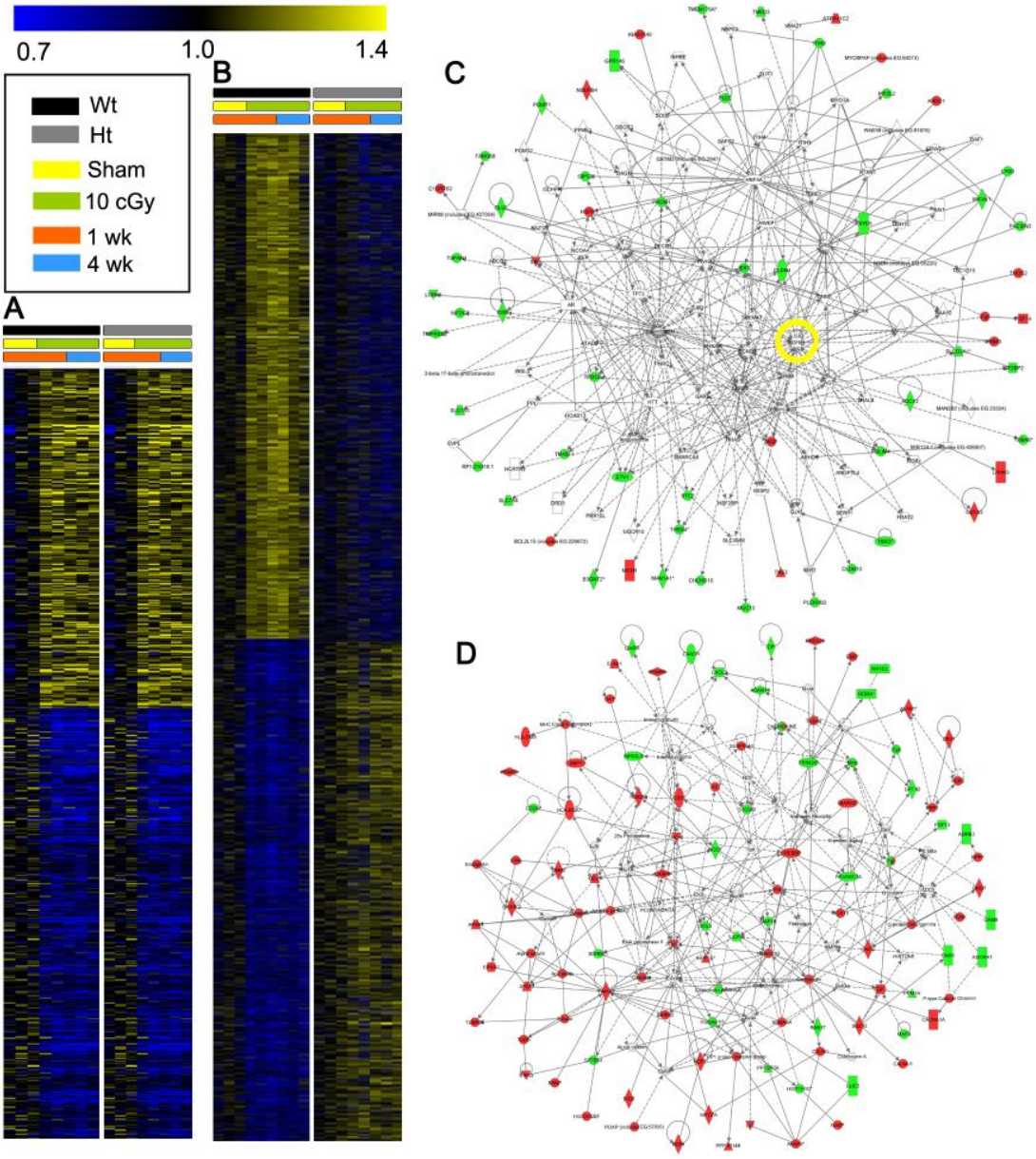

**Figure 5**

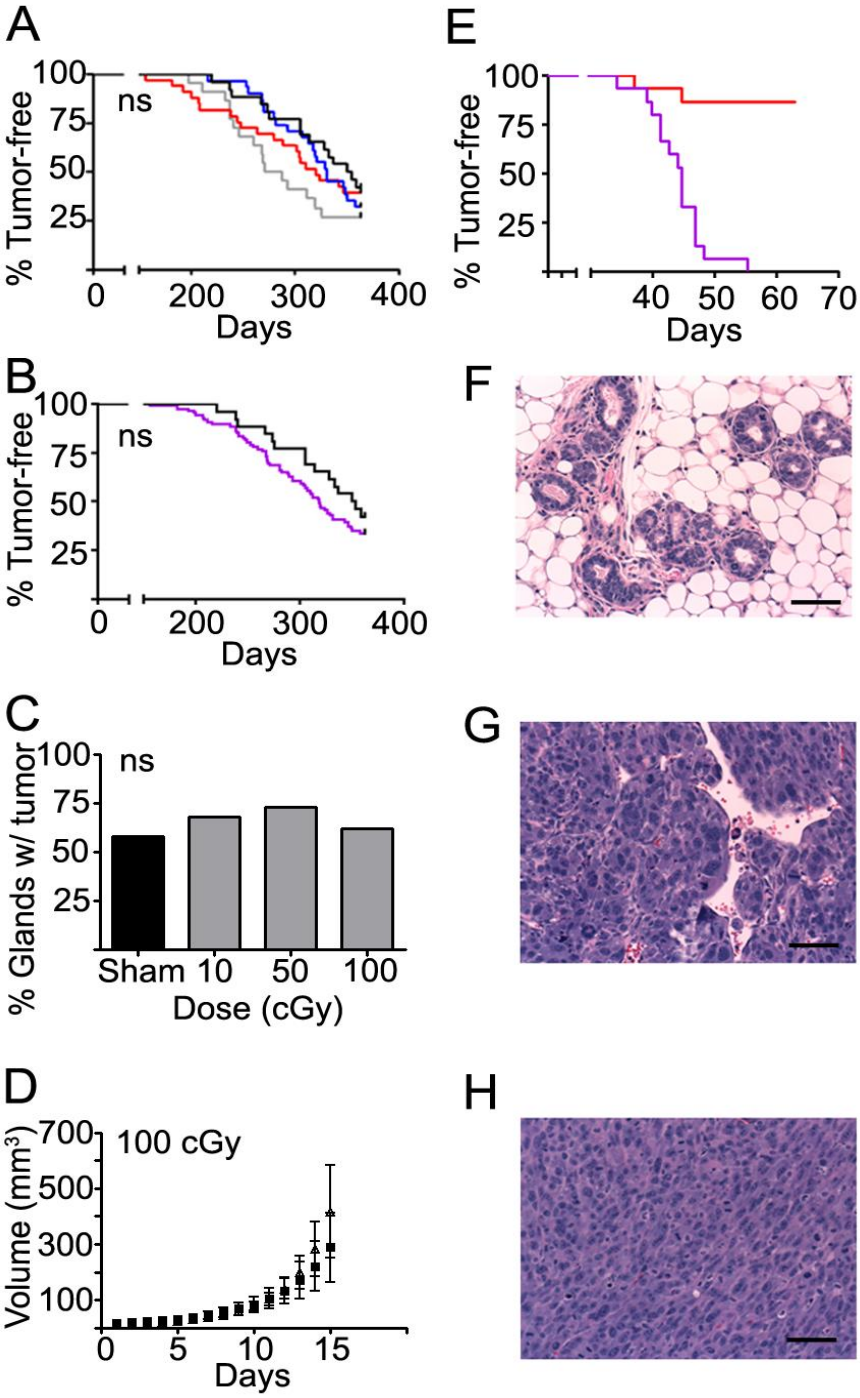
A
100
75
50
25
% Tumor-free
ns
0
200
300
400
Days
E
100
75
50
25
% Tumor-free
40
50
60
70
Days
B
100
75
50
25
% Tumor-free
ns
0
200
300
400
Days
F
C
100
75
50
25
% Glands w/ tumor
ns
Sham
10
50
100
Dose (cGy)
G
D
700
500
300
100
Volume (mm3)
100 cGy
0
5
10
15
Days
H

**Figure 6**

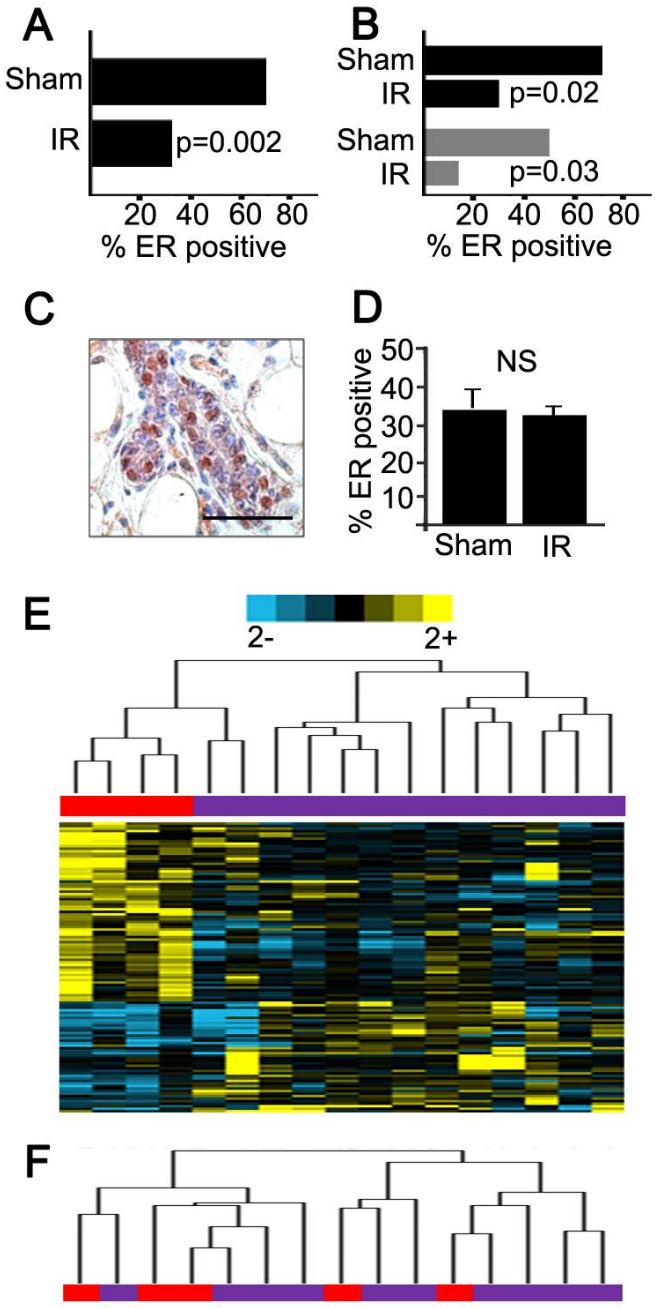
A
Sham
IR
p=0.002
20 40 60 80
% ER positive
B
Sham
IR
p=0.02
Sham
IR
p=0.03
20 40 60 80
% ER positive
C
D
% ER positive
50
40
30
20
10
NS
Sham
IR
E
2-
2+
F

**Figure 7**

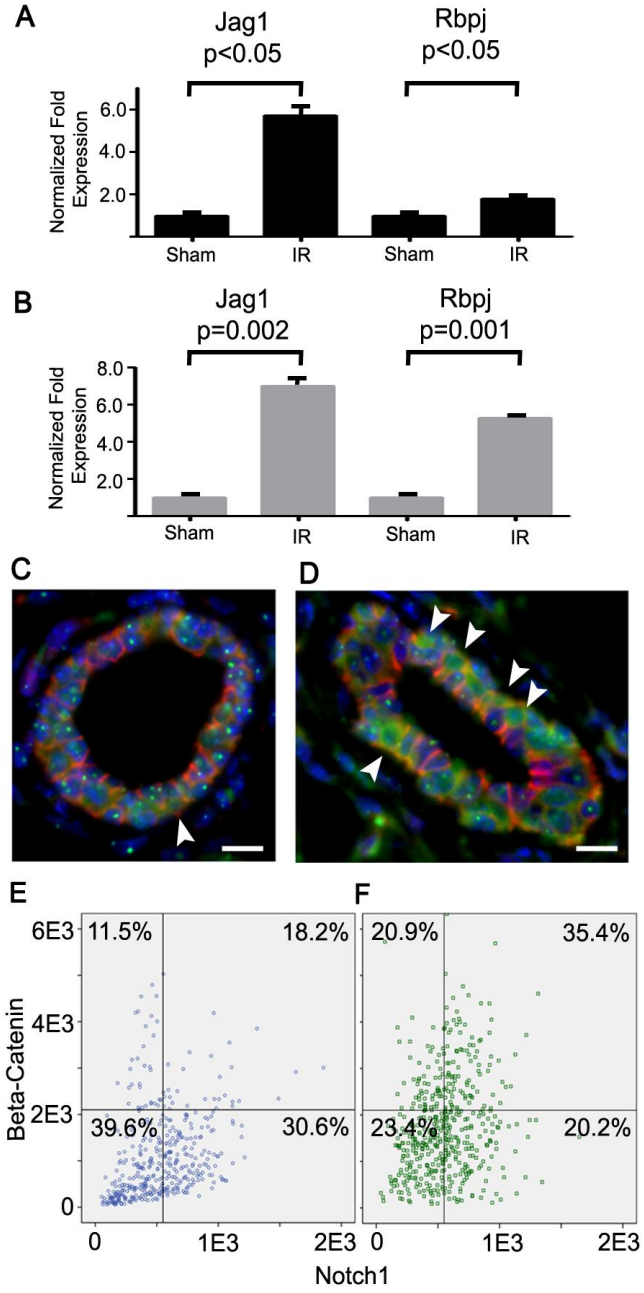
A
Jag1
p<0.05
Rbpj
p<0.05
Normalized Fold Expression
6.0
4.0
2.0
Sham
IR
Sham
IR
B
Jag1
p=0.002
Rbpj
p=0.001
Normalized Fold Expression
8.0
6.0
4.0
2.0
Sham
IR
Sham
IR
C
D
E
F
6E3
4E3
2E3
0
Beta-Catenin
11.5%
18.2%
39.6%
30.6%
20.9%
35.4%
23.4%
20.2%
0
1E3
2E3
0
1E3
2E3
Notch1

**Figure 8**

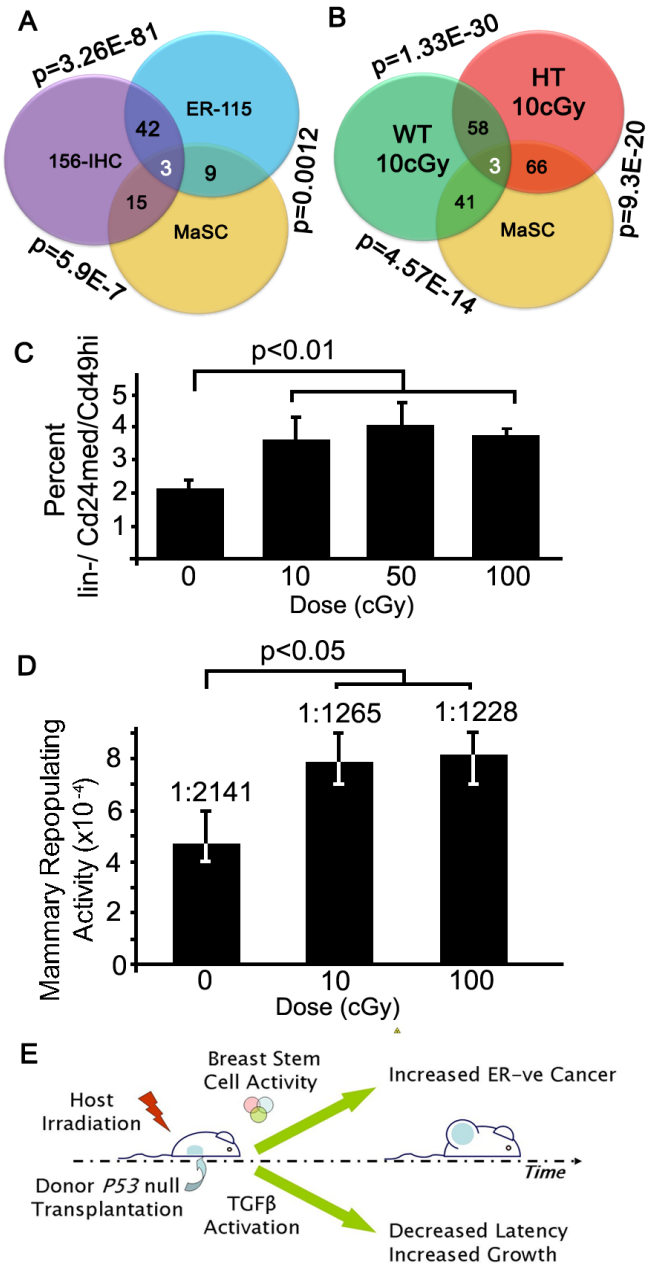
A
p=3.26E-81
ER-115
42
156-IHC
3
9
15
MaSC
p=0.0012
p=5.9E-7
B
p=1.33E-30
HT
10cGy
58
WT
10cGy
3
66
41
MaSC
p=9.3E-20
p=4.57E-14
C
p<0.01
Percent
lin-/ Cd24med/Cd49hi
5
4
3
2
1
0
10
50
100
Dose (cGy)
D
p<0.05
1:1265
1:1228
1:2141
Mammary Repopulating
Activity (x10⁻⁴)
8
6
4
2
0
0
10
100
Dose (cGy)
E
Breast Stem
Cell Activity
Increased ER−ve Cancer
Host
Irradiation
Time
Donor P53 null
Transplantation
TGFβ
Activation
Decreased Latency
Increased Growth

**Figure S1 (Related to Figure 3).** IPA networks of gene interactions amongst the 24-IHC gene profile (top panels), and heatmap of unsupervised hierarchical clustering of the 156-IHC gene profile (bottom panel).

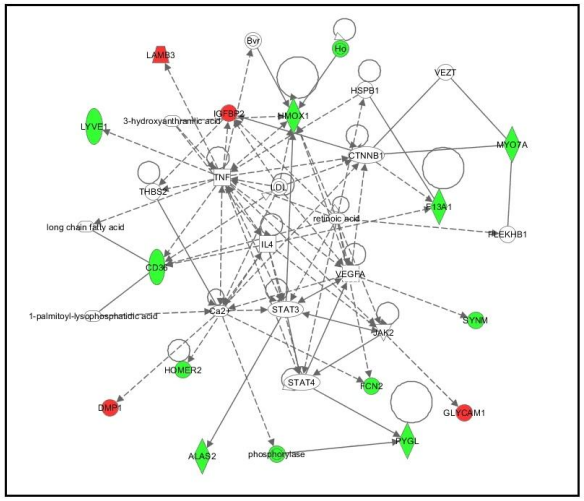


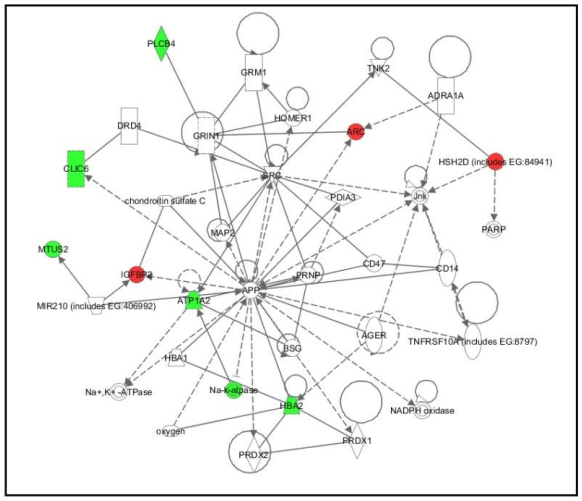


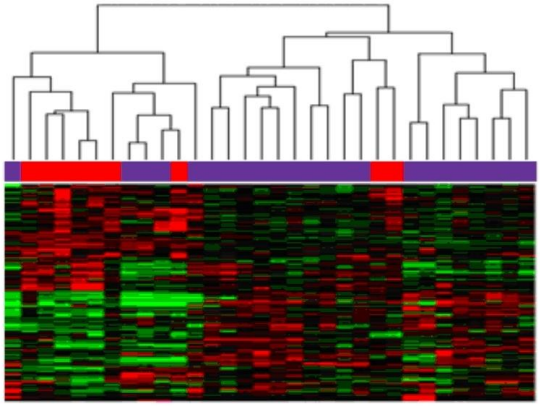

**Table S1 (Related to Figure 2).** Tumor characteristics as a function of host irradiation dose and genotype.

| Balb/c | **Sham** | **10cGy** | **50cGy** | **100cGy** |
|---|---|---|---|---|
| **Tumor Subtype, n/m (%)** | | | | |
| Adenocarcinoma | 13/30 (43) | 10/15 (67) | 14/22 (64) | 8/14 (57) |
| Spindle Cell Carcinoma | 10/30 (33) | 4/15 (27) | 7/22 (32) | 5/14 (36) |
| Squamous Carcinoma | 2/30 (7) | 1/15 (7) | 1/22 (5) | 1/14 (7) |
| Myoepithelioma | 5/30 (17) | 0 | 0 | 0 |
| **Tumor Features, n/m (%)** | | | | |
| DCIS component | | | | |
| Yes | 5/15 (33) | 8/13 (61) | 12/19 (63) | 1/11 (9) |
| Necrotic | | | | |
| Yes | 10/18 (56) | 6/15 (40) | 10/22 (45) | 8/14 (57) |
| Lymphocytic infiltration | | | | |
| Negligable | 0 | 2/15 (13) | 5/22 (23) | 1/13 (8) |
| Mild | 12/18 (67) | 10/15 (66) | 8/22 (36) | 12/13 (92) |
| Moderate | 6/18 (33) | 3/15 (20) | 9/22 (41) | 0 |
| **Markers, n/m (%)** | | | | |
| ER-$\alpha$ | | | | |
| Positive | 20/28 (71) | 4/13 (31) | 6/15 (40) | 6/11 (55) |
| Keratin 14 | | | | |
| Positive | 7/9 (78) | 12/15 (80) | 11/19 (58) | 7/8 (88) |
| Intensity-Weak | 0 | 0 | ND | 0 |
| Intensity-Moderate | 0 | 2/12 (17) | ND | 1/7 (14) |
| Intensity-Strong | 7/7 (100) | 10/12 (83) | ND | 6/7 (86) |
| Keratin 6 | | | | |
| Positive | 8/13 (61) | ND | ND | 7/12 (58) |
| $\alpha$-Smooth muscle actin | | | | |
| Positive | 2/10 (20) | ND | ND | 3/9 (33) |

**Table S2 (Related to Figure 5A-D).** Tumor characterization as a function of *Tgfb1* heterozygote host irradiation dose.

| ***Tgfb1* HT** | **Sham** | **10cGy** | **50cGy** | **100cGy** |
|---|---|---|---|---|
| **Tumor Subtype, n/m (%)** | | | | |
| Adenocarcinoma | 13/27 (48) | 10/25 (40) | 12/19 (63) | 13/25 (52) |
| Spindle Cell Carcinoma | 12/27 (44) | 11/25 (44) | 6/19 (32) | 9/25 (36) |
| Squamous Carcinoma | 0 | 4/25 (16) | 1/19 (5) | 2/25 (8) |
| Myoepithelioma | 2/27 (7) | 0 | 0 | 1/25 (4) |
| **Tumor Features, n/m (%)** | | | | |
| **DCIS component** | | | | |
| Yes | 7/17 (41) | 12/22 (55) | 8/16 (50) | 8/20 (40) |
| **Necrotic** | | | | |
| Yes | 17/25 (68) | 9/25 (36) | 9/18 (50) | 13/23 (56) |
| **Lymphocytic infiltration** | | | | |
| Negligible | 3/25 (12) | 7/24 (29) | 1/19 (5) | 1/22 (5) |
| Mild | 15/25 (60) | 11/24 (46) | 14/19 (74) | 17/22 (77) |
| Moderate | 4/25 (16) | 6/24 (25) | 3/19 (16) | 4/22 (18) |
| Brisk | 3/25 (12) | 0 | 1/19 (5) | 0 |
| **Markers, n/m (%)** | | | | |
| **ER-** | | | | |
| Positive | 8/15 (53) | 3/20 (15) | 5/13 (38) | 6/19 (32) |
| **Keratin 14** | | | | |
| Positive | 7/12 (58) | 15/17 (88) | 11/15 (73) | 9/12 (75) |
| Intensity-Weak | 0 | 0 | 0 | 1/9 (11) |
| Intensity-Moderate | 1/7 (14) | 1/15 (7) | 2/11 (18) | 1/9 (11) |
| Intensity-Strong | 6/7 (86) | 14/15 (93) | 9/11 (82) | 7/9 (78) |
| **Keratin 6** | | | | |
| Positive | 5/13 (38) | ND | ND | 3/9 (33) |
| **-Smooth muscle actin** | | | | |
| Positive | 8/10 (80) | ND | ND | 3/8 (38) |

**Table S3 (Related to Figure 3).** 156 genes modulated by at least 1.5-fold in tumors from irradiated hosts.

| Direction | Affymetrix ID | Gene Symbol |
|---|---|---|
| UP | 1453239_a_at | Ankrd22 |
| UP | 1432344_a_at | Aplp2 |
| UP | 1418687_at | Arc |
| UP | 1438730_at | BC028801 |
| UP | 1423456_at | Bzw2 |
| UP | 1421952_at | Capn6 |
| UP | 1428735_at | Cd69 |
| UP | 1437578_at | Clca2 |
| UP | 1417497_at | Cp |
| UP | 1419697_at | Cxcl11 /// LOC630447 |
| UP | 1418652_at | Cxcl9 |
| UP | 1426005_at | Dmp1 |
| UP | 1458000_at | Dsg1a |
| UP | 1425272_at | Emp2 |
| UP | 1419490_at | Fam19a5 |
| UP | 1436576_at | Fam26f |
| UP | 1429682_at | Fam46c |
| UP | 1418596_at | Fgfr4 |
| UP | 1438558_x_at | Foxq1 |
| UP | 1440342_at | G530011O06Rik |
| UP | 1439015_at | Gfra1 |
| UP | 1448485_at | Ggt1 |
| UP | 1416715_at | Gjb3 |
| UP | 1424927_at | Glipr1 |
| UP | 1424825_a_at | Glycam1 |
| UP | 1442130_at | Hsh2d |
| UP | 1437967_at | http://genome-www4.stanford.edu/cgi-bin/SMD/source/sourceResult?choice=Gene&option=Name&criteria= |
| UP | 1438441_at | Id4 |
| UP | 1423259_at | Id4 /// LOC100045546 |
| UP | 1454159_a_at | Igfbp2 |
| UP | 1421628_at | Il18r1 |
| UP | 1421304_at | Klra2 |
| UP | 1427352_at | Krt79 |
| UP | 1417812_a_at | Lamb3 |
| UP | 1433783_at | Ldb3 |
| UP | 1430551_s_at | Lipm |
| UP | 1419504_at | LOC100047046 /// Mogat1 |
| UP | 1423719_at | LOC632073 /// U46068 |
| UP | 1418723_at | Lpar3 |
| UP | 1454855_at | Magi2 |
| UP | 1427285_s_at | Malat1 |
| UP | 1431385_a_at | Mbtps1 |

| | | |
|---|---|---|
| UP | 1447885_x_at | Nedd9 |
| UP | 1449009_at | OTTMUSG00000005523 /// Tgtp |
| UP | 1435486_at | Pak3 |
| UP | 1436124_at | Pcyt1b |
| UP | 1449374_at | Pipox |
| UP | 1449586_at | Pkp1 |
| UP | 1430700_a_at | Pla2g7 |
| UP | 1419669_at | Prtn3 |
| UP | 1449310_at | Ptger2 |
| UP | 1421073_a_at | Ptger4 |
| UP | 1455347_at | Rtel1 |
| UP | 1420764_at | Scrg1 |
| UP | 1450734_at | Sec16b |
| UP | 1419478_at | Sectm1b |
| UP | 1420378_at | Sftpd |
| UP | 1423024_at | Sh2d1b1 |
| UP | 1449340_at | Sostdc1 |
| UP | 1423323_at | Tacstd2 |
| UP | 1449033_at | Tnfrsf11b |
| UP | 1439680_at | Tnfsf10 |
| UP | 1418158_at | Trp63 |
| UP | 1455377_at | Ttll7 |
| UP | 1418175_at | Vdr |
| UP | 1460657_at | Wnt10a |
| UP | 1436365_at | Zbtb7c |
| UP | 1447870_x_at | 1110002E22Rik |
| UP | 1430674_at | 1700016C15Rik |
| UP | 1436431_at | 1700025G04Rik |
| UP | 1425233_at | 2210407C18Rik |
| UP | 1419643_s_at | 2310057J18Rik /// 2310065H11Rik |
| UP | 1453261_at | 2610035D17Rik |
| UP | 1430162_at | 3830417A13Rik |
| UP | 1418776_at | 5830443L24Rik |
| UP | 1427521_a_at | 9930023K05Rik |
| UP | 1442011_at | A230065H16Rik |
| UP | 1456878_at | AI646023 |
| DOWN | 1425032_at | Abpb |
| DOWN | 1419706_a_at | Akap12 |
| DOWN | 1451675_a_at | Alas2 |
| DOWN | 1438967_x_at | Amhr2 |
| DOWN | 1441618_at | Arhgap29 |
| DOWN | 1452308_a_at | Atp1a2 |
| DOWN | 1448211_at | Atp6v0e2 |
| DOWN | 1432205_a_at | C130038G02Rik |
| DOWN | 1427355_at | Calca |
| DOWN | 1422639_at | Calcb |
| DOWN | 1417266_at | Ccl6 |

| | | |
|---|---|---|
| DOWN | 1419144_at | Cd163 |
| DOWN | 1423166_at | Cd36 |
| DOWN | 1432022_at | Cdgap |
| DOWN | 1452309_at | Cgnl1 |
| DOWN | 1449456_a_at | Cma1 |
| DOWN | 1458934_at | D5Ertd505e |
| DOWN | 1418174_at | Dbp |
| DOWN | 1421276_a_at | Dst |
| DOWN | 1417236_at | Ehd3 |
| DOWN | 1418829_a_at | Eno2 |
| DOWN | 1448876_at | Evc |
| DOWN | 1448929_at | F13a1 |
| DOWN | 1443904_at | Fads6 |
| DOWN | 1416978_at | Fcgrt |
| DOWN | 1418243_at | Fcna |
| DOWN | 1451648_a_at | Folr2 |
| DOWN | 1426594_at | Frmd4b |
| DOWN | 1416411_at | Gstm2 |
| DOWN | 1417883_at | Gstt2 |
| DOWN | 1418645_at | Hal |
| DOWN | 1417714_x_at | Hba-a1 /// Hba-a2 |
| DOWN | 1417184_s_at | Hbb-b1 /// Hbb-b2 |
| DOWN | 1448239_at | Hmox1 |
| DOWN | 1424367_a_at | Homer2 |
| DOWN | 1423180_at | Kcnb1 |
| DOWN | 1456156_at | Lepr |
| DOWN | 1440147_at | Lgi2 |
| DOWN | 1435321_at | Limch1 |
| DOWN | 1424596_s_at | Lmcd1 |
| DOWN | 1417580_s_at | LOC100044204 /// Selenbp1 |
| DOWN | 1451651_at | LOC100044885 /// Vsig4 |
| DOWN | 1418157_at | LOC100046044 /// Nr2f1 |
| DOWN | 1456909_at | LOC676974 |
| DOWN | 1433536_at | Lrp11 |
| DOWN | 1418061_at | Ltbp2 |
| DOWN | 1429379_at | Lyve1 |
| DOWN | 1427040_at | Mdfic |
| DOWN | 1455531_at | Mfsd4 |
| DOWN | 1419605_at | Mgl1 |
| DOWN | 1421977_at | Mmp19 |
| DOWN | 1450430_at | Mrc1 |
| DOWN | 1424933_at | Myo5c |
| DOWN | 1421385_a_at | Myo7a |
| DOWN | 1446990_at | Nfia |
| DOWN | 1438448_at | Otop1 |
| DOWN | 1426259_at | Pank3 |
| DOWN | 1417273_at | Pdk4 |

| | | |
|---|---|---|
| DOWN | 1448995_at | Pf4 |
| DOWN | 1418471_at | Pgf |
| DOWN | 1435771_at | Plcb4 |
| DOWN | 1457029_at | Ppp4r1l |
| DOWN | 1417741_at | Pygl |
| DOWN | 1434914_at | Rab6b |
| DOWN | 1419149_at | Serpine1 |
| DOWN | 1417623_at | Slc12a2 |
| DOWN | 1418395_at | Slc47a1 |
| DOWN | 1418493_a_at | Snca |
| DOWN | 1452604_at | Stard13 |
| DOWN | 1430165_at | Stk17b |
| DOWN | 1455610_at | Synm |
| DOWN | 1418107_at | Tcea2 |
| DOWN | 1435261_at | Tmtc1 |
| DOWN | 1418003_at | 1190002H23Rik |
| DOWN | 1429203_at | 2410076I21Rik |
| DOWN | 1433320_at | 4930519N06Rik |
| DOWN | 1457671_at | 9330120H11Rik |
| DOWN | 1459344_at | 9630019E01Rik |

**Table S4 (Related to Figure 4).** Genes commonly regulated in both wild type and TGFβ1 heterozygote littermates by 10 cGy radiation.

| **UP: Common in both genotypes** | | |
|---|---|---|
| **Affy ID** | **Symbol** | **Fold Change** |
| 1431182_at | Hspa8 | 2.035934833 |
| 1444253_at | Adamts18 | 1.88562875 |
| 1452614_at | Gm566 | 1.727679133 |
| 1419288_at | Jam2 | 1.638208867 |
| 1430306_a_at | Atp6v1c2 | 1.597226 |
| 1424221_at | Susd4 | 1.553738 |
| 1426082_a_at | Slc16a4 | 1.4437834 |
| 1419766_at | Snf1lk | 1.4234349 |
| 1425290_at | Stx19 | 1.4187724 |
| 1424412_at | Ogfrl1 | 1.4177165 |
| 1448700_at | G0s2 | 1.3994897 |
| 1451642_at | Kif1b | 1.3797613 |
| 1453596_at | Id2 | 1.367869867 |
| 1456822_at | Rad23b | 1.366440333 |
| 1441513_at | Tank | 1.3598104 |
| 1439072_at | Slc1a3 | 1.35862485 |
| 1455687_at | Ick | 1.3508295 |
| 1432427_at | Ndufb4 | 1.3498846 |
| 1439313_at | Lphn3 | 1.348262 |
| 1455743_at | Olfml2a | 1.3386785 |
| 1423437_at | Gsta3 | 1.33777677 |
| 1429169_at | Rbm3 | 1.337282867 |
| 1431170_at | Efna3 | 1.3253076 |
| 1450738_at | Kif21a | 1.317572267 |
| 1418606_at | Hoxd10 | 1.316838 |
| 1428932_at | Ttc21a | 1.31485145 |
| 1457598_at | Txnl2 | 1.3104321 |
| 1430650_at | Zfp191 | 1.3065148 |
| 1444004_at | Thoc2 | 1.30435345 |
| 1425808_a_at | Myocd | 1.3005976 |
| 1455333_at | Tns3 | 1.2989487 |
| 1425918_at | Egln3 | 1.29443835 |
| 1453359_at | Exosc1 | 1.2923771 |
| 1448416_at | Mgp | 1.2914075 |

| **DOWN: Common in both genotypes** | | |
|---|---|---|
| **Affy ID** | **Symbol** | **Fold Change** |
| 1416930_at | Ly6d | 0.001715352 |
| 1416274_at | Ctns | 0.113225203 |
| 1419387_s_at | Muc13 | 0.18018838 |
| 1424351_at | Wfdc2 | 0.194352995 |
| 1419518_at | Tuba8 | 0.20925589 |
| 1455434_a_at | Ktn1 | 0.239274377 |
| 1418735_at | Krt4 | 0.24427083 |
| 1417957_a_at | Tspan1 | 0.330924797 |
| 1420378_at | Sftpd | 0.333489185 |
| 1460012_at | Wfdc3 | 0.335398557 |
| 1418252_at | Padi2 | 0.342188797 |
| 1417618_at | Itih2 | 0.348593927 |
| 1422784_at | Krt6a | 0.354497247 |
| 1428988_at | Abcc3 | 0.389366463 |
| 1446771_at | Tuba8 | 0.391899573 |
| 1437673_at | Wnt5a | 0.40269345 |
| 1417156_at | Krt19 | 0.411660393 |
| 1421134_at | Areg | 0.42722667 |
| 1450276_a_at | Scin | 0.4319802 |
| 1452853_at | Carkl | 0.43343457 |
| 1456212_x_at | Socs3 | 0.43729827 |
| 1436791_at | Wnt5a | 0.44297691 |
| 1442115_at | Fam38b | 0.444997897 |
| 1417178_at | Gipc2 | 0.447947547 |
| 1448818_at | Wnt5a | 0.448876153 |
| 1418283_at | Cldn4 | 0.4517666 |
| 1444242_at | Slco2a1 | 0.465972437 |
| 1417343_at | Fxyd6 | 0.46835248 |
| 1417622_at | Slc12a2 | 0.473895853 |
| 1419647_a_at | Ier3 | 0.477387725 |
| 1445186_at | Stc2 | 0.487112117 |
| 1419700_a_at | Prom1 | 0.488231943 |
| 1420913_at | Slco2a1 | 0.49793875 |
| 1419154_at | Tmprss2 | 0.499424423 |

| | | |
|---|---|---|
| 1460723_at | Mc5r | 1.28280025 |
| 1425079_at | Tm6sf2 | 1.27386785 |
| 1448710_at | Cxcr4 | 1.269576567 |
| 1424207_at | Smarca5 | 1.2649768 |
| 1440138_at | Ahdc1 | 1.2635686 |
| 1423566_a_at | Hsp110 | 1.257474853 |
| 1421035_a_at | Magi3 | 1.2557948 |
| 1419128_at | Itgax | 1.412088 |
| 1435747_at | Fgf14 | 1.323115 |
| 1420929_at | Ctnnal1 | 1.369254 |
| 1427090_at | Zbed4 | 1.320285 |
| 1441634_at | Ntng1 | 1.338777067 |
| 1417799_at | Atp6v1g2 | 1.280992867 |
| 1441213_at | MAP3K19 | 1.276724667 |
| 1424297_at | Zfp282 | 1.2748576 |
| 1455148_at | Tmem130 | 1.274185 |

| | | |
|---|---|---|
| 1448788_at | Cd200 | 0.505346097 |
| 1425603_at | Tmem176a | 0.506133123 |
| 1437479_x_at | Tbx3 | 0.513735277 |
| 1451895_a_at | Dhcr24 | 0.52003491 |
| 1418326_at | Slc7a5 | 0.5262313 |
| 1417110_at | Man1a | 0.531924607 |
| 1450009_at | Ltf | 0.537203927 |
| 1435323_a_at | Mboat1 | 0.541856423 |
| 1455266_at | Kif5c | 0.54290913 |
| 1455899_x_at | Socs3 | 0.554682763 |
| 1422607_at | Etv1 | 0.5599803 |
| 1426734_at | Fam43a | 0.57183405 |
| 1420852_a_at | B3gnt2 | 0.582454 |
| 1427418_a_at | Hif1a | 0.5905 |
| 1425503_at | Gcnt2 | 0.597412 |
| 1428572_at | Basp1 | 0.620403 |

**Table S5 (Related to Figure 4).** Genes regulated by 10cGy irradiation only in wild type mammary glands.

| **UP: wildtype irradiated** | | |
|---|---|---|
| **Affy ID** | **Symbol** | **Fold Change** |
| 1448239_at | Hmox1 | 2.8462699 |
| 1437729_at | Rpl27a | 2.656247233 |
| 1418207_at | Fxyd4 | 2.651392667 |
| 1420132_s_at | Pttg1ip | 2.436733733 |
| 1421385_a_at | Myo7a | 2.2925687 |
| 1417602_at | Per2 | 2.275914967 |
| 1427320_at | Copg2as2 | 2.131939633 |
| 1454373_x_at | Ubc | 2.120502767 |
| 1416118_at | Trim59 | 2.110012133 |
| 1425884_at | Bxdc1 | 1.974646533 |
| 1449465_at | Reln | 1.952310267 |
| 1416956_at | Kcnab2 | 1.945471033 |
| 1449851_at | Per1 | 1.891806833 |
| 1436425_at | Ankrd38 | 1.8784835 |
| 1425609_at | Ncf1 | 1.865386333 |
| 1418465_at | Ncf4 | 1.8038053 |
| 1434202_a_at | Fam107a | 1.796454733 |
| 1434987_at | Aldh2 | 1.795853167 |
| 1419378_a_at | Fxyd2 | 1.769300733 |
| 1423478_at | Prkcb1 | 1.769291433 |
| 1449681_at | Hdgf | 1.768159767 |
| 1419282_at | Ccl12 | 1.767192333 |
| 1424265_at | Npl | 1.758355977 |
| 1435375_at | Fam105a | 1.756583967 |
| 1426081_a_at | Dio2 | 1.738955433 |
| 1420158_s_at | Abcf1 | 1.7337025 |
| 1420012_at | Xbp1 | 1.725411867 |
| 1448362_at | Dnajc7 | 1.725210967 |
| 1420053_at | Psmb1 | 1.7183174 |
| 1443033_at | Rbm14 | 1.7035158 |
| 1429432_at | Bat2d | 1.696226417 |
| 1456250_x_at | Tgfbi | 1.691213133 |
| 1419613_at | Col7a1 | 1.683739567 |
| 1439465_x_at | Agbl5 | 1.683427567 |
| 1436716_at | Ppp1r14b | 1.681352567 |
| 1456772_at | Ncf1 | 1.678104333 |

| **DOWN: wildtype irradiated** | | |
|---|---|---|
| **Affy ID** | **Symbol** | **Fold change** |
| 1423858_a_at | Hmgcs2 | 0.246407462 |
| 1454866_s_at | Clic6 | 0.312790537 |
| 1449031_at | Cited1 | 0.419509563 |
| 1436892_at | Spred2 | 0.492231657 |
| 1448530_at | Gmpr | 0.519121227 |
| 1416958_at | Nr1d2 | 0.519973063 |
| 1418649_at | Egln3 | 0.539603343 |
| 1421555_at | Adrb3 | 0.543775887 |
| 1441326_at | Cp | 0.566266907 |
| 1437578_at | Clca2 | 0.573487473 |
| 1450032_at | Slco2a1 | 0.5756616 |
| 1430168_at | Cstad | 0.584658467 |
| 1444320_at | Ddhd2 | 0.585040083 |
| 1422178_a_at | Rab17 | 0.58642767 |
| 1449088_at | Fbp2 | 0.589900627 |
| 1449219_at | Fads3 | 0.594286667 |
| 1460116_s_at | Spred1 | 0.59627362 |
| 1429177_x_at | Sox17 | 0.60321167 |
| 1453592_at | Lrrc39 | 0.61085371 |
| 1448382_at | Ehhadh | 0.61339237 |
| 1434140_at | Mcf2l | 0.614918743 |
| 1432517_a_at | Nnmt | 0.61615891 |
| 1431032_at | Agl | 0.622329253 |
| 1449158_at | Kcnk2 | 0.623295757 |
| 1448756_at | S100a9 | 0.623929617 |
| 1418497_at | Fgf13 | 0.62611588 |
| 1443381_at | Etv4 | 0.629889283 |
| 1417801_a_at | Ppfibp2 | 0.63047527 |
| 1451322_at | Cmbl | 0.631625967 |
| 1418093_a_at | Egf | 0.634136497 |
| 1436994_a_at | Hist1h1c | 0.635212787 |
| 1424123_at | Flvcr2 | 0.636523307 |
| 1435184_at | Npr3 | 0.6379001 |
| 1434172_at | Cnr1 | 0.638053477 |
| 1435504_at | Clip4 | 0.641824317 |
| 1449573_at | Alpk3 | 0.642253687 |

| | | |
|---|---|---|
| 1436077_a_at | Fcho1 | 1.657174933 |
| 1448123_s_at | Tgfbi | 1.646693767 |
| 1460347_at | Krt14 | 1.630177567 |
| 1416871_at | Adam8 | 1.6262493 |
| 1418745_at | Omd | 1.616446667 |
| 1433733_a_at | Cry1 | 1.6084051 |
| 1421005_at | Cep110 | 1.6070901 |
| 1433617_s_at | B4galt5 | 1.5992323 |
| 1425515_at | Pik3r1 | 1.595173 |
| 1426511_at | Susd2 | 1.594506167 |
| 1420697_at | Slc15a3 | 1.593890967 |
| 1434741_at | Rreb1 | 1.592823567 |
| 1423841_at | Bxdc2 | 1.591942867 |

| | | |
|---|---|---|
| 1443518_at | Sgce | 0.644740153 |
| 1439989_at | Tsc1 | 0.649148167 |
| 1419463_at | Clca2 | 0.651393657 |
| 1419721_at | Gpr109a | 0.653334243 |
| 1428853_at | Ptch1 | 0.656679733 |
| 1425203_at | Ddx19b | 0.657143203 |
| 1436990_s_at | Ndg2 | 0.658024023 |
| 1418328_at | Cpt1b | 0.65849033 |
| 1437873_at | Zfp799 | 0.661527287 |
| 1454256_s_at | Aarsd1 | 0.66161418 |
| 1423413_at | Ndrg1 | 0.66238463 |
| 1429024_at | Rbm20 | 0.663942367 |
| 1420906_at | Cd2ap | 0.665083 |

**Table S6 (Related to Figure 4).** Genes regulated by 10cGy irradiation only in *Tgfβ1* +/- mammary glands.

| **UP: TGFb1 +/- irradiated** | | |
|---|---|---|
| **Affy ID** | **Symbol** | **Fold Change** |
| 1425122_at | Fam3b | 8.065317033 |
| 1436739_at | Agtr1a | 6.84627735 |
| 1426039_a_at | Alox12e | 5.481428 |
| 1423405_at | Timp4 | 4.2412618 |
| 1451851_a_at | Csn3 | 4.007569643 |
| 1451478_at | Angptl7 | 3.93495765 |
| 1451510_s_at | Olah | 3.873495 |
| 1417074_at | Ceacam10 | 3.80136525 |
| 1428571_at | Col9a1 | 3.438741367 |
| 1451691_at | Ednra | 3.4220765 |
| 1423858_a_at | Hmgcs2 | 3.3911216 |
| 1416613_at | Cyp1b1 | 3.36675 |
| 1422831_at | Fbn2 | 3.324244267 |
| 1453988_a_at | Ide | 3.1487423 |
| 1454830_at | Fbn2 | 3.125027067 |
| 1418148_at | Abhd1 | 3.114663667 |
| 1431833_a_at | Hmgcs2 | 3.09547605 |
| 1419248_at | Rgs2 | 3.05710385 |
| 1421845_at | Golph3 | 2.956410033 |
| 1450286_at | Npr3 | 2.7712269 |
| 1435670_at | Tcfap2b | 2.659399867 |
| 1450995_at | Folr1 | 2.65527425 |
| 1429157_at | Hhipl2 | 2.6442277 |
| 1448024_at | Npr3 | 2.637571767 |
| 1441801_at | Kctd4 | 2.636219067 |
| 1448830_at | Dusp1 | 2.6324564 |
| 1424855_at | Olah | 2.612785 |
| 1460521_a_at | Obfc2a | 2.565007667 |
| 1416854_at | Slc34a2 | 2.54114285 |
| 1419816_s_at | Errfi1 | 2.539456133 |
| 1448752_at | Car2 | 2.503374333 |
| 1436600_at | Tox3 | 2.429244133 |
| 1420537_at | Kctd4 | 2.426281967 |
| 1435939_s_at | Hepacam2 | 2.361313133 |
| 1422582_at | Lep | 2.359133633 |
| 1449280_at | Esm1 | 2.262209967 |

| **DOWN: TGFb1 +/- irradiated** | | |
|---|---|---|
| **Affy ID** | **Symbol** | **Fold Change** |
| 1449994_at | Epgn | 0.151204292 |
| 1429274_at | Lypd6b | 0.263763277 |
| 1449431_at | Trpc6 | 0.269162657 |
| 1426063_a_at | Gem | 0.3234669 |
| 1438405_at | Fgf7 | 0.34586179 |
| 1420521_at | Papln | 0.3931221 |
| 1455193_at | Zbtb8 | 0.396333513 |
| 1417787_at | Dkkl1 | 0.421502483 |
| 1424733_at | P2ry14 | 0.44945237 |
| 1423952_a_at | Krt7 | 0.457013263 |
| 1434777_at | Mycl1 | 0.462797303 |
| 1428835_at | Myh14 | 0.470676867 |
| 1421117_at | Dst | 0.483266133 |
| 1421075_s_at | Cyp7b1 | 0.485729935 |
| 1454891_at | Cds2 | 0.493119775 |
| 1449773_s_at | Gadd45b | 0.497395403 |
| 1455338_at | A4galt | 0.50777866 |
| 1428977_at | Chst8 | 0.51165516 |
| 1449590_a_at | Mras | 0.518647253 |
| 1460330_at | Anxa3 | 0.518784943 |
| 1419503_at | Stc2 | 0.524135823 |
| 1434188_at | Slc16a12 | 0.5304429 |
| 1424495_a_at | Cklf | 0.531247375 |
| 1418572_x_at | Tnfrsf12a | 0.531683817 |
| 1425002_at | Sectm1a | 0.538353535 |
| 1419282_at | Ccl12 | 0.546586643 |
| 1437152_at | Mex3b | 0.5473138 |
| 1429891_at | Capsl | 0.55359484 |
| 1419722_at | Klk8 | 0.558442035 |
| 1439527_at | Pgr | 0.562017427 |
| 1459646_at | Hs3st6 | 0.56403755 |
| 1440354_at | Elovl7 | 0.56512946 |
| 1437119_at | Ern1 | 0.566177933 |
| 1450065_at | Adcy7 | 0.57065088 |
| 1419379_x_at | Fxyd2 | 0.57077711 |
| 1418571_at | Tnfrsf12a | 0.571829233 |

| | | | | | |
|---|---|---|---|---|---|
| 1416129_at | Errfi1 | 2.247875867 | 1446284_at | Mtss1 | 0.57582772 |
| 1452652_at | Tmem158 | 2.24093245 | 1421141_a_at | Foxp1 | 0.57793595 |
| 1457145_at | Plekhg4 | 2.22620102 | 1451567_a_at | Ifi203 | 0.58049175 |
| 1449031_at | Cited1 | 2.21916535 | 1427956_at | Pcgf1 | 0.58116195 |
| 1437442_at | Pcdh7 | 2.172849667 | 1420647_a_at | Krt8 | 0.583494533 |
| 1416019_at | Dr1 | 2.169630167 | 1421186_at | Ccr2 | 0.58673315 |
| 1415989_at | Vcam1 | 2.159763867 | 1423691_x_at | Krt8 | 0.58925878 |
| 1446269_at | Hbp1 | 2.15569795 | 1420682_at | Chrnb1 | 0.590283887 |
| 1439617_s_at | Pck1 | 2.1535006 | 1454159_a_at | Igfbp2 | 0.596551237 |
| 1430452_at | Cyp20a1 | 2.113511967 | 1431211_s_at | Them5 | 0.598650817 |
| 1454880_s_at | Bmf | 2.088016533 | 1443947_at | Lims1 | 0.606704 |
| 1420349_at | Ptgfr | 2.082686233 | 1423544_at | Ptpn5 | 0.608534 |
| 1439283_at | Osbpl9 | 2.07733855 | 1434145_s_at | Serhl | 0.615426 |
| 1449319_at | Rspo1 | 2.07238633 | 1424542_at | S100a4 | 0.616483 |

**Supplemental Table S7 (Related to Figure 6).** 115 genes modulated in ER-negative tumors from irradiated hosts, as compared to ER-negative tumors from non-irradiated hosts.

| Direction | Affy ID | Symbol |
|---|---|---|
| UP | 1453239_a_at | Ankrd22 |
| UP | 1432344_a_at | Aplp2 |
| UP | 1418687_at | Arc |
| UP | 1449356_at | Asb5 |
| UP | 1428735_at | Cd69 |
| UP | 1421366_at | Clec5a |
| UP | 1417497_at | Cp |
| UP | 1460604_at | Cybrd1 |
| UP | 1443745_s_at | Dmp1 |
| UP | 1425272_at | Emp2 |
| UP | 1438558_x_at | Foxq1 |
| UP | 1416715_at | Gjb3 |
| UP | 1422179_at | Gjb4 |
| UP | 1424927_at | Glipr1 |
| UP | 1448194_a_at | H19 |
| UP | 1448152_at | Igf2 |
| UP | 1417812_a_at | Lamb3 |
| UP | 1436107_at | Lsm8 |
| UP | 1427520_a_at | Myh1 |
| UP | 1427026_at | Myh4 |
| UP | 1452651_a_at | Myl1 |
| UP | 1435529_at | OTTMUSG00000016644 |
| UP | 1422760_at | Padi4 |
| UP | 1435486_at | Pak3 |
| UP | 1419271_at | Pax6 |
| UP | 1435162_at | Prkg2 |
| UP | 1420352_at | Prss22 |
| UP | 1419669_at | Prtn3 |
| UP | 1417262_at | Ptgs2 |
| UP | 1454906_at | Rarb |
| UP | 1420378_at | Sftpd |
| UP | 1418309_at | Tnfrsf11b |
| UP | 1417464_at | Tnnc2 |
| UP | 1416889_at | Tnni2 |
| UP | 1438877_at | Trpm6 |
| UP | 1455377_at | Ttll7 |
| UP | 1427445_a_at | Ttn |
| UP | 1447870_x_at | 1110002E22Rik |
| UP | 1430674_at | 1700016C15Rik |
| UP | 1425233_at | 2210407C18Rik |
| UP | 1453511_at | 2310007B03Rik |
| UP | 1419643_s_at | 2310057J18Rik /// 2310065H11Rik |
| UP | 1455160_at | 2610203C20Rik |

| | | |
|---|---|---|
| UP | 1427521_a_at | 9930023K05Rik |
| DOWN | 1427371_at | Abca8a |
| DOWN | 1422651_at | Adipoq |
| DOWN | 1419706_a_at | Akap12 |
| DOWN | 1451675_a_at | Alas2 |
| DOWN | 1416371_at | Apod |
| DOWN | 1441618_at | Arhgap29 |
| DOWN | 1436453_at | BB144871 |
| DOWN | 1432205_a_at | C130038G02Rik |
| DOWN | 1424041_s_at | C1s /// LOC100044326 |
| DOWN | 1427355_at | Calca |
| DOWN | 1449434_at | Car3 |
| DOWN | 1419684_at | Ccl8 |
| DOWN | 1419144_at | Cd163 |
| DOWN | 1449918_at | Cd209g |
| DOWN | 1423166_at | Cd36 |
| DOWN | 1449193_at | Cd5l |
| DOWN | 1432022_at | Cdgap |
| DOWN | 1417867_at | Cfd |
| DOWN | 1452260_at | Cidec |
| DOWN | 1449456_a_at | Cma1 |
| DOWN | 1419527_at | Comp |
| DOWN | 1448730_at | Cpa3 |
| DOWN | 1416194_at | Cyp4b1 |
| DOWN | 1419204_at | Dll1 |
| DOWN | 1421276_a_at | Dst |
| DOWN | 1417235_at | Ehd3 |
| DOWN | 1427455_x_at | ENSMUSG00000076577 /// Igk /// Igk-C /// Igk-V28 /// LOC100047628 |
| DOWN | 1448929_at | F13a1 |
| DOWN | 1438953_at | Figf /// LOC100047108 |
| DOWN | 1429236_at | Galntl2 |
| DOWN | 1416411_at | Gstm2 |
| DOWN | 1420872_at | Gucy1b3 |
| DOWN | 1417714_x_at | Hba-a1 /// Hba-a2 |
| DOWN | 1417184_s_at | Hbb-b1 /// Hbb-b2 |
| DOWN | 1419407_at | Hc |
| DOWN | 1448696_at | Heph |
| DOWN | 1448239_at | Hmox1 |
| DOWN | 1439231_at | http://genome-www4.stanford.edu/cgi-bin/SMD/source/sourceResult?choice=Gene&option=Name&criteria= |
| DOWN | 1417901_a_at | Ica1 |
| DOWN | 1421653_a_at | Igh /// Igh-2 /// Igh-VJ558 /// LOC544903 |
| DOWN | 1440147_at | Lgi2 |
| DOWN | 1435106_at | Limch1 |
| DOWN | 1418157_at | LOC100046044 /// Nr2f1 |
| DOWN | 1415904_at | Lpl |
| DOWN | 1429379_at | Lyve1 |

| | | |
|---|---|---|
| DOWN | 1419605_at | Mgl1 |
| DOWN | 1421977_at | Mmp19 |
| DOWN | 1450430_at | Mrc1 |
| DOWN | 1421385_a_at | Myo7a |
| DOWN | 1455792_x_at | Ndn |
| DOWN | 1421965_s_at | Notch3 |
| DOWN | 1435553_at | Pdzd2 |
| DOWN | 1441531_at | Plcb4 |
| DOWN | 1416321_s_at | Prelp |
| DOWN | 1428808_at | Prickle2 |
| DOWN | 1418666_at | Ptx3 |
| DOWN | 1417741_at | Pygl |
| DOWN | 1449319_at | Rspo1 |
| DOWN | 1436044_at | Scn7a |
| DOWN | 1429459_at | Sema3d |
| DOWN | 1419100_at | Serpina3n |
| DOWN | 1448889_at | Slc38a4 |
| DOWN | 1418395_at | Slc47a1 |
| DOWN | 1457275_at | Synm |
| DOWN | 1435261_at | Tmtc1 |
| DOWN | 1450798_at | Tnxb |
| DOWN | 1424649_a_at | Tspan8 |
| DOWN | 1420465_s_at | 100039054 /// 2610016E04Rik /// CU041261.1 /// CU104690.1 /// Mup1 /// Mup2 /// OTTMUSG00000007428 /// OTTMUSG00000007431 /// OTTMUSG00000007486 /// OTTMUSG00000008509 /// OTTMUSG00000012492 /// OTTMUSG00000012493 /// OTTMUSG00000015595 |
| DOWN | 1452417_x_at | 2010205A11Rik /// ENSMUSG00000076577 /// Igk /// Igk-C /// Igk-V28 /// LOC100047628 |
| DOWN | 1426154_s_at | 2610016E04Rik /// Mup1 /// Mup2 /// Mup3 |
| DOWN | 1453698_at | 6030451C04Rik |

**References**


Allred, D. C., Wu, Y., Mao, S., Nagtegaal, I. D., Lee, S., Perou, C. M., Mohsin, S. K., O'Connell, P., Tsimelzon, A., and Medina, D. (2008). Ductal Carcinoma In situ and the Emergence of Diversity during Breast Cancer Evolution. Clin Cancer Res *14*, 370-378.

Amundson, S. A., Bittner, M., Chen, Y., Trent, J., Meltzer, P., and Fornace, A. J. J. (1999a). Fluorescent cDNA microarray hybridization reveals complexity and heterogeneity of cellular genotoxic stress responses. Oncogene *18*, 3666-3672.

Amundson, S. A., Do, K. T., and Fornace, A. J. J. (1999b). Induction of stress genes by low doses of gamma rays. Radiat Res *152*, 225-231.

Andarawewa, K. L., Kirshner, J., Mott, J. D., and Barcellos-Hoff, M. H. (2007). TGFb: Roles in DNA damage responses. In Transforming Growth Factor-Beta in Cancer Therapy, Volume II Cancer Treatment and Therapy, S. Jakowlew, ed. (Totowa: Humana Press), pp. 321-334.

Barcellos-Hoff, M. H. (1993). Radiation-induced transforming growth factor b and subsequent extracellular matrix reorganization in murine mammary gland. Cancer Res *53*, 3880-3886.

Barcellos-Hoff, M. H., Derynck, R., Tsang, M. L.-S., and Weatherbee, J. A. (1994). Transforming growth factor-b activation in irradiated murine mammary gland. J Clin Invest *93*, 892-899.

Barcellos-Hoff, M. H., and Medina, D. (2005). New highlights on stroma-epithelial interactions in breast cancer. Breast Cancer Res *7*, 33-36.

Barcellos-Hoff, M. H., Park, C., and Wright, E. G. (2005). Radiation and the microenvironment - tumorigenesis and therapy. Nat Rev Cancer *5*, 867-875.

Barcellos-Hoff, M. H., and Ravani, S. A. (2000). Irradiated mammary gland stroma promotes the expression of tumorigenic potential by unirradiated epithelial cells. Cancer Res *60*, 1254-1260.

Bhowmick, N. A., Chytil, A., Plieth, D., Gorska, A. E., Dumont, N., Shappell, S., Washington, M. K., Neilson, E. G., and Moses, H. L. (2004). TGF-{beta} signaling in fibroblasts modulates the oncogenic potential of adjacent epithelia. Science *303*, 848-851.

Bissell, M. J., Radisky, D. C., Rizki, A., Weaver, V. M., and Petersen, O. W. (2002). The organizing principle: microenvironmental influences in the normal and malignant breast. Differentiation *70*, 537-546.

Bolstad, B. M., Irizarry, R. A., Astrand, M., and Speed, T. P. (2003). A comparison of normalization methods for high density oligonucleotide array data based on bias and variance. Bioinformatics *19*, 185-193.

Bouras, T., Pal, B., Vaillant, F., Harburg, G., Asselin-Labat, M.-L., Oakes, S. R., Lindeman, G. J., and Visvader, J. E. (2008). Notch Signaling Regulates Mammary Stem Cell Function and Luminal Cell-Fate Commitment. Cell Stem Cell *3*, 429-441.

Broeks, A., Braaf, L. M., Wessels, L. F., Van de Vjver, M., De Bruin, M. L., Stovall, M., Russell, N. S., van Leeuwen, F. E., and Van 't Veer, L. J. (2010). Radiation-Associated Breast Tumors Display a Distinct Gene Expression Profile. International journal of radiation oncology, biology, physics *76*, 540-547.

Castiglioni, F., Terenziani, M., Carcangiu, M. L., Miliano, R., Aiello, P., Bertola, L., Triulzi, T., Gasparini, P., Camerini, T., Sozzi, G.*, et al.* (2007). Radiation effects on development of HER2-positive breast carcinomas. Clin Cancer Res *13*, 46-51.

Cicalese, A., Bonizzi, G., Pasi, C. E., Faretta, M., Ronzoni, S., Giulini, B., Brisken, C., Minucci, S., Di Fiore, P. P., and Pelicci, P. G. (2009). The Tumor Suppressor p53 Regulates Polarity of Self-Renewing Divisions in Mammary Stem Cells. Cell *138*, 1083-1095.

Cui, W., Fowlis, D. J., Bryson, S., Duffie, E., Ireland, H., Balmain, A., and Akhurst, R. J. (1996). TGFb1 inhibits the formation of benign skin tumors, but enhances progression to invasive spindle carcinomas in transgenic mice. Cell *86*, 531-542.

de Visser, K. E., Eichten, A., and Coussens, L. M. (2006). Paradoxical roles of the immune system during cancer development. *6*, 24-37.

Deugnier, M.-A., Faraldo, M. M., Teulière, J., Thiery, J. P., Medina, D., and Glukhova, M. A. (2006). Isolation of mouse mammary epithelial progenitor cells with basal characteristics from the Comma-D[beta] cell line. Developmental Biology *293*, 414-425.

Durante, M., and Cucinotta, F. A. (2008). Heavy ion carcinogenesis and human space exploration. Nat Rev Cancer *8*, 465-472.

Ehrhart, E. J., Carroll, A., Segarini, P., Tsang, M. L.-S., and Barcellos-Hoff, M. H. (1997). Latent transforming growth factor-b activation in situ: Quantitative and functional evidence following low dose irradiation. FASEB J *11*, 991-1002.

Fernandez-Gonzalez, R., Illa-Bochaca, I., Welm, B. E., Fleisch, M. C., Werb, Z., Ortiz-de-Solorzano, C., and Barcellos-Hoff, M. H. (2009). Mapping mammary gland architecture using multi-scale in situ analysis. Integr Biol *1*, 80 - 89.

Gonda, T. A., Tu, S., and Wang, T. C. (2009). Chronic inflammation, the tumor microenvironment and carcinogenesis. Cell Cycle *8*, 2005-2013.

Harvey, J. M., Clark, G. M., Osborne, C. K., and Allred, D. C. (1999). Estrogen receptor status by immunohistochemistry is superior to the ligand-binding assay for predicting response to adjuvant endocrine therapy in breast cancer. J Clin Oncol *17*, 1474-1481.

Illa-Bochaca, I., Fernandez-Gonzalez, R., Shelton, D. N., Welm, B. E., Ortiz-de-Solorzano, C., and Barcellos-Hoff, M. H. (2010). Limiting-dilution transplantation assays in mammary stem cell studies. Methods Mol Biol *621*, 29-47.

Inskip, P. D., Robison, L. L., Stovall, M., Smith, S. A., Hammond, S., Mertens, A. C., Whitton, J. A., Diller, L., Kenney, L., Donaldson, S. S*., et al.* (2009). Radiation Dose and Breast Cancer Risk in the Childhood Cancer Survivor Study. J Clin Oncol *27*, 3901-3907.

Jensen, E. V., and Jordan, V. C. (2003). The Estrogen Receptor: A Model for Molecular Medicine. Clin Cancer Res *9*, 1980-1989.

Jerry, D. J., Kittrell, F. S., Kuperwasser, C., Laucirica, R., Dickinson, E. S., Bonilla, P. J., Butel, J. S., and Medina, D. (2000). A mammary-specific model demonstrates the role of the p53 tumor suppressor gene in tumor development. Oncogene *19*, 1052-1058.

Kaplan, H. S., Carnes, W. H., Brown, M. B., and Hirsch, B. B. (1956). Indirect Induction of Lymphomas in Irradiated Mice: I. Tumor Incidence and Morphology in Mice Bearing Nonirradiated Thymic Grafts Cancer Res *16*, 422-425.

Kuperwasser, C., Chavarria, T., Wu, M., Magrane, G., Gray, J. W., Carey, L., Richardson, A., and Weinberg, R. A. (2004). From The Cover: Reconstruction of functionally normal and malignant human breast tissues in mice. PNAS *101*, 4966-4971.

Labbe, E., Lock, L., Letamendia, A., Gorska, A. E., Gryfe, R., Gallinger, S., Moses, H. L., and Attisano, L. (2007). Transcriptional Cooperation between the Transforming Growth Factor-{beta} and Wnt Pathways in Mammary and Intestinal Tumorigenesis. Cancer Res *67*, 75-84.

Land, C. E., Boice, J. D., Shore, R. E., Norman, J. E., and Tokunaga, M. (1980). Breast cancer risk from low-dose exposures to ionizing radiation: Results of parallel analysis of three exposed populations of women. J Natl Cancer Inst *65*, 353-376.

Lim, E., Wu, D., Pal, B., Bouras, T., Asselin-Labat, M.-L., Vaillant, F., Yagita, H., Lindeman, G. J., Smyth, G. K., and Visvader, J. E. (2010). Transcriptome analyses of mouse and human mammary cell subpopulations reveal multiple conserved genes and pathways. Br Ca Res *12*, R21.

Mancuso, M., Pasquali, E., Leonardi, S., Tanori, M., Rebessi, S., Di Majo, V., Pazzaglia, S., Toni, M. P., Pimpinella, M., Covelli, V., and Saran, A. (2008). Oncogenic bystander radiation effects in Patched heterozygous mouse cerebellum. Proc Natl Acad Sci (USA) *105*, 12445-12450.

McCarthy, A., Savage, K., Gabriel, A., Naceur, C., Reis-Filho, J., and Ashworth, A. (2007). A mouse model of basal-like breast carcinoma with metaplastic elements. J Pathol *211*, 389-398.

Medina, D., Kittrell, F. S., Shepard, A., Contreras, A., Rosen, J. M., and Lydon, J. (2003). Hormone Dependence in Premalignant Mammary Progression. Cancer Res *63*, 1067-1072.

Medina, D., Kittrell, F. S., Shepard, A., Stephens, L. C., Jiang, C., Lu, J., Allred, D. C., McCarthy, M., and Ullrich, R. L. (2002). Biological and genetic properties of the p53 null preneoplastic mammary epithelium. Faseb J *16*, 881-883.

Morin Doody, M., Lonstein, J. E., Stovall, M., Hacker, D. G., Luckyanov, N., and Land, C. E. (2000). Breast cancer mortality after diagnostic radiography: findings from the U.S. Scoliosis Cohort Study. Spine *25*, 2052-2063.

NAS/NRC (2006). Health Risks from Exposure to Low Levels of Ionizing Radiation: Phase 2. In Board on Radiation Effects Research (BEIRVII), (Washington: National Academy Press).

Newman, J. C., and Weiner, A. M. (2005). L2L: a simple tool for discovering the hidden significance in microarray expression data. Genome Biol *6*, R81.

Parise, C. A., Bauer, K. R., Brown, M. M., and Caggiano, V. (2009). Breast Cancer Subtypes as Defined by the Estrogen Receptor (ER), Progesterone Receptor (PR), and the Human Epidermal Growth Factor Receptor 2 (HER2) among Women with Invasive Breast Cancer in California, 1998-2004. The Breast Journal *15*, 593-602.

Pavlidis, P., and Noble, W. (2001). Analysis of strain and regional variation in gene expression in mouse brain. Genome Biology *2*, research0042.0041 - research0042.0015.

Prat, A., Parker, J. S., Karginova, O., Fan, C., Livasy, C., Herschkowitz, J. I., He, X., and Perou, C. M. (2010). Phenotypic and molecular charcterization of the claudin-low intrinsic subtype of breast cancer. Br Ca Res *12*, R68.

Purton, L. E., and Scadden, D. T. (2007). Limiting Factors in Murine Hematopoietic Stem Cell Assays. Cell Stem Cell *1*, 263-270.

Saeed, A. I., Sharov, V., White, J., Li, J., Liang, W., Bhagabati, N., Braisted, J., Klapa, M., Currier, T., Thiagarajan, M*., et al.* (2003). TM4: a free, open-source system for microarray data management and analysis. Biotechniques *34*, 374-378.

Savarese, T., Strohsnitter, W., Low, H., Liu, Q., Baik, I., Okulicz, W., Chelmow, D., Lagiou, P., Quesenberry, P., Noller, K., and Hsieh, C.-C. (2007). Correlation of umbilical cord blood hormones and growth factors with stem cell potential: implications for the prenatal origin of breast cancer hypothesis. Breast Cancer Research *9*, R29.

Sell, S., and Pierce, G. B. (1994). Maturation arrest of stem cell differentiation is a common pathway for the cellular origin of teratocarcinomas and epithelial cancers. Lab Invest *70*, 6-22.

Shackleton, M., Vaillant, F., Simpson, K. J., Stingl, J., Smyth, G. K., Asselin-Labat, M. L., Wu, L., Lindeman, G. J., and Visvader, J. E. (2006). Generation of a functional mammary gland from a single stem cell. Nature *439*, 84-88.

Shelton, D. N., Fernandez-Gonzalez, R., Illa-Bochaca, I., Ortiz-de-Solorzano, C., Barcellos-Hoff, M. H., and Welm, B. E. (2010). Use of stem cell markers in dissociated mammary populations. Methods Mol Biol *621*, 49-55.

Tao, L., Roberts, A. L., Dunphy, K. A., Bigelow, C., Yan, H., and Jerry, D. J. (2010). Repression of Mammary Stem/Progenitor Cells by P53 is Mediated by Notch and Separable from Apoptotic Activity. STEM CELLS, N/A-N/A.

Tusher, V. G., Tibshirani, R., and Chu, G. (2001). Significance analysis of microarrays applied to the ionizing radiation response. Proc Natl Acad Sci U S A *98*, 5116-5121.

Wright, E.G. (2010). Manifestations and mechanisms of non-targeted effects of ionizing radiation. Mutat Res *687*, 28-33.

## Chapter 3

## Abstract

### Gene expression of the *Trp53* null BALB/c mouse mammary tumor model recapitulates human breast cancer subtypes

The tumors that spontaneously arise in the *Trp53* null BALB/c mouse mammary transplant model display a diverse histology and expression profiles that are affected by the carcinogenic effects of ionizing radiation mediated through the host microenvironment. In this study we compared the expression profiles of 56 *Trp53* null tumors of the radiation chimera experiments to human breast cancers. The past decade of molecular characterization has underscored the heterogeneity of breast cancer, prompting the consideration that this disease is of at least six subtypes with distinct clinical behaviors requiring specific therapies. Some of these subtypes arise due to specific genomic alterations, while others can be distinguished on the basis of their resemblance to the cell of origin within the mammary epithelium. Genetically engineered mouse models of breast cancer have come to the forefront to elucidate the mammary stem cell hierarchy and its relation to the development of breast cancer subtypes. We show that *Trp53* null BALB/c mouse tumors cluster with several distinct human breast cancer subtypes. Moreover we found that the expression profile based on the shift in estrogen receptor status in tumors from irradiated hosts defines the biology observed in human cancer. Furthermore, we show that the host microenvironment can mediate the effect of radiation to select for specific tumor subtypes and provide evidence that the normal-like class of breast cancer may arise from a progenitor cell of origin. *Trp53* null breast cancer is known for recapitulating aspects of human-breast cancer and our data further affirm its utility in dissecting the etiology of human breast cancers.

**Chapter 3 in context**

The previous chapter showed that host-irradiation was sufficient to promote breast cancer in transplanted *Trp53* null mammary fragments. Those experiments revealed that low dose radiation had persistent effects on tumor development that could be measured a year after exposure in the form of gene expression programs. This final chapter analyzes additional tumors from the radiation chimera experiments and compares them to gene expression profiles of human breast cancers. We show that *Trp53* null mouse tumors recapitulate the human breast cancer transcriptional subtypes and provide evidence suggesting that the normal-like class of human breast cancers may be derived from a mammary progenitor cell of origin.

## Chapter 3

### Introduction

Breast cancer is a complex disease that consists of at least six different subtypes that can identified by gene expression profiling (Perou et al., 2000; Prat et al., 2010; Sorlie et al., 2001) or by immunohistochemical profiling (Rakha et al., 2009; Tang et al., 2009). Marker analysis using the markers estrogen receptor-$\alpha$ (ER), progesterone receptor (PR), human epidermal growth factor receptor-2 (HER2), cytokeratin 5/6 (CK5/6), and cytokeratin 14 (CK14) is more widely used to classify tumors but there is growing appreciation that expression profiles provide not only prognostic value but novel information about the origins and evolution of cancer. The expression profile subclasses are designated luminal-A, luminal-B, HER2, normal-like, and basal-like, with claudin-low believed to be a subtype of basal-like (Prat et al., 2010). The "luminal" and "basal-like" categories of tumors were assigned based on the expression of genes that are also expressed in the luminal (i.e. ER, CK8, CK18) or basal compartment of the normal mammary epithelium (i.e CK5/6, CK14). The category "HER2" was derived from the observed genomic amplification and/or overexpression of the *HER2* gene. Luminal tumors are often low-grade, relatively differentiated, and express ER and PR, while basal-like tumors are often high-grade, poorly differentiated, exhibit metaplastic elements such as spindle and squamous foci, and do not express ER and PR (reviewed in (Perou and Borresen-Dale, 2011)). The distinct characteristics and clinical behaviors of each subtype suggest that detailed understanding of each could improve therapeutic outcomes (Cheang et al., 2009; Liu et al., 2010; Rakha et al., 2007; Rakha et al., 2009; Slamon et al., 2001).

Contemporaneous with the molecular definition of breast cancer subtypes was the ability to isolate a refined population of cells that enrich for mammary stem or progenitor cells using fluorescence activated cell sorting (FACS) (Shackleton et al., 2006; Stingl et al., 2006). Mammary stem cells are capable of symmetric division resulting in two stem cells, or assymetric division resulting in a stem cell and a progenitor cell. Though only a mammary stem cell, and not a progenitor cell, can repopulate a mammary gland in transplantation experiments, progenitors are bi-potent and can give rise mature luminal or mature myoepithelial/alveolar cells that comprise the majority of cells in the mammary ductal system (reviewed in (Visvader and Smith, 2010)). Both stem and progenitor cells likely reside mainly in the basal compartment of the epithelium and detailed FACS analysis revealed that they do not express ER, PR, or HER2 (Asselin-Labat et al., 2006; Sleeman et al., 2007). In addition, the ovarian hormones of estrus and those of pregnancy dramatically affected stem cell activity (Asselin-Labat et al., 2010). These discoveries led to the realization that certain breast cancer subtypes exhibited gene expression profiles that were similar to particular compartments of the stem cell hierarchy.

Breast cancer arising in women carrying the *BRCA1* mutation is a case in point for the utility of linking expression profiles and mammary hierarchy. Female carriers exhibit an expansion of the luminal progenitor population in phenotypically normal breast tissue. The transcriptional nature of these breast tissues, and that of basal-like tumors, is transcriptionally most similar to luminal progenitor cells, not stem cells (Lim et al., 2009). Moreover, knockout and knockdown

studies of the *BRCA1* gene, which regulates stem cell fate decisions, in specific compartments of the stem cell hierarchy has shed light on the origins of the basal-like class of breast cancer (Liu et al., 2008; Molyneux et al., 2010), giving hope that a similar knowledge will be gained for the origin of the other subtypes.

The field of breast cancer has come to recognize the crucial role of the microenvironment in regulating normal mammary morphogenesis and cancer (reviewed in (Bissell et al., 2002a; Sternlicht et al., 2006)). That recognition has been extended to the regulation of stem cells and tumor initiating cells by the microenvironment (reviewed in (Bissell and Inman, 2008; Bissell and Labarge, 2005)). Our studies of ionizing radiation, a known breast carcinogen, revealed that the microenvironment can also mediate radiation's carcinogenic effects (reviewed in (Barcellos-Hoff and Nguyen, 2009; Barcellos-Hoff et al., 2005)). Previous studies showed that the irradiated microenvironment can promote tumor development in epithelial cells that were never irradiated (Barcellos-Hoff and Ravani, 2000). We now show that even low doses of ionizing radiation (the equivalent of several CT scans (Parker et al., 2005)) can promote tumor development of un-irradiated *Trp53* null mammary fragments transplanted into inguinal mammary glands of previously irradiated syngeneic BALB/c recipients. Host-irradiation shortened tumor latency by several months and conferred higher tumor growth rates. These effects were dependent upon host levels of TGF$\beta$1, as host-irradiation did not promote tumors in the haplo-insufficient *Tgfb1* +/- background (Nguyen et al., 2011).

Genetically engineered mouse (GEM) models of breast cancer serve as useful tools for dissecting mechanisms of breast cancer development (Hennighausen and Robinson, 2001; Vargo-Gogola and Rosen, 2007). A limitation of many GEM models is that they may not reflect the diverse biology human breast cancers, since they result from deliberate perturbations of powerful oncogenes or tumor suppressors. In contrast the *Trp53* null BALB/c mammary tumor model shares many features in common with human breast cancer, including a long latency due to a gradual development from hyperplasia to invasive carcinoma, multiple histopathological subtypes, and variable degrees of ER expression (Jerry et al., 2000; Medina et al., 2002). One of the attractive features of the *Trp53* null BALB/c mammary tumor model is that it yields several different histopathological tumor subtypes (i.e. adenocarcinomas, spindle cell carcinomas, and squamous carcinomas) (Jerry et al., 2000; Medina et al., 2002; Nguyen et al., 2011). Furthermore, loss of *Trp53* has been shown to increase mammary stem cell self-renewal and thus numbers (Cicalese et al., 2009a; Tao et al., 2010a), suggesting that an altered stem cell hierarchy, in conjunction with the spontaneous nature of cancer initiating events, may make sense of the diverse histopathological subtypes observed. Perou and colleagues (Herschkowitz et al., 2007) compared gene expression patterns of 13 GEMs to human breast cancers and showed that certain GEMs do resemble human breast cancer subtypes. In that study, they examined five *Trp53* null tumors of the BALB/c strain of mice, and concluded that this model resembles basal-like breast cancers.

Our studies showed that *Trp53* null tumors from irradiated hosts are enriched for a mammary stem cell transcriptional program and were more frequently ER-negative (Nguyen et al., 2011). We identified two signatures that cluster tumors from irradiated hosts relative to those occurring in non-irradiated hosts. In this study we compared the gene expression profiles of 56 *Trp53* null tumors from the irradiated host experiments to human breast cancer and tested the

utility of these signatures in clustering human transcriptional subtypes. We show that a gene profile representing ER status in these mouse tumors also detects ER status in human breast cancers. Lastly, we present evidence suggesting that the normal-like class of breast cancers might be derived from a mammary progenitor cell of origin.

## Methods

Total RNA quality and quantity was determined using Agilent 2100 Bioanalyzer and Nanodrop ND-1000. Affymetrix mouse Genechip MG-430 2.0 arrays were used according to manufacturer's protocol. Background normalization was done by Robust Multichip Average algorithm (Bolstad et al., 2003) using R software v2.10.1 with widgets specific to the Affymetrix platform. Unsupervised hierarchical clustering was done using Gene Cluster v3.0 software and heatmaps were visualized using Java TreeView v1.1.4r3 software. Adjusted data means of gene expression values was centered by medians. Gene clustering was done by an uncentered-correlation and array clustering was done by Spearman Rank correlation. Pathways were identified with Ingenuity Pathway Analysis, or ConceptGen (http://conceptgen.ncibi.org/core/conceptGen/index.jsp). ConceptGen was used to determine significance of overlaps between two gene profiles under standard parameters.

Significance of analysis of microarray (SAM) was done using a two-class analysis with 100 permutations per comparison of the reference class to the target class, followed by a fold-change cut-off of 1.5 (Tusher et al., 2001). For extra stringency, a secondary, thus "tandem," bootstrapping was done by running the above SAM analysis iteratively, removing one sample from the reference class each time (Nguyen et al., 2011). For the TB-199 profile, only genes that were present in 100% of the secondary SAM analyses were included. For the ER-227 profile, genes that were present in at least 75% of the secondary SAM analyses were included.

Pavlidis Template Matching (PTM) (Pavlidis and Noble, 2001) was used to define patterns of genes induced only at one week, only at four weeks, or at both, in irradiated wild type or *Tgfb1* +/- mammary glands ($p<0.05$). The data was derived from GSE18216 generated in (Nguyen et al., 2011).

## Results

### *Trp53* null mouse tumors cluster with different human breast cancer subtypes.

In this study we obtained gene expression profiles of 56 *Trp53* null mouse tumors on a BALB/c background that were either wild type or *Tgfb1* heterozygote hosts, and were either irradiated or not. The mouse genome was "translated" to the human genome by identifying the 998 genes present on both the Affymetrix Human U133A and Mouse 430 2.0 platforms. This set of genes was then used to cluster the mouse tumors with either of two human breast cancer data sets. In both data sets, most of the *Trp53* null mouse tumors grouped within dendrogram clusters that contained a predominant human subtype (Figure 1). 59% (33 of 56) of the mouse tumors co-clustered with the same predominant subtype of human tumors from Pawitan et al. (2005) (Figure 1A) or from Chin et al. (2006) (Figure 1B), showing consistent associations between certain mouse tumors and certain human subtypes. 11 mouse tumors consistently

clustered with human basal-like tumors; 10 with luminal-A/B human tumors; and 12 with clusters containing luminal and normal-like human tumors. Interestingly, 11 of 20 mouse spindle cell carcinomas always clustered together in both human data sets while the remaining nine were distributed across the other sub-trees, suggesting that there are very distinct subsets within tumors of spindle cell morphology. Thus, the data confirm that *Trp53* null model gives rise to diverse transcriptional tumor subtypes similar to those observed in human breast cancer (Perou et al., 2000; Sorlie et al., 2001).

**ERα status of *Trp53* null mouse tumors reflects ER status of human breast cancers.**

The estrogen receptor-α (ER) is one of the most important clinical markers for human breast cancer, since its expression in tumors confers more favorable outcomes (Jensen and Jordan, 2003) and there exist effective therapies that target this protein (Fisher et al., 1998; Hackshaw et al., 2011). Our previous work showed that *Trp53* null tumors that arise from transplantation of un-irradiated *Trp53* null mammary fragments into syngeneic hosts that were previously irradiated were much more likely to be ER-negative (Nguyen et al., 2011). In this study we analyzed the gene expression of those tumors using significance analysis of microarray (SAM) analysis within a tandem-boot-strapping scheme to identify genes modulated by at least 1.5-fold in ER-positive (ER+) tumors compared to ER-negative tumors, and found a profile of 227 genes (designated the ER-277, Table S1). The ER-227 was able to cluster the majority of ER+ mouse tumors from the ER-negative mouse tumors, independent of host-irradiation status or histopathology (Figure 2A). 156 of the ER-227 genes were present on the Affymetrix Human U133A platform and were isolated within each of three independent human breast cancer data sets for which ER status was known. Unsupervised hierarchical clustering of these 156 genes for each data set was done to determine if the ER-227 could cluster human ER+ breast cancers from ER-negative cancers. Indeed, the ER-227 identified subgroups of ER-negative human breast cancers very readily in the data set from GSE7390 (Desmedt et al., 2007), GSE2034 (Wang et al., 2005), and E-TABM-158 (Chin et al., 2006) (Figure 2B-D). The ability of the ER-227, which was derived from tumors assigned as ER+ or ER-negative using the Allred Score (Harvey et al., 1999), to classify ER status in three independent human breast cancer data sets underscores the validity of the marker classification, as well as the human-like quality of the *Trp53* null mouse model.

Comparison of the ER-227 to gene profiles of known biological processes in the ConceptGen database showed that it significantly overlapped with several extracellular matrix programs and several inflammation programs (all $p<0.0005$). Given that breast cancers of the basal-like class tend to be negative for the expression of ER (Sleeman et al., 2007) and often arise from an ER-negative mammary stem (MaSC) or progenitor (MaP) cell of origin (reviewed in (Visvader, 2011)), we compared the ER-277 to gene profiles from enriched populations of MaSCs and MaPs to determine if there was any overlap (Kendrick et al., 2008; Lim et al., 2009; Lim et al., 2010b). Indeed, there was significant overlap between the ER-227 and MaSC or MaP profiles (all $p<1.0E-7$, data not shown), suggesting that the ability of the ER-227 to detect ER status could be understood through the presence of stem- or progenitor-related genes. Supporting this idea are the gene clusters of up-regulated probes representing the human ER-negative tumors detected by the ER-227, which suggest a stem or progenitor cell of origin (data not

shown). Among these genes are P-cadherin (*CDH3*) and cytokeratin 5 (*CK5*), both of which are key genes in the profile that identifies basal-like breast cancer (Laakso et al., 2005; Potemski et al., 2007; Sorlie et al., 2001). Cytokeratin 15 (*CK15*) is expressed in stem cells of the skin (Webb et al., 2004), stem cells in the hair follicle bulge (Ohyama et al., 2006), and putative mammary progenitor cells (Celis et al., 2007). S100 calcium binding protein A8 (*S100A8*) is expressed in ER-negative breast cancers and correlates with the expression of P-cadherin, a basal-like breast cancer gene (Glynn et al., 2010). And the ETS-family transcription factor E74-like factor 5 (*ELF5*) regulates cell fate decisions of alveolar progenitors of the mammary gland (Choi et al., 2009; Oakes et al., 2008). Thus, the correlation of these up-regulated genes with the detection of ER-negative cancers by the ER-227 suggests that ER-negative "cells of origin" are the actual target of this profile (an idea that is reviewed in (Visvader, 2011)).

**The 156-IHC detects human breast cancer subtypes and ER status.**

Our previous study derived a profile of 156 genes (156-IHC) modulated by at least 1.5-fold in un-irradiated *Trp53* null tumors arising in irradiated wild type BALB/c mice and showed that it shared significant overlap with gene profiles of MaSCs (Nguyen et al., 2011). Here, we determined if the 156-IHC could detect human breast cancer subtypes via unsupervised hierarchical clustering. 62 genes of the 156-IHC were present in the Affymetrix Human U133A platform that was used to analyze human breast cancers in three independent cohorts (Chin et al., 2006; Desmedt et al., 2007; Wang et al., 2005). The 156-IHC was able to cluster basal-like cancers apart from luminal-A/B cancers very well, which also correlated with a detection of ER-negative vs. ER+ cancers, respectively (Figure 3A). Furthermore, the 156-IHC was able to segregate ER+ from ER-negative cancers in two other human breast cancer data sets (Figure 3B & C). Interestingly, the gene cluster that was up-regulated within, and thus represented, the clusters of ER-negative tumors are genes involved in stem cell, progenitor cell, or tumor initiating cell activity (data not shown), consistent with the idea that an ER-negative tumor cell of origin, such as mammary stem or progenitor cells, will result in an ER-negative cancer (reviewed in (Visvader, 2011)).

**Host irradiation cooperates with TGFβ1 to determine tumor transcriptional subtypes.**

The tumor promoting effects of host irradiation (decreased latency, increased growth rate) observed in wild type mice was abrogated in *Tgfb1* heterozygote hosts, suggesting that stromal TGFβ1 is a key mediator of this effect (Nguyen et al., 2011). Gene expression analysis was performed on 48 tumors in our published study and the data stored under accession GSE18216 on the Gene Expression Omnibus database. We analyzed an additional eight tumors from irradiated *Tgfb1* +/- host mice, yielding six tumors from non-irradiated heterozygote hosts for comparison with 18 tumors from irradiated heterozygote hosts.

In order to determine the predominant transcriptional biology of tumors arising in irradiated *Tgfb1* +/- hosts compared to those from non-irradiated heterozygote hosts, we used SAM analysis within a tandem-boot-strapping scheme as previously described (Nguyen et al., 2011; Tusher et al., 2001). Interestingly, SAM tandem boot-strap comparison of tumors from non-irradiated wild type hosts to those from non-irradiated heterozygote hosts did not reveal any significantly modulated genes, suggesting that compromised levels of host TGFβ1 alone does

not significantly alter the transcriptional biology of *Trp53* null tumors. We identified 199 genes that were modulated by at least 1.5-fold in tumors that occurred in irradiated *Tgfb1* +/- hosts (designated as the TB-199) (Table S2). The TB-199 was able to segregate tumors of irradiated heterozygote hosts from those of non-irradiated heterozygote hosts under unsupervised hierarchical clustering, independent of ER status or histopathology (Figure 4A). It did not do so when applied to tumors from wild type hosts (Figure 4B). Interestingly, our previous work found a profile of 156 genes (156-IHC, irradiated host core) derived by the same method as for the TB-199, but in tumors from irradiated wild type hosts, that detected host-irradiation by UHC only in wild type hosts (Nguyen et al., 2011). Thus, the effectiveness of both the 156-IHC and TB-199 in detecting host-irradiation is specific to host *Tgfb1* genotype, but host-irradiation, not just compromised host TGF$\beta$1 levels, is required to result in a distinct transcriptional biology within *Trp53* null tumors. However, subtle but important differences in transcription resulting solely from host *Tgfb1* genotype may remain undetected given the highly stringent metric of tandem boot-strapping the SAM analysis, and the sample size of our heterozygote host tumors.

We performed gene network analysis of the TB-199 using Ingenuity Pathway Analysis (IPA) software and found that the top two major networks resemble programs in cellular growth and proliferation, cellular development, and immunological disease (Figure 4C, IPA score=79); and gastrointestinal disease, hepatic system disease, and lipid metabolism (Figure 4D, IPA score=78). IPA also revealed enrichment for cancer related genes, along with inflammatory processes such as recruitment and activation of lymphocytes and phagocytes (all $p<0.005$). Furthermore, gene enrichment analysis comparing the overlap of genes in the TB-199 with gene profiles of known biological processes in published literature using the ConceptGen database revealed that extracellular matrix programs and activation of monocytes, macrophages, and dendritic cells were significantly represented in the TB-199 (all $p<0.005$).

Though the 156-IHC and TB-199 detect host-irradiation status only within their respective host genotypes, there are eight genes that overlap between these two lists. Seven of the eight genes have been reported to be involved in stem cell, progenitor cell, and/or tumor initiating cell activity. Interestingly, five of these seven "stem-related" genes are oppositely regulated between the two profiles, suggesting mechanistic insights into the distinction that results from the combination of host-irradiation and host *Tgfb1* genotype (Table 1). One of the most telling genes in this overlap is tumor protein 63 (*Tp63*), which is a expressed in basal cells of the mammary gland (Ribeiro-Silva et al., 2003) and is associated with other basal markers expressed in metaplastic breast cancers that are believed to be derived from the basal compartment (Reis-Filho et al., 2003). *Tp63* induces stem-like phenotypes when ectopically over-expressed in the MCF7 breast cancer cell line (Du et al., 2010) and is required for the ubiquitous maintenance of stem cell populations in epithelial tissues (Yang et al., 1999). Thus, *Tp63* is a key gene in the gene cluster that represents the basal-like subtype of breast cancers as identified by gene expression profiling (Herschkowitz et al., 2007).

Interestingly, *Tp63* is up-regulated in the 156-IHC, but down-regulated in the TB-199, suggesting that the 156-IHC may be characterized by similarity to basal-like breast cancers, while the TB-199 may resemble other tumor subtypes. Consistent with this idea, inhibitor of differentiation 4 (*Id4*), is also up-regulated in the 156-IHC, but down-regulated in the TB-199.

Id4 is a negative regulator of *BRCA1* (Beger et al., 2001) that is expressed 9-fold higher in basal-like breast cancers over controls (Turner et al., 2007). Mutations or inhibition of the *BRCA1* gene result in a propensity for basal-like breast cancers (Narod and Foulkes, 2004). Along with *Tp63* and *Id4*, insulin-like growth factor binding protein 2 (*Igfbp2*) is also up-regulated in the 156-IHC, but down-regulated in TB-199. *Igfbp2* has also been shown to be involved in the activity of "stem-like" tumor initiating cells (Hsieh et al., 2010; Villani et al., 2010). This inverse pattern suggests that there is a distinction between these signatures. Furthermore, one gene that is present only in the TB-199, *Cd133* (a.k.a. Prominin-1), is a marker of progenitor cells and cancer initiating cells in several cancer types including breast cancer (Wang et al., 2010; Wright et al., 2008a; Zucchi et al., 2008). Thus, based on the inverse expression pattern of *Tp63*, *Id4*, and *Cd133* the 156-IHC may be more basal-like and TB-199 may represent another tumor subtype transcriptional program.

Several recent studies highlighted the similarity of transcriptional programs between basal-like breast cancers and luminal progenitors, supporting the idea that certain tumors may reflect their tumor cell of origin (reviewed in (Visvader, 2011)). To further test the hypothesis that the difference between the 156-IHC and the TB-199 could be understood as cell type specific transcriptional programs, we determined if these two profiles overlap with gene profiles from purified populations enriched with mammary stem cells (MaSCs), mammary progenitor cells (MaPs), or differentiated mammary epithelial cells, since there is evidence that tumor subtypes may reflect their cell of origin (Bouras et al., 2008b; Lim et al., 2009; Molyneux et al., 2010). Gene expression profiles from purified populations of MaSCs or MaPs from human or mouse mammary tissue showed that while MaSC and myoepithelial programs significantly overlapped with both the 156-IHC and TB-199, the luminal progenitor programs distinctly enriched only with the TB-199 (Table 2) (Table S3, overlap lists) (Kendrick et al., 2008; Lim et al., 2009; Lim et al., 2010b). Thus, the feature that distinguishes between the 156-IHC and TB-199 profiles is the presence of a luminal progenitor program in *Trp53* null tumors arising in irradiated *Tgfb1* +/- hosts.

Moreover, this theme of a luminal progenitor program that is specific to irradiated *Tgfb1* +/- hosts was also observed in irradiated normal mouse mammary glands. Nguyen et al. (2011) showed that a low dose (10 cGy) of ionizing radiation resulted in persistent changes in gene expression in the normal mouse mammary gland at one and four weeks after irradiation. Comparison of wild type and *Tgfb1* +/- mice revealed that radiation affects hundreds of genes in a TGFβ-dependent manner. We re-analyzed that data using Pavlidis Template Matching (PTM) (Pavlidis and Noble, 2001) to identify genes that were induced by radiation only at one week, only at four weeks, or at both time points, in each genotype (Table S4). We then determined if the profiles from these time points in each genotype had any overlap with the mammary stem or progenitor profiles from Lim et al. (2010b). Just as was observed between the 156-IHC and TB-199 profiles from irradiated wild type or *Tgfb1* +/- hosts, respectively, the MaSC program was present in both irradiated wild type and *Tgfb1* +/- glands, but the MaP program was present only in *Tgfb1* +/- tissue (Table 3). This result has given insight into a striking result we found in Nguyen et al. (2011) in which *Trp53* null tumors arising in irradiated hosts of either wild type or *Tgfb1* +/- genotype were more frequently ER-negative, with a more dramatic observed in the *Tgfb1* +/- hosts. The PTM analysis presented here suggests that the

more pronounced effect of ER-negative tumors in heterozygote hosts may be because of an expansion in not just the MaSCs, but also MaPs after irradiation. It is known that neither MaSCs or MaPs express ER (Sleeman et al., 2007). Thus, while host irradiation gives rise to ER-negative tumors in both genotypes, the cell of origin may be distinct because radiation expands both MaSCs and MaPs in *Tgfb1* heterozygote hosts.

**The TB-199 detects human breast cancer subtypes.**

Given that the TB-199, like the 156-IHC, significantly overlapped with genes involved in MaSCs and MaPs (Table 2), we determined whether the TB-199 could detect human breast cancer subtypes or ER status via unsupervised hierarchical clustering. 91 genes of the TB-199 were present on the Affymetrix Human U133A platform that was used to analyze human breast cancers in three independent cohorts (Chin et al., 2006; Desmedt et al., 2007; Wang et al., 2005). The TB-199 was able to cluster basal-like tumors apart from luminal-A/B tumors, and to detect ER-negative and ER+ status, respectively (Figure 5A). The TB-199 was also able to detect ER status in the data sets from Desmedt et al. (2007) and Wang et al. (2005) (data not shown).

A study by Perou and colleages (Prat et al., 2010a) derived gene profiles for the claudin-low, basal-like, luminal-A/B, HER2, and normal-like subtypes from a large pool of human breast cancers using SAM analysis. The most interesting aspect of the TB-199 was its ability to detect the normal-like class of breast cancers on Pawitan's patient cohort (Figure 5B). In order to refine these profiles we then used a 3-fold cut-off and selected only genes that were unique to each subtype. To our surprise, the normal-like profile showed significant overlap with the TB-199 profile. Six (*Atp1a2, Slpi*, *Col17a1, Apod, Actg2, Krt5)* of the 91 genes of the TB-199 that were used to cluster Pawitan et al.'s data (2005) significantly ($p<2.0E-5$) overlapped with the normal-like profile derived from Prat et al. (2010).

Given this link between the TB-199 and normal-like cancer profile, we hypothesized that the TB-199 would be able to detect normal-like cancers in other studies. The PMC42 human breast cancer cell line is a bi-potent cell line that can be induced to differentiate into luminal or myoepithelial phenotypes (Whitehead et al., 1983). Caldas and colleagues (Git et al., 2008) showed that PMC42 cells were similar to normal breast tissue by virtue of mRNA and micro-RNA profiling, while being different from luminal or basal-like breast cancer cell lines. We did unsupervised hierarchical clustering of the mRNA gene expression data of the cell lines from Git et al. using the TB-199 profile. The TB-199 was able to segregate the PMC42 cell line apart from the basal-like and luminal cell lines, while maintaining the similarity of the PMC42 cells to normal breast tissue (Figure 5C). Interestingly, the gene cluster that is up-regulated within, and represents, the PMC42 cells (Figure 5C, vertical brown bar) shares a 14 gene overlap with the gene cluster that represents the normal-like tumors detected by the TB-199 in Pawitan's data set (Figure 5B vertical brown bar, and 5D). Furthermore, this normal-like gene cluster of Pawitan's data contains the aforementioned six genes that overlap between the TB-199 and Prat et al.'s (2010) normal-like profile. Thus, the TB-199 signature detects normal-like breast cancers across three independent studies (Git et al., 2008; Pawitan et al., 2005; Prat et al., 2010a). Given the progenitor-like transcriptional program present in the TB-199 and the bi-potent progenitor nature of PMC42 cells, these data suggest that normal-like breast cancers may arise from a mammary progenitor cell of origin.

**Discussion**

The past decade of research has demonstrated that there are distinct transcriptional subtypes of breast cancer (Perou et al., 2000; Sorlie et al., 2001) and that breast cancers contain cancer initiating cells (Al-Hajj et al., 2003) that are refractory to certain therapeutics (Diehn et al., 2009). This has shed light on the inefficacy of certain modes of therapy while highlighting the need for more accurate models that reflect the complexity of this disease. Breast cancer cell lines are the easiest models for experimental manipulation and can reflect important aspects of human breast cancer, such as subtype specificity (Neve et al., 2006) and cancer initiating cells (Lagadec et al., 2010; Phillips et al., 2006). Genetically engineered mouse models provide a higher order complexity that incorporates the intricacies of the entire organism. There are many mouse models that mimic certain aspects of human breast cancer (Vargo-Gogola and Rosen, 2007), but due to the nature of over-expressing an oncogene or removing a tumor suppressor, most yield cancers that are overly aggressive and/or exhibit a single tumor phenotype.

The *Trp53* null BALB/c model has several features in common with human breast cancer, including progression from early stages of hyperplasia, dysplasia, neoplasia, and ductal carcinoma *in situ* (DCIS), to invasive breast cancer that can be one of several different histopathological subtypes. The DCIS stage occurs around six months after puberty, with aneuploidy observed around eight months, and tumors occur with a median latency of 12 months (the approximate mid-life of the mouse). Furthermore, the DCIS lesions can be ER+ or ER-negative, as are the resulting tumors, and to varying degrees (Jerry et al., 2000; Medina, 2002; Nguyen et al., 2011). In this study, gene expression profiling of 56 *Trp53* null tumors provides further evidence of relevance of this tumor model by revealing that these mouse tumors are similar to certain human breast cancer subtypes. Herschkowitz et al. (2007) analyzed the gene expression of many different mouse mammary tumor models, including five *Trp53* null tumors, and showed that each model does show similarity to a certain human subtype. Their conclusion regarding the *Trp53* null model was that it was most similar to the basal-like class. Our analysis of 56 *Trp53* null tumors supported yet expanded this conclusion, since we show that some of our tumors were similar to human basal-like cancers, while others associated with luminal or normal-like cancers.

In addition, we show that the ER-227 profile derived from ER+ *Trp53* null mouse tumors effectively detected ER-status of human breast cancers. An interesting insight from the ER-227 is that its detection of ER status in data sets in which progesterone receptor (PR) and human epidermal growth factor receptor-2 (HER2) expression were known revealed that it also detected PR and HER2 status (data not shown). This suggests that what the ER-227 is actually detecting, via clustering, is the stem/progenitor-like nature of basal-like tumors, which is correlated with the absence of ER (Bouras et al., 2008b; Lim et al., 2009; Molyneux et al., 2010). Supporting this idea are the genes present in the gene cluster of up-regulated probes representing the human ER-negative tumors detected by the ER-227 (data not shown). A number of these up-regulated genes are associated with stem and/or progenitor activity. For example, P-cadherin (*CDH3*) and cytokeratin 5 (*CK5*) are key genes in the profile that identifies

basal-like breast cancer (Laakso et al., 2005; Potemski et al., 2007; Sorlie et al., 2001). Cytokeratin 15 (*CK15*) is expressed in stem cells of the skin (Webb et al., 2004), stem cells in the hair follicle bulge (Ohyama et al., 2006), and putative mammary progenitor cells (Celis et al., 2007). S100 calcium binding protein A8 (*S100A8*) is expressed in ER-negative breast cancers and correlates with the expression of P-cadherin, a basal-like breast cancer gene (Glynn et al., 2010). And the ETS-family transcription factor E74-like factor 5 (*ELF5*) regulates cell fate decisions of alveolar progenitors of the mammary gland (Choi et al., 2009; Oakes et al., 2008). Thus, the ability of the ER-227 to detect ER status is likely due to genes that are active in stem and progenitor cells. This is consistent with the "cell of origin" hypothesis of breast cancer, which posits that breast cancer subtypes share similar transcriptional profiles to their cells of origin (reviewed in (Visvader, 2011)). Application of the cell of origin hypothesis has provided new insights into differences among tumor subtypes. By marker analysis, tumors from BRCA1 mutation carriers are often ER-negative and basal-like, and thus were thought to arise from mammary stem cells. However recent studies showed that *BRCA1* mutations expand the mammary progenitor cell population that gives rise to the tumors, which share similar transcriptional programs to the progenitor cells (Bouras et al., 2008b; Lim et al., 2009; Molyneux et al., 2010).

Our previous work showed that the tumor microenvironment can mediate the carcinogenic effects of ionizing radiation (Barcellos-Hoff and Ravani, 2000) on un-irradiated *Trp53* null transplants that later gave rise to tumors; and that this effect was dependent on TGF$\beta$1 levels in the host (Nguyen et al., 2011). In that study we derived the 156-IHC profile and in this study we derived the TB-199 profile; each were able to detect the effect of host-irradiation on tumors, in wild type or *Tgfb1* +/- hosts, respectively. In this study we showed that both profiles were able to detect human breast cancer subtypes in several independent data sets. Both profiles displayed a proficiency for segregating basal-like from luminal-A/B subtypes, but the unexpected observation was that the TB-199 clearly detected the normal-like subtype. We further confirmed the association between the TB-199 and normal-like subtype by showing that the TB-199 could identify the normal-like PMC42 cell line apart from basal-like and luminal-type cell lines. We also found a significant overlap between the TB-199 and a gene profile of normal-like cancers from Prat et al. (2010a). Interestingly, the TB-199 contains a mammary progenitor transcriptional program and the PMC42 cells are progenitors. Thus, there is compelling indication that normal-like breast cancer may be derived from a mammary progenitor cell of origin. Consistent involvement of the same set of genes in the detection of normal-like cancers across this study and three others suggests that these candidate genes that may be involved in the etiology of normal-like cancers in the *Trp53* null model. Further work will be required to confirm this.

Our analysis of genes induced by radiation in wild type or *Tgfb1* +/- mammary glands at one or four weeks after irradiation showed the presence of a MaSC transcriptional program in both genotypes, but a MaP program only in heterozygote tissue. The *Trp53* gene has been shown to regulate symmetric division of MaSCs, and *Trp53* null status results in a dramatic expansion of this population during the transition from puberty to adulthood (Cicalese et al., 2009a). There is evidence that Notch1 signaling is one of the mediators of this process in *Trp53* null MaSCs (Tao et al., 2010a) and in wild type MaSCs after exposure to low dose radiation (Nguyen et al.,

2011). This made sense of our previous data in which *Trp53* null tumors from irradiated wild type or *Tgfb1* +/- hosts were more frequently ER-negative, but more so in those from irradiated *Tgfb1* +/- hosts (Nguyen et al., 2011). It is likely that this is due to the expansion of both the MaSC and MaP populations in irradiated heterozygote tissues, both of which are ER-negative (Sleeman et al., 2007). The same dose of radiation increased MaSC numbers in wild type mammary glands as evidenced by limiting dilution for repopulating activity and FACS analysis of the cell surface markers Cd24 and Cd29 (Nguyen et al., 2011). We have yet to do this FACS analysis on irradiated *Tgfb1* +/- glands, but our data suggests that we will see an increase in the progenitor population.

In summary, this study highlights the unique qualities of the *Trp53* null BALB/c mammary tumor model, revealing that it recapitulates key human breast cancer transcriptional subtypes. It also yields a transcriptional profile of ER status that is relevant to human breast cancers and provides novel insights into the normal-like subtype of breast cancer. This makes the *Trp53* null BALB/c model highly attractive for *in vivo* mechanistic studies of breast cancer etiology and useful for future studies to examine subtype specific response to therapeutic modalities.

**Figure Legends**

**Figure 1. *Trp53* null mouse tumors co-cluster with different human breast cancer subtypes.** *Trp53* null mouse tumors were clustered along with human breast cancers by combining the mouse and human data sets using the genes that overlap between the Affymetrix Human U133A and Mouse 430 2.0 platforms. Unsupervised hierarchical clustering showed that certain mouse tumors clustered in sub-trees that contained human tumors of a predominant subtype. This was observed when our *Trp53* null tumors were clustered with the data set from (A) Chin et al. (2006) and (B) Pawitan et al. (2005). 59% (33 of 56) of the mouse tumors co-clustered with the same predominant human subtype when combined with either human data set. Human tumors: luminal-A, light blue; luminal-B, dark blue; no subtype, light gray; HER2, green; basal-like, red; normal-like, khaki; white, not applicable or not available. Mouse tumors: adenocarcinoma, pink; spindle cell carcinoma, dark brown; ER+, yellow; ER-negative, orange; sham-irradiated host, red; irradiated-host, purple; wild type host, gray; *Tgfb1* +/- host, black.

**Figure 2. ER-profile of mouse tumors detects ER status of human breast cancers**. (A) ER-227 detects ER status of the *Trp53* null mouse tumors from which it was derived. The effect is independent of host-irradiation status or histopathology of the tumors, and thus specific to ER status. (B-D) Three independent human breast cancer data sets were clustered via unsupervised hierarchical clustering by the 156 genes of the ER-227 that were present on the Human U133A platform. The ER-227 can detect ER status of human breast cancers. ER+, yellow; ER-negative, orange; sham-irradiated host, red; irradiated-host, purple; adenocarcinoma, pink; spindle cell carcinoma, dark brown.

**Figure 3. 156-IHC detects human breast cancer subtypes.**
In Nguyen et al. (2011) SAM analysis identified 156 genes, the 156-IHC, modulated by at least 1.5-fold in *Trp53* null tumors arising in irradiated wild type hosts, compared to those from sham-irradiated wild type hosts. Three independent human breast cancer data sets were clustered via unsupervised hierarchical clustering by the 62 genes of the 156-IHC were present in the Affymetrix Human U133A platform. (A) The 156-IHC segregated basal-like from luminal-A/B tumors and consequently detected their ER status. (B & C) The 156-IHC also detected ER status of human cancers from Wang et al. (2005) and Dedsmedt et al. (2007), respectively.

**Figure 4. Host irradiation in the *Tgfb1* +/- background yields a distinct gene profile.**
SAM analysis identified 199 genes, the TB-199, modulated by at least 1.5-fold in *Trp53* null tumors arising in irradiated *Tgfb1* +/- hosts, compared to those from sham-irradiated heterozygote hosts. (A) The TB-199 detects host irradiation status of the tumors from which it was derived. The effect is independent of ER status or histopathology of the tumors, and thus specific to host-irradiation status. (B) The TB-199 does not detect host-irradiation status in tumors arising in irradiated wild type hosts. Sham-irradiated host, red; irradiated-host, purple; ER+, yellow; ER-negative, orange; adenocarcinoma, pink; spindle cell carcinoma, dark brown. (C) The top gene network within the TB-199 identified by Ingenuity Pathway Analysis (score, 79) includes programs in cellular growth and proliferation, cellular development, and

immunological disease. (D) The second highest ranked IPA network (score, 78) includes programs in gastrointestinal disease, hepatic system disease, and lipid metabolism.

**Figure 5. TB-199 detects normal-like and other human breast cancer subtypes.**
Three independent data sets from human breast cancers were clustered via unsupervised hierarchical clustering by the 91 genes of the TB-199 profile that were present on the Affymetrix Human U133A platform. (A) TB-199 segregates basal-like from luminal-A/B tumors and consequently detected their ER status. (B) TB-199 segregates the various human breast cancer subtypes, but detects the normal-like class of tumors very well. Vertical khaki bar, gene cluster of induced genes representing normal-like tumors. (C) The TB-199 segregates the normal-like PMC42 cell line apart from basal-like and luminal-type cell lines, while maintaining the similarity between PMC42 cells and normal breast tissue. Vertical khaki bar, gene cluster of induced genes representing the PMC42 cells. (D) Gene cluster of induced genes representing normal-like tumors in panel B. Luminal-A, light blue; luminal-B, dark blue; no subtype, light gray; HER2, green; basal-like, red; normal-like, khaki; black, normal breast tissue; white, not applicable.

Figure 1

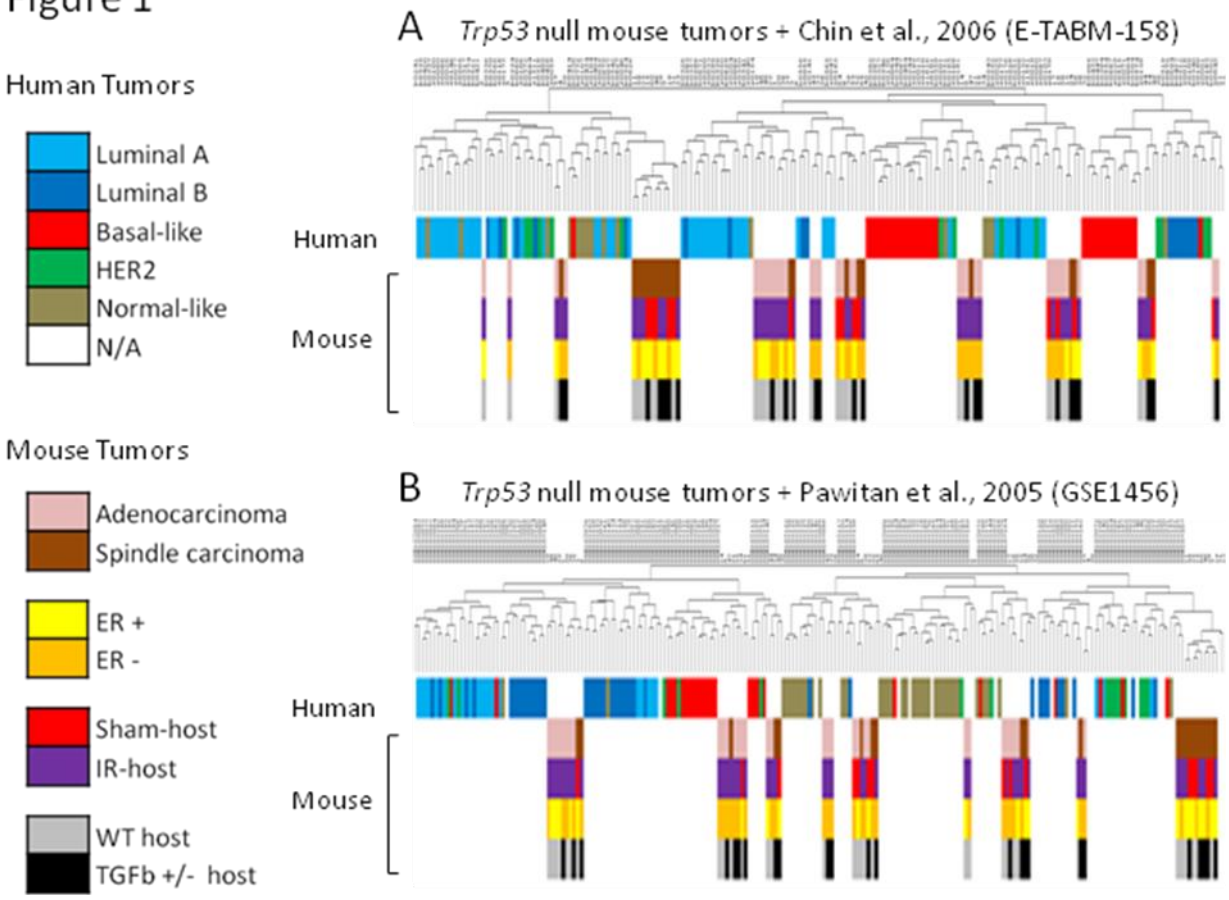
A
Trp53 null mouse tumors + Chin et al., 2006 (E-TABM-158)
Human Tumors
Luminal A
Luminal B
Basal-like
HER2
Normal-like
N/A
Human
Mouse
B
Trp53 null mouse tumors + Pawitan et al., 2005 (GSE1456)
Mouse Tumors
Adenocarcinoma
Spindle carcinoma
ER +
ER -
Sham-host
IR-host
WT host
TGFb +/- host
Human
Mouse

Figure 2

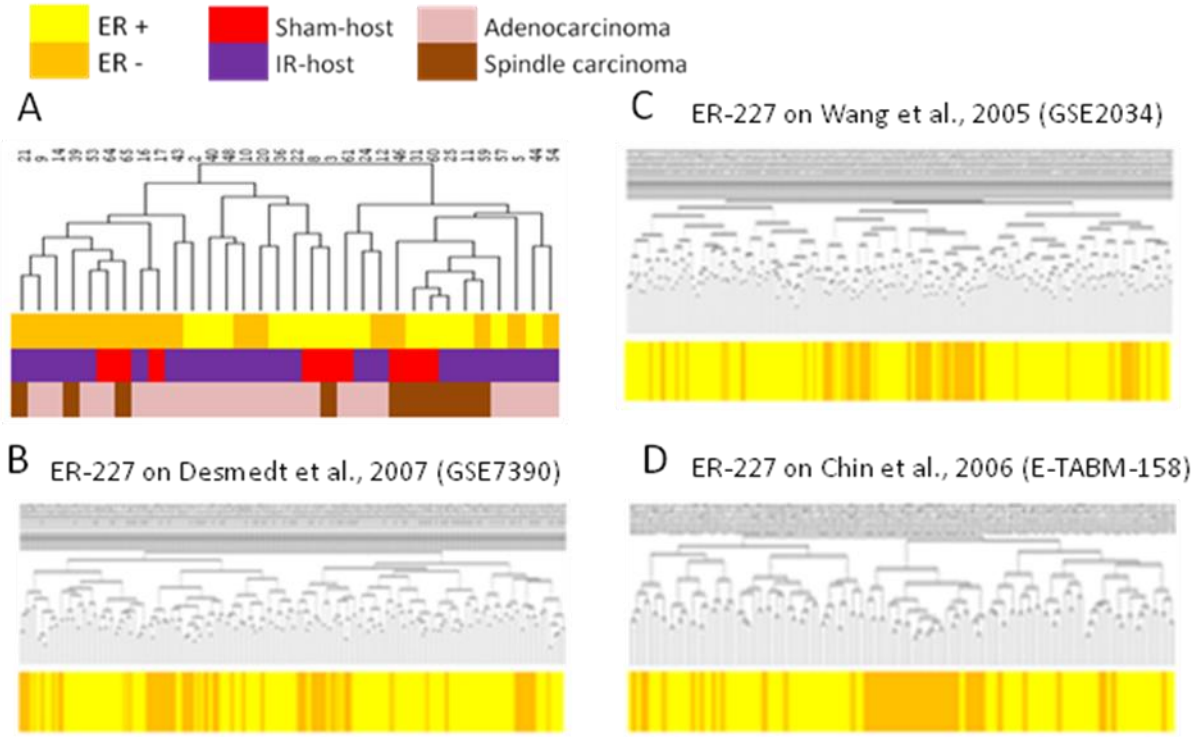
ER +
ER -
Sham-host
IR-host
Adenocarcinoma
Spindle carcinoma
A
C
ER-227 on Wang et al., 2005 (GSE2034)
B
ER-227 on Desmedt et al., 2007 (GSE7390)
D
ER-227 on Chin et al., 2006 (E-TABM-158)

Figure 3

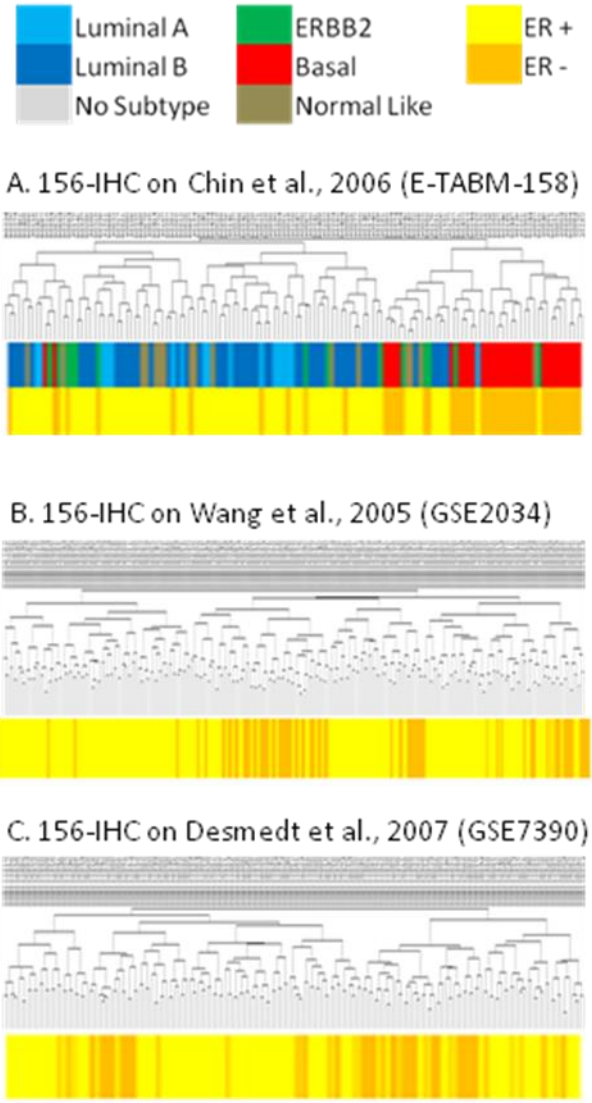
Luminal A
Luminal B
No Subtype
ERBB2
Basal
Normal Like
ER +
ER -
A. 156-IHC on Chin et al., 2006 (E-TABM-158)
B. 156-IHC on Wang et al., 2005 (GSE2034)
C. 156-IHC on Desmedt et al., 2007 (GSE7390)

Figure 4

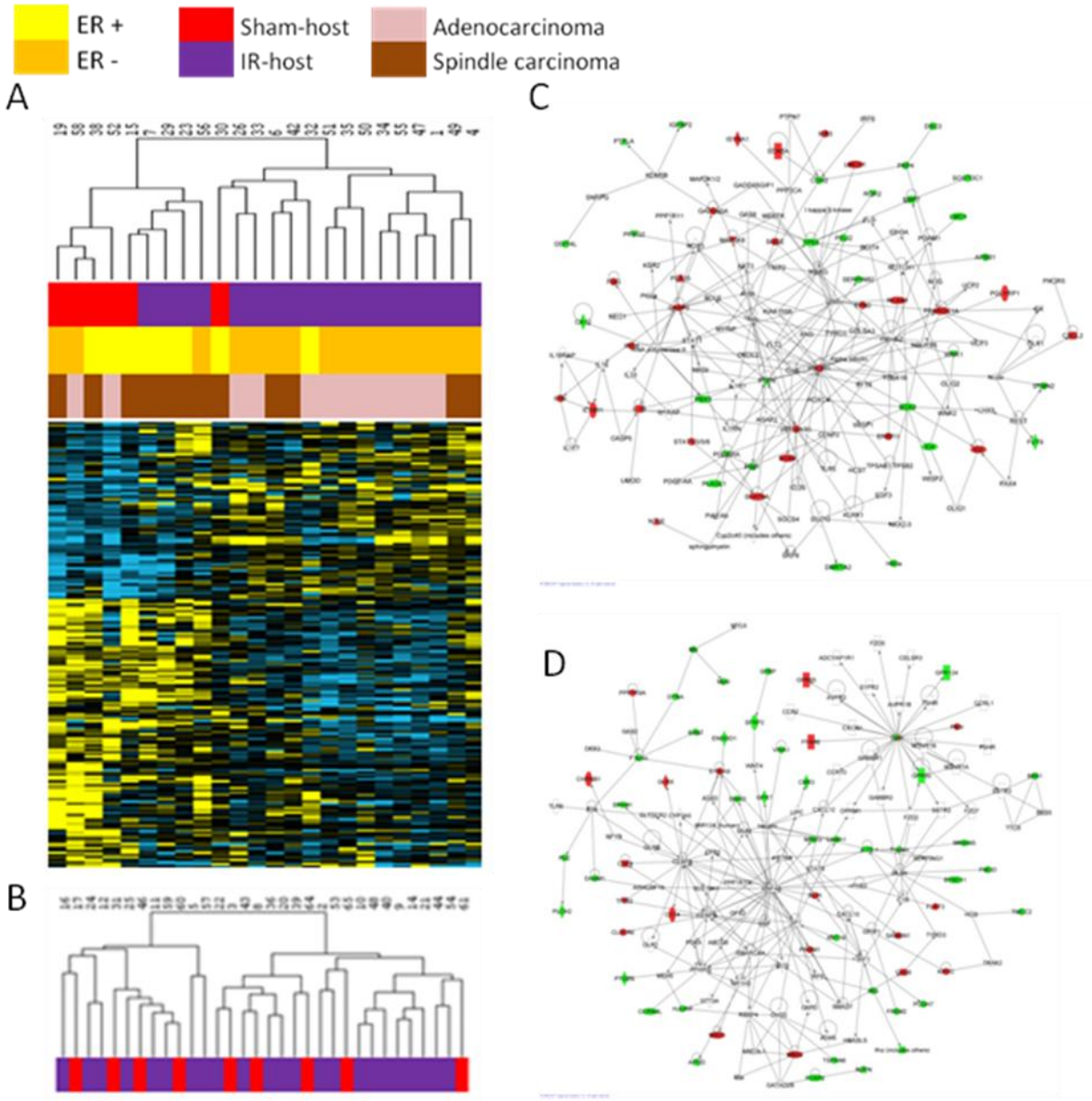
ER +
ER -
Sham-host
IR-host
Adenocarcinoma
Spindle carcinoma
A
B
C
D

Figure 5

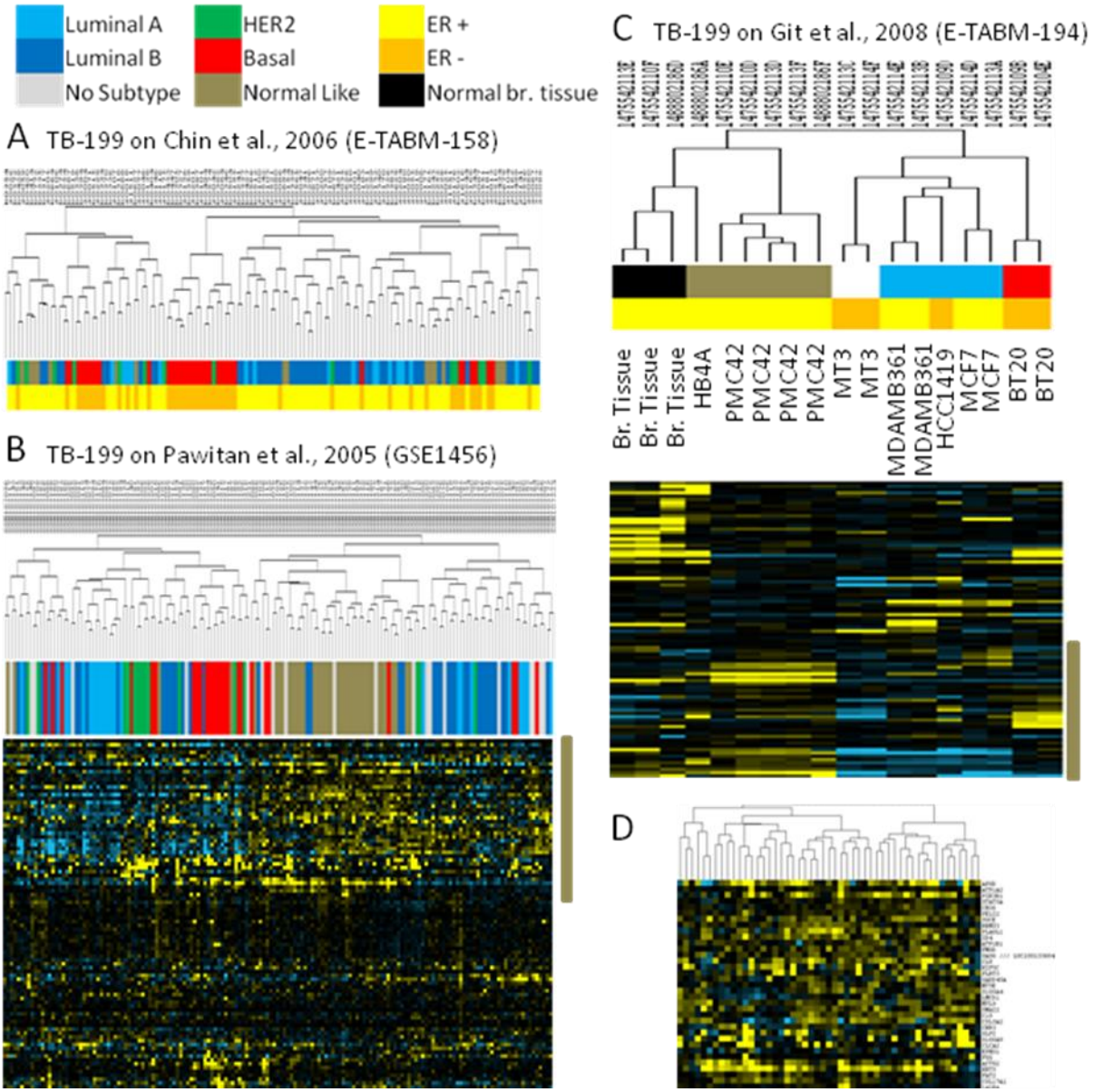
Luminal A
Luminal B
No Subtype
HER2
Basal
Normal Like
ER +
ER -
Normal br. tissue
A TB-199 on Chin et al., 2006 (E-TABM-158)
B TB-199 on Pawitan et al., 2005 (GSE1456)
C TB-199 on Git et al., 2008 (E-TABM-194)
Br. Tissue
Br. Tissue
Br. Tissue
HB4A
PMC42
PMC42
PMC42
PMC42
MT3
MT3
MDAMB361
MDAMB361
HCC1419
MCF7
MCF7
BT20
BT20
D

**Table 1. Overlapping stem- and progenitor-related genes suggest distinction between 156-IHC and TB-199 profiles.**

| | 156-IHC | TB-199 | | | |
|---|---|---|---|---|---|
| Gene Symbol | Direction | Direction | Relevant Function | Tissue | References |
| TP63 | UP | DOWN | TIC, SC,PC | Breast | (Du et al., 2010; Li et al., 2008; Yalcin-Ozuysal et al., 2010) |
| ID4 | UP | DOWN | TIC, PC | Neural, Breast | (Jeon et al., 2008; Turner et al., 2007; Yun et al., 2004) |
| IGFBP2 | UP | DOWN | TIC, PC | Neural, Skin | (Hsieh et al., 2010; Villani et al., 2010) |
| SOSTDC1 | UP | DOWN | TS | Breast, Renal | (Blish et al., 2010; Clausen et al., 2010) |
| ATP1A2 | DOWN | UP | PC | Neural | (Hu et al., 2004; Wright et al., 2003) |
| LMCD1 | DOWN | UP | SP | Occular | (Akinci et al., 2009) |
| ANKRD22 | UP | UP | SC | Embryonic | (Greco et al., 2007) |
| IL18R1 | UP | UP | PC | Breast | (Bertucci et al., 2006; Zhu et al., 2010) |
| | | | | | |
| CD133 | Absent | UP | PC, TIC | Breast | (Lim et al., 2009; Wang et al., 2010; Wright et al., 2008a; Zucchi et al., 2008) |

TIC, tumor initiating cell
SC, stem cell
PC, progenitor cell
SP, side population
TS, tumor suppressor

**Table 2. IHC profiles reflect different mammary stem cell compartments.**

| | 156-IHC | TB-199 | |
|---|---|---|---|
| **Profile Type** | **n, p-value** | **n, p-value** | **References** |
| Mammary Stem Cells (Ms) | 15, p=5.9E-7 | 28, p=1.4E-15 | (Lim et al., 2009) |
| Mammary Stem Cells (Hm) | 17, p=3.6E-5 | 32, p=2.3E-12 | (Lim et al., 2009) |
| Myoepithelial Cells (Ms) | 24, p=5.4E-16 | 45, p=1.2E-35 | (Kendrick et al., 2008) |
| Luminal Progenitors (Hm) | NP | 17, p=1.4E-9 | (Lim et al., 2009) |
| ER- Luminal Cells (Ms) | NP | 14, p=6.4E-10 | (Kendrick et al., 2008) |
| Mature Luminal Cells (Hm) | NP | 13, p=8.4E-5 | (Lim et al., 2009) |
| ER+ Luminal Cells (Ms) | 14, p=1.6E-9 | 13, p=6.9E-7 | (Kendrick et al., 2008) |
| Mammary Stroma (Hm) | 16, p=3.5E-6 | 29, p=2.1E-13 | (Lim et al., 2009) |
| ER- BRCA1 Tumors (Hm) | NP | 12, p=1.5E-4 | (Fernandez-Ramires et al., 2009) |
| Brca1 Serial Tumors (Ms) | 13, p=3.3E-10 | 13, p=1.6E-8 | (Wright et al., 2008b) |
| Brca1 Model (Ms) | 12, p=2.8E-10 | 19, p=3.1E-17 | (Wright et al., 2008b) |
| BRCA1 Breast Canceres (Hm) | 14, p=1.6E-5 | 19, p=4.8E-7 | (van 't Veer et al., 2002) |

n, Number of overlapping genes

p, Significance of overlap via ConceptGen analysis

NP, Not present

Ms, Mouse

Hm, Human

**Table 3. Irradiated mammary glands (10 cGy) exhibit mammary stem and progenitor transcriptional programs**.

Stem and progenitor profiles were derived from Lim et al., 2010.

| | | UP at 1wk | UP at 4wks | UP at 1 & 4wks |
|---|---|---|---|---|
| **Wild type Irradiated** | **Stem Cell Profile** | (26), p=2.51E-8 | (28), p=3.51E-17 | (15), p=05.3E-4 |
| | **Progenitor Cell Profile** | NP | NP | NP |
| | | | | |
| ***Tgfb1* +/- Irradiated** | **Stem Cell Profile** | NP | (40), p=2.087E-17 | (22), p=7.34E-08 |
| | **Progenitor Cell Profile** | NP | (12), p=8.73E-10 | (6), p=2.09E-5 |

(n), Number of overlapping genes

p, Significance of overlap via ConceptGen analysis

NP, Not present

**Table S1. 227 genes (ER-227) modulated by at least 1.5-fold in ER+ *Trp53* null tumors**.
Hm, present on Affymetrix Human U133A platform

| Affy 430 2.0 Probe | Symbol | Direction |
|---|---|---|
| 1440668_at | Adamtsl3 | UP |
| 1451932_a_at | Adamtsl4 | UP |
| 1420970_at | Adcy7 | UP |
| 1422514_at | Aebp1 | UP |
| 1457042_at | AI256396 | UP |
| 1421002_at | Angptl2 | UP |
| 1447272_s_at | Atp10a | UP |
| 1420948_s_at | Atrx | UP |
| 1423586_at | Axl | UP |
| 1418271_at | Bhlhe22 | UP |
| 1427457_a_at | Bmp1 | UP |
| 1423635_at | Bmp2 | UP |
| 1419483_at | C3ar1 | UP |
| 1456523_at | C77713 | UP |
| 1426389_at | Camk1d | UP |
| 1422659_at | Camk2d | UP |
| 1437385_at | Ccbe1 | UP |
| 1419282_at | Ccl12 | UP |
| 1419609_at | Ccr1 | UP |
| 1421186_at | Ccr2 | UP |
| 1422259_a_at | Ccr5 | UP |
| 1449858_at | Cd86 | UP |
| 1450757_at | Cdh11 | UP |
| 1418815_at | Cdh2 | UP |
| 1450876_at | Cfh | UP |
| 1437270_a_at | Clcf1 | UP |
| 1419627_s_at | Clec4n | UP |
| 1421366_at | Clec5a | UP |
| 1434172_at | Cnr1 | UP |
| 1427391_a_at | Col12a1 | UP |
| 1429549_at | Col27a1 | UP |
| 1418441_at | Col8a1 | UP |
| 1419693_at | Colec12 | UP |
| 1450863_a_at | Dclk1 | UP |
| 1448669_at | Dkk3 | UP |
| 1435343_at | Dock10 | UP |

| Affy 430 2.0 Probe | Symbol | Direction |
|---|---|---|
| 1422651_at | Adipoq | DOWN |
| 1419241_a_at | Aire | DOWN |
| 1451675_a_at | Alas2 | DOWN |
| 1416468_at | Aldh1a1 | DOWN |
| 1436538_at | Ankrd37 | DOWN |
| 1460190_at | Ap1m2 | DOWN |
| 1417561_at | Apoc1 | DOWN |
| 1419373_at | Atp6v1b1 | DOWN |
| 1436453_at | BB144871 | DOWN |
| 1452257_at | Bdh1 | DOWN |
| 1418910_at | Bmp7 | DOWN |
| 1455416_at | C130021I20Rik | DOWN |
| 1423954_at | C3 | DOWN |
| 1450429_at | Capn6 | DOWN |
| 1449434_at | Car3 | DOWN |
| 1427482_a_at | Car8 | DOWN |
| 1418509_at | Cbr2 | DOWN |
| 1449918_at | Cd209g | DOWN |
| 1426673_at | Cdh3 | DOWN |
| 1448842_at | Cdo1 | DOWN |
| 1417867_at | Cfd | DOWN |
| 1455435_s_at | Chdh | DOWN |
| 1428573_at | Chn2 | DOWN |
| 1426332_a_at | Cldn3 | DOWN |
| 1418799_a_at | Col17a1 | DOWN |
| 1428571_at | Col9a1 | DOWN |
| 1448730_at | Cpa3 | DOWN |
| 1438694_at | Csn1s2a | DOWN |
| 1420369_a_at | Csn2 | DOWN |
| 1451851_a_at | Csn3 | DOWN |
| 1435435_at | Cttnbp2 | DOWN |
| 1415994_at | Cyp2e1 | DOWN |
| 1416194_at | Cyp4b1 | DOWN |
| 1419204_at | Dll1 | DOWN |
| 1419555_at | Elf5 | DOWN |
| 1442514_a_at | Ell3 | DOWN |

| 1429028_at | Dock11 | UP |
|---|---|---|
| 1435680_a_at | Dpp7 | UP |
| 1448613_at | Ecm1 | UP |
| 1428653_x_at | Elavl1 | UP |
| 1449994_at | Epgn | UP |
| 1438007_at | Fam19a2 | UP |
| 1434993_at | Fam5c | UP |
| 1432262_at | Fam63a | UP |
| 1438035_at | Fam82a1 | UP |
| 1433963_a_at | Fermt3 | UP |
| 1418497_at | Fgf13 | UP |
| 1419376_at | Fibin | UP |
| 1435606_at | Gal3st4 | UP |
| 1423569_at | Gatm | UP |
| 1418776_at | Gbp8 | UP |
| 1422179_at | Gjb4 | UP |
| 1443941_at | Gm447 | UP |
| 1438439_at | Gpr171 | UP |
| 1425357_a_at | Grem1 | UP |
| 1421256_at | Gzmc | UP |
| 1420343_at | Gzmd | UP |
| 1421227_at | Gzme | UP |
| 1418679_at | Gzmf | UP |
| 1422867_at | Gzmg | UP |
| 1443686_at | H2-DMb2 | UP |
| 1420420_at | Hao1 | UP |
| 1418678_at | Has2 | UP |
| 1422851_at | Hmga2 | UP |
| 1440559_at | Hmga2-ps1 | UP |
| 1418761_at | Igf2bp1 | UP |
| 1437103_at | Igf2bp2 | UP |
| 1422053_at | Inhba | UP |
| 1423274_at | Ints6 | UP |
| 1422046_at | Itgam | UP |
| 1440990_at | Kif26b | UP |
| 1433536_at | Lrp11 | UP |
| 1436055_at | Lrrc15 | UP |
| 1418061_at | Ltbp2 | UP |
| 1427040_at | Mdfic | UP |
| 1438467_at | Mgl2 | UP |

| 1418294_at | Epb4.1l4b | DOWN |
|---|---|---|
| 1422438_at | Ephx1 | DOWN |
| 1417023_a_at | Fabp4 | DOWN |
| 1428581_at | Fam178b | DOWN |
| 1420085_at | Fgf4 | DOWN |
| 1418496_at | Foxa1 | DOWN |
| 1448485_at | Ggt1 | DOWN |
| 1424825_a_at | Glycam1 | DOWN |
| 1448810_at | Gne | DOWN |
| 1450990_at | Gpc3 | DOWN |
| 1449279_at | Gpx2 | DOWN |
| 1429086_at | Grhl2 | DOWN |
| 1416368_at | Gsta4 | DOWN |
| 1418186_at | Gstt1 | DOWN |
| 1449482_at | Hist3h2ba | DOWN |
| 1454159_a_at | Igfbp2 | DOWN |
| 1431693_a_at | Il17b | DOWN |
| 1436425_at | Kank4 | DOWN |
| 1455451_at | Kctd14 | DOWN |
| 1415854_at | Kitl | DOWN |
| 1435743_at | Klhl23 | DOWN |
| 1422667_at | Krt15 | DOWN |
| 1424096_at | Krt5 | DOWN |
| 1418363_at | Lalba | DOWN |
| 1417290_at | Lrg1 | DOWN |
| 1452855_at | Ly6k | DOWN |
| 1425253_a_at | Madcam1 | DOWN |
| 1419646_a_at | Mbp | DOWN |
| 1416006_at | Mdk | DOWN |
| 1421836_at | Mtap7 | DOWN |
| 1426941_at | Muc15 | DOWN |
| 1426154_s_at | Mup10 | DOWN |
| 1448465_at | Nipsnap1 | DOWN |
| 1423506_a_at | Nnat | DOWN |
| 1421964_at | Notch3 | DOWN |
| 1425151_a_at | Noxo1 | DOWN |
| 1449281_at | Nrtn | DOWN |
| 1455200_at | Pak6 | DOWN |
| 1426910_at | Pawr | DOWN |
| 1435553_at | Pdzd2 | DOWN |

| | | |
|---|---|---|
| 1417256_at | Mmp13 | UP |
| 1425434_a_at | Msr1 | UP |
| 1421851_at | Mtap1b | UP |
| 1425609_at | Ncf1 | UP |
| 1422974_at | Nt5e | UP |
| 1438684_at | Nuak1 | UP |
| 1460521_a_at | Obfc2a | UP |
| 1431724_a_at | P2ry12 | UP |
| 1428700_at | P2ry13 | UP |
| 1436999_at | Pid1 | UP |
| 1419280_at | Pip4k2a | UP |
| 1421137_a_at | Pkib | UP |
| 1422341_s_at | Pla2g15 | UP |
| 1448749_at | Plek | UP |
| 1452295_at | Pmepa1 | UP |
| 1448379_at | Pot1a | UP |
| 1425527_at | Prrx1 | UP |
| 1421410_a_at | Pstpip2 | UP |
| 1434653_at | Ptk2b | UP |
| 1423331_a_at | Pvrl3 | UP |
| 1417319_at | Pvrl3 | UP |
| 1434295_at | Rasgrp1 | UP |
| 1420620_a_at | Rnf13 | UP |
| 1438306_at | Rnf180 | UP |
| 1422864_at | Runx1 | UP |
| 1415893_at | Sgpl1 | UP |
| 1420818_at | Sla | UP |
| 1417639_at | Slc22a4 | UP |
| 1427483_at | Slc25a24 | UP |
| 1424659_at | Slit2 | UP |
| 1434292_at | Snhg11 | UP |
| 1417697_at | Soat1 | UP |
| 1449264_at | Syt11 | UP |
| 1419537_at | Tcfec | UP |
| 1418547_at | Tfpi2 | UP |
| 1422571_at | Thbs2 | UP |
| 1423182_at | Tnfrsf13b | UP |
| 1421269_at | Ugcg | UP |
| 1422932_a_at | Vav1 | UP |
| 1448594_at | Wisp1 | UP |

| | | |
|---|---|---|
| 1417355_at | Peg3 | DOWN |
| 1418471_at | Pgf | DOWN |
| 1449170_at | Piwil2 | DOWN |
| 1437893_at | Plb1 | DOWN |
| 1437842_at | Plcxd1 | DOWN |
| 1426013_s_at | Plekha4 | DOWN |
| 1416321_s_at | Prelp | DOWN |
| 1425853_s_at | Prlr | DOWN |
| 1448355_at | Prss16 | DOWN |
| 1419669_at | Prtn3 | DOWN |
| 1417323_at | Psrc1 | DOWN |
| 1437161_x_at | Rbpms | DOWN |
| 1449015_at | Retnla | DOWN |
| 1434628_a_at | Rhpn2 | DOWN |
| 1436277_at | Rnf207 | DOWN |
| 1423327_at | Rpl39l | DOWN |
| 1450788_at | Saa1 | DOWN |
| 1417600_at | Slc15a2 | DOWN |
| 1419571_at | Slc28a3 | DOWN |
| 1451139_at | Slc39a4 | DOWN |
| 1418395_at | Slc47a1 | DOWN |
| 1418076_at | St14 | DOWN |
| 1456440_s_at | St8sia6 | DOWN |
| 1460197_a_at | Steap4 | DOWN |
| 1425749_at | Stxbp6 | DOWN |
| 1422973_a_at | Thrsp | DOWN |
| 1418158_at | Trp63 | DOWN |
| 1417957_a_at | Tspan1 | DOWN |
| 1427284_a_at | Ttpa | DOWN |
| 1425753_a_at | Ung | DOWN |
| 1435893_at | Vldlr | DOWN |
| 1453089_at | 3110079O15Rik | DOWN |

| | | |
|---|---|---|
| 1423668_at | Zdhhc14 | UP |
| 1434298_at | Zeb2 | UP |
| 1438531_at | A730054J21Rik | UP |

**Table S2. 199 genes (TB-199) modulated by at least 1.5-fold in tumors from irradiated *Tgfb1* +/- hosts.**

| Affy Probe ID | Symbol | Direction |
|---|---|---|
| 1453239_a_at | Ankrd22 | UP |
| 1422593_at | Ap3s1 | UP |
| 1427465_at | Atp1a2 | UP |
| 1439036_a_at | Atp1b1 | UP |
| 1433827_at | Atp8a1 | UP |
| 1436453_at | BB144871 | UP |
| 1422845_at | Canx | UP |
| 1426165_a_at | Casp3 | UP |
| 1417268_at | Cd14 | UP |
| 1420682_at | Chrnb1 | UP |
| 1417852_x_at | Clca1 | UP |
| 1460259_s_at | Clca1 | UP |
| 1419463_at | Clca2 | UP |
| 1420330_at | Clec4e | UP |
| 1418626_a_at | Clu | UP |
| 1419427_at | Csf3 | UP |
| 1418806_at | Csf3r | UP |
| 1419209_at | Cxcl1 | UP |
| 1417507_at | Cyb561 | UP |
| 1427226_at | Epn2 | UP |
| 1419816_s_at | Errfi1 | UP |
| 1425452_s_at | Fam84a | UP |
| 1425215_at | Ffar2 | UP |
| 1416025_at | Fgg | UP |
| 1429310_at | Flrt3 | UP |
| 1449519_at | Gadd45a | UP |
| 1417399_at | Gas6 | UP |
| 1416593_at | Glrx | UP |
| 1419426_s_at | Gm10591 | UP |
| 1424896_at | Gpr85 | UP |
| 1453596_at | Id2 | UP |
| 1419647_a_at | Ier3 | UP |
| 1424111_at | Igf2r | UP |
| 1421628_at | Il18r1 | UP |
| 1449399_a_at | Il1b | UP |
| 1427381_at | Irg1 | UP |
| 1415977_at | Isyna1 | UP |
| 1422945_a_at | Kif5c | UP |
| 1424596_s_at | Lmcd1 | UP |

| Affy Probe ID | Symbol | Direction |
|---|---|---|
| 1422340_a_at | Actg2 | DOWN |
| 1457128_at | AL024213 | DOWN |
| 1442832_at | Ankrd52 | DOWN |
| 1423893_x_at | Apbb1 | DOWN |
| 1416371_at | Apod | DOWN |
| 1457682_at | Arhgap42 | DOWN |
| 1432032_a_at | Artn | DOWN |
| 1434026_at | Atp8b2 | DOWN |
| 1441656_at | B930068K11Rik | DOWN |
| 1423853_at | BAD-LAMP | DOWN |
| 1437310_at | Bbs1 | DOWN |
| 1455241_at | BC037703 | DOWN |
| 1418910_at | Bmp7 | DOWN |
| 1459838_s_at | Btbd11 | DOWN |
| 1424041_s_at | C1s | DOWN |
| 1430752_at | C330006D17Rik | DOWN |
| 1428485_at | Car12 | DOWN |
| 1427912_at | Cbr3 | DOWN |
| 1424407_s_at | Cbx6 | DOWN |
| 1418815_at | Cdh2 | DOWN |
| 1428902_at | Chst11 | DOWN |
| 1418796_at | Clec11a | DOWN |
| 1418799_a_at | Col17a1 | DOWN |
| 1429549_at | Col27a1 | DOWN |
| 1450625_at | Col5a2 | DOWN |
| 1460248_at | Cpxm2 | DOWN |
| 1452968_at | Cthrc1 | DOWN |
| 1458662_at | Daam1 | DOWN |
| 1444139_at | Ddit4l | DOWN |
| 1441107_at | Dmrta2 | DOWN |
| 1434534_at | Dsc3 | DOWN |
| 1438407_at | Dsel | DOWN |
| 1421117_at | Dst | DOWN |
| 1456069_at | Dtna | DOWN |
| 1426540_at | Endod1 | DOWN |
| 1422438_at | Ephx1 | DOWN |
| 1449280_at | Esm1 | DOWN |
| 1438402_at | Fam171a1 | DOWN |
| 1436948_a_at | Fam70a | DOWN |

| | | |
|---|---|---|
| 1453949_s_at | Lypla1 | UP |
| 1419208_at | Map3k8 | UP |
| 1425803_a_at | Mbd2 | UP |
| 1435548_at | Mrs2 | UP |
| 1426154_s_at | Mup10 | UP |
| 1455104_at | Mxd1 | UP |
| 1426561_a_at | Npnt | UP |
| 1450079_at | Nrk | UP |
| 1422974_at | Nt5e | UP |
| 1416407_at | Pea15a | UP |
| 1449184_at | Pglyrp1 | UP |
| 1425514_at | Pik3r1 | UP |
| 1454254_s_at | PLET1 | UP |
| 1431464_a_at | Pmm2 | UP |
| 1437751_at | Ppargc1a | UP |
| 1456072_at | Ppp1r9a | UP |
| 1419700_a_at | Prom1 | UP |
| 1416601_a_at | Rcan1 | UP |
| 1448756_at | S100a9 | UP |
| 1421457_a_at | Samsn1 | UP |
| 1458813_at | Scn5a | UP |
| 1420688_a_at | Sgce | UP |
| 1428663_at | Sgms2 | UP |
| 1424975_at | Siglec5 | UP |
| 1451489_at | Slc25a35 | UP |
| 1451782_a_at | Slc29a1 | UP |
| 1420914_at | Slco2a1 | UP |
| 1448377_at | Slpi | UP |
| 1419157_at | Sox4 | UP |
| 1421469_a_at | Stat5a | UP |
| 1426337_a_at | Tead4 | UP |
| 1431970_at | Tm7sf4 | UP |
| 1426640_s_at | Trib2 | UP |
| 1436237_at | Ttc9 | UP |
| 1434484_at | Wdnm1-like | UP |
| 1453737_at | Wipf2 | UP |
| 1427104_at | Zfp612 | UP |
| 1430083_at | 2610307P16Rik | UP |
| 1453242_x_at | 2810047C21Rik1 | UP |
| 1453293_a_at | 2810408A11Rik | UP |

| | | |
|---|---|---|
| 1457135_at | Fat2 | DOWN |
| 1451119_a_at | Fbln1 | DOWN |
| 1460412_at | Fbln7 | DOWN |
| 1452799_at | Fggy | DOWN |
| 1419376_at | Fibin | DOWN |
| 1456084_x_at | Fmod | DOWN |
| 1438232_at | Foxp2 | DOWN |
| 1457038_at | Frem2 | DOWN |
| 1457409_at | Fut9 | DOWN |
| 1436115_at | Gm266 | DOWN |
| 1418379_s_at | Gpr124 | DOWN |
| 1455498_at | Gpr50 | DOWN |
| 1417836_at | Gpx7 | DOWN |
| 1440145_at | H60a | DOWN |
| 1450047_at | Hs6st2 | DOWN |
| 1423260_at | Id4 | DOWN |
| 1427216_at | Ifnz | DOWN |
| 1454159_a_at | Igfbp2 | DOWN |
| 1452903_at | Inka1 | DOWN |
| 1421852_at | Kcnk5 | DOWN |
| 1440990_at | Kif26b | DOWN |
| 1448932_at | Krt16 | DOWN |
| 1424096_at | Krt5 | DOWN |
| 1434227_at | Krtdap | DOWN |
| 1418363_at | Lalba | DOWN |
| 1418153_at | Lama1 | DOWN |
| 1418478_at | Lmo1 | DOWN |
| 1452565_x_at | LOC641050 | DOWN |
| 1452855_at | Ly6k | DOWN |
| 1437250_at | Mreg | DOWN |
| 1452670_at | Myl9 | DOWN |
| 1457273_at | Odz2 | DOWN |
| 1419767_at | Padi3 | DOWN |
| 1421193_a_at | Pbx3 | DOWN |
| 1437442_at | Pcdh7 | DOWN |
| 1441994_at | Pcdhb16 | DOWN |
| 1421917_at | Pdgfra | DOWN |
| 1419309_at | Pdpn | DOWN |
| 1419006_s_at | Peli2 | DOWN |
| 1438677_at | Pkp4 | DOWN |
| 1426208_x_at | Plagl1 | DOWN |
| 1436335_at | Plch2 | DOWN |
| 1451718_at | Plp1 | DOWN |

| | | |
|---|---|---|
| 1418746_at | Pnkd | DOWN |
| 1417701_at | Ppp1r14c | DOWN |
| 1435162_at | Prkg2 | DOWN |
| 1434195_at | Prss35 | DOWN |
| 1457493_at | Pten | DOWN |
| 1439747_at | Ptges | DOWN |
| 1456315_a_at | Ptpla | DOWN |
| 1436937_at | Rbms3 | DOWN |
| 1457511_at | Rgs12 | DOWN |
| 1424542_at | S100a4 | DOWN |
| 1427020_at | Scara3 | DOWN |
| 1439768_x_at | Sema4f | DOWN |
| 1419082_at | Serpinb2 | DOWN |
| 1448201_at | Sfrp2 | DOWN |
| 1418673_at | Snai2 | DOWN |
| 1460250_at | Sostdc1 | DOWN |
| 1416967_at | Sox2 | DOWN |
| 1428333_at | Spcs3 | DOWN |
| 1423281_at | Stmn2 | DOWN |
| 1435657_at | Ston2 | DOWN |
| 1428108_x_at | Tmcc2 | DOWN |
| 1422587_at | Tmem45a | DOWN |
| 1418158_at | Trp63 | DOWN |
| 1448501_at | Tspan6 | DOWN |
| 1421694_a_at | Vcan | DOWN |
| 1426399_at | Vwa1 | DOWN |
| 1436746_at | Wnk1 | DOWN |
| 1423836_at | Zfp503 | DOWN |
| 1429835_at | 2310033E01Rik | DOWN |
| 1435639_at | 2610528A11Rik | DOWN |
| 1436362_x_at | 2700079J08Rik | DOWN |
| 1453089_at | 3110079O15Rik | DOWN |
| 1450770_at | 3632451O06Rik | DOWN |
| 1431248_at | 5031426D15Rik | DOWN |
| 1451456_at | 6430706D22Rik | DOWN |
| 1452762_at | 8430436O14Rik | DOWN |
| 1438752_at | A230058F20Rik | DOWN |
| 1438531_at | A730054J21Rik | DOWN |

**Table S3. Overlap of genes between mammary stem or progenitor profiles with the 156-IHC or TB-199.**

All overlaps, p<0.00005

**156-IHC overlap with MaSC profile of Lim et al. (2009)**

| Symbol | Gene ID |
|---|---|
| SERPINE1 | serpin peptidase inhibitor, clade E (nexin, plasminogen activator inhibitor type 1), member 1 |
| PGF | placental growth factor, vascular endothelial growth factor-related protein |
| PKP1 | plakophilin 1 (ectodermal dysplasia/skin fragility syndrome) |
| LEPR | leptin receptor |
| IGFBP2 | insulin-like growth factor binding protein 2, 36kDa |
| GJB3 | gap junction protein, beta 3, 31kDa |
| HOMER2 | homer homolog 2 (Drosophila) |
| TNFSF10 | tumor necrosis factor (ligand) superfamily, member 10 |
| SNCA | synuclein, alpha (non A4 component of amyloid precursor) |
| EHD3 | EH-domain containing 3 |
| SCRG1 | |
| MYO5C | myosin VC |
| SLC47A1 | solute carrier family 47, member 1 |
| ATP6V0E2 | ATPase, H+ transporting V0 subunit e2 |
| C1orf21 | chromosome 1 open reading frame 21 |
| STARD13 | START domain containing 13 |
| CGNL1 | cingulin-like 1 |

**156-IHC overlap with MaSC profile of Lim et al. (2010)**

| Symbol | Gene ID |
|---|---|
| CD36 | CD36 molecule (thrombospondin receptor) |
| PGF | placental growth factor, vascular endothelial growth factor-related protein |
| PKP1 | plakophilin 1 (ectodermal dysplasia/skin fragility syndrome) |
| LAMB3 | laminin, beta 3 |

**TB-199 overlap with MaSC profile from Lim et al. (2009)**

| Symbol | Gene ID |
|---|---|
| COL5A2 | collagen, type V, alpha 2 |
| COL17A1 | collagen, type XVII, alpha 1 |
| VCAN | versican |
| BMP7 | bone morphogenetic protein 7 (osteogenic protein 1) |
| ATP1B1 | ATPase, Na+/K+ transporting, beta 1 polypeptide |
| KRT16 | keratin 16 (focal non-epidermolytic palmoplantar keratoderma) |
| PIK3R1 | phosphoinositide-3-kinase, regulatory subunit 1 (p85 alpha) |
| MXD1 | MAX dimerization protein 1 |
| KRT5 | keratin 5 (epidermolysis bullosa simplex, Dowling-Meara/Kobner/Weber-Cockayne types) |
| GAS6 | growth arrest-specific 6 |
| IGFBP2 | insulin-like growth factor binding protein 2, 36kDa |
| IL1B | interleukin 1, beta |
| FMOD | fibromodulin |
| FBLN1 | fibulin 1 |
| FAT2 | FAT tumor suppressor homolog 2 (Drosophila) |
| DSC3 | desmocollin 3 |
| PTGES | prostaglandin E synthase |
| PLCH2 | phospholipase C, eta 2 |
| SGCE | sarcoglycan, epsilon |
| PTPLA | protein tyrosine phosphatase-like (proline instead of catalytic arginine), member A |
| SLCO2A1 | solute carrier organic anion transporter family, member 2A1 |
| TSPAN6 | tetraspanin 6 |
| SLPI | secretory leukocyte peptidase inhibitor |
| SNAI2 | snail homolog 2 (Drosophila) |

| | |
|---|---|
| ID4 | inhibitor of DNA binding 4, dominant negative helix-loop-helix protein |
| IGFBP2 | insulin-like growth factor binding protein 2, 36kDa |
| EVC | Ellis van Creveld syndrome |
| HOMER2 | homer homolog 2 (Drosophila) |
| TP63 | tumor protein p73-like |
| PLA2G7 | phospholipase A2, group VII (platelet-activating factor acetylhydrolase, plasma) |
| SNCA | synuclein, alpha (non A4 component of amyloid precursor) |
| ARC | activity-regulated cytoskeleton-associated protein |
| MYO5C | myosin VC |
| ATP6V0E2 | ATPase, H+ transporting V0 subunit e2 |
| CGNL1 | cingulin-like 1 |

**156-IHC overlap with myoepithelial profile of Kendrick et al. (2008)**

| Symbol | Gene ID |
|---|---|
| CP | ceruloplasmin (ferroxidase) |
| ATP1A2 | ATPase, Na+/K+ transporting, alpha 2 (+) polypeptide |
| CAPN6 | calpain 6 |
| PGF | placental growth factor, vascular endothelial growth factor-related protein |
| PKP1 | plakophilin 1 (ectodermal dysplasia/skin fragility syndrome) |
| LAMB3 | laminin, beta 3 |
| NEDD9 | neural precursor cell expressed, developmentally down-regulated 9 |
| MMP19 | matrix metallopeptidase 19 |
| LTBP2 | latent transforming growth factor beta binding protein 2 |
| TNFRSF11B | tumor necrosis factor receptor superfamily, member 11b (osteoprotegerin) |
| FCGRT | Fc fragment of IgG, receptor, transporter, alpha |
| GSTM1 | glutathione S-transferase M1 |
| ID4 | inhibitor of DNA binding 4, dominant negative helix-loop-helix protein |
| IGFBP2 | insulin-like growth factor binding protein 2, 36kDa |
| RBMS3 | RNA binding motif, single stranded interacting protein |
| FLRT3 | fibronectin leucine rich transmembrane protein 3 |
| PDPN | podoplanin |
| ATP8B2 | ATPase, Class I, type 8B, member 2 |
| BTBD11 | BTB (POZ) domain containing 11 |
| ZNF503 | zinc finger protein 503 |
| KRTDAP | keratinocyte differentiation-associated protein |
| LAMA1 | laminin, alpha 1 |

**TB-199 overlap with MaSC profile of Lim et al. (2010)**

| Symbol | Gene ID |
|---|---|
| CD14 | CD14 molecule |
| COL5A2 | collagen, type V, alpha 2 |
| COL17A1 | collagen, type XVII, alpha 1 |
| VCAN | versican |
| BMP7 | bone morphogenetic protein 7 (osteogenic protein 1) |
| ATP1B1 | ATPase, Na+/K+ transporting, beta 1 polypeptide |
| KRT16 | keratin 16 (focal non-epidermolytic palmoplantar keratoderma) |
| PCDH7 | protocadherin 7 |
| NT5E | 5'-nucleotidase, ecto (CD73) |
| KRT5 | keratin 5 (epidermolysis bullosa simplex, Dowling-Meara/Kobner/Weber-Cockayne types) |
| ID4 | inhibitor of DNA binding 4, dominant negative helix-loop-helix protein |
| IGFBP2 | insulin-like growth factor binding protein 2, 36kDa |
| IL1B | interleukin 1, beta |
| FMOD | fibromodulin |
| FBLN1 | fibulin 1 |
| PLCH2 | phospholipase C, eta 2 |
| TP63 | tumor protein p73-like |

| | |
|---|---|
| GFRA1 | GDNF family receptor alpha 1 |
| GGT1 | gamma-glutamyltransferase 1 |
| GJB3 | gap junction protein, beta 3, 31kDa |
| EVC | Ellis van Creveld syndrome |
| MAGI2 | membrane associated guanylate kinase, WW and PDZ domain containing 2 |
| TP63 | tumor protein p73-like |
| PLA2G7 | phospholipase A2, group VII (platelet-activating factor acetylhydrolase, plasma) |
| SOSTDC1 | sclerostin domain containing 1 |
| ARC | activity-regulated cytoskeleton-associated protein |
| WNT10A | wingless-type MMTV integration site family, member 10A |
| PTPLA | protein tyrosine phosphatase-like (proline instead of catalytic arginine), member A |
| SNAI2 | snail homolog 2 (Drosophila) |
| STAT5A | signal transducer and activator of transcription 5A |
| GPR124 | G protein-coupled receptor 124 |
| PDPN | podoplanin |
| C14orf37 | chromosome 14 open reading frame 37 |
| BTBD11 | BTB (POZ) domain containing 11 |

**TB-199 overlap with myoepithelial profile of Kendrick et al. (2008)**

| Symbol | Gene ID |
|---|---|
| CBR3 | carbonyl reductase 3 |
| CDH2 | cadherin 2, type 1, N-cadherin (neuronal) |
| COL5A2 | collagen, type V, alpha 2 |
| COL17A1 | collagen, type XVII, alpha 1 |
| BMP7 | bone morphogenetic protein 7 (osteogenic protein 1) |
| C1S | complement component 1, s subcomponent |
| CA12 | carbonic anhydrase XII |
| ATP1A2 | ATPase, Na+/K+ transporting, alpha 2 (+) polypeptide |
| PBX3 | pre-B-cell leukemia homeobox 3 |
| PCDH7 | protocadherin 7 |
| PDGFRA | platelet-derived growth factor receptor, alpha polypeptide |
| LMO1 | LIM domain only 1 (rhombotin 1) |
| NT5E | 5'-nucleotidase, ecto (CD73) |
| KRT5 | keratin 5 (epidermolysis bullosa simplex, Dowling-Meara/Kobner/Weber-Cockayne types) |
| GAS6 | growth arrest-specific 6 |
| ID4 | inhibitor of DNA binding 4, dominant negative helix-loop-helix protein |
| IGFBP2 | insulin-like growth factor binding protein 2, 36kDa |
| FMOD | fibromodulin |

**TB-199 overlap with MaP profile of Lim et al. (2009)**

| Symbol | Gene ID |
|---|---|
| CBR3 | carbonyl reductase 3 |
| APOD | apolipoprotein D |
| PIK3R1 | phosphoinositide-3-kinase, regulatory subunit 1 (p85 alpha) |
| LALBA | lactalbumin, alpha- |
| KIF5C | kinesin family member 5C |
| IGFBP2 | insulin-like growth factor binding protein 2, 36kDa |
| FMOD | fibromodulin |
| GLRX | glutaredoxin (thioltransferase) |
| SLC29A1 | solute carrier family 29 (nucleoside transporters), member 1 |
| FBLN1 | fibulin 1 |
| ARTN | artemin |
| PROM1 | prominin 1 |
| SLPI | secretory leukocyte peptidase inhibitor |
| RGS12 | regulator of G-protein signalling 12 |
| SCARA3 | scavenger receptor class A, member 3 |
| TMEM45A | transmembrane protein 45A |
| UNQ830 | |

| | |
|---|---|
| EPHX1 | epoxide hydrolase 1, microsomal (xenobiotic) |
| GPX7 | glutathione peroxidase 7 |
| FBLN1 | fibulin 1 |
| TP63 | tumor protein p73-like |
| PTPLA | protein tyrosine phosphatase-like (proline instead of catalytic arginine), member A |
| SLCO2A1 | solute carrier organic anion transporter family, member 2A1 |
| PRKG2 | protein kinase, cGMP-dependent, type II |
| SCN5A | sodium channel, voltage-gated, type V, alpha subunit |
| SNAI2 | snail homolog 2 (Drosophila) |
| CHST11 | carbohydrate (chondroitin 4) sulfotransferase 11 |
| SOSTDC1 | sclerostin domain containing 1 |
| RBMS3 | RNA binding motif, single stranded interacting protein |
| CBX6 | chromobox homolog 6 |
| PDPN | podoplanin |
| VWA1 | von Willebrand factor A domain containing 1 |
| PELI2 | pellino homolog 2 (Drosophila) |
| ODZ2 | odz, odd Oz/ten-m homolog 2 (Drosophila) |
| MREG | melanoregulin |
| SCARA3 | scavenger receptor class A, member 3 |
| TMEM45A | transmembrane protein 45A |
| PADI3 | peptidyl arginine deiminase, type III |
| CPXM2 | carboxypeptidase X (M14 family), member 2 |
| BTBD11 | BTB (POZ) domain containing 11 |
| STON2 | stonin 2 |
| HS6ST2 | heparan sulfate 6-O-sulfotransferase 2 |
| FREM2 | FRAS1 related extracellular matrix protein 2 |
| LAMA1 | laminin, alpha 1 |

**TB-199 overlap with profile of ER-negative luminal cells from Kendrick et at. (2008)**

| Symbol | Gene ID |
|---|---|
| CD14 | CD14 molecule |
| CHRNB1 | cholinergic receptor, nicotinic, beta 1 (muscle) |
| CLU | clusterin |
| ATP1B1 | ATPase, Na+/K+ transporting, beta 1 polypeptide |
| PGLYRP1 | peptidoglycan recognition protein 1 |
| KCNK5 | potassium channel, subfamily K, member 5 |
| TRIB2 | tribbles homolog 2 (Drosophila) |
| TTC9 | tetratricopeptide repeat domain 9 |
| FLRT3 | fibronectin leucine rich transmembrane protein 3 |
| FUT9 | fucosyltransferase 9 (alpha (1,3) fucosyltransferase) |
| ESM1 | endothelial cell-specific molecule 1 |
| PELI2 | pellino homolog 2 (Drosophila) |
| PPP1R9A | protein phosphatase 1, regulatory (inhibitor) subunit 9A |
| BTBD11 | BTB (POZ) domain containing 11 |

**Table S4. Genes induced by radiation in wild type and *Tgfb1* +/- mammary glands at 1 or 4 weeks after exposure.**

Human homologues recognized by ConceptGen.

**Induced by at least 1.25-fold at 1 wk in wild type.**

| Symbol | Gene Name |
|---|---|
| ALDH3B1 | aldehyde dehydrogenase 3 family, member B1 |
| ALOX5 | arachidonate 5-lipoxygenase |
| ALOX5AP | arachidonate 5-lipoxygenase-activating protein |
| RUNX3 | runt-related transcription factor 3 |
| CBLB | Cas-Br-M (murine) ecotropic retroviral transforming sequence b |
| CD2 | CD2 molecule |
| CD3D | CD3d molecule, delta (CD3-TCR complex) |
| CD247 | CD247 molecule |
| CD5L | CD5 molecule-like |
| CD8A | CD8a molecule |
| CD8B | CD8b molecule |
| CD19 | CD19 molecule |
| CD22 | CD22 molecule |
| CD80 | CD80 molecule |
| CD86 | CD86 molecule |
| CD34 | CD34 molecule |
| CD37 | CD37 molecule |
| CD40 | CD40 molecule, TNF receptor superfamily member 5 |
| CD40LG | CD40 ligand (TNF superfamily, member 5, hyper-IgM syndrome) |
| CD48 | CD48 molecule |
| CD53 | CD53 molecule |
| CD68 | CD68 molecule |
| CD72 | CD72 molecule |

**Induced by at least 1.25-fold at 4 wks in wild type.**

| Symbol | Gene Name |
|---|---|
| CCBL1 | cysteine conjugate-beta lyase; cytoplasmic (glutamine transaminase K, kyneurenine aminotransferase) |
| CDA | cytidine deaminase |
| CDC25B | cell division cycle 25 homolog B (S. pombe) |
| CDC25C | cell division cycle 25 homolog C (S. pombe) |
| CDKN1C | cyclin-dependent kinase inhibitor 1C (p57, Kip2) |
| CDKN3 | cyclin-dependent kinase inhibitor 3 (CDK2-associated dual specificity phosphatase) |
| CENPE | centromere protein E, 312kDa |
| CENPF | centromere protein F, 350/400ka (mitosin) |
| COL1A1 | collagen, type I, alpha 1 |
| COL1A2 | collagen, type I, alpha 2 |
| COL7A1 | collagen, type VII, alpha 1 (epidermolysis bullosa, dystrophic, dominant and recessive) |
| COL9A3 | collagen, type IX, alpha 3 |
| COL11A1 | collagen, type XI, alpha 1 |
| COL12A1 | collagen, type XII, alpha 1 |
| COL17A1 | collagen, type XVII, alpha 1 |
| CRABP1 | cellular retinoic acid binding protein 1 |
| VCAN | versican |
| ANGPT2 | angiopoietin 2 |
| ANK3 | ankyrin 3, node of Ranvier (ankyrin G) |
| BMPR1B | bone morphogenetic protein receptor, type IB |
| ABAT | 4-aminobutyrate aminotransferase |
| ACRV1 | acrosomal vesicle protein 1 |
| ACTG2 | actin, gamma 2, smooth muscle, enteric |

| | |
|---|---|
| CD74 | CD74 molecule, major histocompatibility complex, class II invariant chain |
| CDKN1A | cyclin-dependent kinase inhibitor 1A (p21, Cip1) |
| CEBPD | CCAAT/enhancer binding protein (C/EBP), delta |
| CHRNB2 | cholinergic receptor, nicotinic, beta 2 (neuronal) |
| CMA1 | chymase 1, mast cell |
| CCR6 | chemokine (C-C motif) receptor 6 |
| CCBP2 | chemokine binding protein 2 |
| CNR2 | cannabinoid receptor 2 (macrophage) |
| CRK | v-crk sarcoma virus CT10 oncogene homolog (avian) |
| CRY1 | cryptochrome 1 (photolyase-like) |
| MAPK14 | mitogen-activated protein kinase 14 |
| CSF1 | colony stimulating factor 1 (macrophage) |
| CSF1R | colony stimulating factor 1 receptor, formerly McDonough feline sarcoma viral (v-fms) oncogene homolog |
| CSF2RB | colony stimulating factor 2 receptor, beta, low-affinity (granulocyte-macrophage) |
| CSK | c-src tyrosine kinase |
| ANG | angiogenin, ribonuclease, RNase A family, 5 |
| ANXA3 | annexin A3 |
| AOAH | acyloxyacyl hydrolase (neutrophil) |
| CFB | complement factor B |
| BLVRB | biliverdin reductase B (flavin reductase (NADPH)) |
| APOD | apolipoprotein D |
| AQP6 | aquaporin 6, kidney specific |
| BST1 | bone marrow stromal cell antigen 1 |
| BTK | Bruton agammaglobulinemia tyrosine kinase |
| SERPING1 | serpin peptidase inhibitor, clade G (C1 inhibitor), member 1, (angioedema, hereditary) |

| | |
|---|---|
| ADAM8 | ADAM metallopeptidase domain 8 |
| ADRBK2 | adrenergic, beta, receptor kinase 2 |
| CAPN6 | calpain 6 |
| ATP6V1G2 | ATPase, H+ transporting, lysosomal 13kDa, V1 subunit G2 |
| KRT14 | keratin 14 (epidermolysis bullosa simplex, Dowling-Meara, Koebner) |
| MGP | matrix Gla protein |
| NDP | Norrie disease (pseudoglioma) |
| PAK3 | p21 (CDKN1A)-activated kinase 3 |
| PAPPA | pregnancy-associated plasma protein A, pappalysin 1 |
| PBX1 | pre-B-cell leukemia homeobox 1 |
| PENK | proenkephalin |
| PLOD2 | procollagen-lysine, 2-oxoglutarate 5-dioxygenase 2 |
| LAMA3 | laminin, alpha 3 |
| STMN1 | stathmin 1/oncoprotein 18 |
| LGALS7 | lectin, galactoside-binding, soluble, 7 (galectin 7) |
| LPP | LIM domain containing preferred translocation partner in lipoma |
| KCNH1 | potassium voltage-gated channel, subfamily H (eag-related), member 1 |
| NT5E | 5'-nucleotidase, ecto (CD73) |
| NTF5 | neurotrophin 5 (neurotrophin 4/5) |
| MAP2 | microtubule-associated protein 2 |
| MARK1 | MAP/microtubule affinity-regulating kinase 1 |
| ROR1 | receptor tyrosine kinase-like orphan receptor 1 |
| MYCN | v-myc myelocytomatosis viral related oncogene, neuroblastoma derived (avian) |
| KIT | v-kit Hardy-Zuckerman 4 feline sarcoma viral oncogene homolog |
| MDK | midkine (neurite growth-promoting factor 2) |

| | | | |
|---|---|---|---|
| ARHGAP4 | Rho GTPase activating protein 4 | MYL2 | myosin, light chain 2, regulatory, cardiac, slow |
| ARHGDIB | Rho GDP dissociation inhibitor (GDI) beta | MEST | mesoderm specific transcript homolog (mouse) |
| RHOH | ras homolog gene family, member H | MFAP4 | microfibrillar-associated protein 4 |
| C1QA | complement component 1, q subcomponent, A chain | NCAM1 | neural cell adhesion molecule 1 |
| C1QB | complement component 1, q subcomponent, B chain | GTF3C1 | general transcription factor IIIC, polypeptide 1, alpha 220kDa |
| C1QC | complement component 1, q subcomponent, C chain | HMMR | hyaluronan-mediated motility receptor (RHAMM) |
| C6 | complement component 6 | IGFBP2 | insulin-like growth factor binding protein 2, 36kDa |
| ACTB | actin, beta | CX3CR1 | chemokine (C-X3-C motif) receptor 1 |
| PTTG1IP | pituitary tumor-transforming 1 interacting protein | NR6A1 | nuclear receptor subfamily 6, group A, member 1 |
| CACNA1A | calcium channel, voltage-dependent, P/Q type, alpha 1A subunit | EGR3 | early growth response 3 |
| ADARB1 | adenosine deaminase, RNA-specific, B1 (RED1 homolog rat) | EIF4G1 | eukaryotic translation initiation factor 4 gamma, 1 |
| ADH7 | alcohol dehydrogenase 7 (class IV), mu or sigma polypeptide | FOXC1 | forkhead box C1 |
| FXYD2 | FXYD domain containing ion transport regulator 2 | GLRB | glycine receptor, beta |
| AP2A2 | adaptor-related protein complex 2, alpha 2 subunit | EPHA4 | EPH receptor A4 |
| AEBP1 | AE binding protein 1 | DIO2 | deiodinase, iodothyronine, type II |
| AIF1 | allograft inflammatory factor 1 | GPX2 | glutathione peroxidase 2 (gastrointestinal) |
| ALAS1 | aminolevulinate, delta-, synthase 1 | DUSP8 | dual specificity phosphatase 8 |
| ALDH2 | aldehyde dehydrogenase 2 family (mitochondrial) | BARX2 | BarH-like homeobox 2 |
| CIITA | class II, major histocompatibility complex, transactivator | LMO4 | LIM domain only 4 |
| NDUFAB1 | NADH dehydrogenase (ubiquinone) 1, alpha/beta subcomplex, 1, 8kDa | LRAT | lecithin retinol acyltransferase (phosphatidylcholine--retinol O-acyltransferase) |
| P2RY6 | pyrimidinergic receptor P2Y, G-protein coupled, 6 | TRAF4 | TNF receptor-associated factor 4 |
| ENPP2 | ectonucleotide pyrophosphatase/phosphodiesterase 2 (autotaxin) | KIAA0256 | |
| PER1 | period homolog 1 (Drosophila) | CP110 | |
| CFP | complement factor properdin | ZNF518 | zinc finger protein 518 |
| SERPINA1 | serpin peptidase inhibitor, clade A (alpha-1 antiproteinase, antitrypsin), member 1 | ZNF7 | zinc finger protein 7 |
| PIK3CD | phosphoinositide-3-kinase, catalytic, delta polypeptide | MIA | melanoma inhibitory activity |

| | | | |
|---|---|---|---|
| PLEK | pleckstrin | ZNF23 | zinc finger protein 23 (KOX 16) |
| PLTP | phospholipid transfer protein | PDE8B | phosphodiesterase 8B |
| PNMT | phenylethanolamine N-methyltransferase | TP63 | tumor protein p73-like |
| PPOX | protoporphyrinogen oxidase | HIST1H3F | histone cluster 1, H3f |
| PRF1 | perforin 1 (pore forming protein) | ALMS1 | Alstrom syndrome 1 |
| SRGN | serglycin | CXCR4 | chemokine (C-X-C motif) receptor 4 |
| IL16 | interleukin 16 (lymphocyte chemoattractant factor) | CTNNAL1 | catenin (cadherin-associated protein), alpha-like 1 |
| IL18 | interleukin 18 (interferon-gamma-inducing factor) | SLC16A5 | solute carrier family 16, member 5 (monocarboxylic acid transporter 6) |
| LCK | lymphocyte-specific protein tyrosine kinase | ZNF282 | zinc finger protein 282 |
| LCP1 | lymphocyte cytosolic protein 1 (L-plastin) | SALL2 | sal-like 2 (Drosophila) |
| LCP2 | lymphocyte cytosolic protein 2 (SH2 domain containing leukocyte protein of 76kDa) | TGM3 | transglutaminase 3 (E polypeptide, protein-glutamine-gamma-glutamyltransferase) |
| INPP5D | inositol polyphosphate-5-phosphatase, 145kDa | TIA1 | TIA1 cytotoxic granule-associated RNA binding protein |
| MMP2 | matrix metallopeptidase 2 (gelatinase A, 72kDa gelatinase, 72kDa type IV collagenase) | TLE2 | transducin-like enhancer of split 2 (E(sp1) homolog, Drosophila) |
| NFATC2 | nuclear factor of activated T-cells, cytoplasmic, calcineurin-dependent 2 | VSNL1 | visinin-like 1 |
| IRF5 | interferon regulatory factor 5 | SMO | smoothened homolog (Drosophila) |
| IRF7 | interferon regulatory factor 7 | RELN | reelin |
| ITGA4 | integrin, alpha 4 (antigen CD49D, alpha 4 subunit of VLA-4 receptor) | PRSS8 | protease, serine, 8 |
| ITGAE | integrin, alpha E (antigen CD103, human mucosal lymphocyte antigen 1; alpha polypeptide) | SOX4 | SRY (sex determining region Y)-box 4 |
| ITGAL | integrin, alpha L (antigen CD11A (p180), lymphocyte function-associated antigen 1; alpha polypeptide) | SOX9 | SRY (sex determining region Y)-box 9 (campomelic dysplasia, autosomal sex-reversal) |
| MRC1 | mannose receptor, C type 1 | SOX11 | SRY (sex determining region Y)-box 11 |
| NFKBIA | nuclear factor of kappa light polypeptide gene enhancer in B-cells inhibitor, alpha | PTGFRN | prostaglandin F2 receptor negative regulator |
| NGFR | nerve growth factor receptor (TNFR superfamily, member 16) | SHMT1 | serine hydroxymethyltransferase 1 (soluble) |
| ITGAM | integrin, alpha M (complement component 3 receptor 3 subunit) | SKP2 | S-phase kinase-associated protein 2 (p45) |
| ITGB2 | integrin, beta 2 (complement component 3 receptor 3 and 4 subunit) | RREB1 | ras responsive element binding protein 1 |
| LRMP | lymphoid-restricted membrane protein | SLC9A5 | solute carrier family 9 (sodium/hydrogen exchanger), member 5 |

| | | | |
|---|---|---|---|
| LSP1 | lymphocyte-specific protein 1 | SLC13A1 | solute carrier family 13 (sodium/sulfate symporters), member 1 |
| NKG7 | natural killer cell group 7 sequence | OSGIN1 | oxidative stress induced growth inhibitor 1 |
| JAK1 | Janus kinase 1 (a protein tyrosine kinase) | GEMIN4 | gem (nuclear organelle) associated protein 4 |
| LY9 | lymphocyte antigen 9 | IRX4 | iroquois homeobox protein 4 |
| LYL1 | lymphoblastic leukemia derived sequence 1 | SUZ12 | suppressor of zeste 12 homolog (Drosophila) |
| MAB21L1 | mab-21-like 1 (C. elegans) | R3HDM1 | R3H domain containing 1 |
| MSR1 | macrophage scavenger receptor 1 | SOSTDC1 | sclerostin domain containing 1 |
| MTCP1 | mature T-cell proliferation 1 | KRT23 | keratin 23 (histone deacetylase inducible) |
| MYO1F | myosin IF | MTCH2 | mitochondrial carrier homolog 2 (C. elegans) |
| NPR1 | natriuretic peptide receptor A/guanylate cyclase A (atrionatriuretic peptide receptor A) | TIAM2 | T-cell lymphoma invasion and metastasis 2 |
| OAS1 | 2',5'-oligoadenylate synthetase 1, 40/46kDa | TJP3 | tight junction protein 3 (zona occludens 3) |
| OAS3 | 2'-5'-oligoadenylate synthetase 3, 100kDa | HSPA4L | heat shock 70kDa protein 4-like |
| GADD45B | growth arrest and DNA-damage-inducible, beta | KIAA1009 | KIAA1009 |
| OMD | osteomodulin | ARHGEF15 | Rho guanine nucleotide exchange factor (GEF) 15 |
| OGN | osteoglycin | DHX30 | DEAH (Asp-Glu-Ala-His) box polypeptide 30 |
| KLRD1 | killer cell lectin-like receptor subfamily D, member 1 | RP4-691N24.1 | |
| MYO7A | myosin VIIA | GLT25D2 | glycosyltransferase 25 domain containing 2 |
| CLDN11 | claudin 11 (oligodendrocyte transmembrane protein) | FBXL7 | F-box and leucine-rich repeat protein 7 |
| MEFV | Mediterranean fever | BAT2D1 | BAT2 domain containing 1 |
| NCF2 | neutrophil cytosolic factor 2 (65kDa, chronic granulomatous disease, autosomal 2) | ARC | activity-regulated cytoskeleton-associated protein |
| NCF4 | neutrophil cytosolic factor 4, 40kDa | LPHN3 | latrophilin 3 |
| FCGR2A | Fc fragment of IgG, low affinity IIa, receptor (CD32) | ZBED4 | zinc finger, BED-type containing 4 |
| FCGR2B | Fc fragment of IgG, low affinity IIb, receptor (CD32) | LPPR4 | |
| FCGR3A | Fc fragment of IgG, low affinity IIIa, receptor (CD16a) | RICH2 | |
| HCK | hemopoietic cell kinase | IRX5 | iroquois homeobox protein 5 |
| HCLS1 | hematopoietic cell-specific Lyn substrate 1 | ARNT2 | aryl-hydrocarbon receptor nuclear translocator 2 |

| | | | |
|---|---|---|---|
| HDC | histidine decarboxylase | SPEG | SPEG complex locus |
| NCKAP1L | NCK-associated protein 1-like | TRAIP | TRAF interacting protein |
| HHEX | hematopoietically expressed homeobox | AMMECR1 | Alport syndrome, mental retardation, midface hypoplasia and elliptocytosis chromosomal region, gene 1 |
| HLA-C | major histocompatibility complex, class I, C | KIF2C | kinesin family member 2C |
| HLA-DMA | major histocompatibility complex, class II, DM alpha | GMEB1 | glucocorticoid modulatory element binding protein 1 |
| HLA-DMB | major histocompatibility complex, class II, DM beta | PLK4 | polo-like kinase 4 (Drosophila) |
| HLA-DOA | major histocompatibility complex, class II, DO alpha | RPP14 | ribonuclease P 14kDa subunit |
| HLA-DQA1 | major histocompatibility complex, class II, DQ alpha 1 | CIT | citron (rho-interacting, serine/threonine kinase 21) |
| HLA-DRA | major histocompatibility complex, class II, DR alpha | RBM14 | RNA binding motif protein 14 |
| HLA-DRB1 | major histocompatibility complex, class II, DR beta 1 | FAM3C | family with sequence similarity 3, member C |
| HMOX1 | heme oxygenase (decycling) 1 | TSPAN2 | tetraspanin 2 |
| HPS1 | Hermansky-Pudlak syndrome 1 | ADAMTS7 | ADAM metallopeptidase with thrombospondin type 1 motif, 7 |
| HSPB1 | heat shock 27kDa protein 1 | INADL | InaD-like (Drosophila) |
| IRF8 | interferon regulatory factor 8 | RNF128 | ring finger protein 128 |
| ID2 | inhibitor of DNA binding 2, dominant negative helix-loop-helix protein | CCNJL | cyclin J-like |
| IFIT2 | interferon-induced protein with tetratricopeptide repeats 2 | LONRF3 | LON peptidase N-terminal domain and ring finger 3 |
| IFNA1 | interferon, alpha 1 | FLJ21062 | |
| IFNA13 | interferon, alpha 13 | C13orf34 | chromosome 13 open reading frame 34 |
| IGFBP7 | insulin-like growth factor binding protein 7 | ATAD5 | ATPase family, AAA domain containing 5 |
| IKBKB | inhibitor of kappa light polypeptide gene enhancer in B-cells, kinase beta | TRPM3 | transient receptor potential cation channel, subfamily M, member 3 |
| IL2RB | interleukin 2 receptor, beta | ADAMTS20 | ADAM metallopeptidase with thrombospondin type 1 motif, 20 |
| IL2RG | interleukin 2 receptor, gamma (severe combined immunodeficiency) | FLJ22184 | |
| IL4R | interleukin 4 receptor | C17orf68 | chromosome 17 open reading frame 68 |
| IL7R | interleukin 7 receptor | ELL3 | elongation factor RNA polymerase II-like 3 |
| IL10RA | interleukin 10 receptor, alpha | IGSF9 | immunoglobulin superfamily, member 9 |
| CTSK | cathepsin K | TMEM181 | transmembrane protein 181 |
| CTSS | cathepsin S | OLFML3 | olfactomedin-like 3 |
| CTSW | cathepsin W | STOX2 | storkhead box 2 |

| | | | |
|---|---|---|---|
| CTSZ | cathepsin Z | LRRN1 | leucine rich repeat neuronal 1 |
| CYBA | cytochrome b-245, alpha polypeptide | KIAA1524 | KIAA1524 |
| CYBB | cytochrome b-245, beta polypeptide (chronic granulomatous disease) | KIAA1543 | KIAA1543 |
| EDNRB | endothelin receptor type B | KIAA1549 | |
| FGF9 | fibroblast growth factor 9 (glia-activating factor) | WNK4 | WNK lysine deficient protein kinase 4 |
| GCH1 | GTP cyclohydrolase 1 (dopa-responsive dystonia) | ZSCAN18 | zinc finger and SCAN domain containing 18 |
| EGFR | epidermal growth factor receptor (erythroblastic leukemia viral (v-erb-b) oncogene homolog, avian) | LRFN4 | leucine rich repeat and fibronectin type III domain containing 4 |
| GFRA2 | GDNF family receptor alpha 2 | GRHL3 | grainyhead-like 3 (Drosophila) |
| FLT4 | fms-related tyrosine kinase 4 | KIAA1244 | KIAA1244 |
| EMP3 | epithelial membrane protein 3 | ZNF462 | zinc finger protein 462 |
| GNGT1 | guanine nucleotide binding protein (G protein), gamma transducing activity polypeptide 1 | LGR6 | leucine-rich repeat-containing G protein-coupled receptor 6 |
| GNS | glucosamine (N-acetyl)-6-sulfatase (Sanfilippo disease IIID) | TNS3 | tensin 3 |
| COCH | coagulation factor C homolog, cochlin (Limulus polyphemus) | SLC12A5 | solute carrier family 12, (potassium-chloride transporter) member 5 |
| ETS1 | v-ets erythroblastosis virus E26 oncogene homolog 1 (avian) | ODF2L | outer dense fiber of sperm tails 2-like |
| CXCR3 | chemokine (C-X-C motif) receptor 3 | TGIF2 | TGFB-induced factor homeobox 2 |
| DNM2 | dynamin 2 | GUF1 | GUF1 GTPase homolog (S. cerevisiae) |
| DOCK2 | dedicator of cytokinesis 2 | CDKAL1 | CDK5 regulatory subunit associated protein 1-like 1 |
| F8 | coagulation factor VIII, procoagulant component (hemophilia A) | BXDC2 | brix domain containing 2 |
| F13A1 | coagulation factor XIII, A1 polypeptide | C14orf106 | chromosome 14 open reading frame 106 |
| FABP1 | fatty acid binding protein 1, liver | PLCXD1 | phosphatidylinositol-specific phospholipase C, X domain containing 1 |
| FANCC | Fanconi anemia, complementation group C | DKFZp762E1312 | |
| FYB | FYN binding protein (FYB-120/130) | TNFRSF19 | tumor necrosis factor receptor superfamily, member 19 |
| GABRA3 | gamma-aminobutyric acid (GABA) A receptor, alpha 3 | CDKN2AIP | CDKN2A interacting protein |
| GRN | granulin | PNRC2 | proline-rich nuclear receptor coactivator 2 |
| DPH2 | DPH2 homolog (S. cerevisiae) | DEPDC1 | DEP domain containing 1 |
| FBLN2 | fibulin 2 | PRPF40A | PRP40 pre-mRNA processing factor 40 homolog A (S. cerevisiae) |
| FCER1G | Fc fragment of IgE, high affinity I, receptor for; gamma polypeptide | ZNF446 | zinc finger protein 446 |

| | | | |
|---|---|---|---|
| FCER2 | Fc fragment of IgE, low affinity II, receptor for (CD23) | CCAR1 | cell division cycle and apoptosis regulator 1 |
| FCGR1A | Fc fragment of IgG, high affinity Ia, receptor (CD64) | IFT122 | intraflagellar transport 122 homolog (Chlamydomonas) |
| TSC22D3 | TSC22 domain family, member 3 | MYO5C | myosin VC |
| DTX1 | deltex homolog 1 (Drosophila) | BAIAP2L1 | BAI1-associated protein 2-like 1 |
| DUSP2 | dual specificity phosphatase 2 | TMEM132A | transmembrane protein 132A |
| CST7 | cystatin F (leukocystatin) | FAM64A | family with sequence similarity 64, member A |
| ALDH1A2 | aldehyde dehydrogenase 1 family, member A2 | FAM70A | family with sequence similarity 70, member A |
| PER2 | period homolog 2 (Drosophila) | LZTFL1 | leucine zipper transcription factor-like 1 |
| GCM2 | glial cells missing homolog 2 (Drosophila) | SLC6A15 | solute carrier family 6, member 15 |
| MFHAS1 | malignant fibrous histiocytoma amplified sequence 1 | HIGD1B | HIG1 domain family, member 1B |
| STK17B | serine/threonine kinase 17b | FXYD4 | FXYD domain containing ion transport regulator 4 |
| CD163 | CD163 molecule | TRIM62 | tripartite motif-containing 62 |
| B4GALT5 | UDP-Gal:betaGlcNAc beta 1,4-galactosyltransferase, polypeptide 5 | NEIL3 | nei endonuclease VIII-like 3 (E. coli) |
| SNAP29 | synaptosomal-associated protein, 29kDa | CRNKL1 | crooked neck pre-mRNA splicing factor-like 1 (Drosophila) |
| LPXN | leupaxin | C14orf50 | chromosome 14 open reading frame 50 |
| CYP7B1 | cytochrome P450, family 7, subfamily B, polypeptide 1 | TTC14 | tetratricopeptide repeat domain 14 |
| KCNK6 | potassium channel, subfamily K, member 6 | SGOL1 | shugoshin-like 1 (S. pombe) |
| NCR1 | natural cytotoxicity triggering receptor 1 | ZNF595 | zinc finger protein 595 |
| LY86 | lymphocyte antigen 86 | RDH10 | retinol dehydrogenase 10 (all-trans) |
| IL27RA | interleukin 27 receptor, alpha | RPESP | |
| C1orf38 | chromosome 1 open reading frame 38 | ADAMTS18 | ADAM metallopeptidase with thrombospondin type 1 motif, 18 |
| NAPSA | napsin A aspartic peptidase | RHOV | ras homolog gene family, member V |
| PIGB | phosphatidylinositol glycan anchor biosynthesis, class B | ANKRD22 | ankyrin repeat domain 22 |
| GMFG | glia maturation factor, gamma | GYLTL1B | glycosyltransferase-like 1B |
| ABCG1 | ATP-binding cassette, sub-family G (WHITE), member 1 | ARHGEF19 | Rho guanine nucleotide exchange factor (GEF) 19 |
| SDC3 | syndecan 3 | SLITRK4 | SLIT and NTRK-like family, member 4 |
| CENTB1 | centaurin, beta 1 | SPIN4 | |
| KIAA0513 | KIAA0513 | EMID1 | EMI domain containing 1 |
| RASSF2 | Ras association (RalGDS/AF-6) domain family 2 | LOC129881 | |
| PTDSS1 | phosphatidylserine synthase 1 | DYNLL2 | dynein, light chain, LC8-type 2 |

| | | | |
|---|---|---|---|
| TATDN2 | TatD DNase domain containing 2 | BNIPL | BCL2/adenovirus E1B 19kD interacting protein like |
| GAB2 | GRB2-associated binding protein 2 | EMB | embigin homolog (mouse) |
| GPR68 | G protein-coupled receptor 68 | MGC29891 | |
| ZAP70 | zeta-chain (TCR) associated protein kinase 70kDa | KIAA1804 | |
| SKAP1 | src kinase associated phosphoprotein 1 | MEX3A | |
| OASL | 2'-5'-oligoadenylate synthetase-like | PALM2 | paralemmin 2 |
| EOMES | eomesodermin homolog (Xenopus laevis) | FBXO32 | F-box protein 32 |
| BECN1 | beclin 1 (coiled-coil, myosin-like BCL2 interacting protein) | GPRASP2 | G protein-coupled receptor associated sorting protein 2 |
| MARCO | macrophage receptor with collagenous structure | C6orf168 | chromosome 6 open reading frame 168 |
| DOK2 | docking protein 2, 56kDa | KIRREL3 | kin of IRRE like 3 (Drosophila) |
| SH2D2A | SH2 domain protein 2A | SERPINB11 | serpin peptidase inhibitor, clade B (ovalbumin), member 11 |
| PSTPIP2 | proline-serine-threonine phosphatase interacting protein 2 | CTTNBP2 | cortactin binding protein 2 |
| PSTPIP1 | proline-serine-threonine phosphatase interacting protein 1 | MYCBPAP | MYCBP associated protein |
| TNFRSF25 | tumor necrosis factor receptor superfamily, member 25 | USP42 | ubiquitin specific peptidase 42 |
| LAPTM5 | lysosomal associated multispanning membrane protein 5 | ZNF644 | zinc finger protein 644 |
| SLC16A6 | solute carrier family 16, member 6 (monocarboxylic acid transporter 7) | ARID5B | AT rich interactive domain 5B (MRF1-like) |
| IL1RL2 | interleukin 1 receptor-like 2 | SLCO5A1 | solute carrier organic anion transporter family, member 5A1 |
| KCNAB2 | potassium voltage-gated channel, shaker-related subfamily, beta member 2 | SPRY4 | sprouty homolog 4 (Drosophila) |
| SAA2 | serum amyloid A2 | TNS4 | tensin 4 |
| TBXAS1 | thromboxane A synthase 1 (platelet, cytochrome P450, family 5, subfamily A) | SYTL1 | synaptotagmin-like 1 |
| TCF7 | transcription factor 7 (T-cell specific, HMG-box) | KIF18A | kinesin family member 18A |
| TCN2 | transcobalamin II; macrocytic anemia | SAMD12 | sterile alpha motif domain containing 12 |
| TFR2 | transferrin receptor 2 | FAM73A | family with sequence similarity 73, member A |
| TGFBI | transforming growth factor, beta-induced, 68kDa | ENTPD8 | ectonucleoside triphosphate diphosphohydrolase 8 |
| TIMP2 | TIMP metallopeptidase inhibitor 2 | RNF207 | ring finger protein 207 |
| TIMP3 | TIMP metallopeptidase inhibitor 3 (Sorsby fundus dystrophy, pseudoinflammatory) | SAMD5 | sterile alpha motif domain containing 5 |
| CLEC3B | C-type lectin domain family 3, member | FAM21A | |

| | |
|---|---|
| | B |
| TNFAIP3 | tumor necrosis factor, alpha-induced protein 3 |
| TNFRSF1B | tumor necrosis factor receptor superfamily, member 1B |
| TNXB | tenascin XB |
| TRAF1 | TNF receptor-associated factor 1 |
| DNAJC7 | DnaJ (Hsp40) homolog, subfamily C, member 7 |
| TNFRSF4 | tumor necrosis factor receptor superfamily, member 4 |
| TXK | TXK tyrosine kinase |
| TYROBP | TYRO protein tyrosine kinase binding protein |
| VTN | vitronectin |
| WAS | Wiskott-Aldrich syndrome (eczema-thrombocytopenia) |
| LAT2 | linker for activation of T cells family, member 2 |
| WEE1 | WEE1 homolog (S. pombe) |
| XBP1 | X-box binding protein 1 |
| PRKCB1 | protein kinase C, beta 1 |
| RBM3 | RNA binding motif (RNP1, RRM) protein 3 |
| EIF2AK2 | eukaryotic translation initiation factor 2-alpha kinase 2 |
| CCL7 | chemokine (C-C motif) ligand 7 |
| LGMN | legumain |
| PSAP | prosaposin (variant Gaucher disease and variant metachromatic leukodystrophy) |
| RFX2 | regulatory factor X, 2 (influences HLA class II expression) |
| CCL22 | chemokine (C-C motif) ligand 22 |
| XCL1 | chemokine (C motif) ligand 1 |
| SOAT1 | sterol O-acyltransferase (acyl-Coenzyme A: cholesterol acyltransferase) 1 |
| PSMB1 | proteasome (prosome, macropain) subunit, beta type, 1 |
| RNASE3 | ribonuclease, RNase A family, 3 (eosinophil cationic protein) |
| RNASE6 | ribonuclease, RNase A family, k6 |

| | |
|---|---|
| | |
| FADS6 | fatty acid desaturase domain family, member 6 |
| TRIM59 | tripartite motif-containing 59 |
| ST8SIA6 | ST8 alpha-N-acetyl-neuraminide alpha-2,8-sialyltransferase 6 |
| CCDC18 | coiled-coil domain containing 18 |
| C2orf55 | chromosome 2 open reading frame 55 |
| DZIP1L | DAZ interacting protein 1-like |
| ASPM | asp (abnormal spindle) homolog, microcephaly associated (Drosophila) |
| LAMA1 | laminin, alpha 1 |
| SLC5A9 | solute carrier family 5 (sodium/glucose cotransporter), member 9 |
| MAGI3 | membrane associated guanylate kinase, WW and PDZ domain containing 3 |
| TMEM130 | transmembrane protein 130 |
| THEM5 | thioesterase superfamily member 5 |
| TMEM184A | |
| TMEM86B | transmembrane protein 86B |
| C11orf82 | |
| BCL6B | B-cell CLL/lymphoma 6, member B (zinc finger protein) |
| LOC653499 | |
| C6orf138 | |

| | |
|---|---|
| ABCE1 | ATP-binding cassette, sub-family E (OABP), member 1 |
| SELPLG | selectin P ligand |
| SPI1 | spleen focus forming virus (SFFV) proviral integration oncogene spi1 |
| PSMB9 | proteasome (prosome, macropain) subunit, beta type, 9 (large multifunctional peptidase 2) |
| SFRP4 | secreted frizzled-related protein 4 |
| SFRS2 | splicing factor, arginine/serine-rich 2 |
| SPN | sialophorin (leukosialin, CD43) |
| ST3GAL1 | ST3 beta-galactoside alpha-2,3-sialyltransferase 1 |
| STAT1 | signal transducer and activator of transcription 1, 91kDa |
| PTPN6 | protein tyrosine phosphatase, non-receptor type 6 |
| PTPRC | protein tyrosine phosphatase, receptor type, C |
| PTPRCAP | protein tyrosine phosphatase, receptor type, C-associated protein |
| SLA | Src-like-adaptor |
| SLAMF1 | signaling lymphocytic activation molecule family member 1 |
| SLC2A3 | solute carrier family 2 (facilitated glucose transporter), member 3 |
| STAT2 | signal transducer and activator of transcription 2, 113kDa |
| STK4 | serine/threonine kinase 4 |
| RAB3IL1 | RAB3A interacting protein (rabin3)-like 1 |
| RYR3 | ryanodine receptor 3 |
| SLC11A1 | solute carrier family 11 (proton-coupled divalent metal ion transporters), member 1 |
| SYK | spleen tyrosine kinase |
| RAC2 | ras-related C3 botulinum toxin substrate 2 (rho family, small GTP binding protein Rac2) |
| PTPN18 | protein tyrosine phosphatase, non-receptor type 18 (brain-derived) |
| PPP1R14B | protein phosphatase 1, regulatory (inhibitor) subunit 14B |
| SIT1 | signaling threshold regulating transmembrane adaptor 1 |
| SLC43A3 | solute carrier family 43, member 3 |
| BLNK | B-cell linker |
| GPR171 | G protein-coupled receptor 171 |

| | |
|---|---|
| CD207 | CD207 molecule, langerin |
| TNFRSF13B | tumor necrosis factor receptor superfamily, member 13B |
| HMHA1 | histocompatibility (minor) HA-1 |
| CLCF1 | cardiotrophin-like cytokine factor 1 |
| PIK3R5 | phosphoinositide-3-kinase, regulatory subunit 5, p101 |
| TNPO3 | transportin 3 |
| SAMHD1 | SAM domain and HD domain 1 |
| PCOLCE2 | procollagen C-endopeptidase enhancer 2 |
| PSD4 | pleckstrin and Sec7 domain containing 4 |
| PIP3-E | |
| HAVCR1 | hepatitis A virus cellular receptor 1 |
| PPP1R16B | protein phosphatase 1, regulatory (inhibitor) subunit 16B |
| GPR160 | G protein-coupled receptor 160 |
| CYFIP2 | cytoplasmic FMR1 interacting protein 2 |
| LAT | linker for activation of T cells |
| TRAPPC3 | trafficking protein particle complex 3 |
| ZNF318 | zinc finger protein 318 |
| SHC2 | SHC (Src homology 2 domain containing) transforming protein 2 |
| FBXO24 | F-box protein 24 |
| SNX5 | sorting nexin 5 |
| PLA2G2D | phospholipase A2, group IID |
| INTU | inturned planar cell polarity effector homolog (Drosophila) |
| IFI44 | interferon-induced protein 44 |
| LYVE1 | extracellular link domain containing 1 |
| RUNDC3A | |
| TREX1 | three prime repair exonuclease 1 |
| CD300A | CD300a molecule |
| CBX3 | chromobox homolog 3 (HP1 gamma homolog, Drosophila) |
| TFEC | transcription factor EC |
| IKZF3 | IKAROS family zinc finger 3 (Aiolos) |
| RALY | RNA binding protein, autoantigenic (hnRNP-associated with lethal yellow homolog (mouse)) |
| KLRK1 | killer cell lectin-like receptor subfamily K, member 1 |
| FCHO1 | FCH domain only 1 |

| | |
|---|---|
| STAB1 | stabilin 1 |
| ANKRD12 | ankyrin repeat domain 12 |
| BICD2 | bicaudal D homolog 2 (Drosophila) |
| KCNH3 | potassium voltage-gated channel, subfamily H (eag-related), member 3 |
| ZBED4 | zinc finger, BED-type containing 4 |
| RABGAP1L | RAB GTPase activating protein 1-like |
| P2RY14 | purinergic receptor P2Y, G-protein coupled, 14 |
| ARHGAP25 | Rho GTPase activating protein 25 |
| IFI44L | interferon-induced protein 44-like |
| RGS14 | regulator of G-protein signalling 14 |
| CLEC4M | C-type lectin domain family 4, member M |
| CUGBP2 | CUG triplet repeat, RNA binding protein 2 |
| CXCR6 | chemokine (C-X-C motif) receptor 6 |
| TNFSF13B | tumor necrosis factor (ligand) superfamily, member 13b |
| CORO2B | coronin, actin binding protein, 2B |
| TPPP | tubulin polymerization promoting protein |
| GRAP | GRB2-related adaptor protein |
| C9orf9 | chromosome 9 open reading frame 9 |
| TSPAN32 | tetraspanin 32 |
| IFI30 | interferon, gamma-inducible protein 30 |
| CLEC10A | C-type lectin domain family 10, member A |
| CORO1A | coronin, actin binding protein, 1A |
| FAM107A | family with sequence similarity 107, member A |
| EBI3 | Epstein-Barr virus induced gene 3 |
| HPSE | heparanase |
| MAP4K1 | mitogen-activated protein kinase kinase kinase kinase 1 |
| INMT | indolethylamine N-methyltransferase |
| KLK8 | kallikrein-related peptidase 8 |
| PLXNC1 | plexin C1 |
| HCST | hematopoietic cell signal transducer |
| GPR83 | G protein-coupled receptor 83 |
| MPHOSPH10 | M-phase phosphoprotein 10 (U3 small nucleolar ribonucleoprotein) |
| NUFIP2 | nuclear fragile X mental retardation protein interacting protein 2 |

| | |
|---|---|
| TBC1D14 | TBC1 domain family, member 14 |
| ZXDC | ZXD family zinc finger C |
| CORO7 | coronin 7 |
| TNFAIP8L2 | tumor necrosis factor, alpha-induced protein 8-like 2 |
| C1orf54 | chromosome 1 open reading frame 54 |
| SNX22 | sorting nexin 22 |
| MAP6D1 | MAP6 domain containing 1 |
| DENND1C | DENN/MADD domain containing 1C |
| FOXRED2 | FAD-dependent oxidoreductase domain containing 2 |
| TRAF3IP3 | TRAF3 interacting protein 3 |
| AKNA | AT-hook transcription factor |
| ACAD10 | acyl-Coenzyme A dehydrogenase family, member 10 |
| LIMD2 | LIM domain containing 2 |
| NPL | N-acetylneuraminate pyruvate lyase (dihydrodipicolinate synthase) |
| AADACL1 | arylacetamide deacetylase-like 1 |
| BCL11B | B-cell CLL/lymphoma 11B (zinc finger protein) |
| FLJ21438 | |
| PDZD4 | PDZ domain containing 4 |
| MYO1G | myosin IG |
| RTN4R | reticulon 4 receptor |
| CXCR7 | chemokine (C-X-C motif) receptor 7 |
| PDXP | pyridoxal (pyridoxine, vitamin B6) phosphatase |
| C1orf63 | chromosome 1 open reading frame 63 |
| SAMSN1 | SAM domain, SH3 domain and nuclear localization signals 1 |
| PARVG | parvin, gamma |
| LRRC4 | leucine rich repeat containing 4 |
| C10orf54 | chromosome 10 open reading frame 54 |
| PCDH15 | protocadherin 15 |
| TOR3A | torsin family 3, member A |
| MS4A6A | membrane-spanning 4-domains, subfamily A, member 6A |
| SECISBP2 | SECIS binding protein 2 |
| ASPHD2 | aspartate beta-hydroxylase domain containing 2 |
| ZNFX1 | zinc finger, NFX1-type containing 1 |
| CXCL16 | chemokine (C-X-C motif) ligand 16 |

| | |
|---|---|
| MS4A7 | membrane-spanning 4-domains, subfamily A, member 7 |
| NFKBIZ | nuclear factor of kappa light polypeptide gene enhancer in B-cells inhibitor, zeta |
| ARHGAP9 | Rho GTPase activating protein 9 |
| PRODH2 | proline dehydrogenase (oxidase) 2 |
| DHX58 | |
| DSCAML1 | Down syndrome cell adhesion molecule like 1 |
| AGBL5 | ATP/GTP binding protein-like 5 |
| CRLF3 | cytokine receptor-like factor 3 |
| TRPV2 | transient receptor potential cation channel, subfamily V, member 2 |
| LAX1 | lymphocyte transmembrane adaptor 1 |
| GIMAP4 | GTPase, IMAP family member 4 |
| STAB2 | stabilin 2 |
| BMP2K | BMP2 inducible kinase |
| FAM46A | family with sequence similarity 46, member A |
| NSUN5 | NOL1/NOP2/Sun domain family, member 5 |
| ARHGAP15 | Rho GTPase activating protein 15 |
| DBNDD2 | dysbindin (dystrobrevin binding protein 1) domain containing 2 |
| SUSD2 | sushi domain containing 2 |
| CRTAM | cytotoxic and regulatory T cell molecule |
| CPXM1 | carboxypeptidase X (M14 family), member 1 |
| BARHL1 | BarH-like 1 (Drosophila) |
| SLAMF8 | SLAM family member 8 |
| TRAT1 | T cell receptor associated transmembrane adaptor 1 |
| HNT | |
| LIME1 | Lck interacting transmembrane adaptor 1 |
| C9orf114 | chromosome 9 open reading frame 114 |
| TREM2 | triggering receptor expressed on myeloid cells 2 |
| GNG2 | guanine nucleotide binding protein (G protein), gamma 2 |
| BANP | BTG3 associated nuclear protein |
| PI15 | peptidase inhibitor 15 |
| C9orf156 | chromosome 9 open reading frame 156 |

| | |
|---|---|
| HERC6 | hect domain and RLD 6 |
| PIH1D1 | PIH1 domain containing 1 |
| LSR | lipolysis stimulated lipoprotein receptor |
| FAM105A | family with sequence similarity 105, member A |
| RHOF | ras homolog gene family, member F (in filopodia) |
| BANK1 | B-cell scaffold protein with ankyrin repeats 1 |
| RALGPS2 | Ral GEF with PH domain and SH3 binding motif 2 |
| RAPGEF6 | Rap guanine nucleotide exchange factor (GEF) 6 |
| CALML5 | calmodulin-like 5 |
| MGC29506 | |
| GALNT7 | UDP-N-acetyl-alpha-D-galactosamine:polypeptide N-acetylgalactosaminyltransferase 7 (GalNAc-T7) |
| TM6SF1 | transmembrane 6 superfamily member 1 |
| GMIP | GEM interacting protein |
| FXYD5 | FXYD domain containing ion transport regulator 5 |
| P2RY13 | purinergic receptor P2Y, G-protein coupled, 13 |
| SLC15A3 | solute carrier family 15, member 3 |
| PLAC8 | placenta-specific 8 |
| MCOLN3 | mucolipin 3 |
| PLA1A | phospholipase A1 member A |
| TMEM71 | transmembrane protein 71 |
| JAKMIP1 | janus kinase and microtubule interacting protein 1 |
| ABCA13 | ATP-binding cassette, sub-family A (ABC1), member 13 |
| SLFN5 | schlafen family member 5 |
| FBXO39 | F-box protein 39 |
| KCNV2 | potassium channel, subfamily V, member 2 |
| C10orf128 | chromosome 10 open reading frame 128 |
| ADAMTS19 | ADAM metallopeptidase with thrombospondin type 1 motif, 19 |
| SLFN13 | schlafen family member 13 |
| BHLHB4 | basic helix-loop-helix domain containing, class B, 4 |

| | |
|---|---|
| C20orf141 | chromosome 20 open reading frame 141 |
| SPIC | Spi-C transcription factor (Spi-1/PU.1 related) |
| PLD4 | phospholipase D family, member 4 |
| DCUN1D3 | DCN1, defective in cullin neddylation 1, domain containing 3 (S. cerevisiae) |
| ALS2CR12 | amyotrophic lateral sclerosis 2 (juvenile) chromosome region, candidate 12 |
| CD200R1 | CD200 receptor 1 |
| MOBKL2C | MOB1, Mps One Binder kinase activator-like 2C (yeast) |
| USP43 | ubiquitin specific peptidase 43 |
| DCBLD2 | discoidin, CUB and LCCL domain containing 2 |
| NFAM1 | NFAT activating protein with ITAM motif 1 |
| FLJ45909 | |
| MS4A8B | membrane-spanning 4-domains, subfamily A, member 8B |
| JAM3 | junctional adhesion molecule 3 |
| INHBE | inhibin, beta E |
| CARD11 | caspase recruitment domain family, member 11 |
| CALML4 | calmodulin-like 4 |
| TIMD4 | T-cell immunoglobulin and mucin domain containing 4 |
| RCSD1 | RCSD domain containing 1 |
| CLEC6A | C-type lectin domain family 6, member A |
| HTRA3 | HtrA serine peptidase 3 |
| EPSTI1 | epithelial stromal interaction 1 (breast) |
| ODF3 | outer dense fiber of sperm tails 3 |
| SLAMF6 | SLAM family member 6 |
| FCRL1 | Fc receptor-like 1 |
| NOSTRIN | nitric oxide synthase trafficker |
| ZBP1 | Z-DNA binding protein 1 |
| COLEC12 | collectin sub-family member 12 |
| LONP2 | lon peptidase 2, peroxisomal |
| KBTBD8 | kelch repeat and BTB (POZ) domain containing 8 |
| GPR174 | G protein-coupled receptor 174 |
| RASSF4 | Ras association (RalGDS/AF-6) domain family 4 |
| SIGLEC10 | sialic acid binding Ig-like lectin 10 |

| | |
|---|---|
| FGD3 | FYVE, RhoGEF and PH domain containing 3 |
| KLHL6 | kelch-like 6 (Drosophila) |
| B3GNT5 | UDP-GlcNAc:betaGal beta-1,3-N-acetylglucosaminyltransferase 5 |
| SLAMF9 | SLAM family member 9 |
| FCRLA | Fc receptor-like A |
| UNC93B1 | unc-93 homolog B1 (C. elegans) |
| MAF1 | MAF1 homolog (S. cerevisiae) |
| NUAK2 | NUAK family, SNF1-like kinase, 2 |
| HSH2D | hematopoietic SH2 domain containing |
| RSAD2 | radical S-adenosyl methionine domain containing 2 |
| UBXD5 | UBX domain containing 5 |
| HVCN1 | hydrogen voltage-gated channel 1 |
| PCGF5 | polycomb group ring finger 5 |
| FAM55C | family with sequence similarity 55, member C |
| LOC390243 | |
| C6orf26 | chromosome 6 open reading frame 26 |
| MCART6 | mitochondrial carrier triple repeat 6 |
| LRRC33 | leucine rich repeat containing 33 |
| LHFPL3 | lipoma HMGIC fusion partner-like 3 |
| BMP8A | bone morphogenetic protein 8a |
| TBC1D10C | TBC1 domain family, member 10C |
| ARHGAP30 | Rho GTPase activating protein 30 |
| FAM78A | family with sequence similarity 78, member A |
| RNASE10 | ribonuclease, RNase A family, 10 (non-active) |
| RSPO2 | R-spondin 2 homolog (Xenopus laevis) |
| KIAA2022 | KIAA2022 |
| SLFN5 | |
| PFN3 | profilin 3 |
| C19orf59 | chromosome 19 open reading frame 59 |
| FGD2 | FYVE, RhoGEF and PH domain containing 2 |
| PI16 | peptidase inhibitor 16 |
| C6orf145 | chromosome 6 open reading frame 145 |
| METRNL | meteorin, glial cell differentiation regulator-like |
| IL4I1 | interleukin 4 induced 1 |
| MUC20 | mucin 20, cell surface associated |

| | |
|---|---|
| AQP11 | aquaporin 11 |
| NRK | Nik related kinase |
| CCDC88B | coiled-coil domain containing 88B |
| TPCN2 | two pore segment channel 2 |
| MCOLN2 | mucolipin 2 |
| LOC255809 | |
| hCG_2015956 | |
| NCF1 | neutrophil cytosolic factor 1, (chronic granulomatous disease, autosomal 1) |
| GIMAP6 | GTPase, IMAP family member 6 |
| PHOSPHO2 | phosphatase, orphan 2 |
| RNF165 | ring finger protein 165 |
| MRC1L1 | mannose receptor, C type 1-like 1 |
| IFIT1L | interferon-induced protein with tetratricopeptide repeats 1-like |
| HIST2H2BF | histone cluster 2, H2bf |

**Induced by at least 1.25-fold at 1 wk in Tgfb1 +/-**

| Symbol | Gene Name |
|---|---|
| CCKBR | cholecystokinin B receptor |
| CCNB1 | cyclin B1 |
| CD247 | CD247 molecule |
| CD151 | CD151 molecule (Raph blood group) |
| LRBA | LPS-responsive vesicle trafficking, beach and anchor containing |
| CDH8 | cadherin 8, type 2 |
| CDH10 | cadherin 10, type 2 (T2-cadherin) |
| CEL | carboxyl ester lipase (bile salt-stimulated lipase) |
| CENPF | centromere protein F, 350/400ka (mitosin) |
| CETN1 | centrin, EF-hand protein, 1 |
| CHKA | choline kinase alpha |
| CHRNA4 | cholinergic receptor, nicotinic, alpha 4 |
| CIDEA | cell death-inducing DFFA-like effector a |
| TBCB | tubulin folding cofactor B |

**Induced by at least 1.25-fold at 4 wks in Tgfb1 +/-**

| Symbol | Gene Name |
|---|---|
| ABCD2 | ATP-binding cassette, sub-family D (ALD), member 2 |
| ATRX | alpha thalassemia/mental retardation syndrome X-linked (RAD54 homolog, S. cerevisiae) |
| CCK | cholecystokinin |
| KRIT1 | KRIT1, ankyrin repeat containing |
| CCNG1 | cyclin G1 |
| CCNG2 | cyclin G2 |
| CCNT2 | cyclin T2 |
| CD36 | CD36 molecule (thrombospondin receptor) |
| CDH11 | cadherin 11, type 2, OB-cadherin (osteoblast) |
| CES1 | carboxylesterase 1 (monocyte/macrophage serine esterase 1) |
| COL3A1 | collagen, type III, alpha 1 (Ehlers-Danlos syndrome type IV, autosomal dominant) |
| COL4A1 | collagen, type IV, alpha 1 |
| COL4A5 | collagen, type IV, alpha 5 (Alport syndrome) |
| COL5A1 | collagen, type V, alpha 1 |

| | | | |
|---|---|---|---|
| CKM | creatine kinase, muscle | COL9A1 | collagen, type IX, alpha 1 |
| ERCC8 | excision repair cross-complementing rodent repair deficiency, complementation group 8 | CPA3 | carboxypeptidase A3 (mast cell) |
| CPB1 | carboxypeptidase B1 (tissue) | CSN3 | casein kappa |
| CPN2 | carboxypeptidase N, polypeptide 2 | CTH | cystathionase (cystathionine gamma-lyase) |
| CRYBA1 | crystallin, beta A1 | CTNNB1 | catenin (cadherin-associated protein), beta 1, 88kDa |
| CSN3 | casein kappa | BCL2L2 | BCL2-like 2 |
| VCAN | versican | BLMH | bleomycin hydrolase |
| BCL2L2 | BCL2-like 2 | APLP2 | amyloid beta (A4) precursor-like protein 2 |
| BICD1 | bicaudal D homolog 1 (Drosophila) | BNIP3L | BCL2/adenovirus E1B 19kDa interacting protein 3-like |
| APOB | apolipoprotein B (including Ag(x) antigen) | SERPINA3 | serpin peptidase inhibitor, clade A (alpha-1 antiproteinase, antitrypsin), member 3 |
| BNIP2 | BCL2/adenovirus E1B 19kDa interacting protein 2 | ABAT | 4-aminobutyrate aminotransferase |
| BRCA1 | breast cancer 1, early onset | AQP7 | aquaporin 7 |
| ARG2 | arginase, type II | ARCN1 | archain 1 |
| ASPH | aspartate beta-hydroxylase | RND3 | Rho family GTPase 3 |
| CACNA1B | calcium channel, voltage-dependent, N type, alpha 1B subunit | ARHGAP5 | Rho GTPase activating protein 5 |
| ATP2B3 | ATPase, Ca++ transporting, plasma membrane 3 | C5 | complement component 5 |
| AGTR1 | angiotensin II receptor, type 1 | OSGIN2 | oxidative stress induced growth inhibitor family member 2 |
| ATP6V1E1 | ATPase, H+ transporting, lysosomal 31kDa, V1 subunit E1 | C11orf9 | chromosome 11 open reading frame 9 |
| KRT14 | keratin 14 (epidermolysis bullosa simplex, Dowling-Meara, Koebner) | ASPH | aspartate beta-hydroxylase |
| KITLG | KIT ligand | CA2 | carbonic anhydrase II |
| P2RX3 | purinergic receptor P2X, ligand-gated ion channel, 3 | CA6 | carbonic anhydrase VI |
| PAX6 | paired box gene 6 (aniridia, keratitis) | ACYP1 | acylphosphatase 1, erythrocyte (common) type |
| PCDH9 | protocadherin 9 | ADAM10 | ADAM metallopeptidase domain 10 |
| PDE1C | phosphodiesterase 1C, calmodulin-dependent 70kDa | CACNB4 | calcium channel, voltage-dependent, beta 4 subunit |
| SLC26A4 | solute carrier family 26, member 4 | ADRB3 | adrenergic, beta-3-, receptor |
| PGGT1B | protein geranylgeranyltransferase type I, beta subunit | ATP1B1 | ATPase, Na+/K+ transporting, beta 1 polypeptide |
| PLS1 | plastin 1 (I isoform) | CALML3 | calmodulin-like 3 |
| PLSCR1 | phospholipid scramblase 1 | CAMK4 | calcium/calmodulin-dependent protein kinase IV |

| | | | |
|---|---|---|---|
| POLR2A | polymerase (RNA) II (DNA directed) polypeptide A, 220kDa | AGL | amylo-1, 6-glucosidase, 4-alpha-glucanotransferase (glycogen debranching enzyme, glycogen storage disease type III) |
| PPP3CB | protein phosphatase 3 (formerly 2B), catalytic subunit, beta isoform | JAG1 | jagged 1 (Alagille syndrome) |
| PPY | pancreatic polypeptide | CASP7 | caspase 7, apoptosis-related cysteine peptidase |
| MID1 | midline 1 (Opitz/BBB syndrome) | ATP6V1B1 | ATPase, H+ transporting, lysosomal 56/58kDa, V1 subunit B1 (Renal tubular acidosis with deafness) |
| AFF1 | AF4/FMR2 family, member 1 | KITLG | KIT ligand |
| LEPR | leptin receptor | P4HA1 | procollagen-proline, 2-oxoglutarate 4-dioxygenase (proline 4-hydroxylase), alpha polypeptide I |
| MMP16 | matrix metallopeptidase 16 (membrane-inserted) | PDCL | phosducin-like |
| NEO1 | neogenin homolog 1 (chicken) | PCDH7 | protocadherin 7 |
| NFATC2 | nuclear factor of activated T-cells, cytoplasmic, calcineurin-dependent 2 | PCK1 | phosphoenolpyruvate carboxykinase 1 (soluble) |
| NFIC | nuclear factor I/C (CCAAT-binding transcription factor) | PDE1A | phosphodiesterase 1A, calmodulin-dependent |
| LPO | lactoperoxidase | PDK4 | pyruvate dehydrogenase kinase, isozyme 4 |
| LRPAP1 | low density lipoprotein receptor-related protein associated protein 1 | ENPP3 | ectonucleotide pyrophosphatase/phosphodiesterase 3 |
| KCNA2 | potassium voltage-gated channel, shaker-related subfamily, member 2 | SERPINF1 | serpin peptidase inhibitor, clade F (alpha-2 antiplasmin, pigment epithelium derived factor), member 1 |
| CITED1 | Cbp/p300-interacting transactivator, with Glu/Asp-rich carboxy-terminal domain, 1 | PEG3 | paternally expressed 3 |
| NOS2A | nitric oxide synthase 2A (inducible, hepatocytes) | ABCB1 | ATP-binding cassette, sub-family B (MDR/TAP), member 1 |
| KCNG1 | potassium voltage-gated channel, subfamily G, member 1 | PHKA1 | phosphorylase kinase, alpha 1 (muscle) |
| MTF1 | metal-regulatory transcription factor 1 | PKHD1 | polycystic kidney and hepatic disease 1 (autosomal recessive) |
| MTM1 | myotubularin 1 | PKNOX1 | PBX/knotted 1 homeobox 1 |
| MYB | v-myb myeloblastosis viral oncogene homolog (avian) | PKP2 | plakophilin 2 |
| KCNQ2 | potassium voltage-gated channel, KQT-like subfamily, member 2 | PMM2 | phosphomannomutase 2 |
| KIF2A | kinesin heavy chain member 2A | POLB | polymerase (DNA directed), beta |
| MC5R | melanocortin 5 receptor | PPM1A | protein phosphatase 1A (formerly 2C), magnesium-dependent, alpha isoform |
| MYH4 | myosin, heavy chain 4, skeletal muscle | PPP2R1B | protein phosphatase 2 (formerly 2A), regulatory subunit A, beta isoform |

| | | | |
|---|---|---|---|
| TNFRSF11B | tumor necrosis factor receptor superfamily, member 11b (osteoprotegerin) | PPP2R2B | protein phosphatase 2 (formerly 2A), regulatory subunit B, beta isoform |
| KIF11 | kinesin family member 11 | PRELP | proline/arginine-rich end leucine-rich repeat protein |
| KRT2 | keratin 2 (epidermal ichthyosis bullosa of Siemens) | LAMB1 | laminin, beta 1 |
| MEF2D | myocyte enhancer factor 2D | MLLT3 | myeloid/lymphoid or mixed-lineage leukemia (trithorax homolog, Drosophila); translocated to, 3 |
| NASP | nuclear autoantigenic sperm protein (histone-binding) | LEP | leptin (obesity homolog, mouse) |
| HELLS | helicase, lymphoid-specific | LEPR | leptin receptor |
| HMGCS2 | 3-hydroxy-3-methylglutaryl-Coenzyme A synthase 2 (mitochondrial) | MMP9 | matrix metallopeptidase 9 (gelatinase B, 92kDa gelatinase, 92kDa type IV collagenase) |
| HNF4A | hepatocyte nuclear factor 4, alpha | LIPA | lipase A, lysosomal acid, cholesterol esterase (Wolman disease) |
| SLC29A2 | solute carrier family 29 (nucleoside transporters), member 2 | FADS3 | fatty acid desaturase 3 |
| IDE | insulin-degrading enzyme | JARID2 | jumonji, AT rich interactive domain 2 |
| IFIT1 | interferon-induced protein with tetratricopeptide repeats 1 | LTBP3 | latent transforming growth factor beta binding protein 3 |
| IFNA1 | interferon, alpha 1 | MT1F | metallothionein 1F |
| IFNA13 | interferon, alpha 13 | KCND2 | potassium voltage-gated channel, Shal-related subfamily, member 2 |
| IHH | Indian hedgehog homolog (Drosophila) | NPR3 | natriuretic peptide receptor C/guanylate cyclase C (atrionatriuretic peptide receptor C) |
| CYLD | cylindromatosis (turban tumor syndrome) | MAOA | monoamine oxidase A |
| LGTN | ligatin | MAP1B | microtubule-associated protein 1B |
| EIF4G2 | eukaryotic translation initiation factor 4 gamma, 2 | MUTYH | mutY homolog (E. coli) |
| ELAVL2 | ELAV (embryonic lethal, abnormal vision, Drosophila)-like 2 (Hu antigen B) | MXI1 | MAX interactor 1 |
| B4GALT1 | UDP-Gal:betaGlcNAc beta 1,4-galactosyltransferase, polypeptide 1 | NTRK2 | neurotrophic tyrosine kinase, receptor, type 2 |
| GJA3 | gap junction protein, alpha 3, 46kDa | KIF5B | kinesin family member 5B |
| GK | glycerol kinase | MATN2 | matrilin 2 |
| CYP27B1 | cytochrome P450, family 27, subfamily B, polypeptide 1 | MBD1 | methyl-CpG binding domain protein 1 |
| DGKB | diacylglycerol kinase, beta 90kDa | MC2R | melanocortin 2 receptor (adrenocorticotropic hormone) |
| ELAVL1 | ELAV (embryonic lethal, abnormal vision, Drosophila)-like 1 (Hu antigen R) | TNFRSF11B | tumor necrosis factor receptor superfamily, member 11b (osteoprotegerin) |

| | | | |
|---|---|---|---|
| FMO4 | flavin containing monooxygenase 4 | KIT | v-kit Hardy-Zuckerman 4 feline sarcoma viral oncogene homolog |
| FOLR1 | folate receptor 1 (adult) | KLC1 | kinesin light chain 1 |
| ERCC1 | excision repair cross-complementing rodent repair deficiency, complementation group 1 (includes overlapping antisense sequence) | MDH1 | malate dehydrogenase 1, NAD (soluble) |
| ESRRB | estrogen-related receptor beta | MYO1C | myosin IC |
| GP1BB | glycoprotein Ib (platelet), beta polypeptide | MYO6 | myosin VI |
| DMBT1 | deleted in malignant brain tumors 1 | PPP1R12A | protein phosphatase 1, regulatory (inhibitor) subunit 12A |
| DMPK | dystrophia myotonica-protein kinase | MFI2 | antigen p97 (melanoma associated) identified by monoclonal antibodies 133.2 and 96.5 |
| NR5A2 | nuclear receptor subfamily 5, group A, member 2 | DYRK1A | dual-specificity tyrosine-(Y)-phosphorylation regulated kinase 1A |
| FUT2 | fucosyltransferase 2 (secretor status included) | EBF1 | early B-cell factor 1 |
| MCHR1 | melanin-concentrating hormone receptor 1 | GTF2A1 | general transcription factor IIA, 1, 19/37kDa |
| GPER | G protein-coupled receptor 30 | GTF2I | general transcription factor II, i |
| DNAH8 | dynein, axonemal, heavy chain 8 | GUCY1B3 | guanylate cyclase 1, soluble, beta 3 |
| FABP3 | fatty acid binding protein 3, muscle and heart (mammary-derived growth inhibitor) | GUSB | glucuronidase, beta |
| FANCD2 | Fanconi anemia, complementation group D2 | GZMA | granzyme A (granzyme 1, cytotoxic T-lymphocyte-associated serine esterase 3) |
| XRCC6 | X-ray repair complementing defective repair in Chinese hamster cells 6 (Ku autoantigen, 70kDa) | GZMB | granzyme B (granzyme 2, cytotoxic T-lymphocyte-associated serine esterase 1) |
| GABRA1 | gamma-aminobutyric acid (GABA) A receptor, alpha 1 | H1F0 | H1 histone family, member 0 |
| GRIA2 | glutamate receptor, ionotropic, AMPA 2 | HDLBP | high density lipoprotein binding protein (vigilin) |
| GRIK1 | glutamate receptor, ionotropic, kainate 1 | HLF | hepatic leukemia factor |
| SLC26A3 | solute carrier family 26, member 3 | NR4A1 | nuclear receptor subfamily 4, group A, member 1 |
| DRD2 | dopamine receptor D2 | HNMT | histamine N-methyltransferase |
| DRD4 | dopamine receptor D4 | HOXD8 | homeobox D8 |
| FARSA | phenylalanyl-tRNA synthetase, alpha subunit | HOXD9 | homeobox D9 |
| GAD1 | glutamate decarboxylase 1 (brain, 67kDa) | HOXD10 | homeobox D10 |
| HMGA2 | high mobility group AT-hook 2 | HPGD | hydroxyprostaglandin dehydrogenase 15-(NAD) |

| | | | |
|---|---|---|---|
| BLZF1 | basic leucine zipper nuclear factor 1 (JEM-1) | HSD11B2 | hydroxysteroid (11-beta) dehydrogenase 2 |
| BCL7C | B-cell CLL/lymphoma 7C | IDE | insulin-degrading enzyme |
| EFTUD2 | elongation factor Tu GTP binding domain containing 2 | IFNGR2 | interferon gamma receptor 2 (interferon gamma transducer 1) |
| NRXN3 | neurexin 3 | IL6ST | interleukin 6 signal transducer (gp130, oncostatin M receptor) |
| PREPL | prolyl endopeptidase-like | EDNRA | endothelin receptor type A |
| TRAF4 | TNF receptor-associated factor 4 | GCDH | glutaryl-Coenzyme A dehydrogenase |
| MICAL2 | microtubule associated monoxygenase, calponin and LIM domain containing 2 | CYP1B1 | cytochrome P450, family 1, subfamily B, polypeptide 1 |
| KIAA0355 | KIAA0355 | FKBP5 | FK506 binding protein 5 |
| KIAA0101 | KIAA0101 | GDI2 | GDP dissociation inhibitor 2 |
| KIAA0494 | KIAA0494 | EHHADH | enoyl-Coenzyme A, hydratase/3-hydroxyacyl Coenzyme A dehydrogenase |
| SFI1 | Sfi1 homolog, spindle assembly associated (yeast) | EIF1AX | eukaryotic translation initiation factor 1A, X-linked |
| YY1 | YY1 transcription factor | GHR | growth hormone receptor |
| ST8SIA2 | ST8 alpha-N-acetyl-neuraminide alpha-2,8-sialyltransferase 2 | GJA1 | gap junction protein, alpha 1, 43kDa |
| PLA2G4C | phospholipase A2, group IVC (cytosolic, calcium-independent) | GJB2 | gap junction protein, beta 2, 26kDa |
| ZNF43 | zinc finger protein 43 | CYP24A1 | cytochrome P450, family 24, subfamily A, polypeptide 1 |
| SYN3 | synapsin III | CYP27A1 | cytochrome P450, family 27, subfamily A, polypeptide 1 |
| JARID1C | jumonji, AT rich interactive domain 1C | DACH1 | dachshund homolog 1 (Drosophila) |
| DNAH17 | dynein, axonemal, heavy chain 17 | ELAVL1 | ELAV (embryonic lethal, abnormal vision, Drosophila)-like 1 (Hu antigen R) |
| WASL | Wiskott-Aldrich syndrome-like | ELF5 | E74-like factor 5 (ets domain transcription factor) |
| TRPA1 | transient receptor potential cation channel, subfamily A, member 1 | FMO2 | flavin containing monooxygenase 2 (non-functional) |
| ACOX2 | acyl-Coenzyme A oxidase 2, branched chain | FMOD | fibromodulin |
| PKD2L1 | polycystic kidney disease 2-like 1 | EPB41L2 | erythrocyte membrane protein band 4.1-like 2 |
| FZD9 | frizzled homolog 9 (Drosophila) | STOM | stomatin |
| EIF4G3 | eukaryotic translation initiation factor 4 gamma, 3 | GM2A | GM2 ganglioside activator |
| CDC23 | cell division cycle 23 homolog (S. cerevisiae) | GMFB | glia maturation factor, beta |
| B4GALT2 | UDP-Gal:betaGlcNAc beta 1,4-galactosyltransferase, polypeptide 2 | GNAI1 | guanine nucleotide binding protein (G protein), alpha inhibiting activity polypeptide 1 |

| | | | |
|---|---|---|---|
| LAPTM5 | lysosomal associated multispanning membrane protein 5 | GADD45A | growth arrest and DNA-damage-inducible, alpha |
| PLA2G6 | phospholipase A2, group VI (cytosolic, calcium-independent) | GPM6B | glycoprotein M6B |
| SLC16A4 | solute carrier family 16, member 4 (monocarboxylic acid transporter 5) | ETV5 | ets variant gene 5 (ets-related molecule) |
| DYRK3 | dual-specificity tyrosine-(Y)-phosphorylation regulated kinase 3 | FUT4 | fucosyltransferase 4 (alpha (1,3) fucosyltransferase, myeloid-specific) |
| DOC2B | double C2-like domains, beta | DNMT3A | DNA (cytosine-5-)-methyltransferase 3 alpha |
| FOXN1 | forkhead box N1 | FABP4 | fatty acid binding protein 4, adipocyte |
| SAA1 | serum amyloid A1 | ACSL3 | acyl-CoA synthetase long-chain family member 3 |
| SLC18A1 | solute carrier family 18 (vesicular monoamine), member 1 | GAB1 | GRB2-associated binding protein 1 |
| TF | transferrin | DR1 | down-regulator of transcription 1, TBP-binding (negative cofactor 2) |
| TGFBR1 | transforming growth factor, beta receptor I (activin A receptor type II-like kinase, 53kDa) | FBN2 | fibrillin 2 (congenital contractural arachnodactyly) |
| TLL2 | tolloid-like 2 | NR3C1 | nuclear receptor subfamily 3, group C, member 1 (glucocorticoid receptor) |
| TNNI2 | troponin I type 2 (skeletal, fast) | TSC22D3 | TSC22 domain family, member 3 |
| TOP2A | topoisomerase (DNA) II alpha 170kDa | EPYC | epiphycan |
| TPMT | thiopurine S-methyltransferase | DUSP1 | dual specificity phosphatase 1 |
| TPTE | transmembrane phosphatase with tensin homology | MFAP5 | microfibrillar associated protein 5 |
| TYR | tyrosinase (oculocutaneous albinism IA) | DDO | D-aspartate oxidase |
| UBC | ubiquitin C | API5 | apoptosis inhibitor 5 |
| UBE2V2 | ubiquitin-conjugating enzyme E2 variant 2 | VNN1 | vanin 1 |
| UGT2B15 | UDP glucuronosyltransferase 2 family, polypeptide B15 | RPS6KA5 | ribosomal protein S6 kinase, 90kDa, polypeptide 5 |
| UCK2 | uridine-cytidine kinase 2 | C5orf13 | chromosome 5 open reading frame 13 |
| ZAN | zonadhesin | VAMP3 | vesicle-associated membrane protein 3 (cellubrevin) |
| CLIP2 | CAP-GLY domain containing linker protein 2 | FADS2 | fatty acid desaturase 2 |
| LAT2 | linker for activation of T cells family, member 2 | SLC4A7 | solute carrier family 4, sodium bicarbonate cotransporter, member 7 |
| CORO2A | coronin, actin binding protein, 2A | PTGES | prostaglandin E synthase |
| XK | X-linked Kx blood group (McLeod syndrome) | AKAP12 | A kinase (PRKA) anchor protein (gravin) 12 |
| MAPK8 | mitogen-activated protein kinase 8 | NFE2L3 | nuclear factor (erythroid-derived 2)-like 3 |

| | | | |
|---|---|---|---|
| RBP3 | retinol binding protein 3, interstitial | FAM115A | |
| SCN2A | sodium channel, voltage-gated, type II, alpha subunit | MTSS1 | metastasis suppressor 1 |
| SMARCE1 | SWI/SNF related, matrix associated, actin dependent regulator of chromatin, subfamily e, member 1 | KEAP1 | kelch-like ECH-associated protein 1 |
| SNAI1 | snail homolog 1 (Drosophila) | RB1CC1 | RB1-inducible coiled-coil 1 |
| PSEN1 | presenilin 1 (Alzheimer disease 3) | DNAJC6 | DnaJ (Hsp40) homolog, subfamily C, member 6 |
| RGS2 | regulator of G-protein signalling 2, 24kDa | ZEB2 | zinc finger E-box binding homeobox 2 |
| RGS16 | regulator of G-protein signalling 16 | KIAA0644 | |
| RHCE | Rh blood group, CcEe antigens | PJA2 | praja 2, RING-H2 motif containing |
| RHD | Rh blood group, D antigen | YWHAG | tyrosine 3-monooxygenase/tryptophan 5-monooxygenase activation protein, gamma polypeptide |
| SOAT1 | sterol O-acyltransferase (acyl-Coenzyme A: cholesterol acyltransferase) 1 | CASK | calcium/calmodulin-dependent serine protein kinase (MAGUK family) |
| SOX5 | SRY (sex determining region Y)-box 5 | SGPL1 | sphingosine-1-phosphate lyase 1 |
| SOX11 | SRY (sex determining region Y)-box 11 | CPNE3 | copine III |
| UAP1 | UDP-N-acteylglucosamine pyrophosphorylase 1 | PRPF4B | PRP4 pre-mRNA processing factor 4 homolog B (yeast) |
| ROBO1 | roundabout, axon guidance receptor, homolog 1 (Drosophila) | ZFP161 | zinc finger protein 161 homolog (mouse) |
| RORA | RAR-related orphan receptor A | MKKS | McKusick-Kaufman syndrome |
| SFTPA2B | surfactant, pulmonary-associated protein A2 | NRIP1 | nuclear receptor interacting protein 1 |
| AKR1D1 | aldo-keto reductase family 1, member D1 (delta 4-3-ketosteroid-5-beta-reductase) | TP63 | tumor protein p73-like |
| SLC1A2 | solute carrier family 1 (glial high affinity glutamate transporter), member 2 | TAF1B | TATA box binding protein (TBP)-associated factor, RNA polymerase I, B, 63kDa |
| SLC1A3 | solute carrier family 1 (glial high affinity glutamate transporter), member 3 | BAZ1B | bromodomain adjacent to zinc finger domain, 1B |
| SLC1A4 | solute carrier family 1 (glutamate/neutral amino acid transporter), member 4 | ZMYM2 | zinc finger, MYM-type 2 |
| PTPRK | protein tyrosine phosphatase, receptor type, K | ZNF207 | zinc finger protein 207 |
| RAB27A | RAB27A, member RAS oncogene family | FZD4 | frizzled homolog 4 (Drosophila) |
| ARMC8 | armadillo repeat containing 8 | HIST2H2AA3 | histone cluster 2, H2aa3 |
| PRKD2 | protein kinase D2 | HIST1H2BL | histone cluster 1, H2bl |
| TNFRSF21 | tumor necrosis factor receptor superfamily, member 21 | MAP7 | microtubule-associated protein 7 |
| TMPRSS11E | transmembrane protease, serine 11E | PIAS2 | protein inhibitor of activated STAT, 2 |

| | | | |
|---|---|---|---|
| SSU72 | SSU72 RNA polymerase II CTD phosphatase homolog (S. cerevisiae) | ZNF229 | zinc finger protein 229 |
| NXPH1 | neurexophilin 1 | B3GALT2 | UDP-Gal:betaGlcNAc beta 1,3-galactosyltransferase, polypeptide 2 |
| SUZ12 | suppressor of zeste 12 homolog (Drosophila) | MBTPS1 | membrane-bound transcription factor peptidase, site 1 |
| CHRDL2 | chordin-like 2 | RNF103 | ring finger protein 103 |
| TMEM158 | transmembrane protein 158 | SPOP | speckle-type POZ protein |
| SLC39A14 | solute carrier family 39 (zinc transporter), member 14 | SRPX | sushi-repeat-containing protein, X-linked |
| R3HDM1 | R3H domain containing 1 | MTMR6 | myotubularin related protein 6 |
| TNPO3 | transportin 3 | SLMAP | sarcolemma associated protein |
| ZNF638 | zinc finger protein 638 | CUL3 | cullin 3 |
| SLCO1B3 | solute carrier organic anion transporter family, member 1B3 | MPDZ | multiple PDZ domain protein |
| SIPA1L1 | signal-induced proliferation-associated 1 like 1 | TFPI2 | tissue factor pathway inhibitor 2 |
| DNM3 | dynamin 3 | OGT | O-linked N-acetylglucosamine (GlcNAc) transferase (UDP-N-acetylglucosamine:polypeptide-N-acetylglucosaminyl transferase) |
| RAI14 | retinoic acid induced 14 | RGS5 | regulator of G-protein signalling 5 |
| C20orf26 | chromosome 20 open reading frame 26 | SUCLG2 | succinate-CoA ligase, GDP-forming, beta subunit |
| SLC7A11 | solute carrier family 7, (cationic amino acid transporter, y+ system) member 11 | ITGA8 | integrin, alpha 8 |
| ZKSCAN5 | zinc finger with KRAB and SCAN domains 5 | WISP1 | WNT1 inducible signaling pathway protein 1 |
| HBP1 | HMG-box transcription factor 1 | RARRES1 | retinoic acid receptor responder (tazarotene induced) 1 |
| KCNV1 | potassium channel, subfamily V, member 1 | RASA1 | RAS p21 protein activator (GTPase activating protein) 1 |
| C1orf107 | chromosome 1 open reading frame 107 | SLC18A2 | solute carrier family 18 (vesicular monoamine), member 2 |
| FBXW8 | F-box and WD repeat domain containing 8 | TAF7 | TAF7 RNA polymerase II, TATA box binding protein (TBP)-associated factor, 55kDa |
| EHF | ets homologous factor | TBL1X | transducin (beta)-like 1X-linked |
| ANGPTL7 | angiopoietin-like 7 | TCF7L2 | transcription factor 7-like 2 (T-cell specific, HMG-box) |
| GPR45 | G protein-coupled receptor 45 | TCF15 | transcription factor 15 (basic helix-loop-helix) |
| ICK | intestinal cell (MAK-like) kinase | DYNLT3 | dynein, light chain, Tctex-type 3 |
| UBOX5 | U-box domain containing 5 | TFAP2B | transcription factor AP-2 beta (activating enhancer binding protein 2 beta) |
| RUFY3 | RUN and FYVE domain containing 3 | TIMP2 | TIMP metallopeptidase inhibitor 2 |

| | | | |
|---|---|---|---|
| MAST1 | microtubule associated serine/threonine kinase 1 | TIMP4 | TIMP metallopeptidase inhibitor 4 |
| LIMCH1 | | TSPAN6 | tetraspanin 6 |
| XPO7 | exportin 7 | TMPO | thymopoietin |
| TBC1D9B | TBC1 domain family, member 9B (with GRAM domain) | CLDN5 | claudin 5 (transmembrane protein deleted in velocardiofacial syndrome) |
| SETX | senataxin | TOP2B | topoisomerase (DNA) II beta 180kDa |
| HECW1 | HECT, C2 and WW domain containing E3 ubiquitin protein ligase 1 | TP53BP2 | tumor protein p53 binding protein, 2 |
| RP11-125A7.3 | | TPP2 | tripeptidyl peptidase II |
| ERC1 | ELKS/RAB6-interacting/CAST family member 1 | TRPS1 | trichorhinophalangeal syndrome I |
| NFASC | neurofascin homolog (chicken) | TSHR | thyroid stimulating hormone receptor |
| SSPO | SCO-spondin homolog (Bos taurus) | TSPYL1 | TSPY-like 1 |
| CEP68 | centrosomal protein 68kDa | TTC3 | tetratricopeptide repeat domain 3 |
| MDN1 | MDN1, midasin homolog (yeast) | UBE2B | ubiquitin-conjugating enzyme E2B (RAD6 homolog) |
| SMG6 | Smg-6 homolog, nonsense mediated mRNA decay factor (C. elegans) | UBE2V2 | ubiquitin-conjugating enzyme E2 variant 2 |
| OBSL1 | obscurin-like 1 | VCAM1 | vascular cell adhesion molecule 1 |
| SRGAP2 | SLIT-ROBO Rho GTPase activating protein 2 | VLDLR | very low density lipoprotein receptor |
| KIAA0415 | | PRKG1 | protein kinase, cGMP-dependent, type I |
| SLC34A2 | solute carrier family 34 (sodium phosphate), member 2 | SCNN1B | sodium channel, nonvoltage-gated 1, beta (Liddle syndrome) |
| DPYSL4 | dihydropyrimidinase-like 4 | SMARCA2 | SWI/SNF related, matrix associated, actin dependent regulator of chromatin, subfamily a, member 2 |
| PDLIM5 | PDZ and LIM domain 5 | MAP2K5 | mitogen-activated protein kinase kinase 5 |
| SLC23A1 | solute carrier family 23 (nucleobase transporters), member 1 | PRKX | protein kinase, X-linked |
| MED13 | thyroid hormone receptor associated protein 1 | PRNP | prion protein (p27-30) (Creutzfeldt-Jakob disease, Gerstmann-Strausler-Scheinker syndrome, fatal familial insomnia) |
| ABCA9 | ATP-binding cassette, sub-family A (ABC1), member 9 | SCNN1G | sodium channel, nonvoltage-gated 1, gamma |
| TNFSF13B | tumor necrosis factor (ligand) superfamily, member 13b | SNCG | synuclein, gamma (breast cancer-specific protein 1) |
| LIAS | lipoic acid synthetase | PSAP | prosaposin (variant Gaucher disease and variant metachromatic leukodystrophy) |
| TANK | TRAF family member-associated NFKB activator | RGS4 | regulator of G-protein signalling 4 |
| FUT9 | fucosyltransferase 9 (alpha (1,3) fucosyltransferase) | SDC1 | syndecan 1 |

| | | | |
|---|---|---|---|
| TOPBP1 | topoisomerase (DNA) II binding protein 1 | SNTB2 | syntrophin, beta 2 (dystrophin-associated protein A1, 59kDa, basic component 2) |
| HSF2BP | heat shock transcription factor 2 binding protein | SOD3 | superoxide dismutase 3, extracellular |
| EDIL3 | EGF-like repeats and discoidin I-like domains 3 | SON | SON DNA binding protein |
| PLK2 | polo-like kinase 2 (Drosophila) | SOX4 | SRY (sex determining region Y)-box 4 |
| UTP14A | UTP14, U3 small nucleolar ribonucleoprotein, homolog A (yeast) | PSMC6 | proteasome (prosome, macropain) 26S subunit, ATPase, 6 |
| RBM12 | RNA binding motif protein 12 | ROBO1 | roundabout, axon guidance receptor, homolog 1 (Drosophila) |
| ABCB8 | ATP-binding cassette, sub-family B (MDR/TAP), member 8 | ROCK1 | Rho-associated, coiled-coil containing protein kinase 1 |
| SEMA4B | sema domain, immunoglobulin domain (Ig), transmembrane domain (TM) and short cytoplasmic domain, (semaphorin) 4B | RORA | RAR-related orphan receptor A |
| ADAM28 | ADAM metallopeptidase domain 28 | RORC | RAR-related orphan receptor C |
| SLC22A7 | solute carrier family 22 (organic anion transporter), member 7 | SFRP2 | secreted frizzled-related protein 2 |
| RNF139 | ring finger protein 139 | SFRS8 | splicing factor, arginine/serine-rich 8 (suppressor-of-white-apricot homolog, Drosophila) |
| PROK2 | prokineticin 2 | SPTBN1 | spectrin, beta, non-erythrocytic 1 |
| BCAN | brevican | PTGFR | prostaglandin F receptor (FP) |
| IL25 | interleukin 25 | RP2 | retinitis pigmentosa 2 (X-linked recessive) |
| AGXT2L1 | alanine-glyoxylate aminotransferase 2-like 1 | RPE | ribulose-5-phosphate-3-epimerase |
| GTDC1 | glycosyltransferase-like domain containing 1 | SH3BGRL | SH3 domain binding glutamic acid-rich protein like |
| NSUN7 | NOL1/NOP2/Sun domain family, member 7 | RPL30 | ribosomal protein L30 |
| TTC21B | tetratricopeptide repeat domain 21B | SHMT1 | serine hydroxymethyltransferase 1 (soluble) |
| TMC5 | transmembrane channel-like 5 | SLC1A3 | solute carrier family 1 (glial high affinity glutamate transporter), member 3 |
| BAALC | brain and acute leukemia, cytoplasmic | SLC2A4 | solute carrier family 2 (facilitated glucose transporter), member 4 |
| CCDC134 | coiled-coil domain containing 134 | STK3 | serine/threonine kinase 3 (STE20 homolog, yeast) |
| SETD6 | SET domain containing 6 | RPS20 | ribosomal protein S20 |
| SPSB1 | splA/ryanodine receptor domain and SOCS box containing 1 | SLC5A1 | solute carrier family 5 (sodium/glucose cotransporter), member 1 |
| HKDC1 | hexokinase domain containing 1 | SYPL1 | synaptophysin-like 1 |

| | | | |
|---|---|---|---|
| PIGZ | phosphatidylinositol glycan anchor biosynthesis, class Z | TACR3 | tachykinin receptor 3 |
| CPEB4 | cytoplasmic polyadenylation element binding protein 4 | IL17B | interleukin 17B |
| TAS1R2 | taste receptor, type 1, member 2 | SERP1 | |
| AADACL1 | arylacetamide deacetylase-like 1 | SCG3 | secretogranin III |
| KIF17 | kinesin family member 17 | OLA1 | GTP-binding protein 9 (putative) |
| KIAA1407 | KIAA1407 | YPEL1 | yippee-like 1 (Drosophila) |
| SYT13 | synaptotagmin XIII | CNOT7 | CCR4-NOT transcription complex, subunit 7 |
| AGXT2 | alanine-glyoxylate aminotransferase 2 | SEC61A1 | Sec61 alpha 1 subunit (S. cerevisiae) |
| FAM20C | family with sequence similarity 20, member C | BAZ2B | bromodomain adjacent to zinc finger domain, 2B |
| FIGNL1 | fidgetin-like 1 | SLC40A1 | solute carrier family 40 (iron-regulated transporter), member 1 |
| KIAA1549 | | CXXC1 | CXXC finger 1 (PHD domain) |
| ZFP14 | zinc finger protein 14 homolog (mouse) | G0S2 | G0/G1switch 2 |
| SLC28A3 | solute carrier family 28 (sodium-coupled nucleoside transporter), member 3 | PODXL2 | podocalyxin-like 2 |
| SLC39A8 | solute carrier family 39 (zinc transporter), member 8 | MYEF2 | myelin expression factor 2 |
| PLEKHA3 | pleckstrin homology domain containing, family A (phosphoinositide binding specific) member 3 | AK3 | adenylate kinase 3 |
| TBX20 | T-box 20 | PLEKHG4 | pleckstrin homology domain containing, family G (with RhoGef domain) member 4 |
| ZBTB26 | zinc finger and BTB domain containing 26 | POT1 | POT1 protection of telomeres 1 homolog (S. pombe) |
| HRASLS | HRAS-like suppressor | INTS6 | integrator complex subunit 6 |
| WDR19 | WD repeat domain 19 | ADAMDEC1 | ADAM-like, decysin 1 |
| PAK7 | p21(CDKN1A)-activated kinase 7 | TOX3 | TOX high mobility group box family member 3 |
| SMURF1 | SMAD specific E3 ubiquitin protein ligase 1 | ZNF638 | zinc finger protein 638 |
| PELI1 | pellino homolog 1 (Drosophila) | CD2AP | CD2-associated protein |
| ZMIZ1 | zinc finger, MIZ-type containing 1 | LYPLA3 | lysophospholipase 3 (lysosomal phospholipase A2) |
| PTBP2 | polypyrimidine tract binding protein 2 | HBP1 | HMG-box transcription factor 1 |
| LMBR1 | limb region 1 homolog (mouse) | CHORDC1 | cysteine and histidine-rich domain (CHORD)-containing 1 |
| HIF3A | hypoxia inducible factor 3, alpha subunit | GABARAPL1 | GABA(A) receptor-associated protein like 1 |
| HHIP | hedgehog interacting protein | PITPNB | phosphatidylinositol transfer protein, beta |
| JOSD3 | Josephin domain containing 3 | SERBP1 | SERPINE1 mRNA binding protein 1 |

| | | | |
|---|---|---|---|
| CENPO | centromere protein O | FBXW2 | F-box and WD repeat domain containing 2 |
| SPC25 | SPC25, NDC80 kinetochore complex component, homolog (S. cerevisiae) | DAPP1 | dual adaptor of phosphotyrosine and 3-phosphoinositides |
| FAM59A | family with sequence similarity 59, member A | RPUSD2 | RNA pseudouridylate synthase domain containing 2 |
| SLC12A5 | solute carrier family 12, (potassium-chloride transporter) member 5 | PLDN | pallidin homolog (mouse) |
| KIAA1239 | KIAA1239 | HIBCH | 3-hydroxyisobutyryl-Coenzyme A hydrolase |
| CCDC91 | coiled-coil domain containing 91 | GCA | grancalcin, EF-hand calcium binding protein |
| OLAH | oleoyl-ACP hydrolase | EHF | ets homologous factor |
| C14orf106 | chromosome 14 open reading frame 106 | ANGPTL7 | angiopoietin-like 7 |
| DKFZp762E1312 | | STX6 | syntaxin 6 |
| ZNF692 | zinc finger protein 692 | AGPAT1 | 1-acylglycerol-3-phosphate O-acyltransferase 1 (lysophosphatidic acid acyltransferase, alpha) |
| URG4 | | CPEB3 | cytoplasmic polyadenylation element binding protein 3 |
| NUP133 | nucleoporin 133kDa | PLEKHA6 | pleckstrin homology domain containing, family A member 6 |
| TEX12 | testis expressed 12 | ABLIM3 | actin binding LIM protein family, member 3 |
| RNF20 | ring finger protein 20 | RAB18 | RAB18, member RAS oncogene family |
| TMPRSS4 | transmembrane protease, serine 4 | ZNF292 | zinc finger protein 292 |
| CLDND1 | claudin domain containing 1 | PDXDC1 | pyridoxal-dependent decarboxylase domain containing 1 |
| SPHK2 | sphingosine kinase 2 | ARHGAP26 | Rho GTPase activating protein 26 |
| SOST | sclerosteosis | KIF1B | kinesin family member 1B |
| DTL | denticleless homolog (Drosophila) | SPG20 | spastic paraplegia 20 (Troyer syndrome) |
| WNT4 | wingless-type MMTV integration site family, member 4 | FBXL7 | F-box and leucine-rich repeat protein 7 |
| HAO1 | hydroxyacid oxidase (glycolate oxidase) 1 | POFUT2 | protein O-fucosyltransferase 2 |
| PPP2R3C | protein phosphatase 2 (formerly 2A), regulatory subunit B'', gamma | BICD2 | bicaudal D homolog 2 (Drosophila) |
| PRPF39 | PRP39 pre-mRNA processing factor 39 homolog (S. cerevisiae) | TRIM2 | tripartite motif-containing 2 |
| TNNI3K | TNNI3 interacting kinase | USP22 | ubiquitin specific peptidase 22 |
| SMOX | spermine oxidase | DOCK9 | dedicator of cytokinesis 9 |
| PHIP | pleckstrin homology domain interacting protein | ZNF629 | zinc finger protein 629 |
| ZNF706 | zinc finger protein 706 | ARHGEF12 | Rho guanine nucleotide exchange factor (GEF) 12 |

| | | | |
|---|---|---|---|
| ASB4 | ankyrin repeat and SOCS box-containing 4 | SLC35A3 | solute carrier family 35 (UDP-N-acetylglucosamine (UDP-GlcNAc) transporter), member A3 |
| DDX49 | DEAD (Asp-Glu-Ala-Asp) box polypeptide 49 | ANGPTL2 | angiopoietin-like 2 |
| KCTD3 | potassium channel tetramerisation domain containing 3 | NET1 | neuroepithelial cell transforming gene 1 |
| CYB5R2 | cytochrome b5 reductase 2 | SERINC3 | serine incorporator 3 |
| HEATR1 | HEAT repeat containing 1 | ACOT2 | acyl-CoA thioesterase 2 |
| HSD17B14 | hydroxysteroid (17-beta) dehydrogenase 14 | RAB40B | RAB40B, member RAS oncogene family |
| NIN | ninein (GSK3B interacting protein) | LANCL1 | LanC lantibiotic synthetase component C-like 1 (bacterial) |
| TMEM106B | transmembrane protein 106B | POLR3C | polymerase (RNA) III (DNA directed) polypeptide C (62kD) |
| PANK1 | pantothenate kinase 1 | IVNS1ABP | influenza virus NS1A binding protein |
| MRPL51 | mitochondrial ribosomal protein L51 | TXNIP | thioredoxin interacting protein |
| PRKAG3 | protein kinase, AMP-activated, gamma 3 non-catalytic subunit | POSTN | periostin, osteoblast specific factor |
| KLHDC8A | kelch domain containing 8A | IMMT | inner membrane protein, mitochondrial (mitofilin) |
| FKBP11 | FK506 binding protein 11, 19 kDa | TLK2 | tousled-like kinase 2 |
| PPP1R14D | protein phosphatase 1, regulatory (inhibitor) subunit 14D | MRVI1 | murine retrovirus integration site 1 homolog |
| GOT1L1 | glutamic-oxaloacetic transaminase 1-like 1 | KHDRBS3 | KH domain containing, RNA binding, signal transduction associated 3 |
| FAM19A4 | family with sequence similarity 19 (chemokine (C-C motif)-like), member A4 | CUGBP1 | CUG triplet repeat, RNA binding protein 1 |
| LRRC34 | leucine rich repeat containing 34 | KCNE3 | potassium voltage-gated channel, Isk-related family, member 3 |
| KLB | klotho beta | TANK | TRAF family member-associated NFKB activator |
| AMOTL1 | angiomotin like 1 | BPNT1 | 3'(2'), 5'-bisphosphate nucleotidase 1 |
| RBM33 | RNA binding motif protein 33 | GNB5 | guanine nucleotide binding protein (G protein), beta 5 |
| VPS13B | vacuolar protein sorting 13 homolog B (yeast) | FUT9 | fucosyltransferase 9 (alpha (1,3) fucosyltransferase) |
| RLBP1L1 | | OGFR | opioid growth factor receptor |
| NKX2-3 | NK2 transcription factor related, locus 3 (Drosophila) | C10orf10 | chromosome 10 open reading frame 10 |
| UBXD4 | UBX domain containing 4 | ABCC9 | ATP-binding cassette, sub-family C (CFTR/MRP), member 9 |
| KLHDC6 | kelch domain containing 6 | MGEA5 | meningioma expressed antigen 5 (hyaluronidase) |
| B3GNT6 | UDP-GlcNAc:betaGal beta-1,3-N-acetylglucosaminyltransferase 6 (core 3 synthase) | LYPLA1 | lysophospholipase I |

| | | | |
|---|---|---|---|
| CMTM2 | CKLF-like MARVEL transmembrane domain containing 2 | VAV3 | vav 3 oncogene |
| UBXD3 | UBX domain containing 3 | AHCYL1 | S-adenosylhomocysteine hydrolase-like 1 |
| CXorf39 | chromosome X open reading frame 39 | FAF1 | Fas (TNFRSF6) associated factor 1 |
| SLC15A4 | solute carrier family 15, member 4 | PWP1 | PWP1 homolog (S. cerevisiae) |
| MAGEB16 | | TBC1D8 | TBC1 domain family, member 8 (with GRAM domain) |
| ZFP92 | | TSPAN2 | tetraspanin 2 |
| STARD6 | START domain containing 6 | ARL4A | ADP-ribosylation factor-like 4A |
| RNF32 | ring finger protein 32 | TOB1 | transducer of ERBB2, 1 |
| SLC32A1 | solute carrier family 32 (GABA vesicular transporter), member 1 | MBNL2 | muscleblind-like 2 (Drosophila) |
| NAT12 | N-acetyltransferase 12 | ENOX2 | ecto-NOX disulfide-thiol exchanger 2 |
| ACVR1C | activin A receptor, type IC | MAP4K5 | mitogen-activated protein kinase kinase kinase kinase 5 |
| SYT6 | synaptotagmin VI | SUPT16H | suppressor of Ty 16 homolog (S. cerevisiae) |
| SLC25A29 | solute carrier family 25, member 29 | LHFPL2 | lipoma HMGIC fusion partner-like 2 |
| C15orf27 | chromosome 15 open reading frame 27 | SEMA3C | sema domain, immunoglobulin domain (Ig), short basic domain, secreted, (semaphorin) 3C |
| TRPM6 | transient receptor potential cation channel, subfamily M, member 6 | UBD | ubiquitin D |
| FAM71A | family with sequence similarity 71, member A | DUSP10 | dual specificity phosphatase 10 |
| SLC5A10 | solute carrier family 5 (sodium/glucose cotransporter), member 10 | SERINC1 | serine incorporator 1 |
| HECTD2 | HECT domain containing 2 | SCOC | short coiled-coil protein |
| DUSP18 | dual specificity phosphatase 18 | OBFC2A | oligonucleotide/oligosaccharide-binding fold containing 2A |
| P117 | | OGFRL1 | opioid growth factor receptor-like 1 |
| LAYN | layilin | STEAP4 | STEAP family member 4 |
| FLJ23861 | | WDR59 | WD repeat domain 59 |
| TAAR1 | trace amine associated receptor 1 | ASB13 | ankyrin repeat and SOCS box-containing 13 |
| RAD9B | RAD9 homolog B (S. cerevisiae) | GRTP1 | growth hormone regulated TBC protein 1 |
| GPR123 | G protein-coupled receptor 123 | ZFHX4 | zinc finger homeodomain 4 |
| PCDH21 | protocadherin 21 | CLMN | calmin (calponin-like, transmembrane) |
| LYK5 | | MOBKL2B | MOB1, Mps One Binder kinase activator-like 2B (yeast) |
| C17orf72 | chromosome 17 open reading frame 72 | CYBRD1 | cytochrome b reductase 1 |
| SYCE1 | synaptonemal complex central element protein 1 | C6orf134 | chromosome 6 open reading frame 134 |

| | | | |
|---|---|---|---|
| TPTE2 | transmembrane phosphoinositide 3-phosphatase and tensin homolog 2 | GRHL2 | grainyhead-like 2 (Drosophila) |
| MYOCD | myocardin | FLJ13611 | |
| FOXP2 | forkhead box P2 | ZNF606 | zinc finger protein 606 |
| LOC113230 | | FHOD3 | formin homology 2 domain containing 3 |
| PALM2 | paralemmin 2 | PDGFD | platelet derived growth factor D |
| CSMD3 | CUB and Sushi multiple domains 3 | CXXC4 | CXXC finger 4 |
| SLC25A25 | solute carrier family 25 (mitochondrial carrier; phosphate carrier), member 25 | TAOK1 | TAO kinase 1 |
| FHAD1 | forkhead-associated (FHA) phosphopeptide binding domain 1 | ARRDC3 | arrestin domain containing 3 |
| OSBPL9 | oxysterol binding protein-like 9 | KIAA1430 | KIAA1430 |
| SLC26A7 | solute carrier family 26, member 7 | CXorf56 | chromosome X open reading frame 56 |
| SLC22A12 | solute carrier family 22 (organic anion/cation transporter), member 12 | STIM2 | stromal interaction molecule 2 |
| WDR17 | WD repeat domain 17 | GPBP1 | GC-rich promoter binding protein 1 |
| DACH2 | dachshund homolog 2 (Drosophila) | RSRC2 | arginine/serine-rich coiled-coil 2 |
| OLFM3 | olfactomedin 3 | BBX | bobby sox homolog (Drosophila) |
| TTC18 | tetratricopeptide repeat domain 18 | ACN9 | ACN9 homolog (S. cerevisiae) |
| DIXDC1 | DIX domain containing 1 | GPAM | glycerol-3-phosphate acyltransferase, mitochondrial |
| GTPBP3 | GTP binding protein 3 (mitochondrial) | GOLPH3 | golgi phosphoprotein 3 (coat-protein) |
| SYNC1 | syncoilin, intermediate filament 1 | MCCC2 | methylcrotonoyl-Coenzyme A carboxylase 2 (beta) |
| PLCD4 | phospholipase C, delta 4 | TNMD | tenomodulin |
| CCDC98 | coiled-coil domain containing 98 | SLC39A8 | solute carrier family 39 (zinc transporter), member 8 |
| BXDC1 | brix domain containing 1 | PLEKHA3 | pleckstrin homology domain containing, family A (phosphoinositide binding specific) member 3 |
| MFSD2 | major facilitator superfamily domain containing 2 | TWSG1 | twisted gastrulation homolog 1 (Drosophila) |
| C15orf23 | chromosome 15 open reading frame 23 | OSGEPL1 | O-sialoglycoprotein endopeptidase-like 1 |
| ZNF541 | zinc finger protein 541 | ARL6IP2 | ADP-ribosylation factor-like 6 interacting protein 2 |
| LINGO1 | leucine rich repeat and Ig domain containing 1 | LMBR1 | limb region 1 homolog (mouse) |
| SPRY4 | sprouty homolog 4 (Drosophila) | MPP5 | membrane protein, palmitoylated 5 (MAGUK p55 subfamily member 5) |
| KIAA1984 | KIAA1984 | KDELC1 | KDEL (Lys-Asp-Glu-Leu) containing 1 |
| ANKRD44 | ankyrin repeat domain 44 | WDR77 | WD repeat domain 77 |
| TMEM107 | transmembrane protein 107 | SLC39A10 | solute carrier family 39 (zinc transporter), member 10 |

| | | | |
|---|---|---|---|
| PAQR8 | progestin and adipoQ receptor family member VIII | ATP10A | ATPase, Class V, type 10A |
| RASL10B | RAS-like, family 10, member B | CREBZF | CREB/ATF bZIP transcription factor |
| ATP9B | ATPase, Class II, type 9B | FAM108C1 | family with sequence similarity 108, member C1 |
| LRRTM1 | leucine rich repeat transmembrane neuronal 1 | JAM2 | junctional adhesion molecule 2 |
| LOC375748 | | RBM25 | RNA binding motif protein 25 |
| OR11H4 | olfactory receptor, family 11, subfamily H, member 4 | RHOJ | ras homolog gene family, member J |
| LBXCOR1 | LBXCOR1 homolog (mouse) | CLK4 | CDC-like kinase 4 |
| SLC6A17 | solute carrier family 6, member 17 | HIVEP3 | human immunodeficiency virus type I enhancer binding protein 3 |
| LOC388931 | | NOL12 | nucleolar protein 12 |
| C3orf16 | chromosome 3 open reading frame 16 | CYP20A1 | cytochrome P450, family 20, subfamily A, polypeptide 1 |
| LCE3B | late cornified envelope 3B | TMCC3 | transmembrane and coiled-coil domain family 3 |
| UST6 | | NIF3L1 | NIF3 NGG1 interacting factor 3-like 1 (S. pombe) |
| C17orf28 | chromosome 17 open reading frame 28 | AASDHPPT | aminoadipate-semialdehyde dehydrogenase-phosphopantetheinyl transferase |
| YIPF6 | Yip1 domain family, member 6 | RETSAT | retinol saturase (all-trans-retinol 13,14-reductase) |
| SLC35E4 | solute carrier family 35, member E4 | C5orf22 | chromosome 5 open reading frame 22 |
| VSIG1 | V-set and immunoglobulin domain containing 1 | WDR33 | WD repeat domain 33 |
| H1FNT | H1 histone family, member N, testis-specific | FAM48A | family with sequence similarity 48, member A |
| SYCN | syncollin | KIF21A | kinesin family member 21A |
| EVX2 | even-skipped homeobox 2 | PPP1R9A | protein phosphatase 1, regulatory (inhibitor) subunit 9A |
| 14-Sep | septin 14 | TMEM48 | transmembrane protein 48 |
| TTC21A | tetratricopeptide repeat domain 21A | TBC1D23 | TBC1 domain family, member 23 |
| RNF182 | ring finger protein 182 | MYNN | myoneurin |
| PHACTR1 | phosphatase and actin regulator 1 | NXT2 | nuclear transport factor 2-like export factor 2 |
| FAM133B | family with sequence similarity 133, member B | KCNQ5 | potassium voltage-gated channel, KQT-like subfamily, member 5 |
| C9orf93 | chromosome 9 open reading frame 93 | CYP26B1 | cytochrome P450, family 26, subfamily B, polypeptide 1 |
| C22orf30 | chromosome 22 open reading frame 30 | SUCNR1 | succinate receptor 1 |
| SENP5 | SUMO1/sentrin specific peptidase 5 | C8orf4 | chromosome 8 open reading frame 4 |
| GSX1 | GS homeobox 1 | UBQLN4 | ubiquilin 4 |

| | |
|---|---|
| GPRIN3 | GPRIN family member 3 |
| RGMB | RGM domain family, member B |
| LOC728160 | |
| RP4-692D3.1 | |
| LOC646851 | |
| CBLN3 | cerebellin 3 precursor |
| LOC441476 | |
| FOXB2 | forkhead box B2 |
| TMPRSS11E2 | |
| tcag7.1294 | |
| LOC729627 | |

| | |
|---|---|
| PRKAG2 | protein kinase, AMP-activated, gamma 2 non-catalytic subunit |
| ANAPC5 | anaphase promoting complex subunit 5 |
| GULP1 | GULP, engulfment adaptor PTB domain containing 1 |
| FAM3B | family with sequence similarity 3, member B |
| ISOC1 | isochorismatase domain containing 1 |
| PTPLAD1 | protein tyrosine phosphatase-like A domain containing 1 |
| ERRFI1 | ERBB receptor feedback inhibitor 1 |
| VPS36 | vacuolar protein sorting 36 homolog (S. cerevisiae) |
| TRNT1 | tRNA nucleotidyl transferase, CCA-adding, 1 |
| PHIP | pleckstrin homology domain interacting protein |
| SUSD4 | sushi domain containing 4 |
| FAM82B | family with sequence similarity 82, member B |
| ANGPTL4 | angiopoietin-like 4 |
| MRPL50 | mitochondrial ribosomal protein L50 |
| DDIT4 | DNA-damage-inducible transcript 4 |
| ING3 | inhibitor of growth family, member 3 |
| SLC38A4 | solute carrier family 38, member 4 |
| RBM28 | RNA binding motif protein 28 |
| ZDHHC2 | zinc finger, DHHC-type containing 2 |
| ARID4B | AT rich interactive domain 4B (RBP1-like) |
| PPM2C | protein phosphatase 2C, magnesium-dependent, catalytic subunit |
| MSL2L1 | male-specific lethal 2-like 1 (Drosophila) |
| FAM20A | family with sequence similarity 20, member A |
| TRIM44 | tripartite motif-containing 44 |
| GOLPH3L | golgi phosphoprotein 3-like |
| KLHL24 | kelch-like 24 (Drosophila) |
| MOBKL1B | MOB1, Mps One Binder kinase activator-like 1B (yeast) |
| PCMTD2 | protein-L-isoaspartate (D-aspartate) O-methyltransferase domain containing 2 |
| C5orf5 | chromosome 5 open reading frame 5 |
| HIST2H3C | histone cluster 2, H3c |
| TTC14 | tetratricopeptide repeat domain 14 |

| | |
|---|---|
| MOSPD2 | motile sperm domain containing 2 |
| TMTC2 | transmembrane and tetratricopeptide repeat containing 2 |
| ADAL | adenosine deaminase-like |
| ABHD3 | abhydrolase domain containing 3 |
| EIF2C4 | eukaryotic translation initiation factor 2C, 4 |
| MUM1L1 | melanoma associated antigen (mutated) 1-like 1 |
| NEDD1 | neural precursor cell expressed, developmentally down-regulated 1 |
| KRT25 | keratin 25 |
| ASB8 | ankyrin repeat and SOCS box-containing 8 |
| ZNF560 | zinc finger protein 560 |
| ACVR1C | activin A receptor, type IC |
| TMEM182 | transmembrane protein 182 |
| PDIK1L | PDLIM1 interacting kinase 1 like |
| MSI2 | musashi homolog 2 (Drosophila) |
| C20orf82 | chromosome 20 open reading frame 82 |
| SNF1LK | SNF1-like kinase |
| MPP7 | membrane protein, palmitoylated 7 (MAGUK p55 subfamily member 7) |
| C5orf33 | chromosome 5 open reading frame 33 |
| STARD4 | START domain containing 4, sterol regulated |
| MUC15 | mucin 15, cell surface associated |
| PLB1 | phospholipase B1 |
| MGC29891 | |
| LYRM5 | LYR motif containing 5 |
| LCOR | ligand dependent nuclear receptor corepressor |
| ARRDC4 | arrestin domain containing 4 |
| DSEL | dermatan sulfate epimerase-like |
| ZFP62 | zinc finger protein 62 homolog (mouse) |
| RBM18 | RNA binding motif protein 18 |
| C20orf72 | chromosome 20 open reading frame 72 |
| FOXQ1 | forkhead box Q1 |
| RAB42 | RAB42, member RAS oncogene family |
| PCMTD1 | protein-L-isoaspartate (D-aspartate) O-methyltransferase domain containing 1 |

| | |
|---|---|
| LONP2 | lon peptidase 2, peroxisomal |
| ACSS1 | acyl-CoA synthetase short-chain family member 1 |
| PARD6B | par-6 partitioning defective 6 homolog beta (C. elegans) |
| DOCK7 | dedicator of cytokinesis 7 |
| DIXDC1 | DIX domain containing 1 |
| KIRREL3 | kin of IRRE like 3 (Drosophila) |
| NCALD | neurocalcin delta |
| GPT2 | glutamic pyruvate transaminase (alanine aminotransferase) 2 |
| SGPP1 | sphingosine-1-phosphate phosphatase 1 |
| LRRC3 | leucine rich repeat containing 3 |
| KBTBD7 | kelch repeat and BTB (POZ) domain containing 7 |
| TSPAN18 | tetraspanin 18 |
| C1orf21 | chromosome 1 open reading frame 21 |
| CLPB | ClpB caseinolytic peptidase B homolog (E. coli) |
| APOLD1 | apolipoprotein L domain containing 1 |
| CDADC1 | cytidine and dCMP deaminase domain containing 1 |
| BMF | Bcl2 modifying factor |
| PLXDC2 | plexin domain containing 2 |
| ZNF799 | zinc finger protein 799 |
| ANGEL2 | angel homolog 2 (Drosophila) |
| RAB2B | RAB2B, member RAS oncogene family |
| C12orf29 | chromosome 12 open reading frame 29 |
| XRCC6BP1 | XRCC6 binding protein 1 |
| ARHGAP24 | Rho GTPase activating protein 24 |
| HOOK3 | hook homolog 3 (Drosophila) |
| C2orf40 | chromosome 2 open reading frame 40 |
| BOC | Boc homolog (mouse) |
| TMEM47 | transmembrane protein 47 |
| C8orf59 | chromosome 8 open reading frame 59 |
| WDR38 | WD repeat domain 38 |
| LOC347475 | |
| MAST4 | |
| WDR53 | WD repeat domain 53 |
| CD164L2 | CD164 sialomucin-like 2 |

| | |
|---|---|
| KCTD4 | potassium channel tetramerisation domain containing 4 |
| ZNF445 | zinc finger protein 445 |
| FAM90A3 | family with sequence similarity 90, member A3 |
| FAM90A15 | family with sequence similarity 90, member A15 |
| FAM101B | family with sequence similarity 101, member B |
| IRF2BP2 | interferon regulatory factor 2 binding protein 2 |
| C17orf58 | chromosome 17 open reading frame 58 |
| RFESD | Rieske (Fe-S) domain containing |
| HIST2H3A | histone cluster 2, H3a |
| C1QTNF9 | C1q and tumor necrosis factor related protein 9 |
| ADAMTSL5 | ADAMTS-like 5 |
| AGBL3 | ATP/GTP binding protein-like 3 |
| PAQR9 | progestin and adipoQ receptor family member IX |
| UBR1 | ubiquitin protein ligase E3 component n-recognin 1 |
| GDPD1 | glycerophosphodiester phosphodiesterase domain containing 1 |
| MAGI3 | membrane associated guanylate kinase, WW and PDZ domain containing 3 |
| DEFB116 | defensin, beta 116 |
| ATP6V1C2 | ATPase, H+ transporting, lysosomal 42kDa, V1 subunit C2 |
| NAP1L5 | nucleosome assembly protein 1-like 5 |
| RSPO1 | R-spondin homolog (Xenopus laevis) |
| HTRA4 | HtrA serine peptidase 4 |
| LOC253012 | |
| EBF3 | early B-cell factor 3 |
| GARNL1 | GTPase activating Rap/RanGAP domain-like 1 |
| PGM2L1 | phosphoglucomutase 2-like 1 |
| CYP4V2 | cytochrome P450, family 4, subfamily V, polypeptide 2 |
| GK5 | glycerol kinase 5 (putative) |
| ZNF438 | zinc finger protein 438 |
| FAM90A20 | family with sequence similarity 90, member A20 |

| | |
|---|---|
| FAM90A17 | family with sequence similarity 90, member A17 |
| FAM90A19 | family with sequence similarity 90, member A19 |
| LOC728849 | |
| HIST2H2AA4 | histone cluster 2, H2aa4 |
| FAM90A13 | family with sequence similarity 90, member A13 |
| FAM90A5 | family with sequence similarity 90, member A5 |
| FAM90A7 | family with sequence similarity 90, member A7 |
| FAM90A14 | family with sequence similarity 90, member A14 |
| FAM90A12 | family with sequence similarity 90, member A12 |
| FAM90A16 | family with sequence similarity 90, member A16 |
| FAM90A8 | family with sequence similarity 90, member A8 |
| FAM90A18 | family with sequence similarity 90, member A18 |
| FAM90A9 | family with sequence similarity 90, member A9 |
| FAM90A10 | family with sequence similarity 90, member A10 |
| RP11-11C5.2 | |

**References**


Akinci, M. A., Turner, H., Taveras, M., and Wolosin, J. M. (2009). Differential gene expression in the pig limbal side population: implications for stem cell cycling, replication, and survival. Invest Ophthalmol Vis Sci *50*, 5630-5638.

Al-Hajj, M., Wicha, M. S., Benito-Hernandez, A., Morrison, S. J., and Clarke, M. F. (2003). Prospective identification of tumorigenic breast cancer cells. Proc Natl Acad Sci U S A *100*, 3983-3988.

Asselin-Labat, M.-L., Shackleton, M., Stingl, J., Vaillant, F., Forrest, N. C., Eaves, C. J., Visvader, J. E., and Lindeman, G. J. (2006). Steroid Hormone Receptor Status of Mouse Mammary Stem Cells. J Natl Cancer Inst *98*, 1011-1014.

Asselin-Labat, M. L., Vaillant, F., Sheridan, J. M., Pal, B., Wu, D., Simpson, E. R., Yasuda, H., Smyth, G. K., Martin, T. J., Lindeman, G. J., and Visvader, J. E. (2010). Control of mammary stem cell function by steroid hormone signalling. Nature *465*, 798-802.

Barcellos-Hoff, M. H., and Nguyen, D. H. (2009). Radiation carcinogenesis in context: how do irradiated tissues become tumors? Health Phys *97*, 446-457.

Barcellos-Hoff, M. H., Park, C., and Wright, E. G. (2005). Radiation and the microenvironment - tumorigenesis and therapy. Nat Rev Cancer *5*, 867-875.

Barcellos-Hoff, M. H., and Ravani, S. A. (2000). Irradiated mammary gland stroma promotes the expression of tumorigenic potential by unirradiated epithelial cells. Cancer Res *60*, 1254-1260.

Beger, C., Pierce, L. N., Kruger, M., Marcusson, E. G., Robbins, J. M., Welcsh, P., Welch, P. J., Welte, K., King, M. C., Barber, J. R., and Wong-Staal, F. (2001). Identification of Id4 as a regulator of BRCA1 expression by using a ribozyme-library-based inverse genomics approach. Proc Natl Acad Sci U S A *98*, 130-135.

Bertucci, F., Finetti, P., Cervera, N., Charafe-Jauffret, E., Mamessier, E., Adelaide, J., Debono, S., Houvenaeghel, G., Maraninchi, D., Viens, P.*, et al.* (2006). Gene expression profiling shows medullary breast cancer is a subgroup of basal breast cancers. Cancer Res *66*, 4636-4644.

Bissell, M. J., and Inman, J. (2008). Reprogramming stem cells is a microenvironmental task. Proc Natl Acad Sci U S A *105*, 15637-15638.

Bissell, M. J., and Labarge, M. A. (2005). Context, tissue plasticity, and cancer: are tumor stem cells also regulated by the microenvironment? Cancer Cell *7*, 17-23.

Bissell, M. J., Radisky, D., Rizki, A., Weaver, V. M., and Petersen, O. W. (2002). The organizing principle: microenvironmental influences in the normal and malignant breast. Differentiation *70*, 537-546.

Blish, K. R., Clausen, K. A., Hawkins, G. A., Garvin, A. J., Willingham, M. C., Turner, J. C., Torti, F. M., and Torti, S. V. (2010). Loss of heterozygosity and SOSTDC1 in adult and pediatric renal tumors. J Exp Clin Cancer Res *29*, 147.

Bolstad, B. M., Irizarry, R. A., Astrand, M., and Speed, T. P. (2003). A comparison of normalization methods for high density oligonucleotide array data based on bias and variance. Bioinformatics *19*, 185-193.

Bouras, T., Pal, B., Vaillant, F., Harburg, G., Asselin-Labat, M. L., Oakes, S. R., Lindeman, G. J., and Visvader, J. E. (2008). Notch signaling regulates mammary stem cell function and luminal cell-fate commitment. Cell Stem Cell *3*, 429-441.

Celis, J. E., Gromova, I., Cabezon, T., Gromov, P., Shen, T., Timmermans-Wielenga, V., Rank, F., and Moreira, J. M. (2007). Identification of a subset of breast carcinomas characterized by expression of cytokeratin 15: relationship between CK15+ progenitor/amplified cells and pre-malignant lesions and invasive disease. Mol Oncol *1*, 321-349.

Cheang, M. C., Chia, S. K., Voduc, D., Gao, D., Leung, S., Snider, J., Watson, M., Davies, S., Bernard, P. S., Parker, J. S.*, et al.* (2009). Ki67 index, HER2 status, and prognosis of patients with luminal B breast cancer. J Natl Cancer Inst *101*, 736-750.

Chin, K., DeVries, S., Fridlyand, J., Spellman, P. T., Roydasgupta, R., Kuo, W.-L., Lapuk, A., Neve, R. M., Qian, Z., and Ryder, T. (2006). Genomic and transcriptional aberrations linked to breast cancer pathophysiologies. Cancer Cell *10*, 529-541.

Choi, Y. S., Chakrabarti, R., Escamilla-Hernandez, R., and Sinha, S. (2009). Elf5 conditional knockout mice reveal its role as a master regulator in mammary alveolar development: failure of Stat5 activation and functional differentiation in the absence of Elf5. Dev Biol *329*, 227-241.

Cicalese, A., Bonizzi, G., Pasi, C. E., Faretta, M., Ronzoni, S., Giulini, B., Brisken, C., Minucci, S., Di Fiore, P. P., and Pelicci, P. G. (2009). The tumor suppressor p53 regulates polarity of self-renewing divisions in mammary stem cells. Cell *138*, 1083-1095.

Clausen, K. A., Blish, K. R., Birse, C. E., Triplette, M. A., Kute, T. E., Russell, G. B., D'Agostino, R. B., Jr., Miller, L. D., Torti, F. M., and Torti, S. V. (2010). SOSTDC1 differentially modulates Smad and beta-catenin activation and is down-regulated in breast cancer. Breast Cancer Res Treat.

Desmedt, C., Piette, F., Loi, S., Wang, Y., Lallemand, F., Haibe-Kains, B., Viale, G., Delorenzi, M., Zhang, Y., d'Assignies, M. S.*, et al.* (2007). Strong time dependence of the 76-gene prognostic signature for node-negative breast cancer patients in the TRANSBIG multicenter independent validation series. Clin Cancer Res *13*, 3207-3214.

Diehn, M., Cho, R. W., Lobo, N. A., Kalisky, T., Dorie, M. J., Kulp, A. N., Qian, D., Lam, J. S., Ailles, L. E., Wong, M.*, et al.* (2009). Association of reactive oxygen species levels and radioresistance in cancer stem cells. Nature *458*, 780-783.

Du, Z., Li, J., Wang, L., Bian, C., Wang, Q., Liao, L., Dou, X., Bian, X., and Zhao, R. C. (2010). Overexpression of DeltaNp63alpha induces a stem cell phenotype in MCF7 breast carcinoma cell line through the Notch pathway. Cancer Sci *101*, 2417-2424.

Fernandez-Ramires, R., Sole, X., De Cecco, L., Llort, G., Cazorla, A., Bonifaci, N., Garcia, M. J., Caldes, T., Blanco, I., Gariboldi, M.*, et al.* (2009). Gene expression profiling integrated into network modelling reveals heterogeneity in the mechanisms of BRCA1 tumorigenesis. Br J Cancer *101*, 1469-1480.

Fisher, B., Costantino, J. P., Wickerham, D. L., Redmond, C. K., Kavanah, M., Cronin, W. M., Vogel, V., Robidoux, A., Dimitrov, N., Atkins, J.*, et al.* (1998). Tamoxifen for prevention of breast cancer: report of the National Surgical Adjuvant Breast and Bowel Project P-1 Study [see comments]. J Natl Cancer Inst *90*, 1371-1388.

Git, A., Spiteri, I., Blenkiron, C., Dunning, M. J., Pole, J. C., Chin, S. F., Wang, Y., Smith, J., Livesey, F. J., and Caldas, C. (2008). PMC42, a breast progenitor cancer cell line, has normal-like mRNA and microRNA transcriptomes. Breast Cancer Res *10*, R54.

Glynn, S. A., Boersma, B. J., Dorsey, T. H., Yi, M., Yfantis, H. G., Ridnour, L. A., Martin, D. N., Switzer, C. H., Hudson, R. S., Wink, D. A.*, et al.* (2010). Increased NOS2 predicts poor survival in estrogen receptor-negative breast cancer patients. J Clin Invest *120*, 3843-3854.

Greco, S. J., Liu, K., and Rameshwar, P. (2007). Functional similarities among genes regulated by OCT4 in human mesenchymal and embryonic stem cells. Stem Cells *25*, 3143-3154.

Hackshaw, A., Roughton, M., Forsyth, S., Monson, K., Reczko, K., Sainsbury, R., and Baum, M. (2011). Long-Term Benefits of 5 Years of Tamoxifen: 10-Year Follow-Up of a Large Randomized Trial in Women at Least 50 Years of Age With Early Breast Cancer. J Clin Oncol.

Harvey, J. M., Clark, G. M., Osborne, C. K., and Allred, D. C. (1999). Estrogen receptor status by immunohistochemistry is superior to the ligand-binding assay for predicting response to adjuvant endocrine therapy in breast cancer. J Clin Oncol *17*, 1474-1481.

Hennighausen, L., and Robinson, G. W. (2001). Signaling pathways in mammary gland development. Dev Cell *1*, 467-475.

Herschkowitz, J. I., Simin, K., Weigman, V. J., Mikaelian, I., Usary, J., Hu, Z., Rasmussen, K. E., Jones, L. P., Assefnia, S., Chandrasekharan, S.*, et al.* (2007). Identification of conserved gene expression features between murine mammary carcinoma models and human breast tumors. Genome Biol *8*, R76.

Hsieh, D., Hsieh, A., Stea, B., and Ellsworth, R. (2010). IGFBP2 promotes glioma tumor stem cell expansion and survival. Biochem Biophys Res Commun *397*, 367-372.

Hu, J. G., Fu, S. L., Zhang, K. H., Li, Y., Yin, L., Lu, P. H., and Xu, X. M. (2004). Differential gene expression in neural stem cells and oligodendrocyte precursor cells: a cDNA microarray analysis. J Neurosci Res *78*, 637-646.

Jensen, E. V., and Jordan, V. C. (2003). The Estrogen Receptor: A Model for Molecular Medicine. Clin Cancer Res *9*, 1980-1989.

Jeon, H. M., Jin, X., Lee, J. S., Oh, S. Y., Sohn, Y. W., Park, H. J., Joo, K. M., Park, W. Y., Nam, D. H., DePinho, R. A.*, et al.* (2008). Inhibitor of differentiation 4 drives brain tumor-initiating cell genesis through cyclin E and notch signaling. Genes Dev *22*, 2028-2033.

Jerry, D. J., Kittrell, F. S., Kuperwasser, C., Laucirica, R., Dickinson, E. S., Bonilla, P. J., Butel, J. S., and Medina, D. (2000). A mammary-specific model demonstrates the role of the p53 tumor suppressor gene in tumor development. Oncogene *19*, 1052-1058.

Kendrick, H., Regan, J. L., Magnay, F. A., Grigoriadis, A., Mitsopoulos, C., Zvelebil, M., and Smalley, M. J. (2008). Transcriptome analysis of mammary epithelial subpopulations identifies novel determinants of lineage commitment and cell fate. BMC Genomics *9*, 591.

Laakso, M., Loman, N., Borg, A., and Isola, J. (2005). Cytokeratin 5/14-positive breast cancer: true basal phenotype confined to BRCA1 tumors. Mod Pathol *18*, 1321-1328.

Lagadec, C., Vlashi, E., Della Donna, L., Meng, Y., Dekmezian, C., Kim, K., and Pajonk, F. (2010). Survival and self-renewing capacity of breast cancer initiating cells during fractionated radiation treatment. Breast Cancer Res *12*, R13.

Li, N., Singh, S., Cherukuri, P., Li, H., Yuan, Z., Ellisen, L. W., Wang, B., Robbins, D., and DiRenzo, J. (2008). Reciprocal intraepithelial interactions between TP63 and hedgehog signaling regulate quiescence and activation of progenitor elaboration by mammary stem cells. Stem Cells *26*, 1253-1264.

Lim, E., Vaillant, F., Wu, D., Forrest, N. C., Pal, B., Hart, A. H., Asselin-Labat, M. L., Gyorki, D. E., Ward, T., Partanen, A.*, et al.* (2009). Aberrant luminal progenitors as the candidate target population for basal tumor development in BRCA1 mutation carriers. Nat Med *15*, 907-913.

Lim, E., Wu, D., Pal, B., Bouras, T., Asselin-Labat, M. L., Vaillant, F., Yagita, H., Lindeman, G. J., Smyth, G. K., and Visvader, J. E. (2010). Transcriptome analyses of mouse and human mammary cell subpopulations reveal multiple conserved genes and pathways. Breast Cancer Res *12*, R21.

Liu, S., Chia, S. K., Mehl, E., Leung, S., Rajput, A., Cheang, M. C., and Nielsen, T. O. (2010). Progesterone receptor is a significant factor associated with clinical outcomes and effect of adjuvant tamoxifen therapy in breast cancer patients. Breast Cancer Res Treat *119*, 53-61.

Liu, S., Ginestier, C., Charafe-Jauffret, E., Foco, H., Kleer, C. G., Merajver, S. D., Dontu, G., and Wicha, M. S. (2008). BRCA1 regulates human mammary stem/progenitor cell fate. Proc Natl Acad Sci U S A *105*, 1680-1685.

Medina, D. (2002). Biological and molecular characteristics of the premalignant mouse mammary gland. Biochimica et Biophysica Acta (BBA) - Reviews on Cancer *1603*, 1-9.

Medina, D., Kittrell, F. S., Shepard, A., Stephens, L. C., Jiang, C., Lu, J., Allred, D. C., McCarthy, M., and Ullrich, R. L. (2002). Biological and genetic properties of the p53 null preneoplastic mammary epithelium. Faseb J *16*, 881-883.

Molyneux, G., Geyer, F. C., Magnay, F. A., McCarthy, A., Kendrick, H., Natrajan, R., Mackay, A., Grigoriadis, A., Tutt, A., Ashworth, A.*, et al.* (2010). BRCA1 basal-like breast cancers originate from luminal epithelial progenitors and not from basal stem cells. Cell Stem Cell *7*, 403-417.

Narod, S. A., and Foulkes, W. D. (2004). BRCA1 and BRCA2: 1994 and beyond. Nat Rev Cancer *4*, 665-676.

Neve, R. M., Chin, K., Fridlyand, J., Yeh, J., Baehner, F. L., Fevr, T., Clark, L., Bayani, N., Coppe, J.-P., and Tong, F. (2006). A collection of breast cancer cell lines for the study of functionally distinct cancer subtypes. Cancer Cell *10*, 515-527.

Nguyen, D. H., Oketch-Rabah, H. A., Illa-Bochaca, I., Geyer, F. C., Reis-Filho, J. S., Mao, J. H., Ravani, S. A., Zavadil, J., Borowsky, A. D., Jerry, D. J.*, et al.* (2011). Radiation Acts on the Microenvironment to Affect Breast Carcinogenesis by Distinct Mechanisms that Decrease Breast Cancer Latency and Affect Tumor Type. Cancer Cell.

Oakes, S. R., Naylor, M. J., Asselin-Labat, M. L., Blazek, K. D., Gardiner-Garden, M., Hilton, H. N., Kazlauskas, M., Pritchard, M. A., Chodosh, L. A., Pfeffer, P. L.*, et al.* (2008). The Ets transcription factor Elf5 specifies mammary alveolar cell fate. Genes Dev *22*, 581-586.

Ohyama, M., Terunuma, A., Tock, C. L., Radonovich, M. F., Pise-Masison, C. A., Hopping, S. B., Brady, J. N., Udey, M. C., and Vogel, J. C. (2006). Characterization and isolation of stem cell-enriched human hair follicle bulge cells. J Clin Invest *116*, 249-260.

Parker, M. S., Hui, F. K., Camacho, M. A., Chung, J. K., Broga, D. W., and Sethi, N. N. (2005). Female breast radiation exposure during CT pulmonary angiography. AJR Am J Roentgenol *185*, 1228-1233.

Pavlidis, P., and Noble, W. (2001). Analysis of strain and regional variation in gene expression in mouse brain. Genome Biology *2*, research0042.0041 - research0042.0015.

Pawitan, Y., Bjohle, J., Amler, L., Borg, A. L., Egyhazi, S., Hall, P., Han, X., Holmberg, L., Huang, F., Klaar, S.*, et al.* (2005). Gene expression profiling spares early breast cancer patients from adjuvant therapy: derived and validated in two population-based cohorts. Breast Cancer Res *7*, R953-964.

Perou, C. M., and Borresen-Dale, A. L. (2011). Systems biology and genomics of breast cancer. Cold Spring Harb Perspect Biol *3*.

Perou, C. M., Sorlie, T., Eisen, M. B., van de Rijn, M., Jeffrey, S. S., Rees, C. A., Pollack, J. R., Ross, D. T., Johnsen, H., Akslen, L. A.*, et al.* (2000). Molecular portraits of human breast tumours. Nature *406*, 747-752.

Phillips, T. M., McBride, W. H., and Pajonk, F. (2006). The response of CD24(-/low)/CD44+ breast cancer-initiating cells to radiation. J Natl Cancer Inst *98*, 1777-1785.

Potemski, P., Kusinska, R., Kubiak, R., Piekarski, J. H., Pluciennik, E., Bednarek, A. K., and Kordek, R. (2007). Relationship of P-cadherin expression to basal phenotype of breast carcinoma. Pol J Pathol *58*, 183-188.

Prat, A., Parker, J. S., Karginova, O., Fan, C., Livasy, C., Herschkowitz, J. I., He, X., and Perou, C. M. (2010). Phenotypic and molecular characterization of the claudin-low intrinsic subtype of breast cancer. Breast Cancer Res *12*, R68.

Rakha, E. A., El-Sayed, M. E., Green, A. R., Lee, A. H., Robertson, J. F., and Ellis, I. O. (2007). Prognostic markers in triple-negative breast cancer. Cancer *109*, 25-32.

Rakha, E. A., Elsheikh, S. E., Aleskandarany, M. A., Habashi, H. O., Green, A. R., Powe, D. G., El-Sayed, M. E., Benhasouna, A., Brunet, J.-S., Akslen, L. A.*, et al.* (2009). Triple-Negative Breast Cancer: Distinguishing between Basal and Nonbasal Subtypes. Clin Cancer Res *15*, 2302-2310.

Reis-Filho, J. S., Milanezi, F., Paredes, J., Silva, P., Pereira, E. M., Maeda, S. A., de Carvalho, L. V., and Schmitt, F. C. (2003). Novel and classic myoepithelial/stem cell markers in metaplastic carcinomas of the breast. Appl Immunohistochem Mol Morphol *11*, 1-8.

Ribeiro-Silva, A., Ramalho, L. N. Z., Garcia, S. B., and Zucoloto, S. (2003). The relationship between p63 and p53 expression in normal and neoplastic breast tissue. Arch Pathol Lab Med *127*, 336-340.

Shackleton, M., Vaillant, F., Simpson, K. J., Stingl, J., Smyth, G. K., Asselin-Labat, M. L., Wu, L., Lindeman, G. J., and Visvader, J. E. (2006). Generation of a functional mammary gland from a single stem cell. Nature *439*, 84-88.

Slamon, D. J., Leyland-Jones, B., Shak, S., Fuchs, H., Paton, V., Bajamonde, A., Fleming, T., Eiermann, W., Wolter, J., Pegram, M.*, et al.* (2001). Use of chemotherapy plus a monoclonal antibody against HER2 for metastatic breast cancer that overexpresses HER2. N Engl J Med *344*, 783-792.

Sleeman, K. E., Kendrick, H., Robertson, D., Isacke, C. M., Ashworth, A., and Smalley, M. J. (2007). Dissociation of estrogen receptor expression and in vivo stem cell activity in the mammary gland

10.1083/jcb.200604065. J Cell Biol *176*, 19-26.

Sorlie, T., Perou, C. M., Tibshirani, R., Aas, T., Geisler, S., Johnsen, H., Hastie, T., Eisen, M. B., van de Rijn, M., Jeffrey, S. S.*, et al.* (2001). Gene expression patterns of breast carcinomas distinguish tumor subclasses with clinical implications. Proc Natl Acad Sci U S A *98*, 10869-10874.

Sternlicht, M. D., Kouros-Mehr, H., Lu, P., and Werb, Z. (2006). Hormonal and local control of mammary branching morphogenesis. Differentiation *74*, 365-381.

Stingl, J., Eirew, P., Ricketson, I., Shackleton, M., Vaillant, F., Choi, D., Li, H. Y. I., and Eaves, C. J. (2006). Purification and unique properties of mammary epithelial stem cells. Nature *439*, 993-997.

Tang, P., Skinner, K. A., and Hicks, D. G. (2009). Molecular classification of breast carcinomas by immunohistochemical analysis: are we ready? Diagn Mol Pathol *18*, 125-132.

Tao, L., Roberts, A. L., Dunphy, K. A., Bigelow, C., Yan, H., and Jerry, D. J. (2010). Repression of Mammary Stem/Progenitor Cells by P53 is Mediated by Notch and Separable from Apoptotic Activity. Stem Cells.

Turner, N. C., Reis-Filho, J. S., Russell, A. M., Springall, R. J., Ryder, K., Steele, D., Savage, K., Gillett, C. E., Schmitt, F. C., Ashworth, A., and Tutt, A. N. (2007). BRCA1 dysfunction in sporadic basal-like breast cancer. Oncogene *26*, 2126-2132.

Tusher, V. G., Tibshirani, R., and Chu, G. (2001). Significance analysis of microarrays applied to the ionizing radiation response. Proc Natl Acad Sci U S A *98*, 5116-5121.

van 't Veer, L. J., Dai, H., van de Vijver, M. J., He, Y. D., Hart, A. A., Mao, M., Peterse, H. L., van der Kooy, K., Marton, M. J., Witteveen, A. T.*, et al.* (2002). Gene expression profiling predicts clinical outcome of breast cancer. Nature *415*, 530-536.

Vargo-Gogola, T., and Rosen, J. M. (2007). Modelling breast cancer: one size does not fit all. Nat Rev Cancer *7*, 659-672.

Villani, R. M., Adolphe, C., Palmer, J., Waters, M. J., and Wainwright, B. J. (2010). Patched1 inhibits epidermal progenitor cell expansion and basal cell carcinoma formation by limiting Igfbp2 activity. Cancer Prev Res (Phila) *3*, 1222-1234.

Visvader, J. E. (2011). Cells of origin in cancer. Nature *469*, 314-322.

Visvader, J. E., and Smith, G. H. (2010). Murine Mammary Epithelial Stem Cells: Discovery, Function, and Current Status. Cold Spring Harb Perspect Biol.

Wang, X. Y., Penalva, L. O., Yuan, H., Linnoila, R. I., Lu, J., Okano, H., and Glazer, R. I. (2010). Musashi1 regulates breast tumor cell proliferation and is a prognostic indicator of poor survival. Mol Cancer *9*, 221.

Wang, Y., Klijn, J. G., Zhang, Y., Sieuwerts, A. M., Look, M. P., Yang, F., Talantov, D., Timmermans, M., Meijer-van Gelder, M. E., Yu, J.*, et al.* (2005). Gene-expression profiles to predict distant metastasis of lymph-node-negative primary breast cancer. Lancet *365*, 671-679.

Webb, A., Li, A., and Kaur, P. (2004). Location and phenotype of human adult keratinocyte stem cells of the skin. Differentiation *72*, 387-395.

Whitehead, R. H., Monaghan, P., Webber, L. M., Bertoncello, I., and Vitali, A. A. (1983). A new human breast carcinoma cell line (PMC42) with stem cell characteristics. II. Characterization of cells growing as organoids. J Natl Cancer Inst *71*, 1193-1203.

Wright, L. S., Li, J., Caldwell, M. A., Wallace, K., Johnson, J. A., and Svendsen, C. N. (2003). Gene expression in human neural stem cells: effects of leukemia inhibitory factor. J Neurochem *86*, 179-195.

Wright, M. H., Calcagno, A. M., Salcido, C. D., Carlson, M. D., Ambudkar, S. V., and Varticovski, L. (2008a). Brca1 breast tumors contain distinct CD44+/CD24- and CD133+ cells with cancer stem cell characteristics. Breast Cancer Res *10*, R10.

Wright, M. H., Robles, A. I., Herschkowitz, J. I., Hollingshead, M. G., Anver, M. R., Perou, C. M., and Varticovski, L. (2008b). Molecular analysis reveals heterogeneity of mouse mammary tumors conditionally mutant for Brca1. Mol Cancer *7*, 29.

Yalcin-Ozuysal, O., Fiche, M., Guitierrez, M., Wagner, K. U., Raffoul, W., and Brisken, C. (2010). Antagonistic roles of Notch and p63 in controlling mammary epithelial cell fates. Cell Death Differ *17*, 1600-1612.

Yang, A., Schweitzer, R., Sun, D., Kaghad, M., Walker, N., Bronson, R. T., Tabin, C., Sharpe, A., Caput, D., Crum, C., and McKeon, F. (1999). p63 is essential for regenerative proliferation in limb, craniofacial and epithelial development. Nature *398*, 714-718.

Yun, K., Mantani, A., Garel, S., Rubenstein, J., and Israel, M. A. (2004). Id4 regulates neural progenitor proliferation and differentiation in vivo. Development *131*, 5441-5448.

Zhu, Y. T., Jia, Y., Hu, L., Qi, C., Prasad, M. K., McCallion, A. S., and Zhu, Y. J. (2010). Peroxisome-proliferator-activated receptor-binding protein (PBP) is essential for the growth of active Notch4-immortalized mammary epithelial cells by activating SOX10 expression. Biochemical Journal *425*, 435–444.

Zucchi, I., Astigiano, S., Bertalot, G., Sanzone, S., Cocola, C., Pelucchi, P., Bertoli, G., Stehling, M., Barbieri, O., Albertini, A.*, et al.* (2008). Distinct populations of tumor-initiating cells derived from a tumor generated by rat mammary cancer stem cells. Proc Natl Acad Sci U S A *105*, 16940-16945.